Formulation of an Integrated Robust Design and Tactics Optimization Process for Undersea Weapon Systems

A Thesis
Presented to
The Academic Faculty

by

Andrew P. Frits

In Partial Fulfillment
of the Requirements for the Degree
Doctor of Philosophy

School of Aerospace Engineering
Georgia Institute of Technology
December, 2004

Formulation of an Integrated Robust Design and Tactics Optimization Process for Undersea Weapon Systems

Approved by:

Dr. Dimitri Mavris, Committee Chair
School of Aerospace Engineering
Georgia Institute of Technology

Dr. Daniel Schrage
School of Aerospace Engineering
Georgia Institute of Technology

Dr. Massimo Ruzzene
School of Aerospace Engineering
Georgia Institute of Technology

Dr. James Craig
School of Aerospace Engineering
Georgia Institute of Technology

Mr. Bill Krol
Naval Undersea Warfare Center

Date Approved:

December 2004

Dedicated to

Sage Orianna Rutledge,

may she have a blessed life.

ACKNOWLEDGEMENTS

I would like to begin by thanking my parents and family, who were supportive of me even though i chose to remain in college for more than a decade. I would like to thank the Office of Naval Research for funding my graduate education. In addition, Bill Krol and Aldu Kusmik from the Naval Undersea Warfare Center deserve special appreciation for the invaluable guidance and tutelage which they provided for me. A special thanks goes to Dr. Neil Weston, who not only initiated this research at ASDL, but also made sure that I never slacked too much. Kristin Kelly and Colin Pouchet provided incredible support in our work on torpedo design. To my close friends, including Brian German, Travis Danner, Tommer Ender, Michael Rutledge, and Thomas A. Dechman III, this work would not have been possible without your support. And finally, to my advisor, Dr. Mavris, the one man whom I can say is personally responsible for my earning a Ph.D., you will always have my respect and gratitude.

TABLE OF CONTENTS

LIST OF TABLES

LIST OF FIGURES

LIST OF ABBREVIATIONS

AMV	Advanced Mean Value Methods.
$\boldsymbol{P_{ck}}$	Probability of Counter-Kill.
$\boldsymbol{P_d}$	Probability of Detection.
$\boldsymbol{P_h}$	Probability of Hit.
$\boldsymbol{P_k}$	Probability of Kill.
$\boldsymbol{R^2}$	Coefficient of Determination.
$\boldsymbol{S/N}$	Signal-to-Noise Ratio.
BW	Beamwidth.
CDF	Cumulative Distribution Function.
DI	Directivity Index.
DoE	Design of Experiments.
FORM	First Order Reliability Methods.
IMP	Integrated Motor-Propulsor.
MCM	Mine Counter-Measures.
MCT	Multiple Classification Tactics.
OEC	Overall Evaluation Criterion.
PDF	Probability Density Function.
POS	Probability of Success.
RSE	Response Surface Equation.
RSM	Response Surface Methodology.
SCEPS	Stored Chemical Energy Propulsion System.
SCT	Single Classification Tactics.
SORM	Second Order Reliability Methods.
TOAD	Torpedo Optimization, Analysis, and Design Program.
TOPSIS	Technique for Ordered Preferencing by Similarity to the Ideal Solution.
UUV	Unmanned Undersea Vehicles.

SUMMARY

In the current Navy environment of undersea weapons development, the engineering aspect of design is decoupled from the development of the tactics with which the weapon is employed. Tactics are developed by intelligence experts, warfighters, and wargamers, while torpedo design is handled by engineers and contractors. This dissertation examines methods by which the conceptual design process of undersea weapon systems, including both torpedo systems and mine counter-measure systems, can be improved. It is shown that by *simultaneously* designing the torpedo *and* the tactics with which undersea weapons are used, a more effective overall weapon system can be created.

In addition to integrating torpedo tactics with design, the thesis also looks at design methods to account for uncertainty. The uncertainty is attributable to multiple sources, including: lack of detailed analysis tools early in the design process, incomplete knowledge of the operational environments, and uncertainty in the performance of potential technologies. A robust design process is introduced to account for this uncertainty in the analysis and optimization of torpedo systems through the combination of Monte Carlo simulation with response surface methodology and metamodeling techniques. Additionally, various other methods that are appropriate to uncertainty analysis are discussed and analyzed.

The thesis also advances a new approach towards examining robustness and risk: the treatment of probability of success (POS) as an independent variable. Examining the cost and performance tradeoffs between high and low probability of success designs, the decision-maker can make better informed decisions as to what designs are most promising and determine the optimal balance of risk, cost, and performance.

These robust design processes are demonstrated on a testbed example, a lightweight torpedo example, a heavyweight torpedo example, and a mine counter-measure system. The dissertation not only develops a framework for robust design, but also develops tools

for the detailed analysis of torpedo systems, the analysis of minehunting systems, and a visualization tool for improved decision-making in the presence of significant amounts of probabilistic data.

Finally, the thesis examines the use of non-dimensionalization of parameters for torpedo design. The thesis shows that the use of non-dimensional torpedo parameters leads to increased knowledge about the scaleability of torpedo systems and increased performance of Designs of Experiments.

The integration of these ideas concerning tactics, robust design with uncertainty, and non-dimensionalization of torpedo parameters has lead to the development of a general, powerful technique by which torpedo and other undersea weapon systems can be fully optimized, thereby increasing performance and decreasing the total cost of future weapon systems.

CHAPTER I

MOTIVATION AND OBJECTIVES

1.1 Need for Advanced Design Methods

Early phases of decision-making in conceptual design are characterized by a high degree of uncertainty in the system. This uncertainty arises from multiple sources, including: lack of detailed analysis tools early in the design process, incomplete knowledge of the operational environment or requirements, and uncertainty in the performance of potential technologies. Yet, in the midst of this uncertainty, decision-makers are often required to make commitments that permanently lock-in final system cost and performance. Figure 1 illustrates how, in today's design process, most of the system cost is committed early in the design process when knowledge of the system is most limited. Today's system engineering world is aspiring to bring more knowledge forward in the design process so that better decisions can be made before a design's final cost is locked-in. Unfortunately, bringing design knowledge forward inherently brings more uncertainty about the system forward, thus creating a need for more advanced design techniques that can handle this uncertainty [213].

1.2 Need for Better Torpedoes

The Navy in general, and the torpedo community in particular, have had their real-dollar budgets decrease significantly. Ship-building, a key indicator of the U.S. Navy budget, is currently at its lowest point since 1950 and the Fleet combat inventory has been cut in half from only 1989 levels [167]. These budget decreases have been occurring since the end of the cold war. Without the direct threat of the Soviet Union, some people perceived that the threat from foreign submarines, and hence the need for advanced undersea weapons, has decreased. However, with the demise of the Soviet Union and the increasingly fractional nature of regional politics, a large export market has been created for relatively inexpensive,

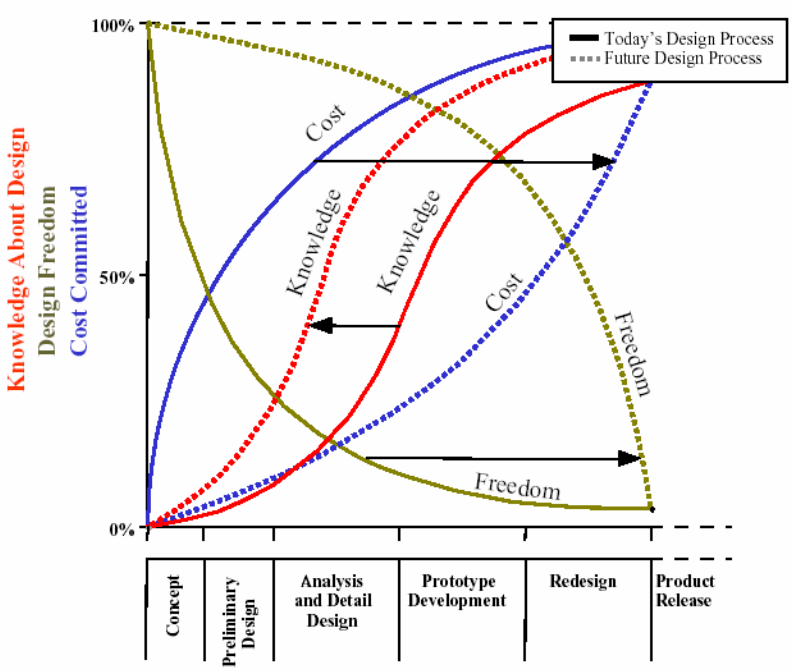

Figure 1: Design Knowledge vs. Cost Committed [53]

yet highly capable, diesel-electric submarines. Germany is advertising its highly advanced type 212 and 214 submarines [91] [92], while Russia is still manufacturing new diesel-electric submarines for export to countries such as the People's Republic of China [192]. A study by the Naval Studies Board of the National Research Council has stated that current undersea weapons will have to be replaced by weapons with "significantly advanced capabilities" in the next 10 to 20 years [174]. These capabilities will need to increase weapon performance, decrease cost, and decrease size so that the payload effectiveness of submarines can be increased.

In addition to increasing submarine threats from foreign navies, ongoing development of unmanned undersea vehicles (UUV's) has opened up new design freedom for torpedoes. Traditionally, US torpedoes have been fixed at two diameters, 12.75 inches and 21 inches, in order to match existing launcher systems. However, with the US military moving towards unmanned systems, the expanding role of combat UUV systems is opening a new range of potential torpedo diameters, from super-small diameter torpedoes to large-diameter, slow-moving UUV systems. This newfound design freedom and associated distancing from

Table 1: Undersea Weapon Design and Optimization Objectives[179]

Program Objectives:
• Develop capabilities for design analyses and evaluation
• Implement and integrate computational & design tools
• Develop distributed design & virtual environment for prototyping
• Optimize design & design process
• Reduce Total Ownership Cost

historical designs, along with the expected revolutionary impact of these UUV systems [57], increases the need for advanced design techniques for torpedo systems.

A change in conceptual design techniques is a vital need in the undersea weapons community. With limited defense budgets and changing national priorities, affordable, cost-effective designs are paramount for next generation torpedo systems. Not only will all future torpedo designs be held to stringent cost goals, but many of the future undersea weapon concepts, such as the super-cavitating torpedo [131], have no evolutionary legacy from which to draw upon. As such, these concepts have the potential for even more risk, so adequate analysis of the system uncertainty from the start is crucial.

The Navy has repeatedly expressed its desires in expanding methods for conceptual design techniques relating to future undersea weapon systems. In fact, the Office of Naval Research has a four-year, six-and-a-half million dollar program to examine nothing other than Undersea Weapon Design and Optimization with the specified task to "Design infrastructure and tools that support affordable undersea weapons" [179]. The stated objectives of this multi-million dollar program are listed in Table 1.

1.3 Need for Tactics in Design

In the current Navy environment of undersea weapons development, the engineering aspect of design is decoupled from the development of the tactics with which the weapon is

employed. The current approach utilizes a group of intelligence experts and warfighters, drawing from knowledge that includes experience with previous weapons systems, wargaming scenarios, and threat assessments, who generate a preliminary set of 'desired' torpedo attributes. Warfare analysis groups then use complex engagement programs and tactical considerations to refine these preliminary attributes into point performance requirements for a future torpedo system, i.e., they specify a required maximum velocity, range, and turn rate. In addition, the requirements often include a desire to minimize vehicle traits such as radiated noise, with constraints placed on maximum allowable noise. Torpedo designers then use engineering analysis tools to translate these requirements into feasible torpedo designs that meet the specified criteria. The modern-day process is detailed in Figure 2.

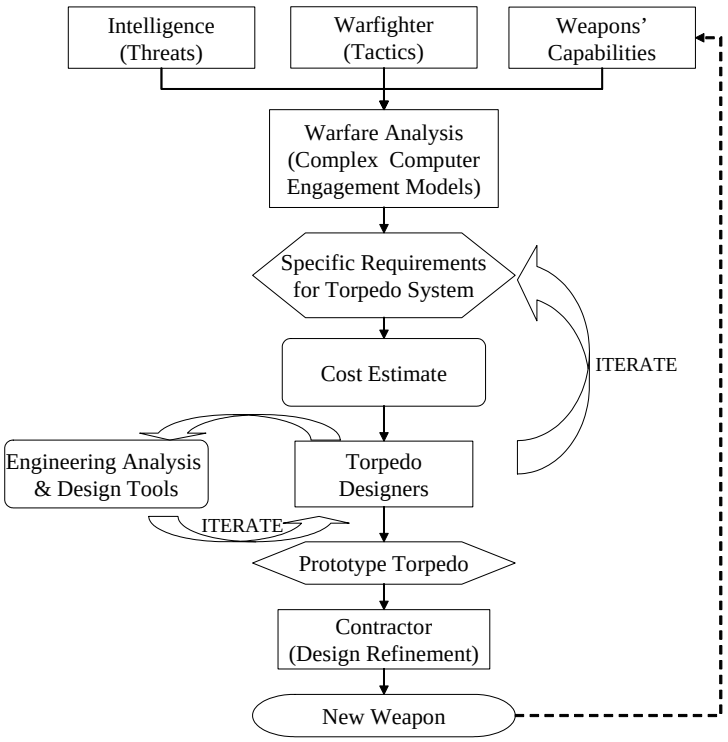

Figure 2: Existing Torpedo Design Paradigm (Adapted from [81])

Unfortunately, from the total systems perspective, this design paradigm may not produce optimal designs. For one, it leads to a situation in which the tactics with which a weapon is employed are developed independently from the weapon itself. The tactics are

generally derived not from design knowledge of potential systems, but from experience with current operational systems, in conjunction with threat assessments, to develop required torpedo performance attributes to best defeat future threats. These performance attributes are set as requirements and passed down to torpedo designers, who then use their engineering models and available technologies to create a torpedo system that meets the analysts' specifications. Once this newer and more capable torpedo is introduced into service, the Fleet will often create a new set of tactics that best utilizes the capabilities of the new system. The tactics are therefore continuously developed and refined using a torpedo with static performance. This system of tactics development, then torpedo design, then tactics re-development creates a never-ending cycle in which the weapon system is never truly optimized for the tactics with which it is employed. This lack of interaction between the warfare analyst and the weapon designer prevents the weapon system from reaching its greatest potential effectiveness.

Another drawback of this system is that weapon requirements are given to torpedo designers as a point condition, i.e., a specific speed and range are defined. These point conditions limit the torpedo designer to developing a torpedo that fits into a tightly constrained design space, curtailing design freedom and excluding potentially feasible designs that may better fulfill the mission via a different set of performance parameters.

Therefore, to truly optimize a weapon system, the tactical employment of the weapon and engagement models must be considered concurrently with the engineering analysis of the weapon. This concept introduces a new paradigm, in which mission analysis and weapon design are considered simultaneously. The inclusion of mission analysis, and the exploration of different combinations of tactics and performance, allows for the creation of an optimal weapon system. In addition, instead of designing to a rigid set of point requirements, the designer now has the flexibility to adjust either torpedo performance attributes or the tactical employment to reach the required level of mission effectiveness, greatly expanding the design space and generating more freedom for the design process.

One of the goals of this research is to illustrate an environment in which the effects of change in both engineering parameters and tactical parameters are analyzed simultaneously

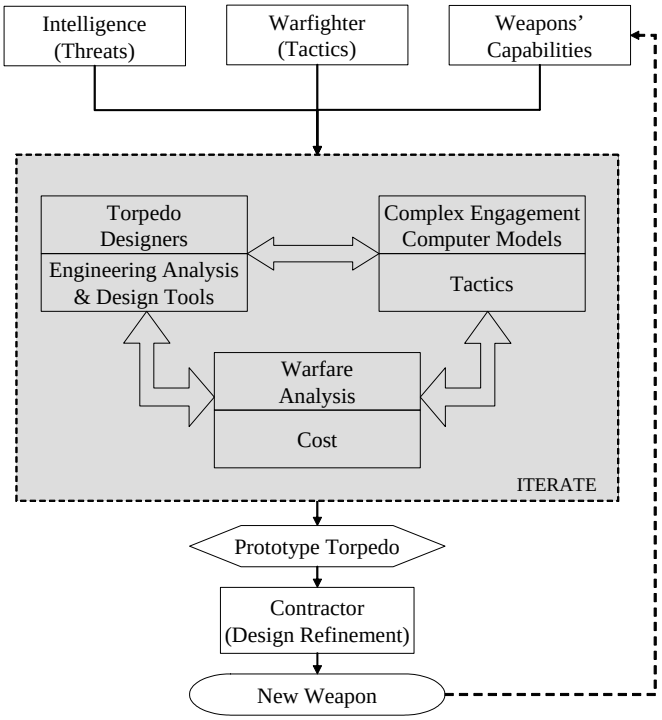

Figure 3: Proposed Torpedo Design Paradigm (Adapted from [81])

to determine their impact on overall torpedo effectiveness. Thus, the linkages between design variables, weapon performance, and tactics can be more thoroughly understood, and a vehicle with the greatest overall effectiveness can be created. This new paradigm is illustrated in Figure 3.

Though it might be expected that the military has already embraced the simultaneous design of torpedoes and tactics analysis, this is not the case. Two separate groups of researchers, using two distinct set of analysis tools, work on these problems. Unfortunately, the linkages between these two groups only occur at high levels in the force/management structure, and the "link is not as tight as it should be [132]". As another torpedo researcher stated, there is "nothing of note on the simultaneous development of tactics and design in subs and torpedoes" and that "it is an open research question in general [244]". Clearly the military has not yet embraced the simultaneous development of design and tactics analysis.

In addition to studying the effect of tactics integration with the design of torpedoes, the use of tactics coupled with design will be studied for another undersea weapon application:

mine counter-measure systems. These mine counter-measures are not only a driving need in the Navy today, but readily lend themselves to studies that involve tactics integration.

1.4 Need for Mine Counter-Measures

Mine counter-measure (MCM) systems are an absolutely critical need for the Navy. "The use of mines and countermeasures to mines has figured significantly in every major armed conflict and nearly every regional conflict in which the United States has been involved since the Revolutionary War [228]." In fact, since World War II, the United States has lost more ships to enemy mines than to all other sources combined. Figure 4 shows the mechanism of attack against all US ships damaged or sunk between 1950 and 1999; the devastating impact that mines have had on U.S forces is readily apparent. Naval mines have also been employed with significant effect by the United States. At the end of World War II, the United States began an intensive mining campaign against Japanese harbors. As a result of this campaign, during the last five months of Word War II, the Japanese lost 670[1] ships to mines, including almost every vessel left in the Japanese inventory, and almost equal to U.S. losses to German submarines during the entire war[2] [70].

Currently, mines are fielded by more than 50 countries, with over 300 distinct types of mines in service [66]. Mines are cheap and affordable, yet can create massive amounts of damage, both in wrecked equipment and human lives. In the case of the USS Samuel B. Roberts, a single mine that cost an estimated $1,500 to build and deploy was able to inflict nearly $100 million of damage to the U.S. warship [32] and seriously injuring 10 sailors [173]. In fact, many were amazed that the warship was not sunk, with a corresponding catastrophic loss of life. A photograph of the damage to the warship is shown in Figure 5. Similar cases abound, where mines purchased for thousands of dollars have done tens of millions of dollars in damage to US ships.

The need for effective minehunting capabilities has been stated at the highest levels of

[1]Some sources place this number closer to 300 ships, due to discrepancies concerning whether very small Japanese junkers should be counted as ships [136]

[2]Note that this number refers to only U.S. losses to German submarines, not total *Allied* losses to German submarines.

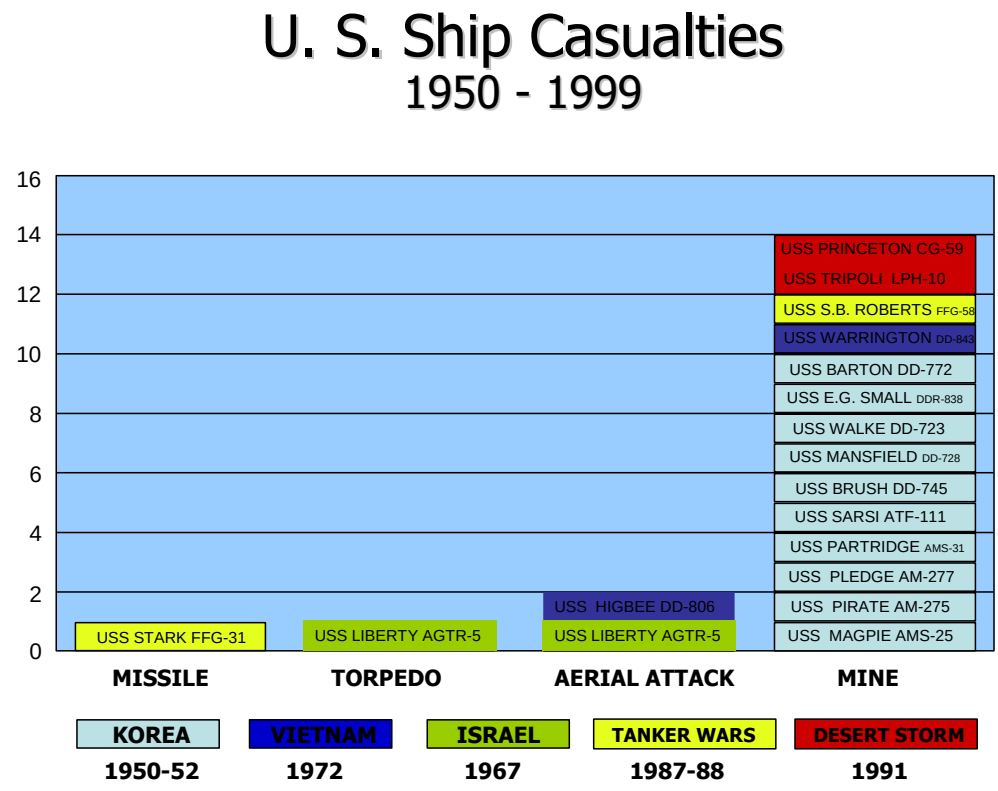

Figure 4: Casualties for US Ships from 1950-1999 [14]

the Navy. In 1999, the Navy Strategic Planning Guidance Manual said, "Naval forces must remain capable of operating regardless of a future adversary's area denial strategy[3] [1]." As bluntly spoken by Admiral Johnson, Chief of Naval Operations, "mine warfare is a unique Navy core capability that must become a prime warfighting area we all treat as important as strike [117]."

In order to better handle these mine threats, the Navy is looking at many advanced systems. Many of these systems are autonomous, unmanned undersea vehicles (UUVs). UUVs are particularly well-suited for mine-hunting scenarios [85], as the environment is not only exceptionally dangerous (the Germans lost 282 ships while minesweeping in World War II [136]), but also requires long loiter times. In many cases, these UUVs will be physically replacing human swimmers in the minehunting and neutralization role [140]. The

[3]Area denial strategy refers to mining large areas of ocean, in order to deny an enemy the ability to safely use the area

Figure 5: Mine Damage to the USS Samuel B. Roberts [29]

Navy is examining many such UUV systems, including the Long-Term Mine Reconnaissance System (LRMS), to conduct reconnaissance of mine-fields [67]. While developing these mine counter-measure systems, it has been found that the tactics, or search patterns, with which these systems are being used is highly influential on their design [83] [98].

Since minehunting search patterns greatly influence the vehicle design, mine counter-measure systems represent a field where it is critical that design and tactics be developed simultaneously. This field of developing optimized searching techniques and unmanned vehicles applies not only to mine counter-measure systems, but as Gage discusses [84], there are many other military applications for which minehunting design methods and tactics are directly applicable: "intelligent land mine deployment [143], ... reconnaissance, sentry duty, communications relay [124], maintenance inspection, carrier deck FOD (foreign object) disposal [82], and ship hull cleaning [75]."

Future plans for Navy mine counter-measure systems are very aggressive. Currently, there are 17 MCM detachments tasked with dedicated MCM missions [32]. Unfortunately, during wartime operations, it is often impossible to assign a dedicated MCM asset to every group of U.S. ships. As a result, the U.S. is attempting to develop an "organic" mine

counter-measure capability. This process entails the inclusion of mine counter-measure capabilities into generic warfighting vessels, so that dedicated MCM platforms would not be required [32] [66]. With such a system, whenever a U.S. task force encounters a situation where mine counter-measure systems are needed, the vessels would have inherent, "organic" MCM capabilities, without the need to wait for dedicated MCM assets to arrive.

Unfortunately, deploying these organic MCM systems requires that new, advanced MCM systems must be developed. Because the systems will be deployed on vessels already full of combat systems, the new MCM equipment will not have much space available to it. In addition, there will be much less of a willingness on the part of a commander to put a warship in harm's way for MCM activities. These facts mean that new types of mine counter-measure systems need to be developed so that the military may implement this "organic" capability. Therefore, design techniques must be developed to address the future of these new mine counter-measure systems, and these techniques must account for both the tactics with which the systems are used, and the uncertainty that inherently surround minehunting.

1.5 Need for Accounting of Uncertainty

Uncertainty exists in nearly every facet of engineering, from manufacturing, to design, to reliability and human interactions; the list encompasses nearly every element of engineering. The study of methods to deal with uncertainty in the physical world has been a fundamental problem for engineers and has interested scientists for several centuries. LaPlace in his 1820 work, "A Philosophical Essay on Probabilities", wrote about how uncertainty and the mathematics used to predict it, probability, pervade all areas of science.

> I present here without the aid of analysis the principles and general results of this theory, applying them to the most important questions of life, which are indeed for the most part only problems of probability. Strictly speaking, it may even be said that nearly all our knowledge is problematical; and in the small number of things which we are able to know with certainty, even in the mathematical sciences themselves, the principal means of ascertaining truth —

induction, and analogy — are based on probabilities; so that the entire system of human knowledge is connected with the theory set forth in this essay [137].

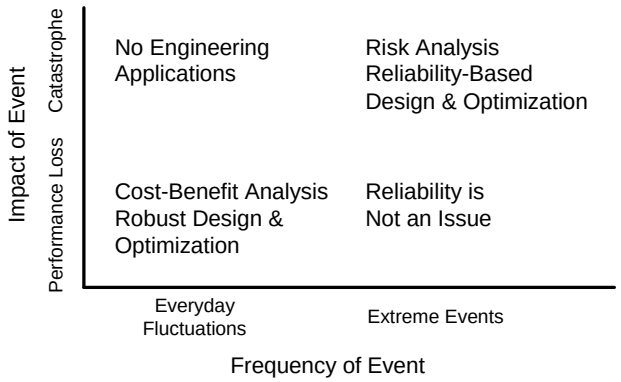

Figure 6: Uncertainty Classification [111]

At the system-level, uncertainty can generally be divided into two levels, each with its own developing field, reliability analysis and robust analysis. Reliability analysis generally deals with preventing catastrophic failings (Figure 6) while robustness deals with maintaining good system performance at off-design conditions. Additionally, reliability analysis concentrates on extreme events, or the so-called 'tails' of uncertainty distributions, while robust design focuses on the behavior near the mean. This concept is illustrated in Figure 7. While reliability analysis has been around for many years, robust design is a rapidly growing field, being first popularized in Japan by Taguchi and then transitioning to the United States starting in 1980 [76].

Using advanced design methods to characterize and analyze this uncertainty early in the design process is one method that helps bring system knowledge forward in the design process, as shown in Figure 1. By estimating the uncertainty, the decision-maker gains better knowledge of the risks and rewards of various system configurations, thereby leading to better-informed decisions.

A recent NASA study determined that uncertainty based design is a critical need in the aerospace industry, yet still has many barriers to overcome before it is fully adopted [246]. These barriers are both cultural and technical in nature; the authors propose that

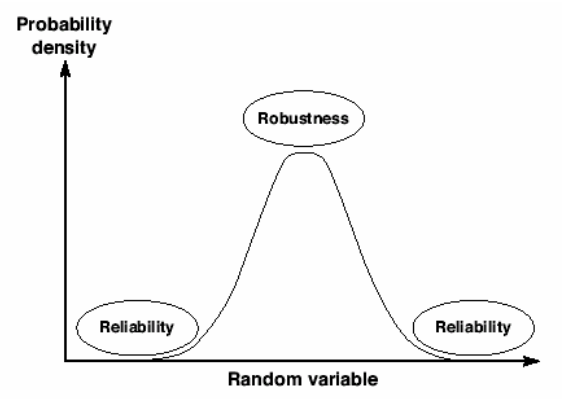

Figure 7: Reliability versus Robustness on Probability Density Functions [246]

uncertainty-based design methods are not sufficiently developed to be fully adopted by industry. However, once these barriers are overcome, the authors listed several benefits of uncertainty-based design [246]:

1. Confidence in analysis tools will increase
2. Design cycle time, cost, and risk will be reduced
3. System performance will increase while ensuring that reliability requirements are met
4. Designs will be more robust
5. The methodology can assess systems at off-nominal conditions

This need to account for uncertainty is not specific to the aerospace industry, and also applies to undersea vehicles. Yukish, in his paper on undersea vehicle conceptual design, states that for key attributes of conceptual design of complex systems in general, and undersea vehicles in particular, "the uncertainty of design parameters is often many percentage points of their absolute value [243]". Thus, uncertainty must be taken into account when dealing with optimal design of undersea weapon systems.

1.6 System-of-Systems Ramifications

The inclusion of tactics as an integrated part of the design process is essentially taking a system-of-systems approach to the problem. In this manner, the system in question (in

Table 2: System of System Analogies

Component System	Larger System
Torpedo Design	Submarine Engagements
Commercial Aircraft Design	National Airspace System [87]
Fighter Aircraft Design	Air Campaign Analysis [213]
Missile Design	Aircraft Engagements
Armored Fighting Vehicle	Future Combat System [23] [208]
Coast Guard Cutter	Integrated Deepwater System [225]
Communication Satellite	Constellation of Communications Satellites
Personal Air Vehicle	Future Transportation System [52] [54]

this case the torpedo or minehunter) is not being designed to meet an arbitrary set of requirements, but instead, is being designed concurrently with the larger system in which it is being used; the larger system in this case being the submarine warfighting environment. This type of design process, in which the larger system is being modeled, analyzed, and optimized concurrently with the component system, is being increasingly studied in the world of design. In fact, the techniques used for this study, integrating torpedo design and tactics, can be used as a basis for techniques for any number of system-of-system problems. A list of examples where system-of-systems level analyses would be beneficial is given in Table 2.

1.7 Overall Research Objectives

The primary goal of this dissertation is to formulate a means to better design torpedo systems. The development of such a mechanism requires the examination of many factors, including the effects of tactics on the performance of torpedoes and the many uncertainties involved in the torpedo design process itself. Additionally, the use of normalized and non-dimensional parameters will be examined for potential benefit in the torpedo conceptual design process. By taking these new factors into account in the early phases of torpedo design, a method for a more effective, more robust design of torpedoes can be created.

Unfortunately, due to the lack of engagement models available for torpedo research, the means was not available to fully couple the torpedo tactics with torpedo design. As a result, only the impact of tactics on torpedo design was demonstrated, and a second application,

focusing on the mine counter-measure design problem, was added. The mine counter-measure problem proved to have very tractable tactics, making it easier to demonstrate the linkage between tactics and design optimization for an undersea weapon system.

1.8 Research Questions and Hypothesis

The research questions stand as follows:

1. *When determining total weapon effectiveness, how significant is the tactical environment with which a system is used compared to torpedo design decisions?*

2. *If tactics account for a significant portion of total weapon effectiveness, can conceptual design decisions still be made that have more than marginal improvements on total weapon effectiveness? Can the optimization of tactics and conceptual design be synergistically combined to create an even more effective weapon system? Can this synergy be demonstrated on a mine counter-measure system?*

3. *When dealing with uncertainty, can probability of success be treated as an independent variable in conceptual design? If so, can it be used to select the torpedo design that has the best tradeoff between cost and risk?*

4. *What are the best combinations of metamodeling and uncertainty-analysis measures of merit to use when in the initial stages of robust conceptual torpedo design?*

5. *What normalization schemes for torpedo design parameters can be used to simplify the conceptual design process?*

The hypothesis for the research is as follows:

A new, more effective design process can be created for conceptual torpedo design. This process, by accounting for the effects from both uncertainty and the tactical environment in which the torpedo is employed, will significantly improve on current design processes for torpedoes.

Table 3: Dissertation Outline

Background	Ch. 1	Motivation
	Ch. 3	Uncertainty and Metamodeling
	Ch. 2	Torpedo Design and Tactics, Mine Counter-Measures
Formulation	Ch. 4	Proposed Methods (Traveller Example)
	Ch. 5	Research Tools Development
Implementation and Results	Ch. 6	Torpedo Design Application
	Ch. 7	Tactics Integration (Torpedo & Minehunter Example)
	Ch. 8	Non-Dimensionalization in Torpedo Design
	Ch. 9	Conclusions

1.9 Dissertation Outline

This dissertation can loosely be divided into three sections: background, formulation, and results. These sections are split among 9 Chapters, as shown in Table 3. The background section consists of the first three chapters. Chapter 1 introduces the motivation for this work along with the research objectives, questions, and hypothesis. Chapter 2 provides a background in torpedo design, with a general overview of torpedo systems, submarine tactics, and mine counter-measure systems. Chapter 3 gives a background in probabilistics, response surface methodology, Monte Carlo methods, and multi-objective decision-making. Chapter 4 lays out the formulation of the proposed approach and gives some preliminary results. Chapter 5 then discusses the development of analysis tools required for the research. These tools include the Torpedo, Optimization, Analysis, and Design (TOAD) program for the design of torpedo systems and a torpedo design visualization environment developed in Matlab.

The remaining chapters contain results and example implementations of the work. Chapter 6 shows how the proposed research approach can be used in the design of torpedo systems. Chapter 7 looks at the inclusion of tactics into the design process, both for torpedo systems and mine counter-measures. Chapter 8 examines the creation of non-dimensional parameters for facilitating the sizing and optimization of torpedo systems. Finally, Chapter 9 summarizes the progress to date and suggests future research plans.

CHAPTER II

INTRODUCTION TO UNDERSEA WEAPONS AND TACTICS

2.1 Background in Torpedo Design

Throughout history, the United States Navy has remained at the forefront of torpedo design. The first wartime use of a torpedo occurred in the United States, when the one-man submarine, called the *Turtle*, failed to sink the British ship HMS *Eagle* in 1776 [88]. The United States was also the location of the first successful submarine attack when, in 1864, the Confederate submarine *Hunley* sank the USS *Housatonic* during the U.S. Civil War. In that war, 22 Union ships and 6 Confederate ships were sunk[1] by torpedoes [88]. Though at the beginning of the Second World War US torpedo designs were not the most advanced in the world, the United States still used their submarines and torpedoes effectively, sinking 5,631,117 tons of Japanese vessels, accounting for 55% of the total Japanese vessels sunk during the war. The US submarine force accomplished this feat while employing only 1.6% of the Navy's total personnel [200]. Even though the United States submarine history was impressive throughout World War II, it was still dwarfed by the performance of the German submarine fleet. The German forces sank almost 11 million tons of allied vessels; though at the cost of losing 785 submarines [136]. The German submarines were effective all across the Atlantic, as is evident from Figure 8.

Today, the United States retains the lead in torpedo design, with torpedo systems currently in service that can be launched from submarines, surface ships, helicopters, fixed-wing aircraft, and rockets [2]. Unfortunately, even though the United States maintains the most advanced fleet of nuclear submarines, the front-line torpedo used by those submarines,

[1]The number of Union ships sunk is debated, some authors place the number at 29, but they include very small vessels like ships' launches; likewise some authors put the number of Confederate ships sunk at only one (the ironclad *Albemarle*) with five damaged [168]

Figure 8: Dots Represent Shipping Losses in the Atlantic from Jan. 1942 - May 1943 [103]

the Mark-48 Mod 7 ADCAP, is a highly evolutionary design with origins dating back to 1963 [88]. Current Navy plans predict that this torpedo will be in use through the year 2026 [227], amounting to a total lifespan of over 60 years! New torpedo designs that focus on non-evolutionary designs will be necessary to retain the United States' technical lead throughout the 21^{st} century.

Some photographs of various U.S. torpedo systems have been included. Figure 9 shows the devastating firepower of a Mk-48 heavyweight torpedo. Figure 10 shows a Mk-46 lightweight torpedo being launched off the side of a ship. Figure 11 shows the loading of a Mk-48 heavyweight torpedo onto a submarine. The figure gives a good idea of the size

of these torpedoes compared to humans.

Figure 9: Live-Fire Test of a Mk-48 Heavyweight Torpedo [56]

2.1.1 Common Torpedo Design Requirements

Torpedoes must fit many requirements to be useable by the Navy. They have performance requirements, generally in the area of range, maximum velocity, radiated noise, and sonar performance. Secondly, there are strenuous safety requirements, and, finally, there are physical compatibility requirements. Any new torpedo must retain compatibility with existing torpedo handling and launch systems. This compatibility requirement sets a maximum requirement on torpedo length and weight. In addition, it firmly fixes the diameter of the torpedo. Practically every US torpedo in the inventory is one of two diameters, either

Figure 10: Ship Launch of a Mk-46 Lightweight Torpedo [177]

Figure 11: Loading of Mk-48 Heavyweight Torpedo [68]

21 inches for a 'heavyweight class' or 12.75 inches for a 'lightweight' class torpedo. Heavyweight class torpedoes are used exclusively in nuclear attack and ballistic missile submarines to launch at standoff distances against potential threats, both surface and submerged. The lightweight weapon is used by aircraft and helicopters, who generally 'drop' their weapon

Table 4: Table of Modern Torpedo Characteristics [2][4][5][56][68]

Torpedo	**Mk-48**	**Speafish**	**Tigerfish**	**Tp62**	**Mk-46**	**Mk-50**	**Mk-60**
Fleet	US Navy	Royal Navy	Royal Navy	Swedish Navy	US Navy	US Navy	US Navy
Mission	Submarine Launched	Submarine Launched	Submarine Launched	Submarine Launched	Air & Surface Launched	Air & Surface Launched	Submarine Launched Mine
Diameter (in)	**21**	**21**	**21**	**21**	**12.75**	**12.75**	**21**
Length (in)	240	276	254	236	102.36	114.1	132
Weight (lb_m)	4000	4075	3414	2897	517.65	800.42	2056
Velocity (kts)	55	70	35	50	45	55	---
Range (nmi)	20.5	12.5	7	21.5	6	8	---
Power (hp)	---	1000	---	400	---	201.2	---
Warhead (lb_m)	650	660	750	440	98	100	Launches Mk-46
Propulsion	Piston Engine	Gas Turbine	Electrical	Piston Engine	Piston Engine	SCEPS	---
Fuel	Otto-II	Otto-II + HAP	Chloride Silver-Zinc Oxide Batteries	H_2O_2	Otto-II	SF_6	---

closer to the target, or by surface ship launchers, which use either tube launchers or launch the torpedo via a rocket booster. The lightweight systems have significantly less range than the heavyweights, but are used as close-in weapons by surface ships against enemy submarines, or, for long range encounter, are dropped by anti-submarine warfare aircraft in the immediate vicinity of the enemy. A table showing examples of modern torpedo characteristics is given in Table 4. Note that only two torpedo diameters, 21 inches and 12.75 inches, are listed in the table. This listing reflects the fact that these are the only two operational diameters in use. Figure 12 gives a side-by-side comparison of torpedo sizes.

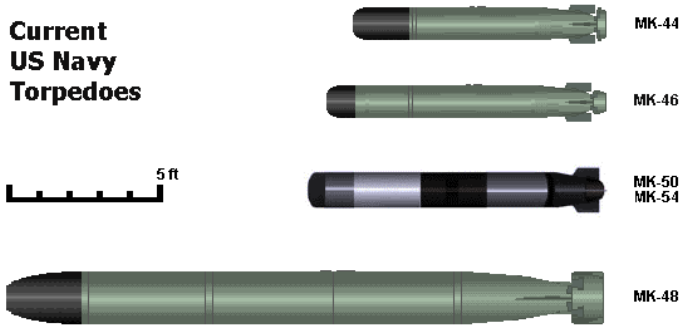

Figure 12: Comparison of Sizes for U.S. Torpedoes [68]

In addition to physical size, most torpedoes have several characteristics in common. Nearly all torpedoes have a propulsion system (undersea mines are an example of a "torpedo" system that does not), which includes an engine or motor, a propeller, and a linkage between the two, often including a gearbox. The motor setup is generally at the back end of the torpedo, providing power both for propulsion and auxiliary systems (called hotel power). In front of the propulsion components is the energy section, containing either fuel for an engine or batteries for an electric motor. In front of this section lies the detonator and the warhead. Finally, the very front of the torpedo houses the sonar and the guidance, navigation, and control electronics, or the 'brains' of the torpedo. These systems are purposely located at the front of the torpedo so that the sonar can point forward and to isolate it as much as possible from the noisy engine machinery. A diagram of a typical torpedo is given in Figure 13.

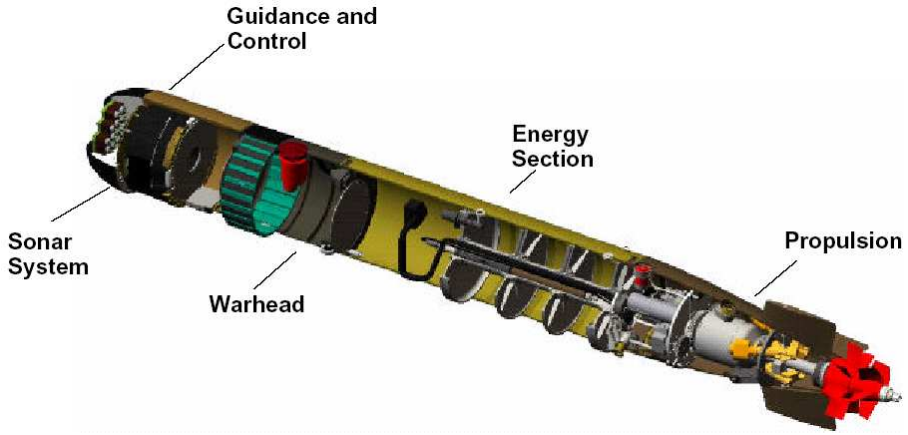

Figure 13: Inner Components of a Torpedo [133]

Figure 14 shows the key sonar parameters in the torpedo system. These parameters include the directivity index, or how strong the sonar is, the beam-resolution, or how small an area can be examined, and the beam-width, which describes how large a search-field is present for the torpedo. An entire sonar system can be approximated by these parameters.

One distinct advantage of torpedo design is that a torpedo system can be easily broken into individual sections based upon their function. In addition, since these functionally divided torpedo components operate sufficiently independently, that they can be individually

Table 5: Sizing Rules for Torpedo Sections

Name	Description / Sizing Rules	Inputs	Outputs	Ref
Outer Shell	Sized based upon outer diameter, with extra width allocated for the torpedo shell structure and noise decoupling layer	Depth Outer diameter Decoupling layer thickness	Inner diameter Shell weight	[27]
Sonar	Sized to fit an array aperture of sufficient size to generate needed beamwidth and directivity index	Directivity index Beamwidth Beam resolution	Hotel power Length Weight	[35][120] [161][162]
Guidance Navigation and Control	Sized to fit all of the electronic boards needed for sonar DSP and vehicle control	Directivity index Board spacing Board thickness	Hotel power Length Weight	[161] [162]
Buoyancy	Mostly empty section that provides buoyancy to the vehicle, may contain inflatable balloons, or telemetry systems for test rounds	Length	Weight	—
Warhead	Sized to fit a warhead of a given size, calculates the explosive effectiveness of either conventional or shaped charges, calculates probability of warhead destroying target	Charge weight Conventional or Shaped	$P_{destroy}$ Equivalent explosive wt. Length Weight	[25] [26][27]
Fuel Section	Determines amount of fuel (and therefore energy) available to the motor	Length Fuel type	Available energy Weight	[90]
Battery Section	Determines how many batteries can fit into system and the amount of energy available	Battery type	Available energy Weight	[63] [90][144]
Motor	Converts battery power to shaft horsepower, sized to meet a horsepower requirement	Shaft-horsepower	η_{motor} Length Weight	[196]
Engine	Burns fuel to create shaft horsepower, may be a piston, turbine, or other power-extraction process	Shaft-horsepower Motor type	η_{motor} Length Weight	[71][90]
Afterbody	Fairs the torpedo diameter near the rear, contains control surfaces, actuators, may contain gear-box	—	Length Weight	[90]
Control Fins	Stabilizes the torpedo and banks the torpedo in a skid-to-turn fashion	# fins Aspect ratio Surface area	Turn rate Weight	—
Propulsor (Pumpjet)	Ducted propulsor that provides thrust	RPM Cavitation depth	η_{prop} Length Weight	[80] [90][158]
Integrated Motor-Propulsor (IMP)	An integrated motor and propulsor	RPM Shaft-horsepower Cavitation depth	η_{motor} η_{prop} Length Weight	[80][90] [158][196]

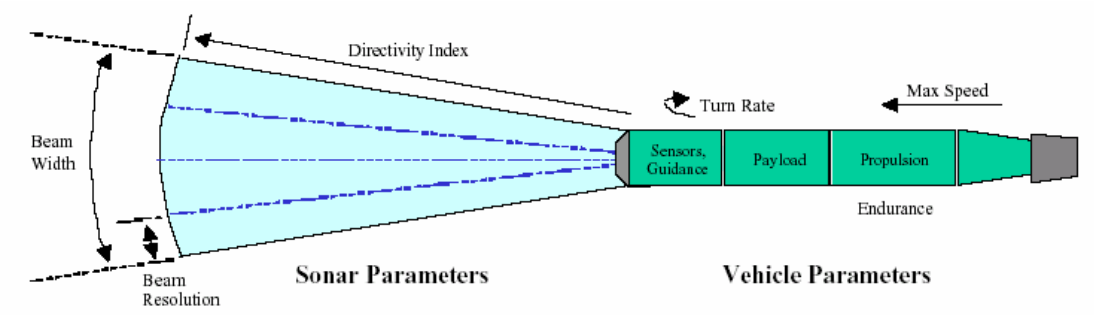

Figure 14: Key Torpedo Parameters [134]

sized [28]. Thus, a torpedo can be generated by sizing each torpedo section independently, then stacking the entire system together. Table 5 describes each individual component (or section) of the torpedo. For each component, the table gives the general sizing philosophy of the section, along with general inputs and outputs.

Compared to other weapon systems, another unusual characteristic of torpedoes is that they are regularly used in test-firings (without warheads) for realistic combat training. The torpedoes are then retrieved from the ocean, refurbished, refueled, and returned to service. Thus, the life-cycle cost of the torpedo is in many ways driven as much by the refurbishment cost as much as the acquisition cost.

2.1.2 Torpedo System Alternatives

Besides simply choosing the diameter, there are other characteristics that dictate torpedo design. The biggest single decision in torpedo design is the selection of the propulsion system. Many propulsion systems are available. Very early torpedoes used either no propulsion (pre-Civil War), stored compressed gas, or flywheels [88]. WWII torpedoes were primarily of two varieties, one using external combustion to create steam for a turbine and the other using electric power [168] [169] [170].

Modern torpedo systems have a wide range of propulsion system options available. Traditional systems burn a liquid monopropellant called Otto fuel, but other other modern systems also burn Hydroxyl Ammonium Perchlorate (HAP) fuel in addition to Otto [90] [186]. Another alternative is the advanced stored-chemical propulsion systems (SCEPS)

used in the Mk-50. This propulsion system creates energy through the chemical reaction of sulfur hexa-flouride (SF_6) and water (H_2O) [90]. The layout of the SCEPS system for a Mk-50 Advanced Lightweight Torpedo is shown in Figure 16. In addition to fuel type, these fuel burning systems may use either a reciprocating engine or a turbine engine for power extraction.

Super-cavitating torpedoes represent a radical departure from traditional torpedo design. Super-cavitating torpedoes are high-speed torpedoes, which can travel hundreds of miles per hour. They work by generating a travelling through a "bubble" of gaseous water vapor, thus reducing the overall drag [13]. A schematic of a super-cavitating system is shown in Figure 15. These new super-cavitating systems represent a dramatic need for advanced design techniques for the torpedo community, as there is no historical precedent and multiple revolutionary technologies are required to create an operational system.

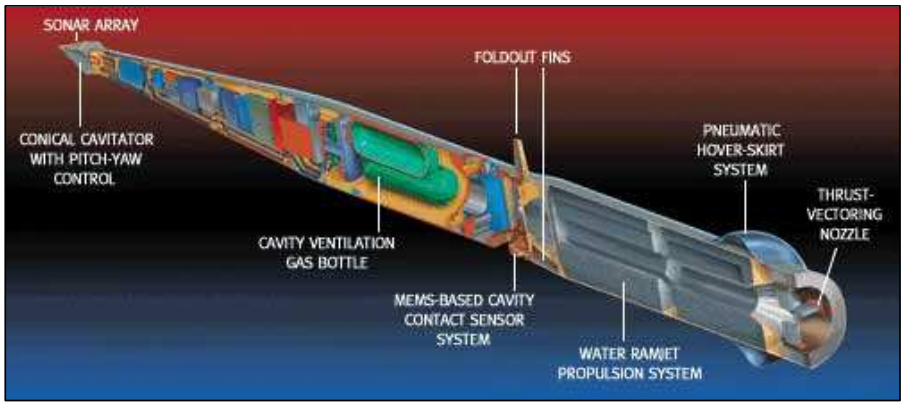

Figure 15: Schematic of a Super-Cavitating Torpedo System [13]

A less dramatic, though equally revolutionary change in the torpedo community has been a move towards developing all electric torpedo systems. In these cases, no fuel is present in the torpedo, instead, large banks of batteries or fuel cells are used to power an electric motor, either linked via a crankshaft to a propulsor or directly sharing components with the propeller, called an integrated motor propulsor system (IMP) [166]. Electric systems have advantages over thermo-chemical systems in that they are safer (no combustible fuels), tend to be quieter, and are faster and cheaper to refurbish after torpedo trial runs. In particular,

the IMP systems enjoy these advantages and have the potential to further reduce both weight and noise by decreasing the amount of motor machinery while still taking advantage of performance-increasing pumpjet effects [233]. A diagram of the rear of an IMP system is shown in Figure 17. Even with these advantages of all-electric systems, traditional fuel-based torpedo systems are still sometimes preferred because they currently supply the most power and endurance. The choice of propulsion systems (and hence fuel type) is a big driver on torpedo design. The various fuel systems for modern torpedoes are shown in Table 4.

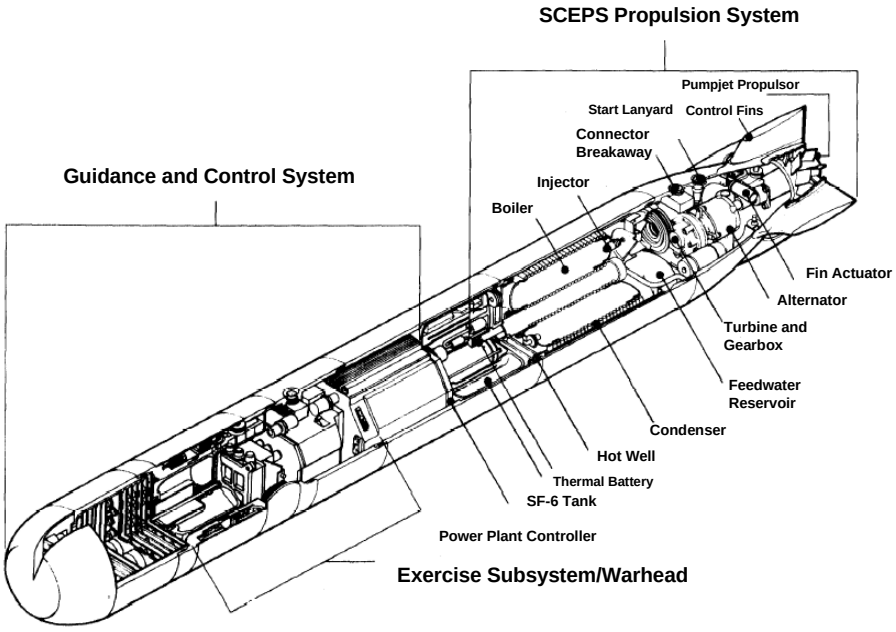

Figure 16: Schematic of a SCEPS Propulsion System [226]

2.2 Tactics

2.2.1 Basic Submarine Tactics

When dealing with submarine engagements, the potential tactical situations and possible responses are nearly limitless. However, the myriad of tactical decisions and alternatives can be broken down to a single goal: to detect and either avoid or attack a threat without the threat detecting you. The submarine is the original stealth vehicle, while submerged it is completely invisible to any modern day radar or optical technology. The only effective way

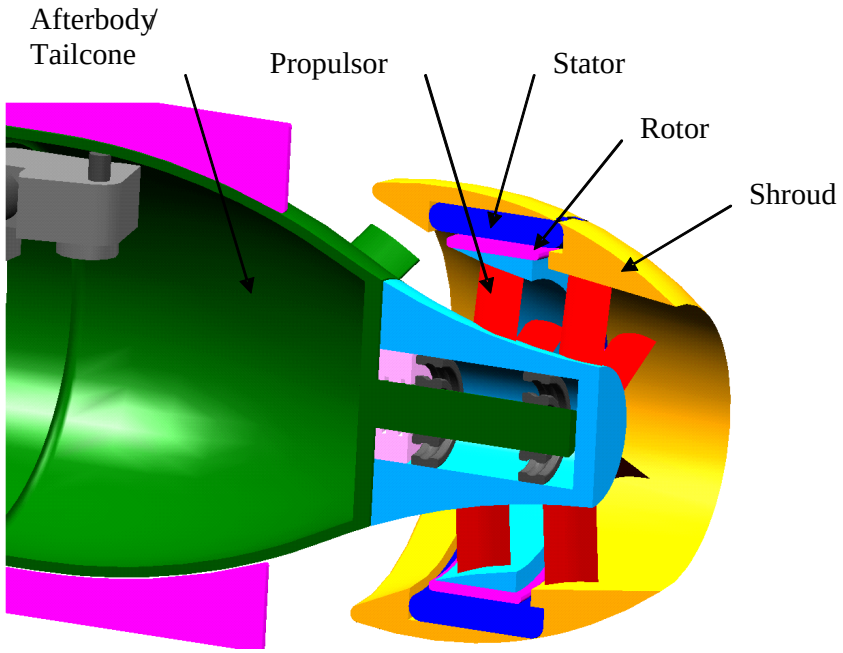

Figure 17: Integrated Motor-Propulsor System (IMP) [196]

to detect submerged submarines is through acoustic energy[2], either actively transmitted into the water or passively 'listening' for enemy submarines. Thus, the goal of modern submarine warfare is to remain as quiet as possible and hence, undetectable [41].

Undersea warfare is characterized by a continuous lack of knowledge concerning the exact location of enemy vessels. Thus, a large portion of undersea warfare is concerned with the means and mechanisms of acquiring information about the position of the target. To a large degree, undersea warfare deals almost exclusively with triangulation tactics, sonar capabilities, and acoustics. In fact, submarine maneuvering is largely driven by this need to take acoustic readings from several positions in order to better localize the target.

However, regardless of the tactics taking place, in a submarine-on-submarine encounter, two parameters can be used to define the system-of-systems effectiveness. The first parameter, P_{kill}, is the probability that the friendly submarine successfully launches a torpedo against the threat submarine, the torpedo successfully hits the submarine, and the warhead

[2]Aircraft may also detect submerged submarines through the use of Magnetic Anomaly Sensors (MAD). However, these sensors only work at very close ranges and cannot be used by undersea vehicles

causes enough damage to defeat the enemy submarine. The P_{kill} parameter, often represented by $\boldsymbol{P_k}$, is a number between zero and one, representing this probability of destroying the threat submarine. A P_k of one is desired.

The second key parameter, $P_{counterkill}$, is essentially the reverse of P_{kill}. $P_{counterkill}$ refers to the ability of the target, or threat submarine, to detect the friendly submarine, launch a torpedo against it, and destroy it. $P_{counterkill}$, or simply $\boldsymbol{P_{ck}}$, also varies between zero and one, with zero representing the optimum, or greatest survivability.

For this analysis work, instead of working with P_{kill}, a separate parameter will be used, P_{hit}. This parameter indicates the probability of successfully hitting the enemy submarine with a torpedo (P_{hit}). The new term is different from the P_{kill} term because it excludes the probability that a torpedo hit will succeed in destroying a submarine. Such lethality analysis is generally very rigorous, requiring large, time-consuming, classified models, and will not be included in this work.

- P_{hit} ($\boldsymbol{P_h}$): The fraction of starting geometries from which the threat submarine is hit. This criterion is an indicator of how successful the friendly submarine is at striking the target. A P_h of 1.0 represents a 100% mission success rate. P_{hit} is directly analogous to P_{kill}.

2.2.2 Tactics Analysis Programs

The defense department has modeling programs of all types and sizes. These computer programs run the gamut from analyzing a single vehicle component, such as a sizing tool for electric motors [196], to a model that determines the final outcome of military campaigns, such as the Integrated Theater Engagement Model (ITEM) [204]. Soban succinctly illustrates the complete scope of military modeling levels and their inherent tradeoffs in Figure 18. Soban discusses the three primary levels of military models: engineering models that examine a single platform or sub-system, mission models that examine how the platforms perform in an encounter, and campaign models that address the overall performance of all the assets in a theater.

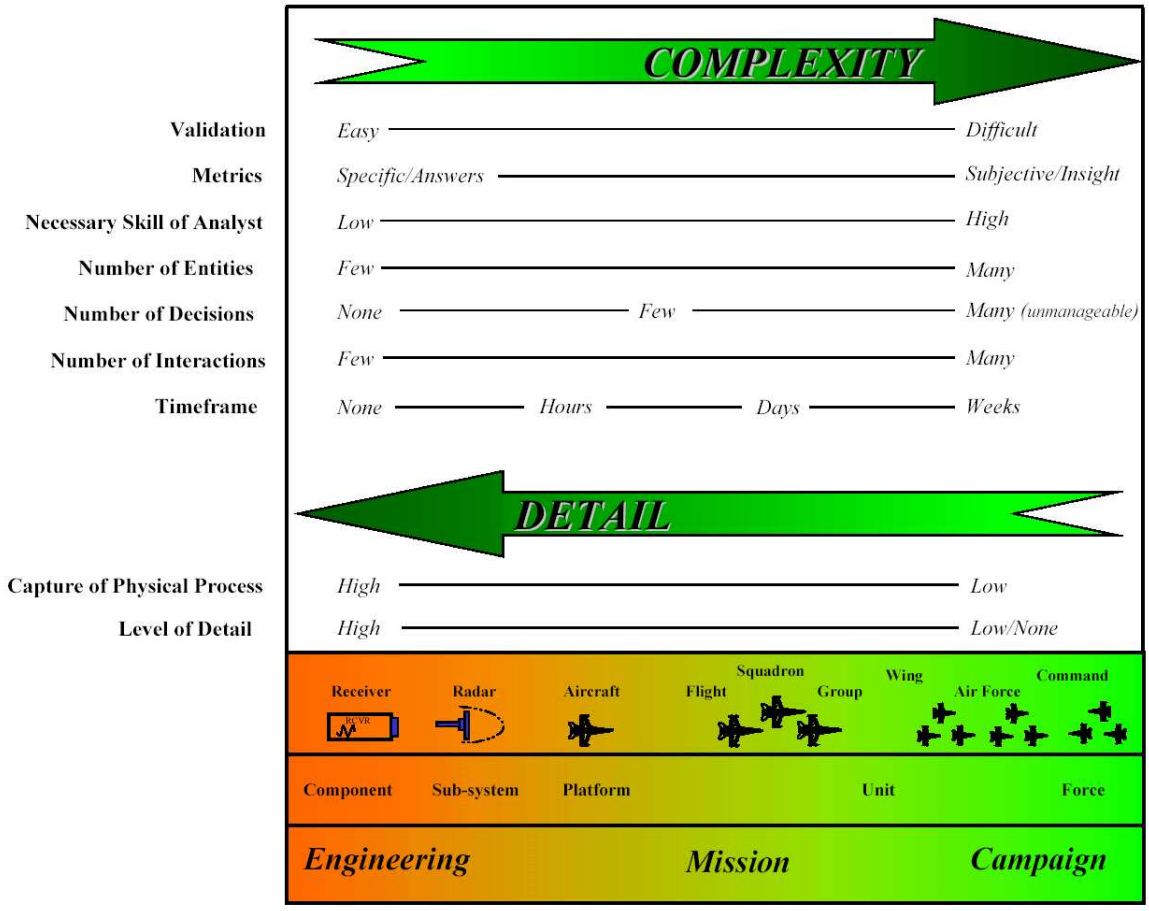

Figure 18: Various Levels of Military Modeling [213]

The defense department has computer tools that provide analysis at each of these levels. However, as discussed by Soban [213], Hines [105], and Kurtz [132], there is insufficient linking of these computer programs between model levels. Because these linkages are lacking, it is difficult to propagate changes at the platform or sub-system level up through the mission level to the campaign levels. Therefore, there is much work to be done on appropriate mechanisms to link these computer models together, on determining the best way to propagate information between them, and to examine how these models can work together to provide better solutions.

There are many mission-level torpedo and mine warfare analysis tools that have been developed by the defense department. These programs include the Multi-Warfare Systems Evaluator (MWSE) [30], the Autonomous Littoral Warfare Systems Evaluator (ALSWE)

[30] [62], the Technology Requirements Model at the Applied Research Laboratory at Penn State [30] [242], and the Object-oriented, Rule-Based Interactive System (ORBIS) developed at the Applied Physics Lab at Johns Hopkins University [104]. All of these models have a high degree of complexity and have been in development for years. In addition, they have several characteristics in common which are required for an undersea engagement model:

- They all require parametric vehicle characteristics
- They all have some level of acoustics modeling
- They all have some type of parameterized tactics
- They all use Monte Carlo simulations to account for the inherent randomness of battlefield encounters

Unfortunately, though these models exist, they were not available to the researchers at the Georgia Institute of Technology. As a result, simplified tactics models had to be developed to illustrate the linkages between tactics and design. However, these models were developed with the same key characteristics as the military counter-parts.

2.3 Mine Counter-Measures Strategy and Design

Mine counter-measures are divided into two types of techniques, minehunting and minesweeping. Minehunting involves "employment of sensor and neutralization systems, whether air, surface, or subsurface, to locate and dispose of individual mines [7]". Minehunting is generally time-intensive and requires that each mine be individually detected, identified, and neutralized. Minesweeping, on the other hand, deals with "the technique of clearing mines using either mechanical, explosive, or influence sweep equipment [7]". Minesweeping is nothing more than attempting to blindly destroy all of the mines in the region. This destruction can be conducted by deploying large assault breaching systems (as in Figure 19), dropping bombs from aircraft, or using a magnetic pulse or fake acoustic signature to 'trick' the mines into prematurely detonating. Minehunting is generally preferred to minesweeping; as stated by Rear Admiral Jose Betancourt, "hunt when you can, sweep when you must [22]."

The mine counter-measure analysis in this work will focus exclusively upon minehunting problems. These minehunting systems involved towed sensors, unmanned undersea vehicles (Figure 20), and aircraft based sensors and weapons (Figure 21). In minehunting, the search platform, or combination of cooperative platforms, must be able to detect a target, identify the target as a mine, and neutralize the threat. However, the research work presented here focuses on the use of a single unmanned undersea vehicle. The UUV design problem was chosen because it is very similar to a torpedo design problem, allowing similar approaches to be used for both systems.

Figure 19: Assault Breaching Systems for Mine Sweeping [22]

Figure 20: Mine-Hunting UUV [176]

Figure 21: Mine-Hunting Helicopter System [232]

The goal of mine counter-measures is to clear a path so that ships may travel a 'safe' corridor through an enemy mine-field. This path is often called a Q-route, is generally 1,000 yards wide, and is usually intentionally placed where minehunting conditions are optimal [228]. Figure 22 shows an example Q-route. The necessary width of this corridor is a function of the number of ships that much pass through, the size of these ships, and their navigational error. Building an inter-connecting sequence of these Q-routes will allow shipping to transit from port to port and port to deep-water. Mine counter-measures strategies focus on the creation of this corridor, even to the extent that a Defense Department operations manual says that if MCM assets are not available, then a corridor should be created by driving all friendly vessels in a straight line through a minefield [228]! This approach, which the military defines as "channelization", is a potentially expensive method for clearing mines, but illustrative of the sometimes desperate nature of the needs involved. Later in

a campaign, mine counter-measure forces may focus on clearing the entire minefield, both for humanitarian purposes and so that the entire region may be opened to unrestricted shipping.

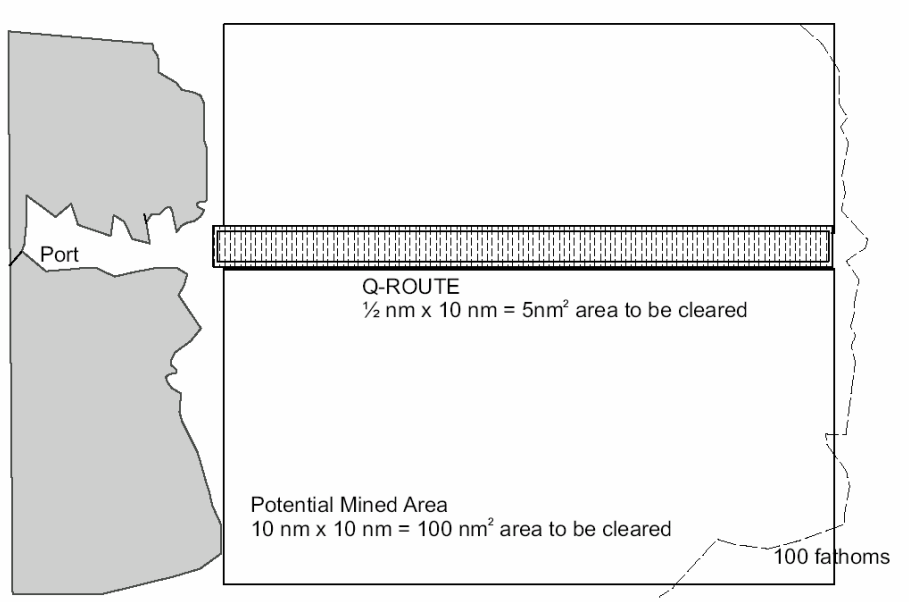

Figure 22: Diagram of Q-Route for Safe Passage Through Minefields [228]

2.3.1 Minehunting Process

Prosecuting a single mine requires that several distinct tasks be completed. Each of these tasks has a probability of occurring, a probability of a false alarm, and a time associated with it. The process for minehunting is laid down in Figure 23, with the individual steps defined in Table 6. As the mine hunter sweeps the mine field, it is attempting to 'detect' a target amidst the clutter. Detection is defined as identifying anything that is not background, for example a rock, etc. There is a single probability, $\boldsymbol{P_d}$ (probability of detection), that an object is detected from the background. Once an object has been detected, the mine hunter then checks to see if the object is similar to a mine: is the object a mine-like contact or not? A mine-like contact is an object that is not a natural feature of the background and is potentially a mine, for instance, a discarded refrigerator, piece of junk, or decoy would be considered a mine-like contact. This attempt to determine if the contact is mine-like is called

a classification attempt. The classification attempt has associated with it a probability of identifying a mine as mine-like (P_{cmm}), probability of falsely identifying a non-mine-like contact as mine-like (P_{cnm}), and a time associated with the physical classification process (T_c) [193] [212]. An object that is not classified as mine-like is removed as a false target.

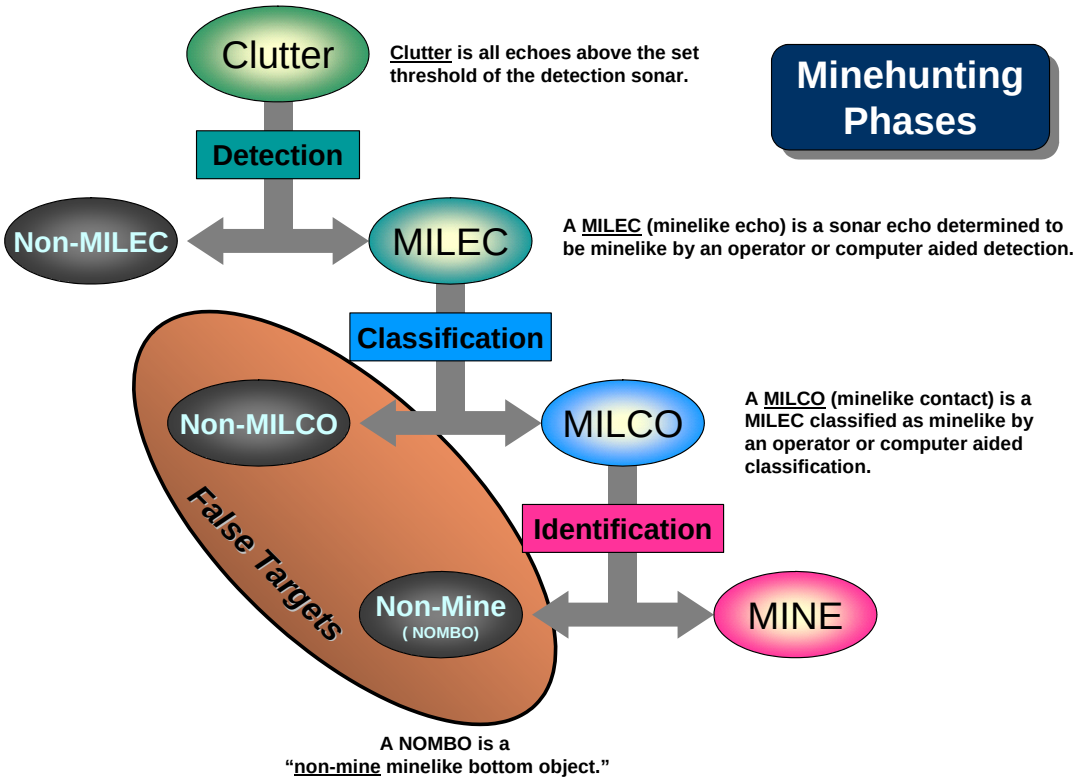

Figure 23: Minehunting Process [175]

Once the contact has been classified as being a mine-like object, the next step is to fully identify the mine. Identifying the mine entails verifying that the object is in fact a mine, and, in addition, attempting to identify what type of mine is present. This identification process generally requires a second, higher fidelity sensor to accomplish, which explains why it is divided into a separate task. This sensor can either be on the same platform that detected the mine-like contact, or could be on a separate platform that is brought to bear on the contact. For instance, a UUV may be used to locate and classify the mine, then a helicopter with an advanced LIDAR unit may be tasked with the job of classifying the mine

and neutralizing it with a super-cavitating projectile (see Figure 21). The identification step has the same parameters as the classification step, with a probability of correctly identifying a mine as a mine (P_{imm}), a probability of incorrectly identifying a non-mine as a mine (P_{inm}), and a time required to identify the mine (T_i) [193] [212].

The final step in the minehunting process is the neutralization of the mine. Neutralization involves detonating the mine, rupturing the mine, or damaging the internal components of the mine [193]. Again, mine neutralization has two parameters associated with it, the probability of neutralizing the mine (P_n) and the time required to neutralize the mine (T_n) [193] [212]. These probabilistic and temporal parameters that are used for detection, classification, identification, and neutralization of mines can be used to completely characterize a minehunting system as well as build computer models to estimate minehunting effectiveness. Note that each of these parameters is, to some extent, a function of not only the minehunter, but also of the background conditions and the type of mine being prosecuted (some mines are more difficult to detect, take longer, etc.) [193]. As a result uncertainty is inherently involved with any calculations when dealing with minehunting problems. A summary of these minehunting parameters is given in Table 6.

Table 6: Parameters Defining Minehunting Process

Abbr.	**Subset**	**Definition**
P_d		Probability of detecting an object
P_c		Probability of classifying an object
	P_{cmm}	Probability of classifying a mine as mine-like
	P_{cnm}	Probability of classifying a non-mine as mine-like
T_c		Time to classify object
P_i		Probability of identifying a mine-like object
	P_{imm}	Probability of correctly identifying a mine
	P_{inm}	Probability of incorrectly identifying a non-mine
T_i		Time to identify object
P_n		Probability of neutralizing object
T_n		Time to neutralize object

2.3.2 Minehunting Sensors

Probability of detection (P_d) is a function of the distance between the target and the sensor. The correlation between the probability of detection and distance to the target is generally described using a lateral range curve. The lateral range curve is defined as "the probability that the target will be detected if its track relative to the searcher is a straight line infinitely long in both directions with [a] closest point of approach [236]." Lateral range to the target is defined as the closest point of approach to the target and is easiest to visualize in the case of a straight sensor track, as illustrated in Part A of Figure 24. The lateral range curve then defines the probability of detecting the target as the seeker passes by at the distance given. The curve represents the cumulative chance of finding the target as the searcher closes and then withdraws from the target. An example lateral range curve is shown in Part B of Figure 24. These lateral range curves are not necessarily fixed for a given sensor; they are also a function of the object being detected and operating conditions. Figure 25 illustrates how the lateral range curve for a single sensor can varying depending upon the search conditions.

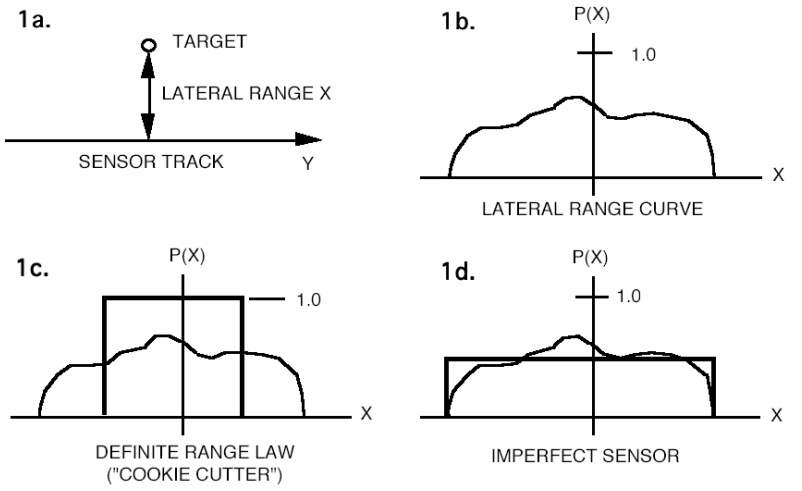

Figure 24: Lateral Range Curves for Sensors [84]

Two simplifications of lateral range curves are often made in mine counter-measure analysis. One simplification is that the sensor is 'perfect', meaning it will always detect an

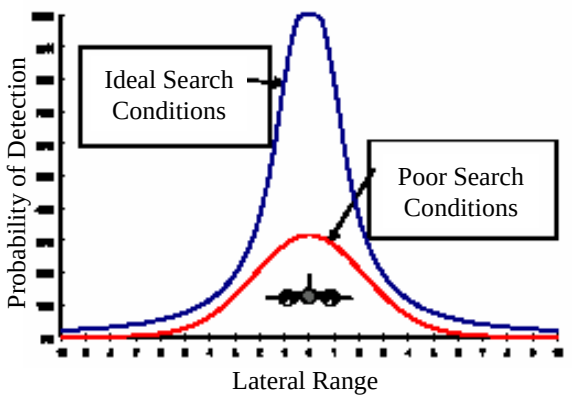

Figure 25: Changing Lateral Range Curve for a U-Boat Sensor [37]

object that is inside of its sensor radius. This type of sensor can be quantized via a single value (sensor radius), with a lateral range curve looking like the example in Part C of Figure 24. Anything inside this sensor radius will automatically be detected by the sensor.

Another lateral range curve simplication is to assume an 'imperfect' sensor. This sensor assumes that there is a fixed, yet finite probability of detecting an object that comes inside of the seeker radius. With this type of sensor model there is no advantage to coming closer to the object. The sensor is, however, not considered to be perfect because there is only a finite chance of target detection. This type of sensor is characterized by two parameters, a sensor radius and a detection probability. An example lateral range chart for this sensor is shown in Part D of Figure 24. This imperfect model is more accurate that the 'perfect' or 'cookie-cutter' sensor model, but significantly less complex than having a full lateral range curve. For the mine counter-measure analysis in this work, an 'imperfect' sensor model is assumed. For a real-world sensor, an 'equivalent sensor radius' for constructing an imperfect sensor model can be estimated by calculating the sensor sweep radius at which the number of missed detections inside of the radius equals the number of valid detections outside of the sweep radius [44]. An example of this definition is shown in Figure 26.

2.3.3 Minehunting Search Strategies

The field of search theory first developed in World War II when it was desired to make optimal use of the large amounts of resources being dedicated to search for enemy submarines.

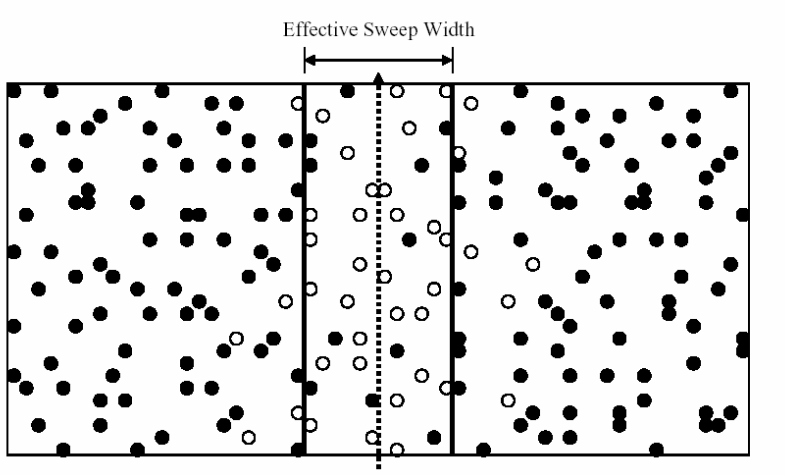

Figure 26: Definition of Sweep Radius for an Imperfect Sensor – When the Number of Missed Detections Inside the Radius Equals the Number of Detections Outside the Sweep Radius [44]

The two definitive sources on search strategies are considered to be Koopman [130] and Stone [215] [216]. However, although extensive theoretical work is being undertaken in the field of search theory, the subject can be simplified into a few basic techniques.

There are two styles of minehunting search strategies available. The first is an unstructured, or random search pattern. In this situation, a "search perimeter" is defined and the minehunter travels in a randomly selected straight line until it either reaches the search perimeter, detects an object, or travels a set distance. At this point, the minehunter then randomly selects a new path and begins travelling anew [98] [109]. This type of search strategy is useful because it requires very little programming. In addition, it is beneficial when there are multiple searchers, because coordination between searchers is unnecessary, and in these situations the system will be in inherently robust to the loss of a single searcher. The disadvantage of the random search is that the overall search rate is lower, the middle of the search zone is often 'over-searched', and it is sometimes difficult for the vehicle to determine when the search perimeter has been reached. These random searches can be parameterized by designating the search step length and then selecting whether a new direction will be taken each time an object is discovered or only when a fixed distance is travelled.

A second type of search pattern is a patterned, or "complete" search [109]. In this type

of search, a pre-programmed route is followed by the searching vehicle. This path is often a raster-scan, or parallel-path search, such as shown in Figure 27. This type of a raster-scan search pattern is convenient because it is easy to program and can easily be parameterized based on the distance between individual sweeps. However, other patterns exist, such as a spiral pattern (Figure 28). The advantage of a structured search pattern is that the search area is never covered twice and the highest overall search rate can be achieved [236]. Another advantage is that an accurate estimate of search-rate can be estimated using a structured search pattern.

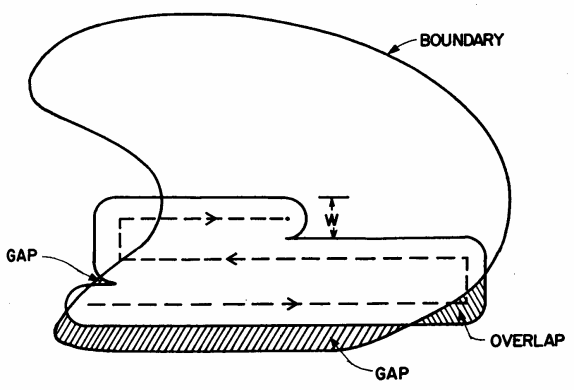

Figure 27: Raster Search Pattern [236]

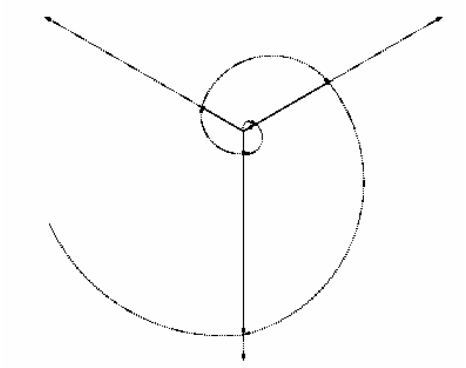

Figure 28: Spiral Search Pattern [36]

Unfortunately, there are many problems associated with a structured pattern. For one, it requires the searching vehicle to be more complex: the vehicle must always know where

it is and where it is going, and, in the case of a coordinated search between multiple vehicles, all the vehicles must communicate with each other. In addition, navigational error can play a significant role in the effectiveness of a structured search pattern. In fact, many structured search patterns are designed with overlap in the search tracks in order to account for navigational errors [102].

Another decision when selecting the search pattern is whether to use a "Single Classification Tactic (SCT)" or a "Multiple Classification Tactic (MCT)" [193]. A single classification tactic occurs when a single classification attempt is made for each target. Thus, if an object is detected and then classified as a non-mine, the object will be 'stored' in memory as a non-mine and will not be re-examined in future encounters. The advantage of this technique is that the searcher does not waste time re-examining objects that have already been classified as non-mines. The disadvantage of this technique occurs when a mine is incorrectly classified as a non-mine, because the system will never re-examine its work.

A multiple classification tactic implies the opposite. Each time an object is detected, the system will attempt to re-classify it as a mine or a non-mine. The advantage of this system is that it is simpler (the searcher does not have to remember previously classified targets) and it is more robust, because if the searcher runs into a mine that was incorrectly classified as a non-mine, it will attempt to re-classify the mine, allowing for the opportunity to correctly classify the mine. The disadvantage of this technique is that it is slower, as a significant amount of time can be spent continually classifying non-mines.

Monte Carlo analysis is the most common analysis used for minehunting problems. This style of analysis is needed because of the random number and placement of mines, the randomness of the search pattern and navigational error, and the inherent uncertainty associated with detection probabilities. Most theoretical minehunting research today is conducted via the use of these Monte Carlo techniques as the primary form of analysis. Current research into mine counter-measure systems focuses on elements such as how to optimize the search pattern [109], how to link multiple searchers together [102], and how to develop better UUV designs [238] or better sensors [141] [194]. These research thrusts are summarized in an article discussing the Navy's vision for UUV development [73]. Unfortunately,

even though much research is being done and great strides have been made developing these elements of the mine counter-measure system, there has yet to be much research coupling the design elements with the search optimization process.

2.3.4 Measures of Effectiveness

The two key measures of effectiveness for mine counter-measure systems are time and risk [193]. The goal is to minimize the amount of time that it takes to neutralize an enemy minefield. Minimization of this time allows task forces to conduct operations in the mined area more quickly, as well as freeing mine counter-measure assets for additional missions. This measure of effectiveness is generally quoted as the amount of time it takes to reach a specified level of neutralization of the minefield. The other key measure of effectiveness is the risk to ships that will be traversing the channel. The overall goal of mine counter-measures is to reduce the likelihood of ships suffering damage from mines. This goal is generally represented as the percent clearance, or percent neutralization, of the minefield. However, since the number of mines in an area is never exactly known (barring a situation in which perfect intelligence exists), the exact value of percent clearance will never be known in an operational setting, it therefore must be represented as a probabilistic value.

CHAPTER III

LITERATURE REVIEW OF UNCERTAINTY AND METAMODELING

3.1 Definition of Uncertainty

The seemingly simple act of defining uncertainty can become quite daunting. There are many definitions of uncertainty in the literature, with many authors attempting to bring their personal or disciplinary perspective into the picture. Some of the over-arching definitions include: Hazelrigg, "Any time that we conduct an experiment for which we cannot predict the outcome, that is, when the sample space contains more than one element with nonzero probability, we say that there is uncertainty [101]", Bandte, "Uncertainty ... is defined as the error between a mathematical model and reality, arising mainly as a result of a lack of knowledge available for constructing the model [149]", and Haldar "The occurrence of multiple outcomes without any pattern is described by terms such as uncertainty [99]". In many cases, the simple dictionary definition of uncertainty is adequate, "the quality or state of being ... indefinite or indeterminate [165]".

It is common in the literature not to attempt a single, over-arching definition of uncertainty, but instead to break uncertainty down into several sources, defining each source individually. These definitions have the benefit of adding more specificity to the understanding of uncertainty. Some of these definitions are given in Table 7.

Table 7: Uncertainty Definitions [45][59][97][181][182][201]

Author	Name	Definition
Du	Input Parameter Uncertainty	Variability of input values
	Model Parameter Uncertainty	Uncertainty due to limited information in estimating characteristics of model parameters
	Parameter Uncertainty	Input parameter uncertainty + model parameter uncertainty
	Model Structure Uncertainty	Uncertainty in the model structure itself, including validity of built-in assumptions in the model
Gu	Approximation Error	Error in how to model physics
	Algorithm Error	Error in use or implementation of model
	Bias Error	Approximation error + algorithm error
	Precision Error	Manufacturing error in design variables
Crespo	Unstructured Uncertainty	Inability to precisely specify the model
	Structured Uncertainty	Inability to specify the value of the parameters for a model
Robinson	Uncertainty from External Parameters	External system parameters with which the user doesn't have sufficient info
	Uncertainty from Internal Parameters	Internal to the system parameters which may vary
	Uncertainty from System Model	Difference between the modeling technique and reality
	Observational Uncertainty	Measurement error
Oberkampf	Aleatory Uncertainty	Inherent variation associated with the physical system or the environment under consideration
	Epistemic Uncertainty	Lack of knowledge or information in any phase or activity of the modeling process fundamentally caused by incomplete information or incomplete knowledge of some characteristic of the system or its environment
	Error	Recognizable deficiency in any phase or activity of modeling and simulation that is not due to lack of knowledge

Of these definitions, Oberkampf gives the most complete for the purposes of the work in this thesis. Oberkampf divides uncertainty into three categories. The first is aleatory uncertainty, which he also calls variability. It is defined as "inherent variation associated with the physical system or the environment under consideration [182]." It represents sources such as manufacturing error and typically has a known range and can be defined using a probability distribution.

The second type of uncertainty is epistemic uncertainty, resulting from "lack of knowledge or information in any phase or activity of the modeling process [182]." This uncertainty is a result of incomplete information or knowledge about the system or its environment. It can occur when the actual physics of a behavior is unknown and there is insufficient experimental evidence to model it, or when the physical environment is unknown (such as landing the first spacecraft on Mars). Oberkampf suggests that it is difficult to adequately capture epistemic uncertainty through probability distributions, because the exact distributions will rarely be known. He suggests the use of either "subjective probability distributions", which are probability distributions that, to some extent, are based on expert experience, or more advanced techniques, such as interval analysis, fuzzy logic, and possibility theory.

The third type of uncertainty as stated by Oberkampf is called error, which is a "recognizable deficiency in any phase or activity of modeling and simulation that is not due to lack of knowledge [181]." Oberkampf subcategorizes error into two types, acknowledged and unacknowledged. Acknowledged errors results from creating a math model that includes simplifications or approximations or discretization of problems. The magnitude of these errors is generally known by the user, thus they can be reasonably estimated. Unacknowledged errors are blunders or bugs introduced into the problem. Unacknowledged errors are practically impossible to estimate, and should be removed through redundant procedures and good programming protocols. A summary of Oberkampf's definitions is given in Table 8.

Note also that the nature of uncertainty will change with time for a project. As progression is made through the various engineering phases, conceptual, preliminary, and detailed, new data and new test techniques are used, thus reducing and reshaping the uncertainty

Table 8: Oberkampf's Uncertainty Definitions [181][182]

Error	Definition	Example	Treatment
Aleatory Uncertainty	Inherent variation associated with the physical system or the environment under consideration	Manufacturing Flaws	Probability Distributions
Epistemic Uncertainty	Lack of knowledge or information in any phase or activity of the modeling process fundamentally caused by incomplete information or incomplete knowledge of the system or its environment	Unknown Physics, Unknown Environment	Subjective Probability Distributions, Other Methods
Acknowledged Error	Recognizable deficiency in any phase or activity of modeling and simulation that is not due to lack of knowledge	Simplification of Physics, Discretization	Probability Distributions
Unacknowledged Error	Mistakes or blunders	Bugs	Eliminate as Much as Possible

about the system. An example by Mavris, in Figure 29, shows how uncertainty varies throughout the life of an aircraft project. When including uncertainty in an analysis, it is important to use an uncertainty model that is applicable to both the engineering system and the current phase of the engineering project.

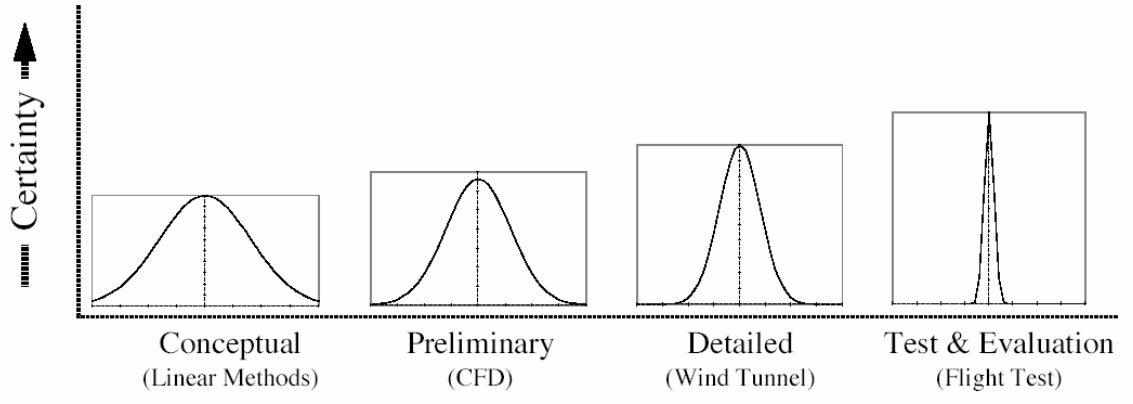

Figure 29: Fidelity Evolution for Aircraft Drag Prediction [153]

3.2 Probabilistics Background

The most common mathematical techniques used to handle uncertainty comes from the field of probability. One of the cornerstones of probabilistics is the use of continuous random variables. These variables, as the name implies, vary continuously within a range of values. The likelihood of the variable being a particular value is characterized through the probability density function, $f(x)$. The probability that a number lies between a and b can

be found by integrating the probability density function (abbreviated PDF), as in Equation 1.

$$P(a \leq X \leq b) = \int_a^b f(x)dx \tag{1}$$

An example probability density function is in Figure 30. Note that the area under the curve represents the probability of the number occurring. The area of the shaded region in Figure 30 is the probability of a single occurrence of a number between a and b. Since the total probability of a number existing is always 1, the total area of a probability density function must always equal 1.

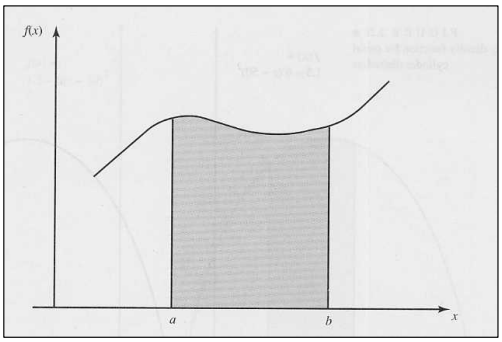

Figure 30: Probability Density Function [100]

The cumulative distribution function (CDF) shows the probability that a random number is less than or equal to a specified value. It is found by integrating the corresponding probability density function, as in Equation 2.

$$F(x) = P(X \leq x) = \int_{-\infty}^{x} f(y)dy \tag{2}$$

The cumulative distribution function is similar to the probability density function as it completely defines a probability distribution, the results are simply shown in a different format. A probability density function can always be obtained from a cumulative distribution function, and vice-versa.

Several probability density functions have been defined by statisticians; the most important of which is undoubtedly the Gaussian, or normal distribution. It is defined as Equation

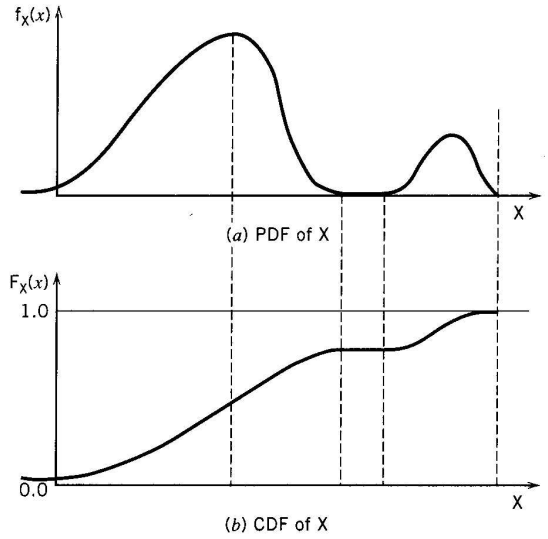

Figure 31: Example Probability Density Function and Corresponding Cumulative Distribution Function [99]

3 and shown in Figure 32.

$$f(x) = \frac{1}{\sigma\sqrt{2\pi}}\, e^{-\frac{(x-\mu)^2}{2\sigma^2}} \tag{3}$$

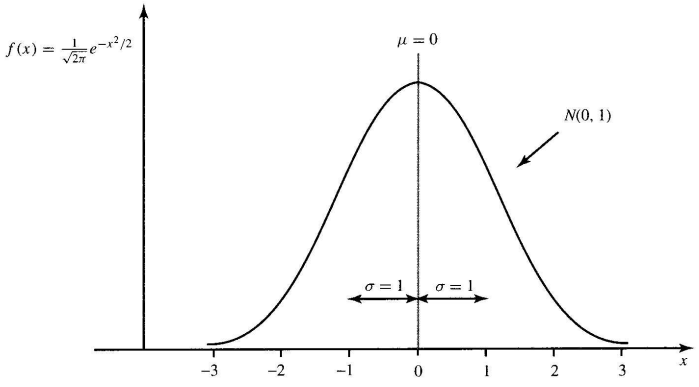

Figure 32: Normal Probability Distribution[100]

Two parameters are used to control the shape of the normal distribution, μ, which is the mean of the distribution, and σ, which is defined as the standard deviation of the

distribution. The calculation of the mean of a sampled set of data is given in Equation 4, where n is the total number of values present and y_i is a single data point. The standard deviation, also defined as the square root of the variance, of a sampled set of data can always be estimated through the formula in Equation 5. Thus, if a set of data is available, and the user either knows that the set fits a normal distribution or that it can be approximated as a normal distribution, Equation 4 and Equation 5 can be used to calculate the parameters of the distribution.

$$\mu = \bar{y} = \frac{\sum_{i=1}^{n} y_i}{n} \tag{4}$$

$$\sigma = \sqrt{\frac{\sum_{i=1}^{n} (y_i - \bar{y})^2}{n-1}} \tag{5}$$

The reason for the importance of the normal distribution is the central limit theorem, "which states that the sum of many small random effects is normally distributed [218]." Thus, when a large enough number of quasi-independent random distributions (of any form) are added together, the resulting distribution will tend towards a normal distribution. Because of the behavior predicted by the central limit theorem, there is a tendency to use normal distributions even though the exact distribution of a parameter may not be known, on the assumption that, if a summation of a large number of smaller random events is driving the larger random event, then the uncertain parameter will tend towards a normal distribution. Other probability distributions are also defined and can be used in probabilistic analysis. They are particularly useful when sufficient data about an uncertain parameter is known so that an appropriately fitting distribution can be used. These other probability distributions include the uniform distribution, log-normal, triangular, and Weibull, etc. [100].

3.3 Methods to Characterize Uncertainty

Historically, probability distributions have been used to characterize uncertainty. But, as pointed out by Oberkampf, for some types of uncertainty simple probability distributions are not adequate to capture the uncertainty. As Oberkampf states in one paper, if there is not

sufficient data to reliably estimate the form and parameters of the probability distribution, simply choosing a probability distribution function and ranges associated with the function may be wildly inadequate [182]. This behavior is particularly true when dealing with epistemic uncertainty (uncertainty due to lack of knowledge). Fortunately, there have been many developments in alternative methods by which uncertainty can be handled. These methods, which are not based upon probability, are often called 'possibilistic', and were designed for situations in which statistical data about parameters is not available [246].

One such method is interval analysis. For interval analysis, potential ranges are defined for the unknown parameters. No assumptions are made about the distribution of the parameter within the chosen range. Then, when the system is being analyzed, interval arithmetic is used to perform mathematical operations with the interval numbers. In its most basic form, a combinatorial approach is utilized which analyzes the endpoints of the intervals. However, by employing such a method, the results will show the worst case, or overly conservative, results. In many ways, interval analysis is used to determine the worst-case propagation of uncertainty [246].

Fuzzy set analysis has been examined as early as 1965 [245]. Fuzzy logic was developed for use when the knowledge concerning uncertainty distributions is incomplete or inaccurate. "The central concept of fuzzy logic is the membership function, which represents the degree of membership of the fuzzy variable within a fuzzy set [246]". A set of mathematical rules is created around these fuzzy sets. These methods are also called possibilistic methods, because 'possibility functions' are used instead of probability functions. Figure 33 shows a graphical comparison of the membership functions for interval analysis, fuzzy logic, and probabilistic analysis.

Chen completed a study comparing fuzzy logic and possibility-based analysis against traditional probabilistic approaches for designing to avoid failure. Chen showed that when accurate uncertainty distributions are known, probabilistic methods are clearly preferable, however, "when limited information is available for the uncertainty... the probabilistic method might produce unsafe designs. In these cases, a possibility-based method is better [38]". Even though these possibility methods may be beneficial when appropriate statistical

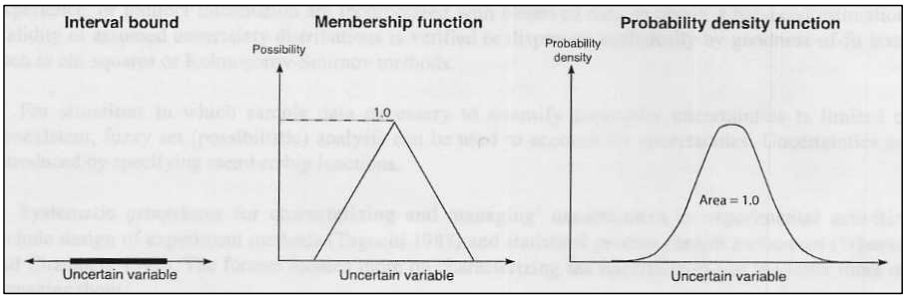

Figure 33: Various Uncertainty Descriptions [246]

data is not available, they still have drawbacks. According to Langley, "Existing algorithms for possibilistic methods tend to be computationally intensive [135]", so they may not provide any benefit in terms of analysis time.

In addition, when distribution information is not available, some researchers will simply apply a uniform distribution across all the known parameters. Using a uniform distribution, there is an equal likelihood of all events occurring, thus preference is not given to any particular outcome. This type of approach has been used in design space exploration, before firm decisions about the vehicle have been made and the entirety of the design space needs to be explored [122].

3.4 Metamodeling (Surrogate Modeling)

When dealing with probabilistic analysis, particularly when using schemes such as Monte Carlo simulation, large numbers of analysis runs may be required, often reaching tens and even hundreds of thousands of runs. Unfortunately, even in an age of increasing computer processing speeds, many computational models simply cannot run quickly enough to be reasonable for a Monte Carlo approach. Fortunately, a process exists by which a complex analysis tool (a computer simulation, or actual experimental results) can be simplified and represented in a computationally efficient manner. This approximation process requires the construction of a metamodel of the system.

Essentially, metamodeling is a process by which a physical experiment or complex computer model is represented by a simpler function. Metamodels, also called surrogate models,

are used so that slow experimental or computationally intensive processes can be replaced by fast, easy-to-use approximations. Accuracy of the original process is thereby traded for computational speed.

Metamodels are often combined with other statistical sampling processes, such as Designs of Experiments, in order to generate as much information about a process or computer program with as few trials as possible. Designs of Experiments are similar to the original work of Taguchi [219], who used pre-specified trials, or experiments, to identify the main effects of design variables and to analyze interactions between design variables. Taguchi focused on running experiments based upon predefined arrays of runs, now called Taguchi arrays. These types of pre-specified trials were also developed in the field of statistics, culminating in a suite of tools called Design of Experiments that supplement Taguchi methods. Designs of Experiments (DoE) consist of a predetermined set of orthogonal experiments, or runs, from which the complete behavior of a system can be determined. The goal of a DoE is to generate the greatest amount of knowledge about the design space with the fewest number of runs. As Montgomery defines them, Designs of Experiments are a "test or series of tests in which purposeful changes are made to the input variables of a process or system so that we may observe and identify the reasons for change in the output response [171]." Thus, the Design of Experiments is an *intelligent* selection of analysis runs that is made, so that the general behavior of a computer model can be approximated without the need for extensive repetitions of runs.

Several types of Designs of Experiments exist, the simplest such DoE is a full-factorial experiment. In this type of DoE, each variable in the design space is divided into a number of distinct levels, generally 2 or 3. The design space is then sampled at each combination of the levels for all the design variables. While this type of DoE is the easiest to implement, it requires the largest number of runs, particularly troublesome when a large number of design variables are involved. Less computationally expensive Design of Experiments have been developed, such as the Box-Behnken and the Central Composite Design. These DoEs use the statistical principal of orthogonality to separate the effects of design variables and variable interactions, thereby producing a similar amount of knowledge about the design

Table 9: Potential Designs of Experiments (Adapted from [122] [172])

Design of Experiment	Number of Runs (N-Variables)	Number of Runs for 7 Vars
2-Level Full Factorial	2^N	128
3-Level Full Factorial	3^N	2,187
Central Composite Design	$2^N + 2N + 1$	143
Box-Behnken	—	57
D-Optimal Design	$(N+1)(N+2)/2$	36
Taguchi*	—	27

* Main effects and some interactions only [17]

space to full factorial experiments, but at a fraction of the number of runs. Software exists, such as JMP [116] and Design-Expert [214], that not only have these common, predefined sets of experiments, but also have algorithms that can be used to create custom DoEs. Table 9 shows some DoEs and the number of associated runs with each. Figure 34 shows a graphic representation of a Designs of Experiments in three dimensions.

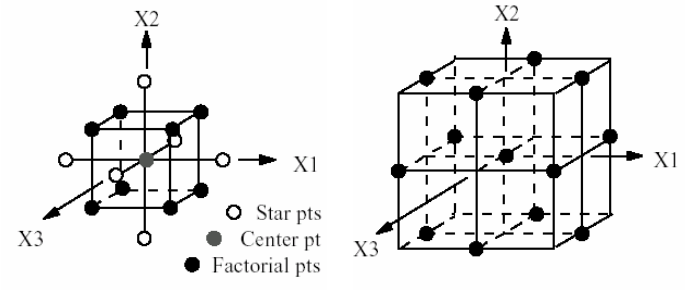

Figure 34: 3-D Pictorial Representation of a Central Composite Design (left) and Box-Behnken Design [211]

The results of the Designs of Experiments can then be used to generate the approximate models, or metamodels.The process by which Designs of Experiments are used to generate metamodels is shown in Figure 35. The process often begins with the use of a screening test. A screening test is used when there is a cumbersome number of design variables. The screening test is a scaled down, lower order DoE (with fewer runs), specifically designed to capture only first-order effects, excluding higher order effects and interactions. The results of the screening test DoE can be used to determine which design variables do not contribute much to the variability of the results. These design variables can then be discarded so that

there is a more manageable number. Next, a larger Design of Experiments is used and a predictive model, or metamodel, is created for the design space. This metamodel can then be used to explore the entire design space. When the specific metamodels being used are response surface equations, this process is referred to as Response Surface Methodology (RSM), which is becoming a common practice in aerospace conceptual design [122] [154].

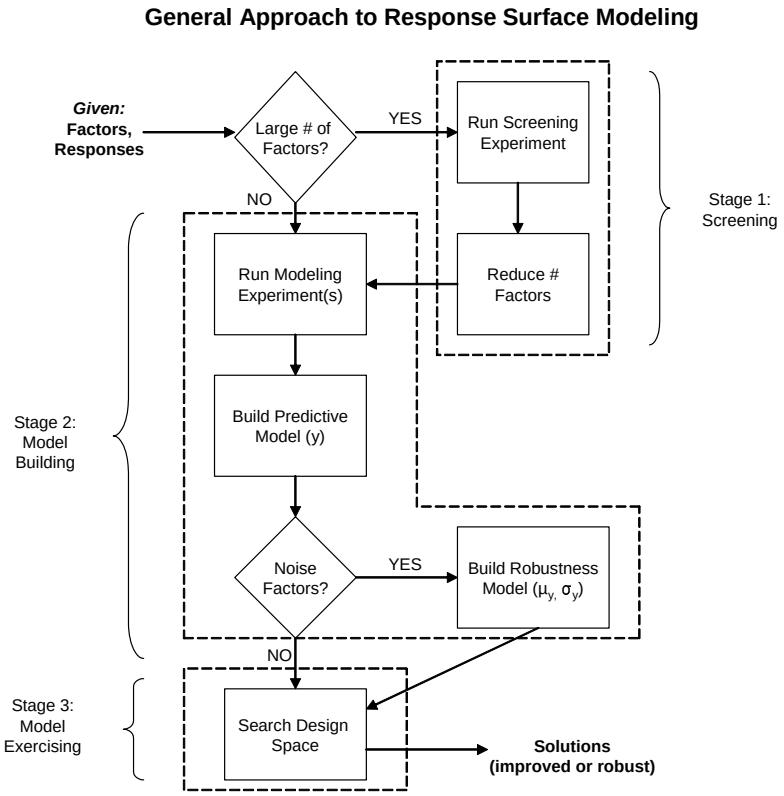

Figure 35: Design of Experiments and Metamodeling Approach [128]

One of the biggest drawbacks of coupling Designs of Experiments with metamodels is the difficulty excluding infeasible regions of the design space. Since Designs of Experiments often select the 'corners' of the design space, it is quite common to have DoE points that do not converge to valid solutions. There are few alternatives available to address this problem of analysis cases failing while developing the metamodel. One alternative is to simply ignore the failed cases, particularly if there are only a small number present [123]. Another possibility is to shrink the ranges of the design space variables until all of the analysis runs are feasible [123]. Unfortunately, shrinking the design space can unnecessarily discard valid

regions from the metamodel, resulting in the unnecessary exclusion of valid potential designs [78]. But, simply discarding failed cases may inappropriately include infeasible design space in the metamodel. Non-dimensionalization of DoE variables represents a potential technique that could be used to address this problem. Potential non-dimensionalization schemes for torpedo design variables and their ramifications are discussed at length in Chapter 8. Regardless of the metamodel used, care should be taken to insure that the final results from the metamodel are feasible.

3.4.1 Potential Metamodels

There are many different types of metamodels available. The most commonly used is a polynomial regression. A polynomial regression is a simple least-squares linear regression of the analysis data [178]. Polynomial regressions can take many forms including: first-order, second-order, or third-order forms. A common form of polynomial regressions are second-order equations that include cross-terms which account for interactions between input variables. These second order polynomial regressions, as shown in Equation 6, are known as response surface equations and are the most common form of metamodels. An example two-variable response surface equation is given in Equation 7. Once this response surface equation is generated, the equation can be used to replace the analysis tool. Thus, a time-consuming analysis tool can be replaced with an approximate, simple equation.

$$y = b_0 + \sum_{i=1}^{n} b_i x_i + \sum_{i=1}^{n} b_{ii} x_i^2 + \sum_{i=1}^{n-1} \sum_{j=i+1}^{n} b_{ij} x_i x_j + \epsilon \tag{6}$$

y is the approximated response
x_i are the design variables
b_0 is the intercept
b_i are regression coefficients for main effects
b_{ii} are coefficients for quadratic effects
b_{ij} are coefficients for interactions
ϵ is the approximation error

$$y = b_0 + b_1 x_1 + b_2 x_2 + b_{11} x_1^2 + b_{22} x_2^2 + b_{12} x_1 x_2 \tag{7}$$

Response surface equations are very common metamodeling tools and have been used in a variety of research, from power systems [180], to aircraft [155] [184], helicopters [15], missiles [64] [77], propulsion systems [203], and larger system of systems studies such as the US Air Transportation System [86] [87]. They have also been used in previous research directly relating to torpedo design [20] [71].

One of the greatest difficulties in metamodeling is the fitting of non-linear behavior. Second order response surface equations inherently fit only second order behavior. Sometimes, this level of fit is not sufficient to capture the behavior of the actual model. In these cases, a better approximation can often be made by increasing the order of the underlying polynomial regression being used. Alternatively, McDonald showed that the act of transforming the variable being modeled before creating the regression (as by taking the natural log or the square root) can often lead to significantly better model fits. In this case the transformation works by removing non-linear effects that cause problems for the linear regressions. Using an appropriate variable transformation can be highly beneficial in improving the performance of a polynomial regression [164].

A second common type of metamodel that is good at handling non-linear effects is Kriging. Kriging models were originally developed for the field of geostatistics and were introduced to engineering applications by Matheron [145]. A Kriging model contains both a polynomial representation of a system and an error term. It is of the form shown in Equation 8, where y(x) is the response of interest, f(x) is the polynomial approximation, and Z(x) is an estimated error term. Thus, the Kriging model builds off of the polynomial regression by estimating an error term. However, in actual use it is often easier to simply represent the underlying f(x) function of the Kriging model as a constant. For many problems, the error term alone is sufficient to accurately model the system [211]. The error term is found through a complex process that entails examining the correlation between all the sampled data points, the expected correlation of the point to be estimated, and the use of a predefined correlation function. Specific methods to implement Kriging metamodels are discussed in References [46], [211], and [230]

$$y(x) = f(x) + Z(x) \tag{8}$$

Kriging has some advantages over polynomial regressions. For one, it does not assume a polynomial fit, such as quadratic, so it does not assume the order of the system behavior and is therefore good at fitting non-linear behavior. Secondly, Kriging can be used to either fit the data points exactly, interpolate between them, or smooth the data and not perfectly fit the data points. This behavior, either interpolation or data smoothing, is a function of the form of the error function used in Equation 8 [46]. The primary disadvantage of Kriging is its increased complexity over polynomial regressions.

A third metamodeling approach calls for the use of Radial Basis Functions. Radial Basis Functions are another interpolative scheme, providing a metamodel estimate based upon a selected basis function and the radial distance to all the data points in the system. The equation for radial basis functions is given as

$$f(x) = \sum_{i=1}^{M} \beta\phi(||x - x_i||)$$

summed over all the available data points where β is chosen such that $f(x_i) = F(X_i)$, meaning that the data points are fit exactly, and ϕ is one of several potential classes of radial basis functions such as cubic $\phi(r, c) = (r + c)^3$ or Gaussian $\phi(r, c) = r^2 \ln(cr)$ as described in [163] and [190].

As these three metamodeling approaches become more and more common in the engineering world, work has been done comparing these metamodels. Volovoi showed that Kriging models performed significantly better than response surface equations [230] [231]. Work by Jin and Simpson in Reference [114] and [115] showed that Kriging models worked especially well for non-linear problems. Jin and Simpson noted that radial basis functions tend to over-fit the problem, adding artifical non-linear effects. However, they did note that for relatively linear problems, polynomial regressions achieved very reasonable fits with a very minimal amount of effort. Thus, Jin and Simpson's final recommendation was to quickly fit any problem to a polynomial regression, then, only if the fit of the polynomial did not look good, move to the more complex Kriging method.

Other metamodeling methods also exist, but will not be addressed in this thesis. These methods include the use of neural networks [206] [207] and the use of Gaussian Processes [47] [48]. Radial basis functions have also been used in conjunction with neural networks [12] [185]. In addition, work has been done recently in the use of adaptive polynomial regressions [114]. A good survey of various metamodeling techniques was done by Simpson, et. al., in Reference [210]

3.4.2 Measures of Goodness

When developing a metamodel, it is imperative that the user determine the quality of the model fit before using it to replace a complex analysis tool. There are many criteria to judge the goodness of the response surface equation; one such criterion is the coefficient of determination, or $\boldsymbol{R^2}$, which measures the proportion of the variability in the data accounted for by the polynomial model [99]. R^2 varies between 0 and 1, but since metamodels generally represent deterministic (and therefore completely repeatable) computer experiments, the user should expect large R^2 values, on the order of 0.99 or better. The formula for R^2 is given in Equation 9. Other measures of model goodness include actual versus predicted plots and residual plots, or scatter plots (Figure 36). Actual versus predicted plots chart the value predicted by the response surface equation versus the 'real' value generated by the analysis codes. The plots show how well each of the data points was predicted; a perfectly predicting metamodel will result in a straight line at a 45 degree angle on the plot. Scatter plots are used to show the distribution of the error for the metamodel. The amount of error between the predicted value and the actual value is shown as a function of the predicted value, thus illustrating trends between the error and the response. Scatter plots are given their name because in an ideal situation, there should be no discernable trends to the distribution, it should appear as random points on the plot. Discernable trends in the scatter plots indicate that the polynomial model is not capturing all the system behavior; there may be additional higher order effects present, etc. Kirby and Barros provide an excellent set of methods by which the goodness of response surface equations can be measured [18] [122].

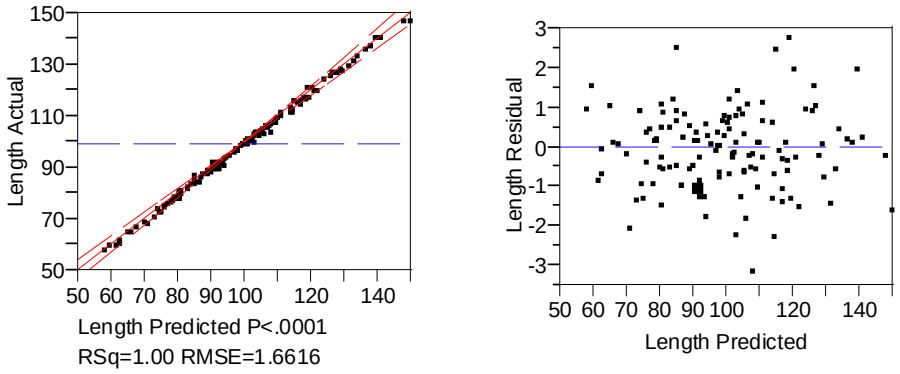

Figure 36: Actual versus Predicted for a Response Surface Equation (left) and Residual Plot (right)

$$R^2 = \frac{\sum_{i=1}^{n}(\hat{y}_i - \bar{y})^2}{\sum_{i=1}^{n}(y_i - \bar{y})^2} \text{ where,} \tag{9}$$

y_i is the i^{th} true value,

$\hat{y}$ is the predicted value,

and $\bar{y}$ is the mean value

Unfortunately, the above measures of merit can only be used on metamodels that do not perfectly fit the data, such as polynomial regressions. Models that are based upon interpolation, such as Kriging models or radial basis functions, cannot use these measures of merit. The reason is that these measures of merit look at how closely the actual data points are fitted. But, since Kriging and Radial Basis Functions are interpolative models, they always include the original data points in the model, therefore, even if the model is a poor fit, it will still have an R^2 equal to one and no residual! The best way to examine the goodness of these models is to check the accuracy of the metamodel with additional randomly selected analysis runs. When checking against random points, it is common to look at the average error, sum-square error, and maximum error (see Equation 10). Such comparisons against random points are the best metric by which any metamodel should be validated before it is used. It is the metric used by Simpson and Volovoi when they compared multiple metamodels [114] [230].

$$\text{Average Absolute Error: } \frac{1}{n}\sum_{i=1}^{n}\frac{|y_{t_i}-y_{m_i}|}{y_{t_i}} \tag{10}$$

$$\text{Sum Square Error: } \frac{1}{n}\sum_{i=1}^{n}(y_{t_i}-y_{m_i})^2$$

$$\text{Maximum Error: } max\left\{\frac{|y_{t_i}-y_{m_i}|}{y_{t_i}}\right\} \text{ for } i=1,2,\ldots,n$$

$$\text{where: } y_m = \text{metamodel approximation}$$

$$\text{and } y_t = \text{true result from analysis}$$

The user must validate the metamodel for each of the system responses, such as overall length, velocity, etc. Even if the metamodel does a good job of capturing some of the responses, this does not imply that the metamodel will be effective for other responses; each response must be individually verified. However, if the metamodels are unsatisfactory, there are methods to improve their performance. The user may always choose to add more modeling and simulation runs to the metamodel. Another mechanism is to reduce the ranges of the design variables being modeled. If using a polynomial regression, another technique is to add higher order terms to the regression, fitting a 3rd order equation instead of a 2nd order equation or adding more cross terms. For Kriging, a new error form may be helpful, and for radial basis functions, a new basis function ($\phi(r)$) may be beneficial. Finally, the user may always attempt to circumvent the problem by performing a variable transformation on the results [164] or attempting to non-dimensionalize the variables.

3.4.3 Pareto Plots and Prediction Profiles

The information from Designs of Experiments and metamodels can be used for a variety of additional purposes. For one, the information from the Design of Experiments can be used to generate Pareto charts, which are charts that show the relative effect that each design variable has on the output variables. An example Pareto chart is shown for a single torpedo response in Figure 37. The chart lists each design variable in descending order of contribution, uses bar charts to show the relative contribution of each design variable to the variability of the response, and also graphs the cumulative effect on the variability.

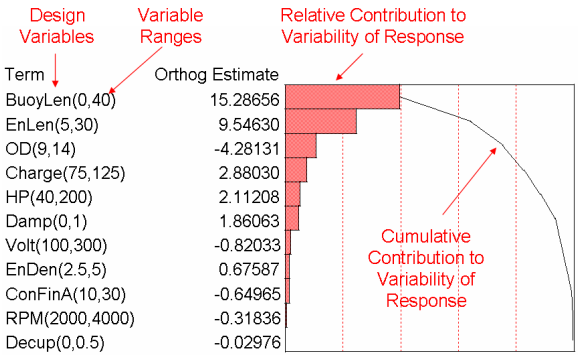

Figure 37: Example Pareto Chart

The prediction profile is another tool that uses the information contained in metamodels to show how the design variables affect the overall system responses. Prediction profiles are created through the SAS Institute's JMP statistical software package and are useful in summarizing the behavior of a complex system. An example prediction profile is given in Figure 38. In the prediction profile, the center values along the x-axis indicate the current settings of the design variables, around these current settings are the minimum and maximum ranges of the design variables. In the JMP software package, these settings can be dynamically altered through the GUI. The center values on the y-axis show the system performance or system metrics resulting from the current design variable settings. Another beauty of this tool is that it shows the partial derivatives, or trendlines, of each of the design variables. These trendlines make the interactions between each design variable and performance characteristics clear. For instance, it is apparent from Figure 38 that by increasing the motor horsepower, the maximum velocity significantly increases, but at the cost of also increasing the weapon length. Another interesting point provided by the prediction profile is that increasing the diameter will decrease the length, but there is an optimal diameter for highest velocity. One key advantage of the JMP software is that the prediction profiler is an interactive system, so changing the value of an input variable will immediately result in the user seeing the effects on the system response and on the individual trendlines, allowing the user to quickly make tradeoffs between the various system design variables and responses.

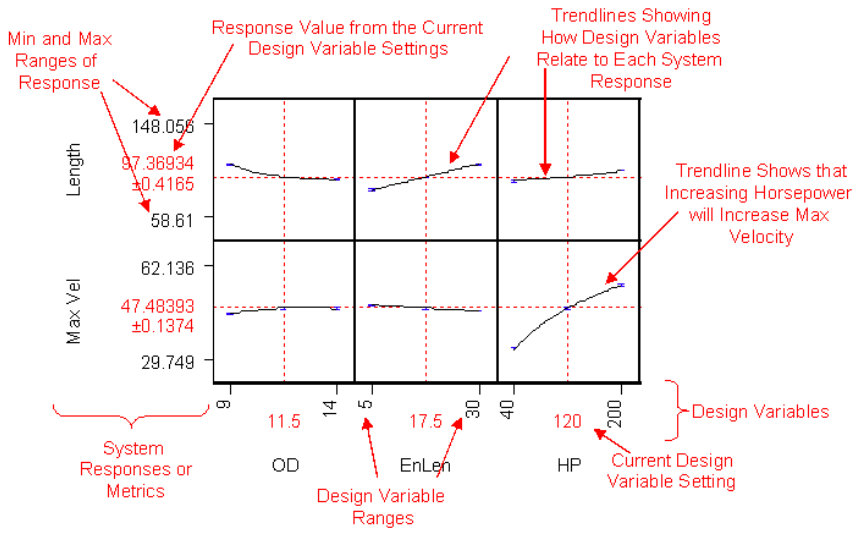

Figure 38: Example Prediction Profile

These prediction profiles can be used in two ways. First, they provide insight into the behavior of the system. The user can examine the trendlines to determine if the system behaves as predicted, e.g., one would expect that a torpedo with a smaller horsepower engine would have a lower velocity. This expected trend can be verified by observing whether the trendlines in the prediction profile indicate this effect. Though this means the prediction profile can be used as a diagnostic tool to ensure that the appropriate trends are being captured in the analysis program and the metamodel.

A second use of the prediction profile is for optimization. Since the prediction profile is set in a dynamical GUI environment, the user can use the computer mouse to alter the variable settings until an optimum is reached. In addition, the JMP software allows for the automated optimization of the torpedo design variables for any set of optimization criteria. Thus, a response surface equation can be quickly optimized using only the prediction profile.

3.4.4 k-Factors to Model Technology and Uncertainty

It is often necessary to model new technologies in the modeling and simulation tool. Unfortunately, the physics of the new technology may be overly complex or may not have been fully developed. However, Kirby developed a means to model ambiguous technologies in an analysis tool without necessarily modeling the complete physics. She suggested using

Disciplinary Metrics	Technologies Considered: T1	T2	T3
k factor 1 (O&S)	+4%	~	-10%
k factor 2 (Drag)	~	-3%	~
k factor 3 (RDT&E)	-1%	~	-2%
k factor 4 (Fuel burn)	-2%	-2%	+3%

Figure 39: Example "k-Factors" Representing Technologies [121]

multipliers, or "k-factors", on disciplinary metrics to model the effects of technology [121] [122] [150]. Taken together, a set of "k-factors" can be used to model the impact, both positive and negative, of a new technology. Figure 39 has an example where technologies (T1, T2, and T3) are represented through a series of "k-factors" (K1, K2, K3, and K4). Note that these "k-factors" are multipliers on internal disciplinary metrics, and represent both the advantages and disadvantages of using a tool.

Another use of "k-factors" is in the modeling of uncertainty in the analysis tool. Uncertainty analysis capability can be directly built into a simulation tool through these "k-factors". These "k-factors" can be used to account for uncertainty by randomly adding either benefits or degradations to the system components. In addition, "k-factors" can be built into metamodels, such as response surface equations, so that uncertainty analysis can be conducted independent of running the analysis program.

3.5 Use of Uncertainty in Analysis Methods

Many uncertainty analysis methods originated from the realm of structures and reliability. Many of these methods have gravitated into the robust design world. The most basic uncertainty analysis method is Monte Carlo Simulation. Monte Carlo simulation was developed by Stanislaw Ulam, a Polish physicist working on building hydrogen bomb for the United States. It was named after the gambling casinos of Monte Carlo in Monaco [108] [218].

Essentially, Monte Carlo simulation consists of direct, random sampling involving large numbers of trials. Monte Carlo simulation came into its own as a legitimate analysis method

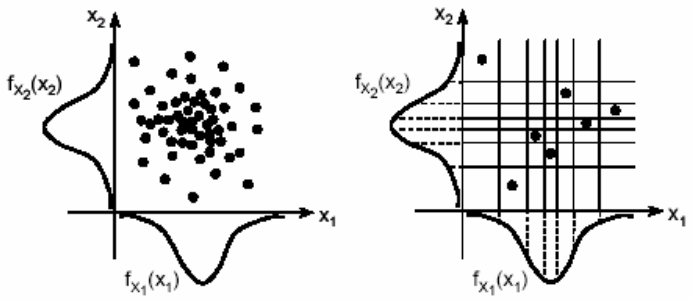

Figure 40: Monte Carlo Descriptive Sampling [125]

once computer speeds were fast enough to allow large numbers of trials. Given an infinite number of trials, Monte Carlo techniques theoretically provide the actual answer. In reality, Monte Carlo solutions are still approximate, as only a finite number of runs are made, but they are often treated as providing the 'exact' results (provided sufficient runs are made) by authors when dealing with probability problems [221]. The precision of Monte Carlo results is inversely proportional to the square root of the number of runs made, $\frac{1}{\sqrt{n_{sample}}}$, therefore to improve the estimate by a factor of 2, four times as many runs need to be generated [209].

One of the great advantages of Monte Carlo techniques is that they are not subject to the 'curse of dimensionality'. As the number of uncertain variables increases, many schemes have an exponential increase in the required number of analysis runs required to achieve a solution. Monte Carlo techniques do not have this problem [108]. The great disadvantage of Monte Carlo, however, is that it is very intensive computationally. Tens of thousands, often hundreds of thousands of runs may be required to achieve a good solution.

A great deal of research has been done throughout the past several decades to decrease the amount of analysis runs required for Monte Carlo simulations. One such technique is descriptive sampling, which uses smarter selections of random points to decrease the number of Monte Carlo runs [125] [205]. A representative sketch of descriptive sampling is given in Figure 40.

Another set of uncertainty analysis methods developed from the world of structural reliability. These methods include advanced mean value methods (AMV), first-order reliability

methods (FORM), and second-order reliability methods (SORM) [16] [19] [99] [221]. These methods generally work by first assuming that each input parameter exists at its mean value. Then, first or second-order Taylor approximations are made for the model using subsequent analysis runs or data known from the distributions of the input parameters. These approximations are then used to estimate the most probable point, which, taken from the reliability definitions, means the point at which failure is most likely to occur [99]. Similar to these methods are also sensitivity-based approaches, in which "rather than sampling across known distributions or ranges for uncertain design parameters, gradients for performance parameters are taken with respect to the uncertain design parameters [125]". Many researchers have used these methods to further develop robust design tools, including Green [96], Langley [135], Du [58] [60] [61], and Gu [97].

Another common means of decreasing the amount of computation time required to run Monte Carlo simulations is through the use of metamodels. Instead of expensive function calls, response surface methodology can be used to generate response surface equations or other metamodels that approximate the complex analysis tool. The Monte Carlo simulation can then use these approximate metamodels in lieu of the full analysis tool. Since the metamodels run at a fraction of the time of the analysis tool, computationally expensive Monte Carlo runs can be reduced to reasonable runtimes. This technique has been successfully used for the probabilistic design of complex systems by many researchers, including Mavris [149] [150], Koch [127], and Qu [195]. One interesting use of metamodeling for probabilistic design was completed by DeLaurentis. Instead of replacing the analysis module with a metamodel, the analysis was sampled at points throughout the design space using full Monte Carlo simulation in conjunction with a high-fidelity analysis tool. The resulting CDFs from this analysis were then discretized and response surface equations created from these discretized CDFs. Thus, instead of approximating the design space for the use of Monte Carlo simulation, DeLaurentis instead approximated the *results* of the Monte Carlo simulation [53] [55].

Applications for these methods have been very diverse, extending far from the field of structural reliability analysis. Current applications run the gamut from Mars missions

[51] to engine sizing [156] [203] to aircraft design problems [152]. These techniques have been used for single discipline analysis such as aerodynamics [187] [217] and have also been extended to larger system-of-system studies [54] [213].

3.6 Multi-Objective Criteria with Uncertainty

Design with uncertainty inherently requires the use of multi-objective methods. This is due to the fact that even when only a single objective metric is present, treating this metric with uncertainty inherently generates two objectives, one based upon the 'goodness' of the metric, generally estimated by the mean, μ, and the other based upon the 'variability' of the metric, often treated as a standard deviation or variance. As described by Chen, when dealing with robust design, a single objective is generalized into two aspects, "optimizing the mean of performance" and "minimizing the variation of performance" [39]. Thus, even what originally is a single-objective decision problem becomes, at a minimum, a bi-objective problem in the presence of uncertainty. Therefore, multi-objective decision making techniques are a necessity when dealing with uncertainty in robust design problems.

Several methods exist to aid in the solution of multiple objective problems. These methods include utility functions that collapse multiple objectives into single values, such as weighted sums and signal-to-noise ratios, as well as methods that look at comparisons of multiple solutions, such as TOPSIS or efficiency frontiers.

3.6.1 Signal-to-Noise Ratios

Signal-to-noise ($\boldsymbol{S/N}$) ratios were originally implemented in robust design problems by Taguchi as a method to account for both the mean and the variance of an attribute as a single value [219, 220]. Essentially, signal-to-noise ratios consist of a comparison of the mean of a response to its standard deviation. Taguchi states that the "S/N ratio is a measure of robustness; the higher the ratio, the less harm variations cause to the system [220]." In the case of a maximization problem, if the standard deviation is small compared to the mean, then the problem has a large signal-to-noise ratio. Conversely, if the standard deviation is large compared to the mean, then the problem has a poor signal-to-noise ratio. Separate

signal-to-noise ratios have been created for use in three separate types of problems, maximization problems (S/N_{Large}), traditional minimization problems (S/N_{Small}), and problems where the goal of the optimization problem is to reach an objective value (S/N_{Target}), often called a 'target optimization' or 'nominal the best' problem. The formulas for the three signal-to-noise ratios are given in Equation 11 through Equation 13.

$$S/N_L = -10\, log_{10}\left[\frac{1}{n}\sum_{i=1}^{n}\left(\frac{1}{y_i}\right)^2\right] \tag{11}$$

$$S/N_S = -10\, log_{10}\left[\frac{1}{n}\sum_{i=1}^{n} y_i^2\right] \tag{12}$$

$$S/N_T = \quad 10\, log_{10}\left(\frac{\bar{y}^2}{s^2}\right) \tag{13}$$

$$\bar{y} = \frac{1}{n}\sum_{i=1}^{n} y_i$$

$$s = \left(\frac{1}{n-1}\sum_{i=1}^{n}(y_i - \bar{y})^2\right)$$

Signal-to-noise ratios are a useful technique because they reduce bi-objective robust design problems into single-objective problems, however, they come with several drawbacks. One drawback is that Taguchi has devised over 70 distinct signal-to-noise ratios, each useful in various applications [17] [188]. Thus, choosing the most appropriate signal-to-noise ratio may be a cumbersome task and often involves a trial-and-error approach [188]. In many cases using the wrong signal-to-noise ratio may result in less than optimal results. For example, according to Box and Leon, S/N_T is only appropriate to use when the standard deviation is proportional to the mean, otherwise a different signal-to-noise ratio transformation needs to be used [24] [138]. Taguchi himself states that "It is very important to choose appropriate S/N ratios to solve various quality engineering problems [220]." Thus, it may be difficult to decide what the appropriate signal-to-noise ratio is for every problem.

An additional problem with signal-to-noise ratios is the inability to distinguish between an improvement in signal (mean) versus an improvement in variability (noise). For example, an improved signal-to-noise ratio may have either a more optimal mean or smaller variability, but this difference is indistinguishable to the user. Taguchi also mentions that the lack of

knowing the total variation indicated by the S/N ratio is a drawback of the metric [220].

3.6.2 Weighted Sums

Weighted sums are the simplest, most common form of utility functions. Weighted sums consist of a simple summation of the independent objective parameters, along with a user-specified 'weighting' value assigned to each term. The weighting values typically are constrained such that all the weighting values add to one. The general form of a weighted sum is given in Equation 14.

$$\text{minimize: } \sum_{i=1}^{k}(w_i\, f_i(x)) \tag{14}$$

$$\text{where } f_i(x) \text{ represents the } i^{th} \text{ objective}$$

$$\text{and } w_i \text{ represents the } i^{th} \text{ weighting value}$$

Oftentimes, instead of simply summing the objective values, a 'baseline' alternative will be chosen. The weighted sums are then compared against this 'baseline' alternative, as in Equation 15. This formulation is also called an overall evaluation criterion (OEC), and becomes a criterion that includes all the appropriate disciplinary and overall vehicle metrics [151]. An advantage of overall evaluation criteria is that both minimization and maximization objectives can be included in the same minimization function. Overall evaluation criterion formulations have been used in many applications, including missile systems [89], military aircraft [151], and commercial aircraft [150].

$$\text{minimize: } OEC = w_1\Big(\frac{\text{Min Metric 1}}{\text{Metric}_{Baseline}\ 1}\Big)+w_2\Big(\frac{\text{Min Metric 2}}{\text{Metric}_{Baseline}\ 2}\Big)+w_3\Big(\frac{\text{Metric}_{Baseline}\ 3}{\text{Max Metric 3}}\Big)+\ldots \tag{15}$$

Weighted sums easily fit into a bi-objective robust design problem, which originally starts as a minimization of a single parameter, $f(x)$. In these problems, the robust objective can be expressed as a weighted sum with the goal of minimizing both the mean (μ_f) of the response and the standard deviation (σ_f) of the response (Equation 16). Weighting factors can be applied to stress either the minimization of the mean or the variance.

$$\text{minimize: } w_1\,\mu_f + w_2\,\sigma_f \tag{16}$$

Hwang mentions that utility functions will ensure non-dominated solutions and will achieve satisfactory solutions when the weighting parameters are correctly assessed. Non-dominated solutions are important because they represent solutions in which there is not an obviously preferable alternative. As described by Hwang, "a non-dominated solution is one in which no one objective function can be improved without a simultaneous detriment to at least one of the other objectives [112]." Unfortunately, when it comes to weighted sums, Hwang mentions that it is difficult to generate the best weighting factors before the analysis is done, and also mentions that in many cases the objective function is not additively separable [112].

3.6.3 Efficiency Frontiers

Efficiency frontiers deal with the creation of a Pareto-front of non-dominated solutions. The efficiency frontier graphically shows the set of these optimal, non-dominated solutions. An example Pareto front, or efficiency frontier, is given in Figure 41, which shows the non-dominated solutions for a finance problem, dealing with capital asset pricing. The frontier is defined by the set of alternatives that represent the most return for a given risk. Efficiency frontiers have the advantage over weighted sums in that the entire range of potential solutions is visible to the decision-maker, thus the decision-maker can make the decision about the best alternative after the analysis data has been gathered. As in Figure 41, the decision-maker can quickly use the efficiency frontier to determine the amount of risk he or she is willing to accept in exchange for a specific return on investment.

Efficiency frontier methods work exceptionally well on bi-objective decision-making problems, which, as stated earlier, result whenever single-objective problems are changed into robust design problems. However, even though these methods are best visualized for bi-objective problems, they can be expanded for larger numbers of objectives. Efficiency Frontier techniques deal with the creation of the set of non-dominated solutions of the problem. Once this frontier is created, the user may select any solution that he or she desires,

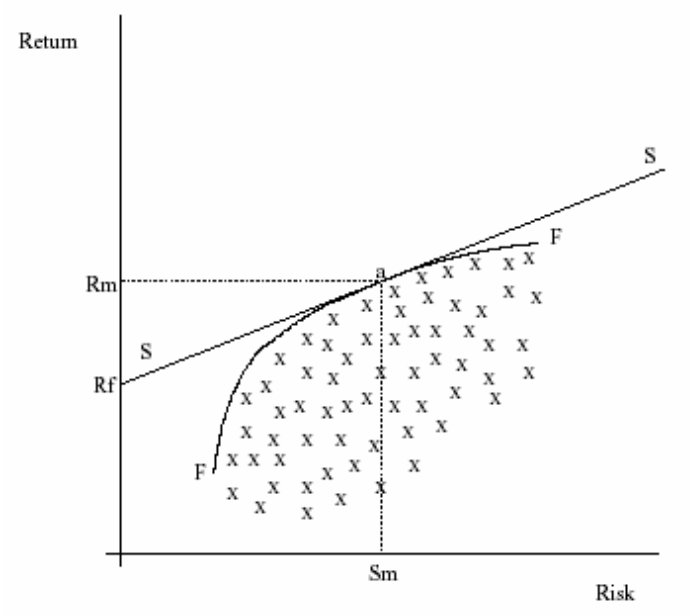

Figure 41: Example Pareto Front for Capital Asset Pricing [69]

each solution representing an 'optimal' candidate for a given trade-off between the two objective parameters. Another method to select the 'best' solution from the pareto front is to look at the 'utopia' solution, which is the hypothetical solution that would occur if the decision-maker could have the best of both worlds, which in the robust world means having the design with the optimal mean and the minimum variability. The decision-maker may choose to pick the real alternative that has the smallest Euclidean distance to this utopia solution.

Points on the efficiency frontier can be calculated in a number of ways. The simplest manner is the use of a weighted sum. For the bi-objective robust design problem, the corresponding weighted sum would be that shown in Equation 16. Any optimal solution to this weighted sum will create a point on the efficiency frontier. Additional points on the frontier can be generated by selecting a range of weighted values. Unfortunately, using weighted sums to create efficiency frontiers has many drawbacks. For one, as proven by Das and Dennis, every point on the efficiency frontier can be calculated by a weighted sum only if the frontier is convex in shape. If the efficiency frontier is not convex in shape, weighted sums cannot be used to find points in the non-convex regions of the efficiency

frontier [49]. An example of the geometric argument provided by Das and Dennis for a non-convex frontier is given in Figure 42. In order for a point to be found through the use of a weighted sum, the point must have a unique tangent drawn through it. Thus, in Figure 42, the convex points R, M, and Q may be found via a weighted sum, but point P may not.

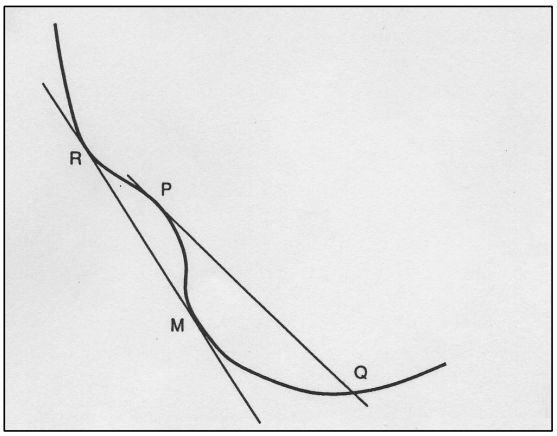

Figure 42: Geometric Argument Illustrating How Weighted Sums can only Find Convex Points in Efficiency Frontiers [49]

The second drawback to using weighted sums to calculate efficiency frontiers is the fact that, even when the efficiency frontier is convex in nature, an even distribution of weighted sums will not create an even distribution of pareto points [49]. Thus, the use of weighted sums may generate pareto fronts with large gaps of missing information. Figure 43 provides such an example.

Chen and Zhang, along with other researchers, have developed an alternate method for finding the optimal points on the efficiency frontier [40] [248]. These authors suggest using a compromise programming approach. The compromise programming approach first requires running an optimization to determine the 'utopia' point for each parameter. For example, if the mean and standard deviation were to be simultaneously minimized, the user would first find the solution with the minimum mean without regard to standard deviation, and then vice-versa. These points correspond to the end-points of the efficiency frontier; the hypothetical 'utopia' point is created as a combination of these two points. These 'utopia' points, for the function $f(x)$, are defined as $[\mu_f^*, \sigma_f^*]$.

Next, the authors redefine the traditional bi-objective robust design optimization problem, finding x such that $f(x)$ minimizes $[\mu_f, \sigma_f]$, to a problem that minimizes the closeness to the utopia point, as shown in Equation 17.

$$\begin{aligned} &\text{minimize: } \beta \\ &\text{subject to: } w_1\Big(\frac{\mu_f}{\mu_f^*} - 1.0 + \Delta_1\Big) \leq \beta \\ &\text{and } w_2\Big(\frac{s_f}{s_f^*} - 1.0 + \Delta_2\Big) \leq \beta \end{aligned} \tag{17}$$

The authors then show that using this compromise programming approach instead of a weighted sum approach leads to an even spacing of Pareto points and can handle non-convex regions [40]. Figure 43 shows the difference between a standard weighted-sum approach and a compromise programming approach in finding the efficiency front. Note that for the compromise programming approach,, the Pareto points are evenly distributed throughout the frontier and the non-convex regions in the center are fully captured.

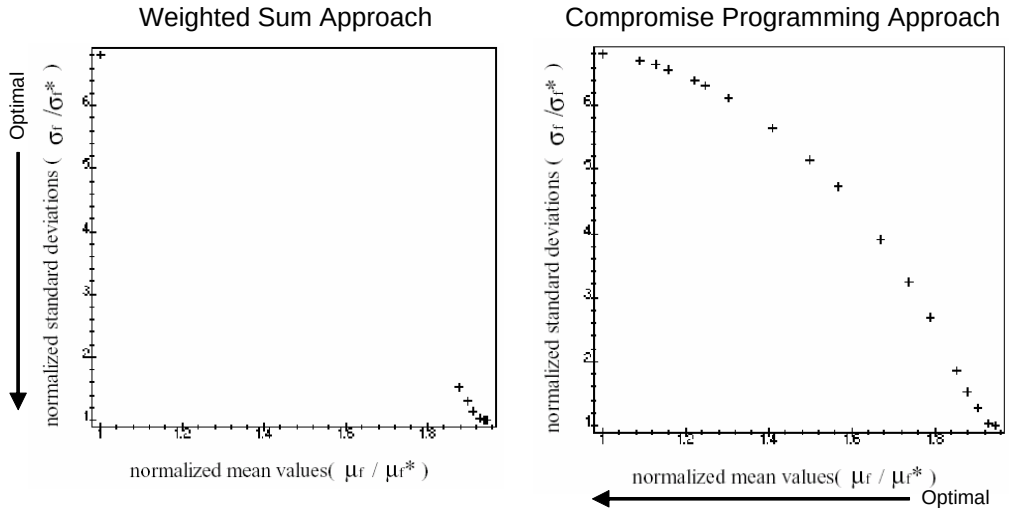

Figure 43: Comparison of Pareto Frontier from Weighted Sum and Compromise Programming Methods [40]

The authors, along with work by Tind and Wiecek, also show that a quadratic approximation of the efficiency frontier can be made at any Pareto point. Thus, the frontier in the neighborhood of any Pareto point can be examined without the need for additional

optimization runs [223] [247].

Other methods are also being developed to generate an even distribution of points on the Pareto front. One promising example is the Normal Boundary Intersection method being developed by Das and Dennis [50].

In addition to these techniques for reducing the computational requirements in the creation of efficiency frontiers, metamodels may also been used. Wilson, et. al., showed that they could create Pareto frontiers through the use of metamodels [239]. The authors first constructed Kriging and response surface equation metamodels of the design space. Then, since the existence of metamodels made subsequent function calls computationally inexpensive, an exhaustive grid-search was conducted to find the location of the Pareto, or efficiency, frontier. The location of the frontier was then refined through the use of actual analysis runs at the Pareto points. By this means the authors were able to quickly generate efficiency frontiers for convex, non-convex, and discontinuous spaces.

Roth, et. al., combined a metamodel with a genetic algorithm to efficiently search out the Pareto frontier in an engine technology problem [202]. Brown and Thomas also suggested the use of genetic algorithms to find the efficiency frontier for complex naval architecture problems [31] [222].

In addition to grid-search or genetic algorithms that use metamodels to locate the efficiency frontier, metamodels could also be used with existing compromise programming approaches to generate the efficiency frontier even faster, a potentially useful application when dealing with dimensionally expansive systems.

3.6.4 TOPSIS

TOPSIS stands for Technique for Ordered Preference by Similarity to the Ideal Solution. It is another method for selecting the best choice from a selection of alternatives. As such, in order to use this method, a set of alternatives must already be generated. This set may come from minimizing various weighted sums or overall-evaluation criteria, the creation of an efficiency frontier, or even the random creation of designs. TOPSIS then works by choosing the hypothetical optimal design (called the positive ideal solution) and the hypothetical

worst design (called the negative ideal solution). The positive ideal solution is identical to the 'utopia' solution defined for efficiency frontiers. TOPSIS then chooses the design that has the smallest Euclidean distance to the positive ideal solution and the largest Euclidean distance to the negative ideal solution. A geometric representation of the TOPSIS method is shown in Figure 44. In this figure, A^* represents the positive ideal solution, A^- represents the negative ideal solution, and, though A_1 is closest to the ideal solution, A_2 is the preferred solution because it is significantly further from the negative ideal solution. The TOPSIS preference system is very close to that of efficiency frontiers, however it includes the concept of a negative ideal solution as well as a positive ideal solution.

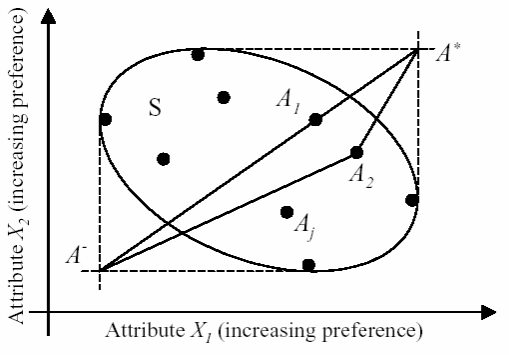

Figure 44: Geometric Representation of TOPSIS Approach[113]

3.6.5 Probability of Success

Though not a multi-attribute decision making technique in of itself, probability of success can be used as an important part of the multi-attribute decision-making process. Probability of success (POS) is defined by Bandte as "the envelope objective function or overall evaluation criterion ... measuring the probability of satisfying all criteria [16]." It is the chance of a probabilistically designed vehicle *simultaneously* meeting all design requirements, whether they be given by physical constraints such as weight and length, performance constraints such as velocity and range, or systems effectiveness constraints such as probability of hit and probability of evade. The equation for probability of success, assuming N number of trials and M number of constraints, is given in Equation 18. A POS of one indicates that

the design is guaranteed to meet all the stated requirements (assuming that the uncertainty was adequately captured), while a POS of zero indicates that the system will never simultaneously meet all of the design requirements.

Probability of success is useful when dealing with uncertainty analysis because it shows the likelihood that a given design will meet all of the design constraints. The probability of success metric has another key advantage because it collapses a multiple objective function into a single value. "This new objective function, called probability of success, allows for the use of any standard single-objective optimization technique available [16]," thus, the probability of success metric allows for the large number of single-objective optimization schemes to be used to solve multi-objective robust design problems. Conceptually, the probability of success metric is not difficult to comprehend, and can be stated quite simply as in Equation 19. However, even though the metric is seemingly straightforward, its usefulness is quite profound.

$$POS = \frac{1}{N}\sum_{i=1}^{N}\prod_{j=1}^{M}\left\{ \begin{array}{cc} 1 & for \;\; z_{j_{min}} \leq z_j \leq z_{j_{max}} \\ 0 & otherwise \end{array} \right\} \tag{18}$$

$$POS = \frac{\text{Number of 'Successful' Trials}}{\text{Total Number of Trials}} \tag{19}$$

3.7 Joint-Probability Analysis and Decision-Making

Joint probability analysis is based upon multi-variate probability theory. Instead of constructing univariate probability distributions for each parameter, the analysis instead focuses on developing a probability model that accounts for multiple probabilistic parameters simultaneously. This multi-variate probability model can better handle interactions between variables than single-variable probability models.

For example, the standard normal distribution is given in Equation 3. From this equation, an analysis could be conducted that estimates the behavior of the distribution based upon two figures: the mean, μ, and the standard deviation, σ. However, if the effect of two random variables were taken together, the effect is not the same. One might assume that the output of two random variables could be estimated using four parameters: the two

means (μ_x and μ_y) and the two standard deviations (σ_x and σ_y). The resulting probability model is then shown as Equation 20.

$$p(x,y) = \frac{1}{2\pi\sigma_x\sigma_y}\, e^{-\frac{1}{2}\left(\frac{(x-\mu_x)^2}{2\sigma_x^2} + \frac{(y-\mu_y)^2}{2\sigma_y^2}\right)} \tag{20}$$

Unfortunately, Equation 20 makes a very large assumption, namely, that the two normal probability distributions are independent of each other. However, Wallace observed that for many engineering systems an assumption of independence is made, but this assumption is often not correct. Wallace showed that for some engineering problems, inappropriate assumptions about model independence can cause errors of greater than 50% [235]. Therefore, an approach must be taken that accounts for the dependencies, or correlations, between probability distributions. A better approximation for the normal distribution is to use the bi-variate normal distribution, shown in Equation 21 [110].

$$p(x,y) = \frac{1}{2\pi(1-\rho^2)^{1/2}\sigma_x\sigma_y}\, e^{\left[\frac{-1}{2(1-\rho^2)}\left(\frac{(x-\mu_x)^2}{2\sigma_x^2} - 2\rho\left(\frac{x-\mu_x}{\sigma_x}\right)\left(\frac{y-\mu_y}{\sigma_y}\right) + \frac{(y-\mu_y)^2}{2\sigma_y^2}\right)\right]} \tag{21}$$

This bi-variate normal distribution now accounts for not only the independent properties of each univariate distribution, but also accounts for the coupling, or correlation, between the two probabilistic parameters, via the correlation coefficient ρ. An illustration of the bi-variate normal distribution and the impact of its design parameters is shown in Figure 45 and Figure 46.

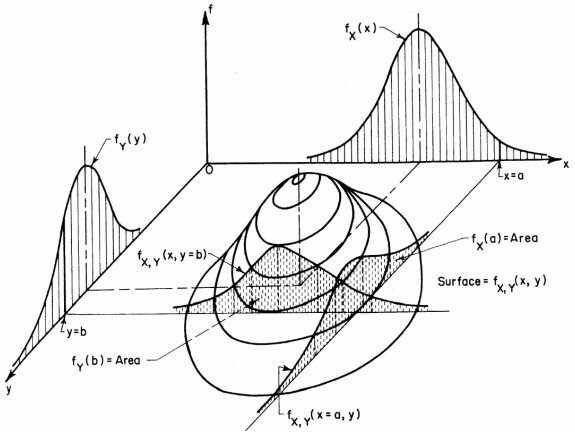

Figure 45: Joint Probability Distribution [11] [16]

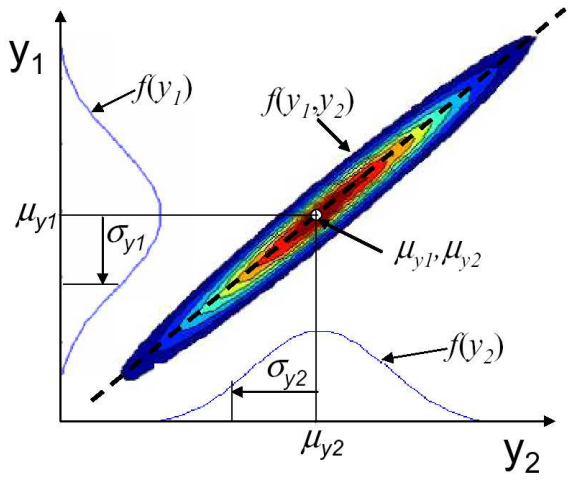

Figure 46: Multi-Variate Probability Terms [235]

The correlation coefficient, which can be estimated via Equation 22 [100], describes how the two distributions trend together. The correlation coefficient has a value between -1 and 1. A value of -1 implies that the distributions are opposite each other, so when a high value is generated for one distribution, a low value will be generated for the other distribution. A value of zero means that no correlation exists between the distributions, and a value of 1 implies that they trend together. Figure 47 illustrates how the correlation coefficients affect a random sample.

$$\rho = \frac{COV(X,Y)}{\sigma_x \ \sigma_y} = \frac{\Sigma_{i=1}^{n}(x_i - \bar{x})(y_i - \bar{y})}{\sqrt{\Sigma_{i=1}^{n}(x_i - \bar{x})^2}\sqrt{\Sigma_{i=1}^{n}(y_i - \bar{y})^2}} \tag{22}$$

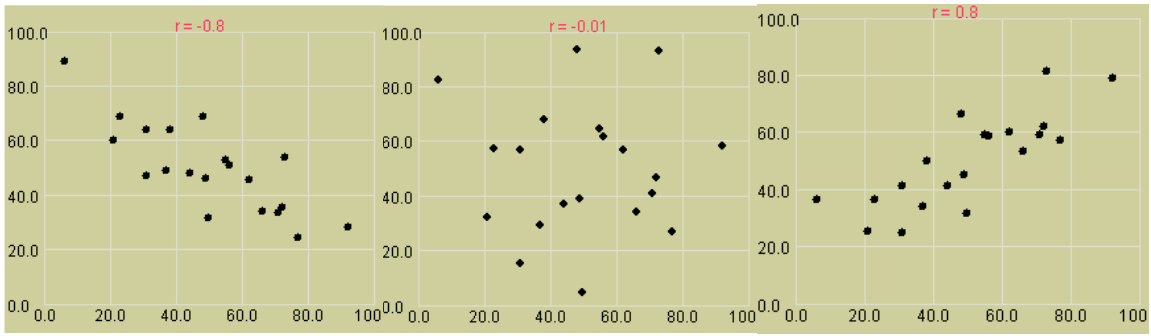

Figure 47: Correlation Coefficients ($\rho = -.8$, $\rho = 0$, and $\rho = 0.8$, respectively) (adapted from [118])

Bandte describes how the bi-variate normal distribution is useful for design applications, because now, when a coupled, multi-variate probabilistic response needs to be modeled, a smooth function can be fit to the data, allowing this new analytical probability model to be used in later analysis [16]. For example, if multiple probabilistic responses are estimated using this approach, then the probability of success can be calculated by simply integrating this model. This method allows for multi-variate probability data to be modeled using only a handful of parameters. In addition to using a smooth probability model, Bandte suggests that an Empirical Distribution Function may also be used to calculate the probability of success, which consists of a brute-force Monte Carlo estimation of the probability models [16].

For cases where more than two variables exist, the bi-variate normal distribution can be expanded to N-dimensions, as discussed by Bandte and Tong [16] [224]. Unfortunately, the N-dimensional normal distribution is not always defined. When the correlation coefficient is too negative, corresponding to the case that $\rho < 1/(1-N)$, the multi-variate normal distribution is not defined [16], so it cannot be used for every problem. However, both Bandte and Wallace propose that in these situations, and situations when the underlying probability distributions are non-normal, alternative multi-variate probabilistic distributions could be used instead [16] [234].

3.8 Numerical Optimization Techniques

At some point in the process of conceptual design numerical optimization techniques will have to be employed to find the best solutions. There are many types of numerical optimization techniques available for this task. Each of these numerical optimization techniques has various advantages and disadvantages, making their appropriateness for individual optimization problems vary. Since there are too many optimization techniques to discuss in detail, a few broad types of optimization processes will be discussed here, as they are relevant for many of the optimization problems discussed later.

One of the basic classes of optimizers are path-building optimizers. These class of optimizers includes a wide array of individual optimization techniques: Powell's method [191],

Fletcher Reeve's method [74], and sequential quadratic programming [229]. These methods solve the problems by various techniques, but have the common approach of generally developing numerical gradient information and then taking a path-building approach, where the optimizer steps to the optimal solution. These traditional optimizers work very well for smooth, continuous design problems. With a well-behaved problem, they tend to move quickly towards a solution, with the fewest overall number of function calls.

Unfortunately, these gradient-based optimizers are not good at handling discontinuous spaces. In addition, unless special adaptations are made, they are not able to handle discrete variables. They also assume that the space is unimodal; they therefore will find only a local optimum in a multimodal space. When handling multimodal problems, multiple starting points might need to be used for these gradient-based methods to find the global solution, a technique that significantly increases the runtime for the optimizer. And, finally, because the optimizers are estimating gradients numerically, they are very sensitive to noise in the analysis tool. Even if only a small amount of noise is present, the resulting gradients may be dramatically off, destroying the effectiveness of the optimizer. When such noise is present in the analysis there are precious few techniques to reduce the effects of this noise on the optimizer. One approach is to increase the step-size for taking numerical derivatives. This method will reduce the relative impact of the numerical noise on the calculated gradient. However, if the step size is made too large, the gradient information will not be sufficiently local in nature, causing additional problems for the optimizer.

A second set of optimizers are random searches. These optimizers are the most straightforward, with the quickest implementation time. These optimizers work through either a grid-search or random search, testing a pre-selected number of points in the design space. The advantage in these techniques, besides the short set-up time, is that discontinuous, noisy, and discrete problems can be handled with little difficulty. In addition, random searches will find the global optimum in the design space, not just the local optimum. Random search also has the added benefit of being very amiable for distributed computing, allowing for more resources to be quickly brought to bear to solve the optimization problem. The disadvantage with the random search is that very large numbers of function calls are

Table 10: Comparison of Optimization Techniques

Optimization Technique	Setup Time	# of Function Calls	Requires Smooth Functions	Handles Discrete Variables	Multi-Modal	Handles Noisy Problems
Gradient-Based	Significant	Few	Yes	No	No	No
Random Search	Minimal	Most	No	Yes	Yes	Yes
Genetic Algorithms	Significant	Many	No	Yes	Yes	Yes

required, not to mention that the method is decidedly inelegant.

Random searches belong to a larger set of optimization techniques known as stochastic techniques. These techniques are based upon the concept that some random calculations are used by the optimizer. Besides just random search, two other stochastic optimization techniques are simulated annealing and genetic algorithms [183]. Genetic algorithms are the most common, whereby the design variables are stored as a "chromosome", then random permutations of this chromosome are constructed and compared to each other [93]. Genetic algorithms have advantages in that they are insensitive to noise, work very well with discrete variables, and can find the global optimum. Unfortunately, they take a lot more function calls than path-building or gradient-based approaches, though they tend to be more efficient than random searches. They also have a longer set-up time than random searches. Genetic algorithms have been used for design problems for a number of years [203] [222].

The field of numerical optimization is quite expansive, and a full treatment in this document is impossible. However, several useful optimization techniques have been identified and are summarized in Table 10.

3.9 Advanced Engineering Software

Advanced engineering software are computer programs that are designed to facilitate complex engineering tasks. This genre of software works by linking together independent analysis programs so that the outputs from one program flow down to the inputs of other programs. This linkage allows the user to run an entire engineering simulation, utilizing multiple, distinct analysis modules, with the single click of a button. iSIGHT is an example

of one such analysis program [65]. It couples the ability to link multiple analysis programs together with several other features that facilitate engineering studies and optimization once the engineering environment has been established. iSIGHT has built in utility for the the running of Designs of Experiments and the creation of metamodels, both polynomial regression models and Kriging models.

In addition, iSIGHT has built-in deterministic optimizers that utilize sequential-quadratic programming to find optimum responses for constrained, non-linear optimization problems. Finally, iSIGHT has built-in probabilistic design methods for robust design. These methods include the ability to select a probabilistic distribution for an input variable, the use of Monte Carlo simulation to determine output distributions, and the use of optimization schemes for probabilistic analysis [129]. Many researchers have successfully used iSIGHT for various multidisciplinary design problems [8] [94] and probabilistic design problems with uncertainty [125] [126].

iSIGHT is not the only available tool for this type of integration. In addition to iSIGHT, a program called ModelCenter, developed by Phoenix integration, has nearly identical capabilities [189]. SAIC has also developed a similar software capability called ENVISION [240] [241]. Finally, Buonano showed that many of the same capabilities present in ModelCenter and iSIGHT can also be accomplished in a custom-built Matlab framework, with faster overall execution times [33].

3.10 Non-Dimensionalization in Design

Non-dimensionalization is a common practice in engineering fields, particularly aerospace. It is used to create automatically scaling parameters that can be used to represent a vehicle design regardless of the actual size of the vehicle. Non-dimensionalization is a process that can be conducted when the physics of the problem is not fully understood or is overly complex. Essentially, by multiplying system variables together until groups of like units are created, non-dimensional parameters are created. Furthermore, these non-dimensional parameters tend to be system drivers. These drivers are crucial for proper scaling, a key to accurate preliminary design. The method for non-dimensionalization is formalized with

the Buckingham-Pi theorem, which states that any complete equation can be written such that all the variables are dimensionless in form [9] [139]. Table 11 shows some examples of non-dimensional items commonly used in aerospace engineering. Though these types of non-dimensionalization are very common in the field of conceptual design of aircraft [147] [199], they are less common in overall torpedo design.

Table 11: Examples of Non-Dimensionalization

Name	Scaling Purpose	Formula
Coefficient of Lift	Lift	$C_L = \frac{L}{1/2\rho v^2 S}$
Coefficient of Drag	Drag	$C_D = \frac{D}{1/2\rho v^2 S}$
Mach Number	Compressibility Effects	$M = \frac{v}{a}$
Reynolds Number	Viscous Effects	$Re = \frac{\rho v x}{\mu}$
Thrust-to-weight	Aircraft Propulsion	$\frac{T_{SL}}{W_{TO}}$
Wing Loading	Aircraft Size and Wing Area	$\frac{W_{TO}}{S}$

These non-dimensional parameters are also useful in the running of Designs of Experiments. When running DoEs, small ranges must often be chosen for the input variables, because the DoE may often pick incompatible inputs, causing the analysis program to fail. An aircraft example might be the DoE choosing a low value for absolute thrust and a high value for payload. In such a case, the analysis program will return a bad result, such as zero for flight range, because the aircraft physically lacks the engine thrust required to takeoff. Thus, the ranges of the variables on DoEs must be kept small so that the smallest absolute thrust is still sufficient to fly the heaviest vehicle. However, by running a DoE using non-dimensional, or even normalized parameters, this problem can be partially alleviated. For instance, by using thrust-to-weight ratio ($\frac{T_{SL}}{W_{TO}}$) instead of absolute thrust, the vehicle thrust will automatically scale itself as a heavier vehicle is required. This scaling allows for a larger range of input variables in the Design of Experiments, since the input variables are scaling themselves to appropriate values, allowing the analysis program to run more smoothly.

CHAPTER IV

RESEARCH FORMULATION

4.1 Formulation of an Integrated, Robust Design Hierarchy

The research questions stated in Section 1.8 can be broken into three primary research tasks. The first research task focuses on the inclusion of uncertainty in the design process and the development of a robust design process that uses probability of success as a key variable for decision-making. A visualization tool was also developed to assist with decision-making during the design process. The second research task looks at the inclusion of tactics in conceptual design. This research task examines the effects of tactics on the design of undersea weapons. It first explores the relative impact of tactics on torpedo design. The analysis then looks at the concurrent optimization of tactics and design parameters for a mine counter-measure application. Finally, the third research task looks at the use of non-dimensionalization or normalization of torpedo design parameters to improve the performance of torpedo analysis when used in conjunction with Designs of Experiments or other analysis tools.

4.1.1 Robust Design Metric

A robust design methodology is required in order to account for the uncertainty inherent in any complex design process. The design methodology illustrated here is a robust, over-arching framework for probabilistic analysis. This framework illustrates specific tasks that need to be conducted for probabilistic analysis, however, the specific mechanisms for accomplishing each task are left to the user. This plug-and-play style framework allows the user to select the most appropriate tool to be used for each step, depending upon the specific nature of the problem at hand. The framework includes discussions as to which individual tools are useful at each step and lists the reasons why some tools are preferred over others. The specific tools that are applicable for each step are covered in more detail

in the background chapter (Chapter 3).

The key step in creating this robust design process is the development of a good metric that accounts for all of the probabilistic information. Adding probabilistics to a process inherently makes responses more difficult to characterize. For instance, Figure 48 shows an example torpedo problem from an historical design perspective. On the left-hand side of the figure is a design space with a single design point illustrated. This design point represents a single physical torpedo design. On the right-hand side of this figure is the response space or performance of the system. With historical, deterministic design techniques a single vehicle design maps to a single response. In this type of a deterministic environment, the response can be definitively characterized as either meeting the design constraints or failing to meet the constraints.

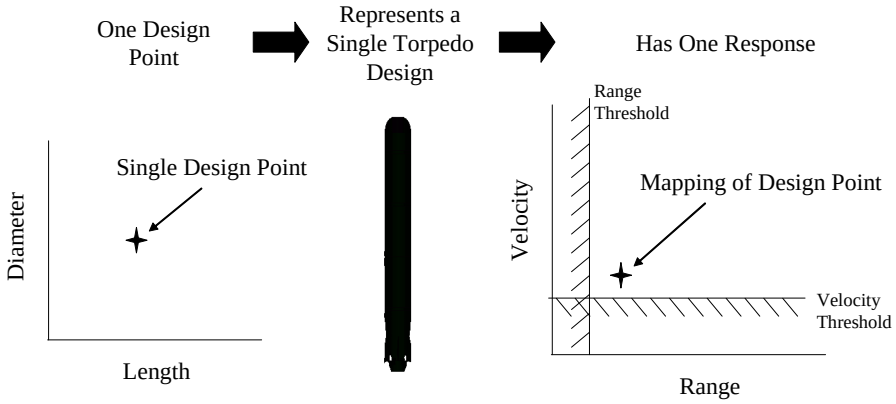

Figure 48: All Constraints are Satisfied All of the Time

However, as discussed earlier, designs are never fully deterministic. There is always some uncertainty or probabilistic response to a design. Thus, a more accurate interpretation of the design process is given in Figure 49. This figure shows the same design point from Figure 48, but now, this single design point maps to a probabilistically represented response space. It is now impossible to definitively characterize this design point as either meeting or failing to meet the design requirements

Therefore, a metric of merit is needed that can be used to identify which portion of the valid, or 'successful' response space is met by the design (Figure 50). A very powerful

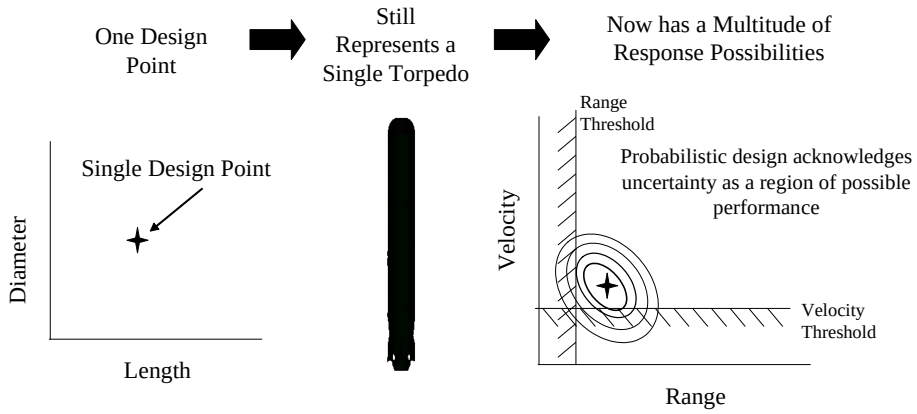

Figure 49: A Metric is Needed to Quantify the "Successful" Region

metric to use is the concept of probability of success, as introduced in Section 3.6.5. The probability of success is graphically shown in Figure 51. The probability of success is a single metric that succinctly captures all the information about the region of the response space that meets the design requirements. The probability of success value collapses all of this probabilistic data into a single value, thus making the multi-dimensional response easier to use for interpretation, visualization, and optimization. In many ways, the probability of success concept is directly analogous to the quantity of risk inherent in the system. A high probability of success indicates that the system can be considered low risk: in all probability, it will meet all of the design requirements. A low probability of success indicates a risky system: the chances of it fully satisfying all of the mission goals is low.

The new design goal is now to develop the system with probability of success in mind. In this environment, the designer is attempting not to meet specific design requirements, but instead is looking at the *probability* of meeting the design requirements. The goal of the designer is therefore to select the design variables that give the desired probability of success with the lowest cost. The new design environment is more like the environment illustrated in Figure 52, where the design point is optimized to provide an improved probability of success.

A key goal of this research is to develop risk vs. reward curves for torpedo systems which will show the relations between performance, cost, and the probability of meeting

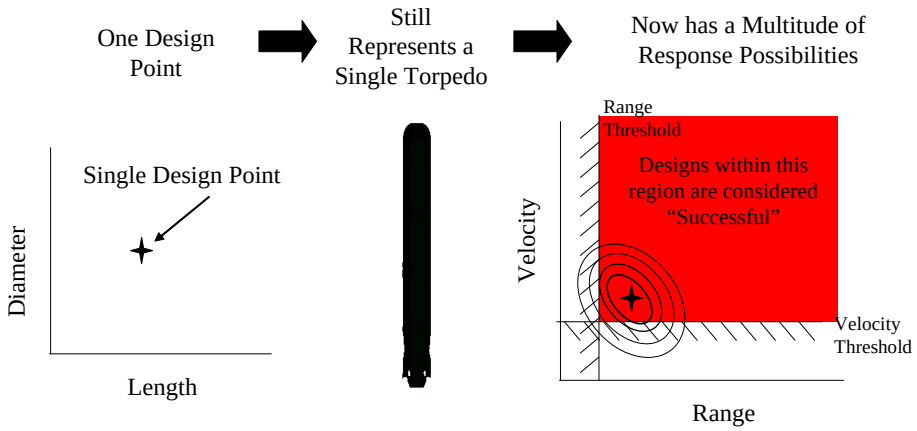

Figure 50: Probability of Success can be used to Quantify the Likelihood of a Successful Design

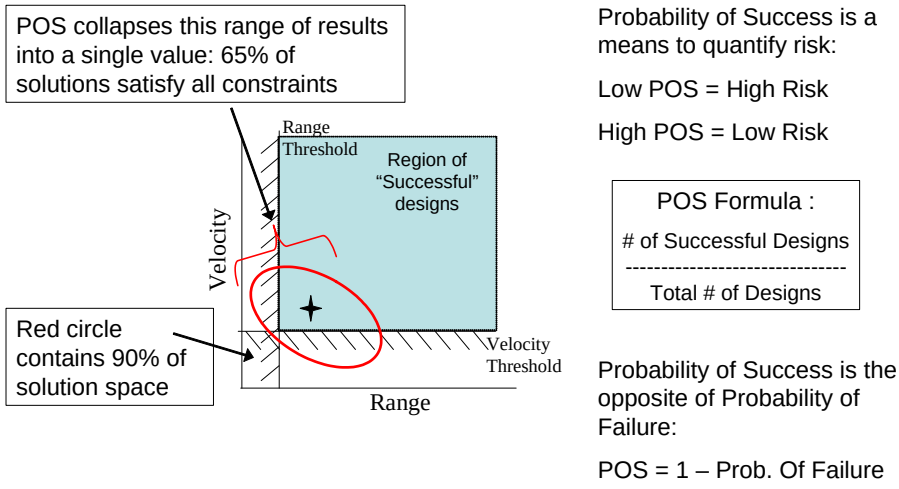

Figure 51: Visual Definition of Probability of Success

design requirements (now considered probability of success), all in an environment that is accounting for uncertainty. These risk vs. reward charts will be used to provide the decision-maker more insight into the tradeoffs between probability of success, performance, and cost.

Figure 53 shows a hypothetical cost versus probability of success curve. Each design point on the design chart (left-hand side of Figure 53) corresponds to a single optimum solution for a given probability of success. By finding optimal solutions for multiple POS values, the Pareto Frontier for cost versus POS can be established. The probability of

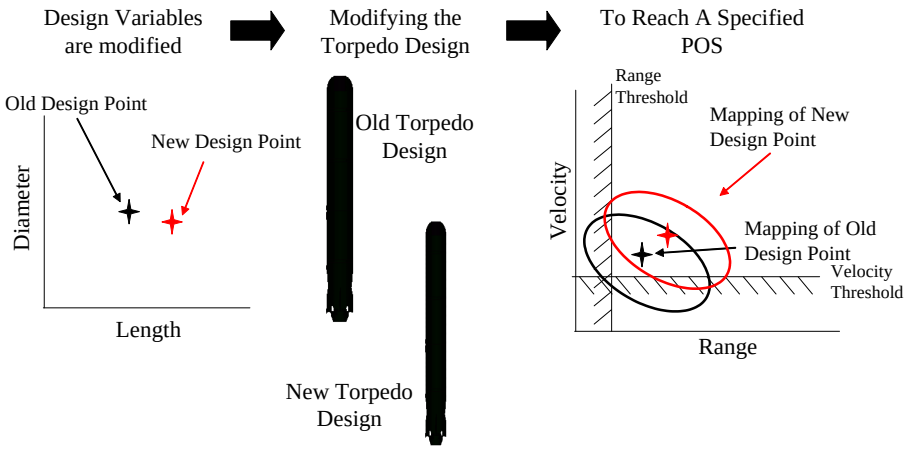

Figure 52: Designing for Probability of Success can Decrease the Likelihood of Constraint Violation

success chart (right-hand side of Figure 53) shows the optimum, or lowest cost solution for each probability of success. By collecting this data, a POS-cost frontier can be created *before making a decision*, allowing the decision-maker to make a better informed tradeoff as to what probability of success, or associated system risk, he or she is willing to accept, since the implications on cost are immediately known.

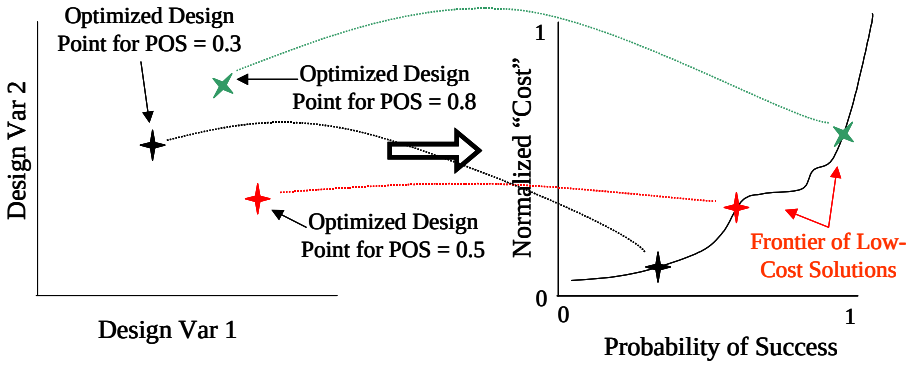

Figure 53: Translation of Design Space to Cost versus Probability of Success

This type of information will also be useful when comparing two potential design alternatives. As Figure 54 shows, the relative cost versus probability of success can be shown simultaneously for two alternatives. With this information, the decision-maker can quickly determine which alternative is the best to pursue, depending upon the amount of risk that

he or she is willing to accept.

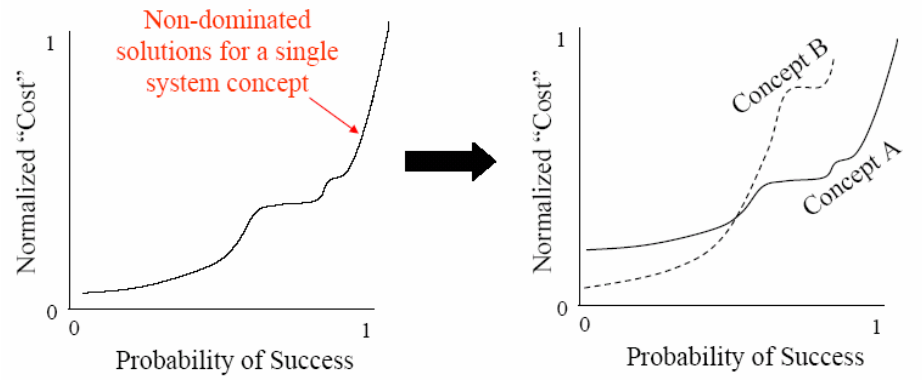

Figure 54: Hypothetical Cost versus POS for Multiple Alternatives

4.1.2 Robust Design Process

The full framework for the robust design process is provided in Figure 55. Again, each step in the framework is somewhat generic in nature, with specific methods able to be 'dropped' into the framework as the problem warrants, meaning that the framework can be custom-tailored to the problem at hand. The first step in this framework is the requirements definition.

4.1.2.1 Step 1: Define Requirements

Before any research can be conducted, the goals of the analysis and potential problems need to be identified. Furthermore, specific system requirements or constraints should be laid out, if they are known. For example, a torpedo may be given a maximum length constraint, or a minimum range constraint.

During this phase of the design process, the metrics of merit should also be identified. The metrics of merit are used to indicate the key goals that differentiate various concepts. For instance, these goals might mean designing a vehicle that weighs the least or has the lowest cost. Or, for a torpedo example, it might be the development of a torpedo system that has the highest overall probability of kill. Multiple goals, or measures of merit, may be chosen. Multiple measures of merit can easily be combined together using the multiple objective decision methods described in Section 3.6, such as weighted sums or TOPSIS.

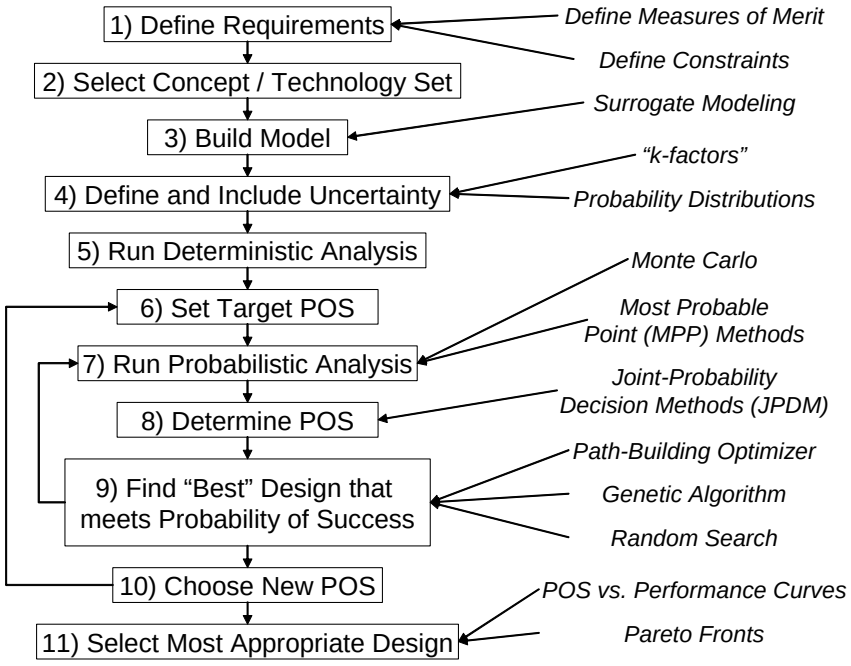

Figure 55: Robust Design Process

These measures of merit may also be probabilistic in nature. For instance, the cost value might be calculated as a probability distribution instead of a point value. In these cases, the probabilistic response must be reduced to a single numerical value, so that it can later be optimized. Therefore, the measure of merit might be defined as the mean of the probabilistic cost value. Or, the measure of merit might be a weighted sum of probabilistic values, such as the mean of the response plus the standard deviation. Finally, the probabilistic measure of merit might be represented as a signal-to-noise ratio. These techniques are discussed in Section 3.6.1 and 3.6.2.

4.1.2.2 Step 2: Select Concept / Technology Set

The next step is to define or select which concepts will be examined, or, which sets of technologies will be placed in the system. Several distinct systems may be examined in order to compare them against each other. It may also be advantageous to define a "baseline" system, which uses common technologies. This baseline system may then be used as a basis of comparison for other concepts. For a torpedo example, different concepts might be a

piston-driven torpedo, an all-electric torpedo, or a super-cavitating torpedo.

4.1.2.3 Step 3: Build Model

In order for an analysis to be conducted, a computer model must be developed. This model must be automated, with as little human interaction as possible (preferably involving no human interaction). Automation is a requirement because the model will be called a multitude of times. This automation should include the ability for the model to be given a set of analysis runs, then have the model conduct the runs and automatically return the results. This level of integration is necessary for later design steps. Advanced engineering environments, as described in Section 3.9, can be used to integrate and automate existing computer tools together.

It is also possible to replace an analysis tool with a metamodel. The advantages to this technique are that metamodels are inherently automated (being little more than a series of equations) and can execute quickly. Extensive techniques for metamodel development and validation are provided in Section 3.4.

In addition, the computer model should incorporate as many facets of the vehicle and its environment as appropriate for the problem. A full system-of-systems model, in which the complete tactical environment with which the vehicle operates is included, provides the most relevant mechanisms for selecting robust solutions.

4.1.2.4 Step 4: Define and Include Uncertainty

The next step in the design process is to define the uncertainty and include it in the analysis tool. Uncertainty is most commonly defined via a probability distribution, but, as discussed in Section 3.3, there are many other methods to characterize this uncertainty. The uncertainty definition that is most appropriate for the problem should be selected. Note that, if multiple concepts are being analyzed, it may be necessary that the uncertainty be individually defined for each concept, depending upon the differences between concepts and the amount of information available.

The second task is the inclusion of this uncertainty into the analysis tool. The analysis tool may already include the capability of analyzing uncertainty, the capability may need to

be added, or the uncertainty could be modeled as "k-factors" as discussed in Section 3.4.4.

4.1.2.5 Step 5: Run Deterministic Analysis

The next step is to generate a baseline point from which to start the analysis. The analysis code (or metamodel) should be run without uncertainty to generate a single, deterministic response. From this response, the performance of the analysis model can be determined as well as validated. In addition, extra deterministic runs may be conducted so that Pareto plots and prediction profiles may be generated. The process for the generation of this plots is described in Section 3.4.3. These tools can then be used to gain an understanding of the design space before large-scale probabilistic analysis is undertaken.

4.1.2.6 Step 6: Set Target Probability of Success

The simplest of all the steps, step 6 requires the selection of a target probability of success. This target probability of success will serve as an initial point for the probabilistic analysis, and later will be the starting point in the determination of the Pareto front.

4.1.2.7 Step 7: Run Probabilistic Analysis

Step 7 is computationally expensive and may require significant amounts of time to set up. It requires the ability to run a probabilistic analysis at the current design point. This analysis must account for all the mechanisms by which uncertainty was included into the problem in Step 4. Potential methods include all of the techniques discussed in Section 3.5, including Monte Carlo techniques, descriptive sampling, and advanced mean value methods. The appropriate probabilistic technique to use is a function of the problem, the analysis run-time, the required fidelity of the results, and the computational power available. Again, an appropriate technique should be selected that best fits the particular problem being solved, there is no one-step solution.

4.1.2.8 Step 8: Determine Probability of Success

The probability of success for the previous probabilistic analysis must now be calculated. There are two primary mechanisms for the calculation of the probability of success. One may use brute-force techniques to simply count the number of individually successful designs

divided by the total number of designs. Or, it may also be possible to estimate the means, standard deviations, and correlation coefficients of the responses in step 7 and use these values to estimate the probability of success. Advanced mean value methods, such as first-order reliability methods, will return a probability of failure value, which can quickly be converted into a probability of success value. These processes are discussed in detail in Section 3.7.

4.1.2.9 Step 9: Optimize to Meet Probability of Success

The next step in the robust design process is to use an optimizer to find the best design that meets the probability of success target defined in Step 6. The best design is defined as the design with the best measure of merit value (as defined in Step 1) that meets the minimum required probability of success. As discussed in Section 3.8, there are many valid choices of optimizers to use. These optimizer choices include gradient-based optimizers, genetic algorithms, or random search. Gradient-based optimizers generally require the fewest number of runs, however, they are very sensitive to noise. When these optimizers are used, it will be necessary to have very accurate estimates of the probability of success at each design point; if Monte Carlo techniques are being used, this entails very large numbers of runs. Also, the probabilistic space is likely to be multi-modal, so multiple starting points will be required to use a gradient-based optimizer.

Genetic algorithms and random searches have advantages because they are significantly less sensitive to noise. Looking back at Figure 7, robust design is only focused on the center region of the probability distribution; the tails are inconsequential. Thus, if Monte Carlo techniques are being used in conjunction with a random search, these optimizers may require significantly less function calls at each design point than a gradient-based optimizer, and may even require fewer function calls overall. Again, the tails of the distributions are only important to the gradient-based optimizer because all of the noise from the system must be removed for the optimizer to perform adequately. A completely random search has the added advantage in that it could be used to simultaneously identify the entire Pareto front for the system, it does not have to be repeated for multiple probability of success

values.

4.1.2.10 Step 10: Choose New Probability of Success

Once the best design for the selected probability of success has been identified, a new probability of success is selected, and steps 6 through 10 are repeated. This process is repeated until the optimum solutions for an entire range of probability of success values have been identified. Note, however, that if a technique such as a random search is used for Step 9, it may not be necessary to repeat the process for multiple probability of success values, as the results of a single random search, with sufficient runs, can be used to identify the entire Pareto front.

In addition, instead of simply selecting an evenly distributed range of probability of success values to capture the Pareto front, the efficiency frontier techniques in Section 3.6.3 could be used to more smartly select the best POS points to analyze. In addition, these techniques include methods to approximate the Pareto front, so that fewer probability of success optimizations may need to be made.

4.1.2.11 Step 11: Select Most Appropriate Design

The final step in the design process is the creation of the Pareto front. This Pareto front would then include every design that represented a distinct, optimum system for the given probability of success. In essence, this process leads to the creation of a product similar to Figure 54. Using this figure, the decision-maker can then intelligently examine the probabilistic results of the analysis. Using this knowledge that details the linkage between cost (or other applicable measure of merit) and probability of success, or risk, the decision-maker can decide what level of risk that he or she is willing to pay for. In addition, the decision-maker can make informed tradeoffs between competing technology sets. This concept of selecting a risk value is similar to the defense department's push, starting in 1995, to make cost an independent variable [119]. As stated by DoD Directive 5000.1: "All participants in the acquisition system ... shall view cost as an independent variable [3]". The new goal will no longer be to make cost an independent variable, but instead *make probability of success an independent variable.* This technique is superior to simply designing

for a single weighted sum, signal-to-noise ratio, or loss function, because the decision-maker is able to visualize the tradeoffs in value and risk *before* the final decision is made.

Again, the framework presented here allows for the plug-and-play type of inclusion of the appropriate tool at each point in the process. Table 12 shows a summary of the steps in the framework, as well as appropriate tools for each step. The table should be used as the primary guide for using this design process.

4.1.3 Robust Design Examples

Several example applications have been analyzed via this robust design process. These examples explore different types of problems, with relevant solutions provided for each. Through these examples the design process will be illustrated, validated, and have its usefulness demonstrated.

4.1.3.1 Traveller Problem

The first example is demonstrated in Section 4.2.1. This is a 2-dimensional example which explores the ability of a traveller to most efficiently cross over a mountain range. This example is purely hypothetical and is intended as a demonstration of the design process. Even though the problem has only two dimensions, it still illustrates the effectiveness of the method in characterizing the results of a multi-modal problem with both uncertainty and multiple alternatives present.

4.1.3.2 Torpedo Analysis using Metamodels

The next example of the robust design environment is shown in Section 6.1. This application looks at using the robust design environment to examine a heavyweight torpedo system. In order to conduct the analysis, a metamodel is developed using a torpedo analysis tool. The example compares the results for two technology sets: a piston-driven torpedo and an all-electric torpedo. Two different optimization techniques are also compared.

4.1.3.3 Torpedo Analysis with Direct Simulation

The third example of the robust design environment is given in Section 6.2. This example is similar to the previous example where a torpedo design is analyzed. However, the example

Table 12: Overview of Robust Design Framework

Process	Description	Relevant Techniques
Step 1: Define Requirements	Define system requirements and measures of merit	Multi-Objective Methods, Probabilistic Measures of Merit (Sec 3.6)
Step 2: Select Concept/ Technology Set	Select concepts, or groups of technologies, that will be examined	Develop "Baseline" System
Step 3: Build Model	Develop an automated, physics-based computational analysis model	Metamodeling Techniques (Sec 3.4) Advanced Engineering Environments (Sec 3.9)
Step 4: Define and Include Uncertainty	Mathematically characterize the uncertainty and include it in the analysis model	Probability Distributions, Fuzzy Logic, Interval Bounds (Sec 3.1, 3.3) "k-factors" (Sec 3.4.4)
Step 5: Run Deterministic Analysis	Analyze a single deterministic point, analyze validity of modeling tool, develop Pareto charts, etc., to understand the design space	Pareto Charts Prediction Profiles (Sec 3.4.3)
Step 6: Set Target POS	Set a target probability of success value for initial optimization	—
Step 7: Run Probabilistic Analysis	Execute probabilistic analysis around the design point to retrieve statistical data	Monte Carlo Methods Descriptive Slamping Mean Value Methods (Sec 3.5)
Step 8: Determine POS	Determine the probability of success value for the point based upon the statistical results in Step 7 and the requirements from Step 1	Estimate Empirical Density Function JPDM Methods (Sec 3.7)
Step 9: Optimize to Meet Target POS	Using an optimizer, repeat the probabilistic analysis from Step 7 and Step 8 until the 'best' system is found that meets the target probability of success	Graident-Based Optimizer Genetic Algorithm Random Search (Sec 3.8)
Step 10: Select New POS	Select a new probability of success target, then repeat steps 7-9, in order to create a range of 'optimum' solutions	Efficiency Frontier Approximations (Sec 3.6.3)
Step 11: Select Most Appropriate Design	Create the Pareto front of optimal solutions from Step 10, allow the decision-maker to use this pareto front to determine the most appropriate design or design alternative	—

differs because a metamodel is no longer used, instead, the analysis is conducted using direct simulation of the torpedo analysis tool. The study is conducted both for a heavyweight torpedo system and a lightweight torpedo system.

4.1.4 Integration of Tactics with Design

4.1.4.1 Effect of Tactics on Torpedo Design

The original goal of this work was to analyze the implementation of a torpedo design tool in conjunction with a modeling and simulation tool that accounted for submarine maneuvers, submarine tactics, the acoustic environment, and various methods for the tactical employment of torpedoes. Unfortunately, such analysis tools, in order to be accurate enough to be useful, are exceptionally complex and tend to be proprietary or classified in nature. As such, it was impossible to obtain the use of appropriate analysis tools for this paper. Instead, an engagement analysis tool was developed that examined the likelihood of a torpedo system being able to locate and prosecute a target (called P_{hit}), without regards to the actual tactics used by the submarine. Because of the limited modeling capabilities developed, a full system-of-systems optimization, linking submarine tactics to torpedo design, could not be performed. Instead, an examination of the impact of the tactical situation at torpedo launch on the design of the torpedo and on the likelihood that it will hit the target. The results of this analysis are shown in Section 7.1.

4.1.4.2 Optimization of Mine Counter-Measure Tactics and Design

A second tactics integration and optimization example was performed by examining the effects of combining tactics and design parameters for mine counter-measure, or minehunting missions. This analysis problem was chosen because the tactics of minehunting and minehunter design could be easily characterized. This easy characterization allows for a real illustration of the advantages that can be gained by exploring the simultaneous optimization of the vehicle design and the tactics, something that could not be illustrated for the torpedo design problem (as mentioned in the previous section). In order to conduct the minehunting optimization, a minehunting analysis tool was developed for which the percent clearance of a minefield could be calculated as a function of time. Uncertainty,

in the form of an unknown number of mines, errors in the track of the minehunter, and uncertainty in the probability of detection, were added to the problem. An example mine counter-measure system was then optimized, both from the standpoint of examining tactics and design parameters individually, and then by examining them simultaneously. This example is discussed in detail in Section 7.2.

4.1.5 Creation of Non-Dimensional Parameters for Torpedo Design

Finally, a study was conducted that looked at ways to improve the method by which torpedoes are characterized in the early phases of design. This improvement focuses on replacing the traditional dimensional design parameters with non-dimensional parameters. By changing the design variables, torpedo characterizations can be created that are more robust, and, equally importantly, work better in the modeling and simulation framework required for the robust design process. The analysis, given in Chapter 8, discusses a method to determine which parameters are effective for torpedo design and shows which parameter combinations are useful.

Figure 56 provides an illustration of the example problems, including how they relate to both each other and the major thrusts of the dissertation.

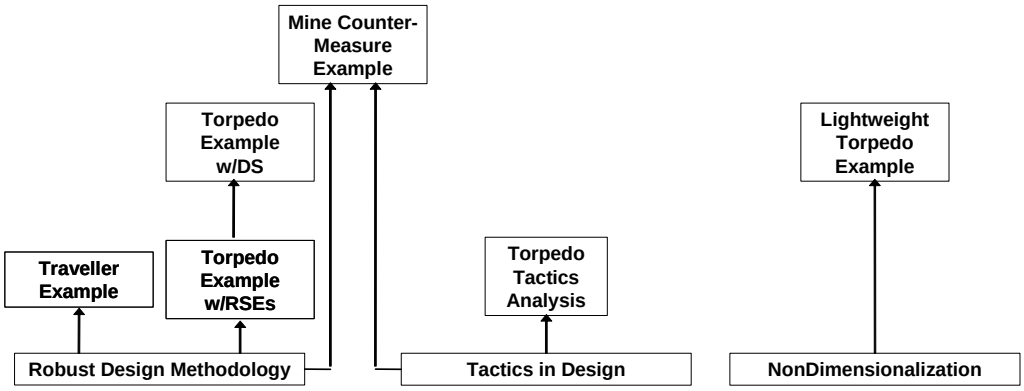

Figure 56: Guide to Methodology Demonstrations

4.2 Illustration of Robust Design Methodology

4.2.1 Problem Setup

The design methodology proposed in Section 4.1.2 is illustrated with a 2-dimensional example. The goal of this example is to create a curve the demonstrates the variation of probability of success as a function of the performance of the system, similar to the hypothetical curves shown in Figure 54. This problem was designed to execute quickly to allow for Monte Carlo analysis, remain in two dimensions for easy visualization, and be as intuitive as possible, so that the design process might be transparent.

The example problem consists of a hypothetical traveller desiring to cross the region between two mountains. The topography of the scenario, with an optimal path illustrated by a dashed line, is shown in Figure 57. The goal of the traveller is to move from the lower-left corner (0,0) location to the upper-right corner (1,1) location, spending the least amount of energy (or time) possible. The traveller is penalized both for increasing height and for walking extra horizontal distance. An objective function for the problem is shown in Equation 23. By changing the relative weightings of α and β in this function, the traveller can be driven towards preferring a longer, less hilly path (low α) or a shorter, more hilly path (low β). In this case, the objective function is analagous to a travel time, with extra time being required to both travel vertical distances and to travel in a round-about manner. The weightings on the objective function would then relate to how quickly a traveller can travel vertically (β) versus how quickly a person could travel horizontally (α). The final addition to the problem is the inclusion of a maximum-height constraint, prohibiting a path from entering a region greater than a specific height.

$$objective = \min(\alpha \cdot \Delta Distance + \beta \cdot \Delta Height) \tag{23}$$

The design variables for this problem were, for ease of implementation, limited to two. In order to fully define a path using only two variables, it was decided that the path would consist of two line segments, one beginning at the start location, one ending at the end location, and both meeting at a 'kink' location in the middle. The x- and y-location of this

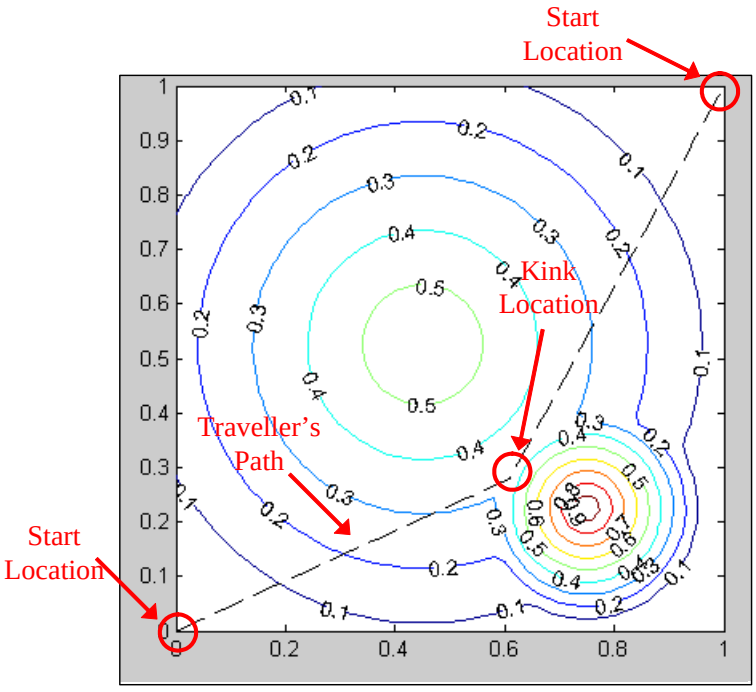

Figure 57: Mountain Topography with Optimal Path

kink point is defined by the two design variables. Figure 57 shows the optimal path for traversing the mountains, with a 'kink' location located at $x = 0.61, y = 0.28$. Using this approach, two design variables, each ranging from zero to one, can capture a large field of potential paths through the mountains.

This design problem was chosen as a testbed for these techniques because of many promising features. For one, since the problem is two-dimensional, it is easily visualizable. Secondly, and just as importantly, the presence of two mountains in the topography makes the problem inherently multi-modal. Figure 58 shows contours of constant objective function, where the objective function has both α and β set to one. As can be seen, there is a minimum in the 'ridge' formed between the two mountains, along with minimums in the corners of the design space. The minimums in the corners of the space correspond to a traveler moving around the mountains.

The design process for this example can be laid out as in Figure 59. Note that the requirements have now been stated, that the traveller find the shortest route under a specified height constraint, and a Matlab model constructed. The next step is the definition of

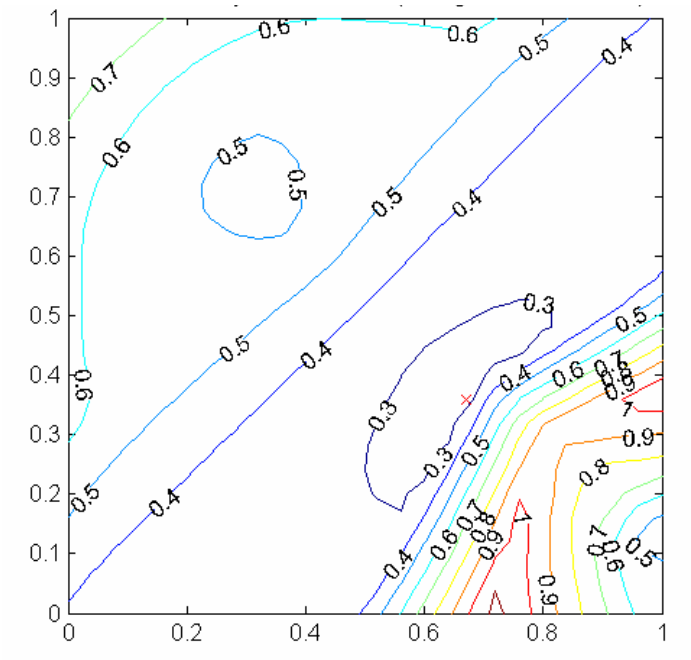

Figure 58: Contours of Objective Function for Kink Locations

uncertainty in the problem, which will be added as probabilistic distributions around the mountain heights. The final solutions will be generated via a metamodel generated from a grid search, and the selection of the designs will come from a gradient-based optimizer.

4.2.2 Addition of Uncertainty

Once the deterministic problem was defined and subsequently solved, uncertainty was added to the problem. In this case, uncertainty was added to the heights of the mountains. This uncertainty would be characteristic of a scenario in which the traveller was not fully aware of the mountain heights before beginning travel. Each mountain height was varied randomly based upon a normal distribution, centered around the original height (0.6 for the wider mountain and 1.0 for the larger mountain). The normal distribution was given a standard deviation of 0.125.

Figure 60 shows the distributions of the mountain height centered around the mean. The distribution results are shown for a 25,000 case Monte Carlo run. The figure also shows what happens to the objective function results when the deterministically determined optimal path is calculated through the Monte Carlo analysis. Note that now, instead of the

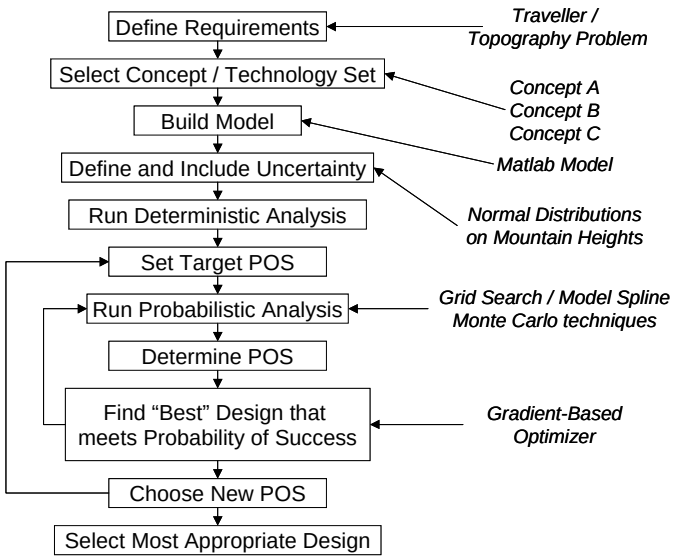

Figure 59: Design Process as Applied to Traveller Example

objective function returning a single objective value for the path, it returns a distribution of objective values, based upon the distribution of the mountains. The effect on the objective function is significant, in many cases, the performance is 50% worse or 50% better than the expected deterministic value, clearly indicating a wide range in performance. Also note that the maximum height that the traveller takes is no longer constant. According to the data in Figure 60, in over 15% of the runs the traveller followed paths that violated that 0.4 maximum height constraint. Since this maximum height constraint is the only constraint in the problem, the probability of success, or the probability of simultaneously meeting all constraints, is 0.85 or 85%.

In order to speed future analysis, a metamodel was created of the design space. Since the design space consists of only two dimensions, a simple 36×36 point grid-search was used. Monte Carlo runs were made for each of these points to generate a grid of mean objective function, signal-to-noise-ratio, and probability of success for each sampled design point. Plots of these results are shown in Figure 61. The metamodel then consisted of a cubic spline interpolation of the 1296 points in the 36×36 grid.

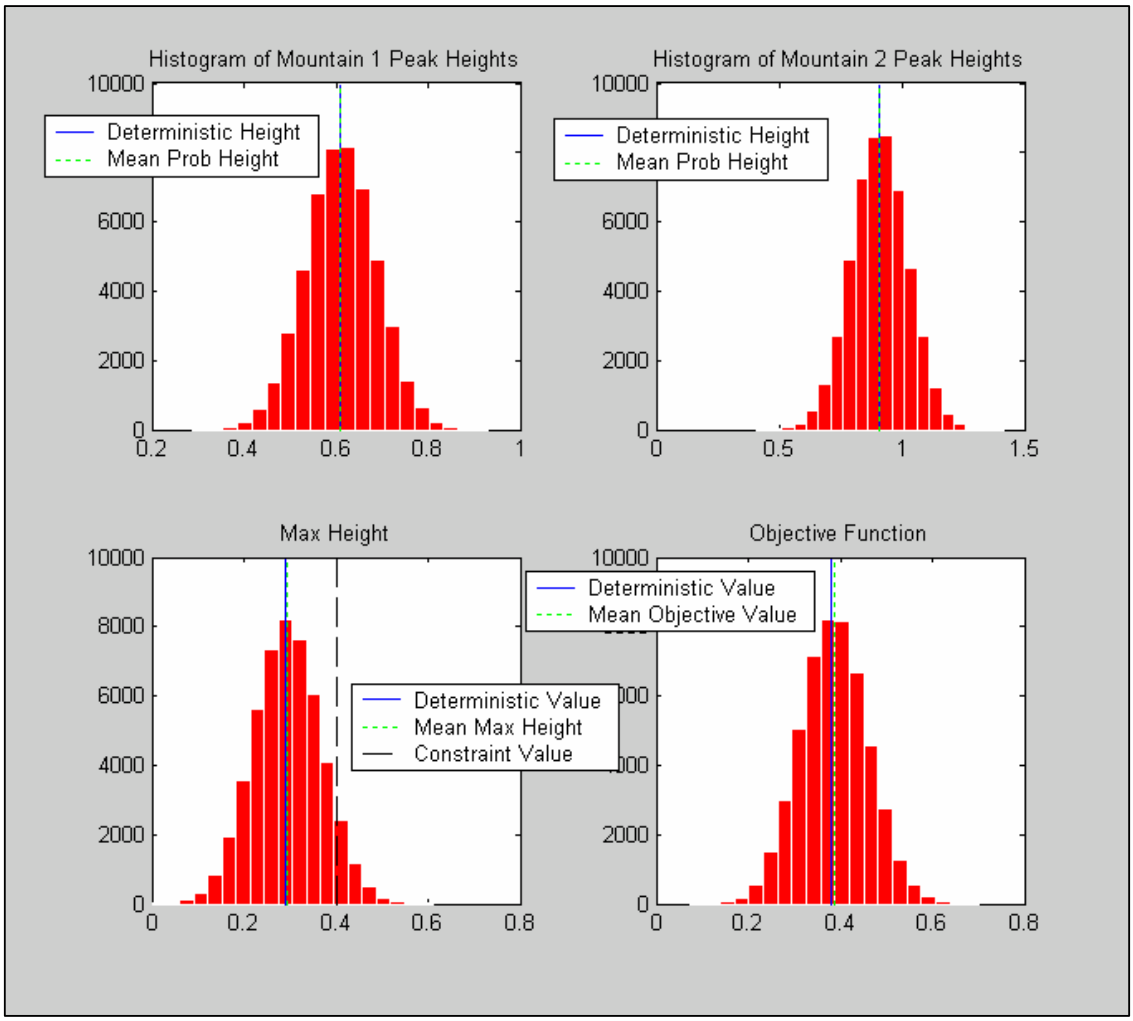

Figure 60: Input Probability Density Functions for the Mountain Heights and Output Distributions for Maximum Path Height and Objective Function

4.2.3 Problem Results

The built-in Matlab optimizer, called 'fmincon' [146], which is a traditional, constraint-based, sequential quadratic programming optimizer, was used to perform optimizations on the metamodel of the probabilistic design space. The goal of the optimizer was to find the location of the path with the smallest mean objective function while remaining within a specified probability of success. For instance, for a required probability of success 0.8, the analysis program would return a mean objective function of 0.43. Thus, if the designer wishes to be 80% confident of reaching his or her goal without violating the maximum

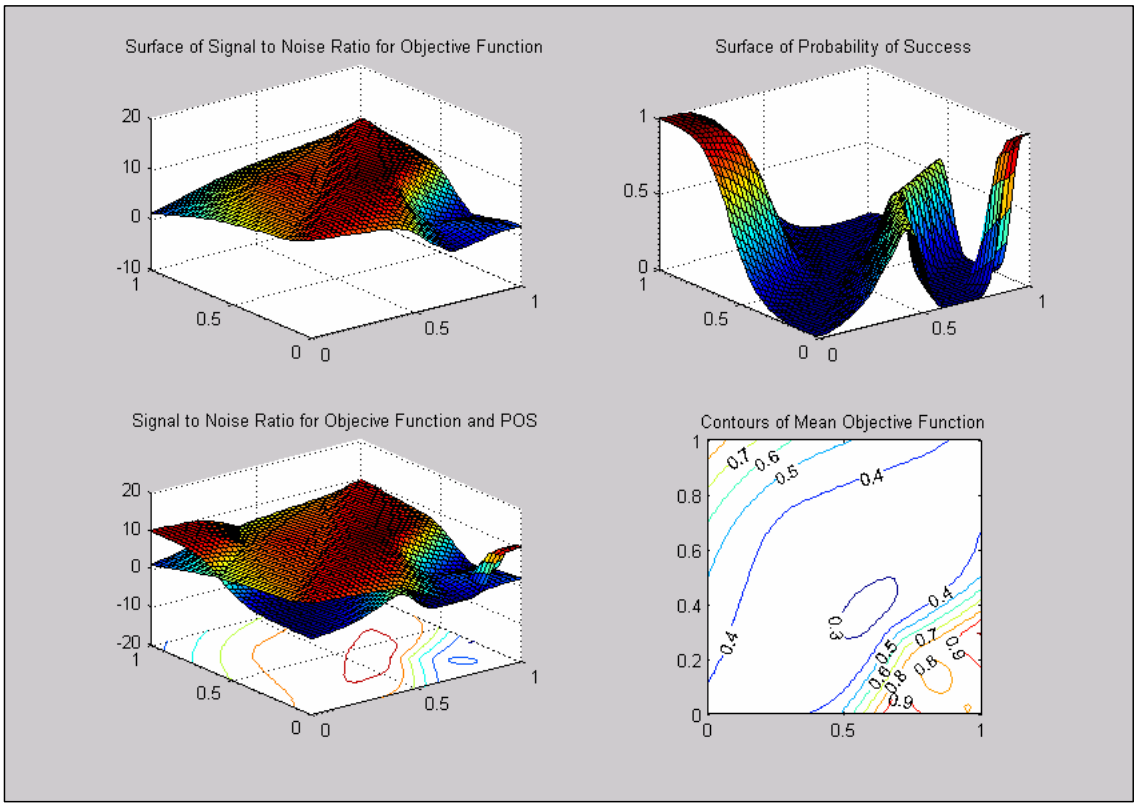

Figure 61: Example Probabilistic Contours for S/N Ratio, Mean Objective Function, and Probability of Success

height constraint, the best value for the mean of objective function that can be obtained is 0.43. Table 13 shows example results for varying probability of successes. Note that as the probability of success decreases, or relaxes, the objective function improves.

These results can be shown graphically, as in Figure 62. Remember that for these figures a lower mean travel time is better and a higher probability of success is less risky. Thus, the perfect solution would be a travel time of zero with a 100% probability of success, which corresponds to a point in the lower right corner of the graph.

In many respects, the curve in Figure 62 behaves as expected. Decreasing the probability of success results in decreasing the mean of the objective function. This is tantamount to saying that increasing the risk that is acceptable allows for an increase in the performance of the system, a very intuitive result and typical of hypothetical risk versus reward curves, as shown in an example investment-risk curve of Figure 63. The trends between the two

Table 13: Optimum Mean of Objective Function vs. Probability of Success

Probability of Success	Opt. Mean Obj. Function
0.20	0.29
0.40	0.29
0.60	0.39
0.80	0.43
0.90	0.48
0.99	0.80

figures are the same: as the risk increases, the reward increases.

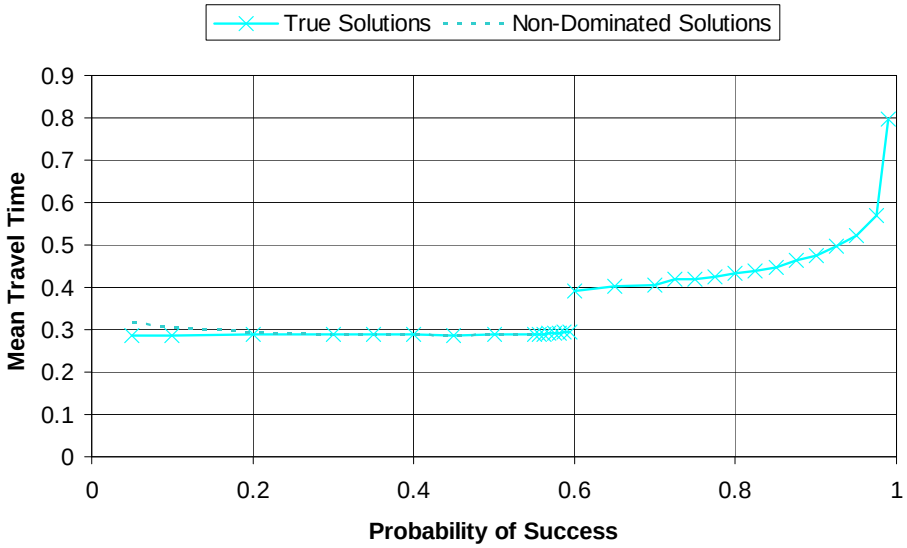

Figure 62: Optimum Mean of Objective Function versus Probability of Success

Some unexpected behavior happens in the left side of the objective function versus probability of success curve (see also Figure 64). In this region, the performance of the system actually increases as the risk is increased, as indicated by the dashed line. This behavior most likely occurs due to the use of an equality constraint on meeting the probability of success. At some point, these equality constraints may 'over-constrain' the solution, driving the solution to a non-optimal answer. Two lines are used in Figure 62 and Figure 64, the dotted line represents the sometimes non-optimal equality constraint values, while solid lines represent the 'best' solution for a given minimum probability of success. These solutions are found when inequality constraints are used, they represent the non-dominated set

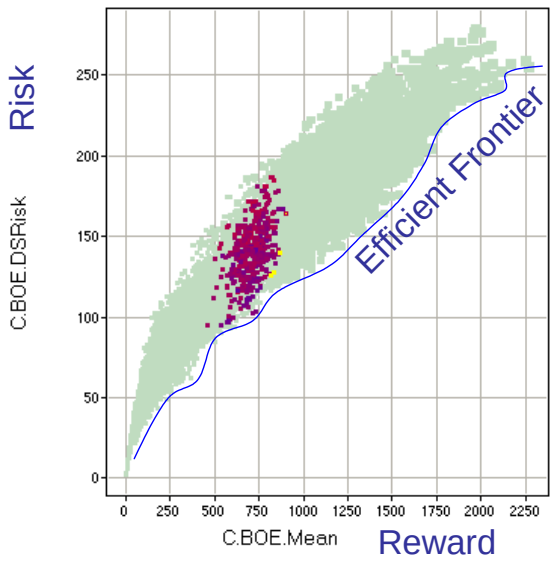

Figure 63: Example Risk vs. Reward Curve with Efficiency Frontier [197]

of solutions.

The second oddity in the figure is the discontinuous 'jump' that occurs at a probability of success equal to 0.6. Each point on the figure represents an optimized solution. Therefore, it would be expected that as the probability of success increases slightly, the optimum would also change slightly, resulting in only a small change in the performance of the system. This continuous change occurs throughout most of the figure which results in the smooth curvature. However, since the example problem is multi-modal in nature, the jump in the figure corresponds to the solution discontinuously changing from one region of the design space to a completely different region. The reason for the discontinuous behavior is because the best solution meets a constraint boundary where it can no longer increase in probability of success. Thus, when a higher probability of success is called for, a feasible solution in this region of the design space is not available, so the solution must be found in a different region of the design space, with less optimal characteristics. In many respects, it can be thought of as a completely different 'family' of solutions in the design space.

If each optimized result were required to be only a small step from the previous result, then the results would be continuous throughout the entire range of risks. Results with this new constraint are shown in the graph in Figure 65. The line of optimal results now

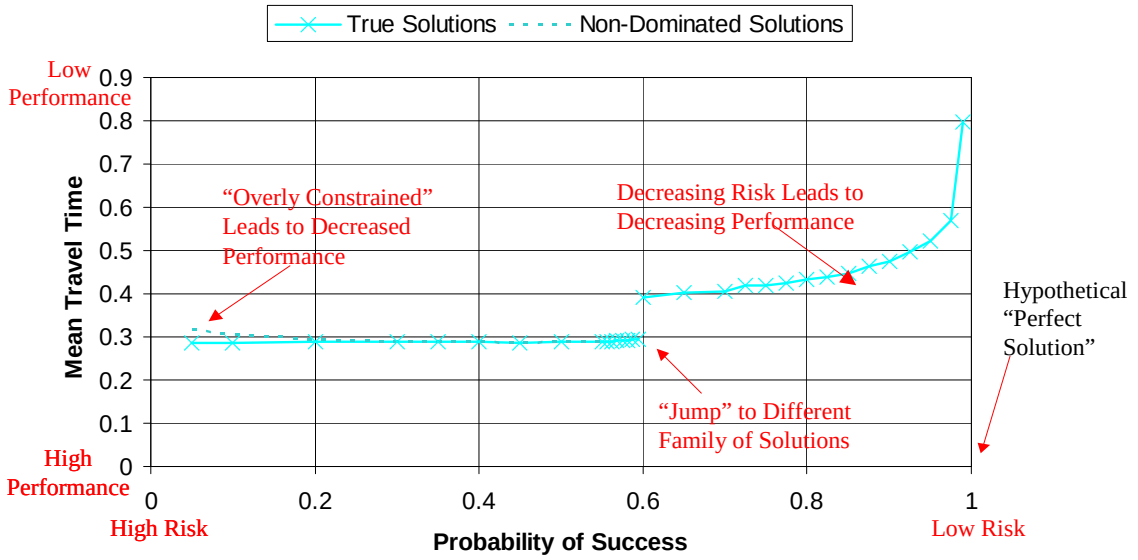

Figure 64: Optimum Objective Function versus Probability of Success Explained

extends continuously down to a POS near zero. The lower (or better performing) solution still ends abruptly at a probability of success of 0.6. This abrupt ending is due to the fact that the solution has hit a constraint 'wall' in this region, with no additional solutions in the same neighborhood that have an acceptable POS. The lesser performing family of solutions (upper line) is completely dominated by the lower line until the point is reached at which the lower set of solutions are no longer feasible.

Figure 66 is a path-inset figure. It shows the same set of optimal solutions as the previous figures, but also contains insets showing the values for the optimal traveller path for each probability of success. Note that there is not much variation between the first two insets. The optimal solution stays in the same general area, which explains why the curve is smooth between these points. However, in the third inset, the optimal solution has jumped from the valley between the two mountains to a path moving around the mountains. This jump, resulting from the multi-modal nature of the design space, is what leads to the discontinuous region in the curve. The next inset shows that the design point moves a little further, but is in the same neighborhood, again illustrating the fact that when the solution remains in the same neighborhood, there is a smooth curve for POS versus travel time. The last inset indicates yet another jump in the design space, which explains the strong kink

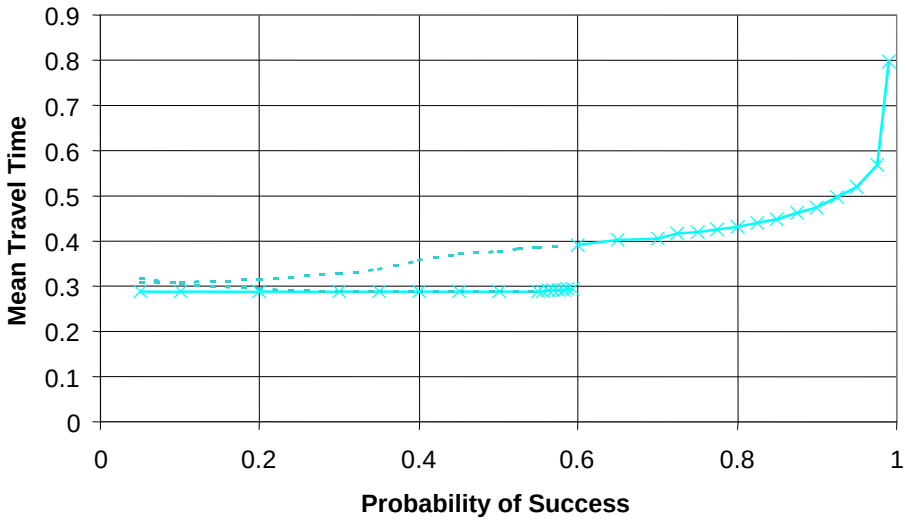

Figure 65: Optimum Objective Function versus Probability of Success w/ Equality Constraints

at the end of the function. This kink at the right-hand side of the figure might better be represented by another discontinuous break, representing the jump in the optimal solution.

Essentially what Figure 66 tells the user is this: the fastest route across the terrain is to travel in the region between the two mountain peaks. But, since the traveller isn't certain about the true mountain heights, this is the riskiest path to take. A safer path (with corresponding higher probability of success) is to go around the larger mountain, but it is likely that this path will be slower than through the valley. Finally, if the traveller wishes to be certain that the trip is successful, going completely around both mountains will ensure a successful trip, but will take the longest time.

4.2.4 Multiple Alternatives

To further examine options for the decision-maker, the mountain topography was again optimized with a second set of parameters used for the objective function. Having a different objective function is akin to using a completely alternative concept for solving the problem. The objective function parameters (α and β) for the initial results had α heavily penalizing the traveler for going long distances and only lightly penalizing the traveler for going uphill. The second concept has the majority of the penalty for going uphill, with small penalties

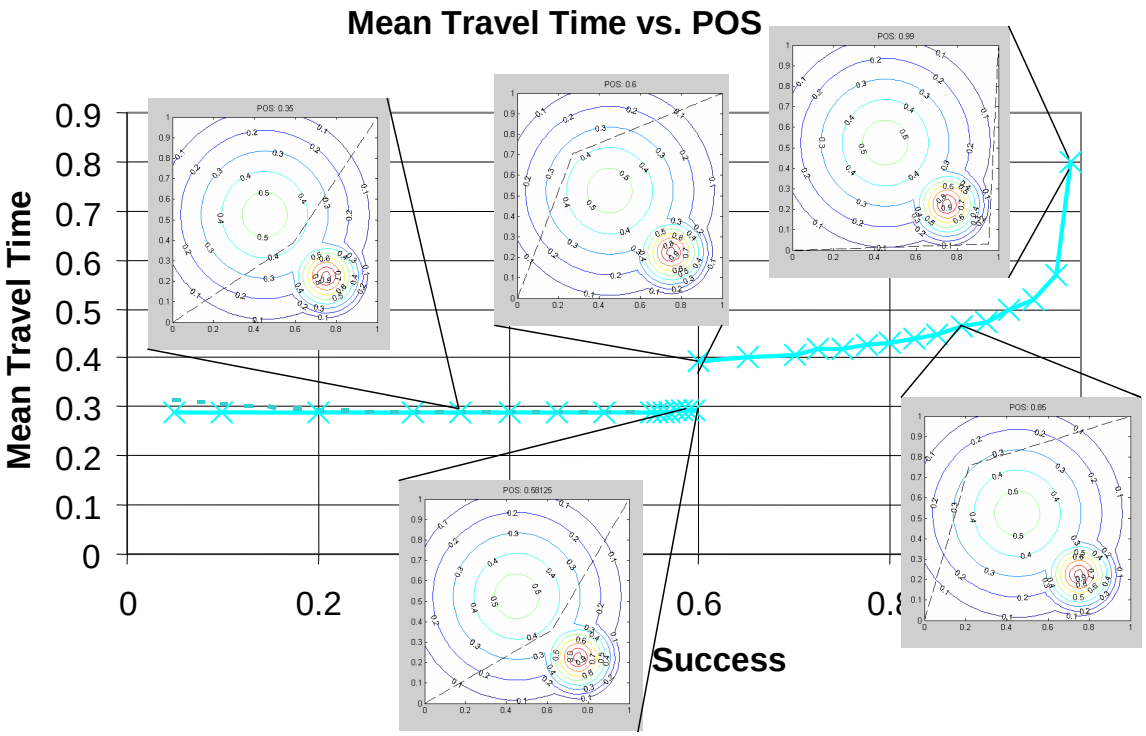

Figure 66: Optimum Objective Function versus Probability of Success w/ Path Insets

for extra horizontal distance. The first concept has a preference for climbing, while the second has a preference for flat land. The new values for the objective function are given in Table 14.

The probability of success versus optimal solution for the two different concepts is shown in Figure 67. As is evident in the figure, the solution for the flat-land preference alternative consists of a straight line. This straight line is due to the fact that the alternative's optimal travel time occurs when it travels completely around the mountains, which also corresponds to the best probability of success. The dashed line for the alternative was generated by constraining the alternative to travel a path with a probability of success exactly equal to the value specified, i.e., an equality constraint was used for POS instead of an inequality constraint. Again, the equality constraint can force the traveller to travel a sub-optimal path. The mean travel time of Alternative Two over these paths greatly increases, as the traveller is forced to travel over the mountain, as opposed to the optimal route, around the mountain. The straight line therefore represents the set of non-dominated solutions.

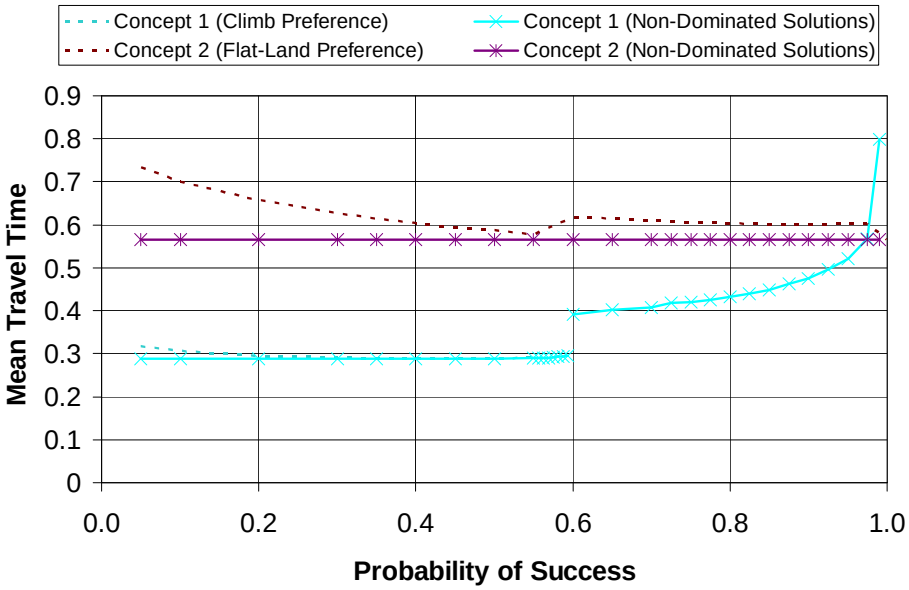

Figure 67: Optimum Objective Function versus Probability of Success for Two Alternatives

Table 14: Objective Function Weightings for Alternatives

		α	β	
Alternative	Preference	Unwillingness to Travel Extra Distance	Unwillingness to Travel Vertically	Maximum Height Constraint
One	Climbing	1.2	0.6	0.4
Two	Flat Land	0.6	1.4	0.4
Three	Baseline	1.0	1.0	0.4

Figure 67 is very useful to a decision-maker, outlining the relative advantages of two distinct concepts. Clearly, if the decision-maker is willing to accept some measure of risk, or a probability of success less than 1.0, Alternative One is the most beneficial, since it has a lower travel time for points where the POS is less than 1.0. However, if the decision-maker is not willing to accept any risk, then Alternative Two is the most beneficial concept, since it has the lowest travel time at a probability of success of 1.0.

As a further example, a third concept was added, with an evenly weighted objective function. Since this path corresponds to having neither a preference for going over the mountains or around the mountains, the concept is a compromise between the climbing preference and the flat-land preference. The three alternatives are summarized in Table 14.

Figure 68 shows the optimized paths when the third alternative is added. Note that this concept always performs worse than Alternative One and Alternative Two. Again, valuable information is provided to the decision-maker, who now realizes that there is no benefit in looking at the compromise alternative, as both the other alternatives are better performers over the entire range of possible risk.

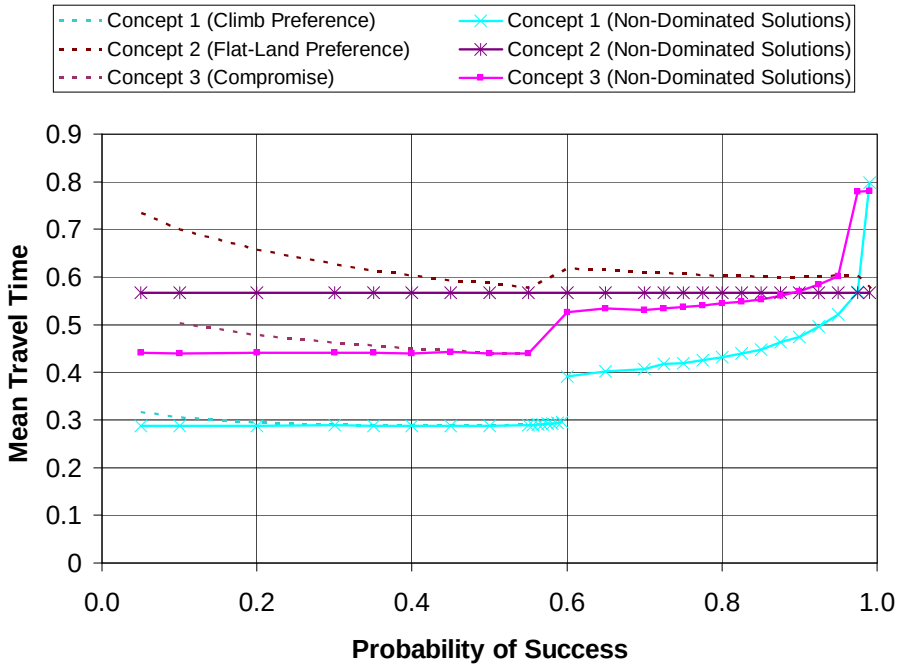

Figure 68: Optimum Objective Function versus Probability of Success for Three Alternatives

The same analysis was repeated for a second mountain topography (created by adjusting the locations of the two mountains). The results are shown in Figure 69. Again, similar behavior is visible as in the earlier example. The compromise alternative's optimal path is always dominated and thus would not be a wise selection. Similarly, Alternative One outperforms Alternative Two at lower probability of successes. However, if a probability of success near 1.0 is desired, then Alternative Two is the preferable concept.

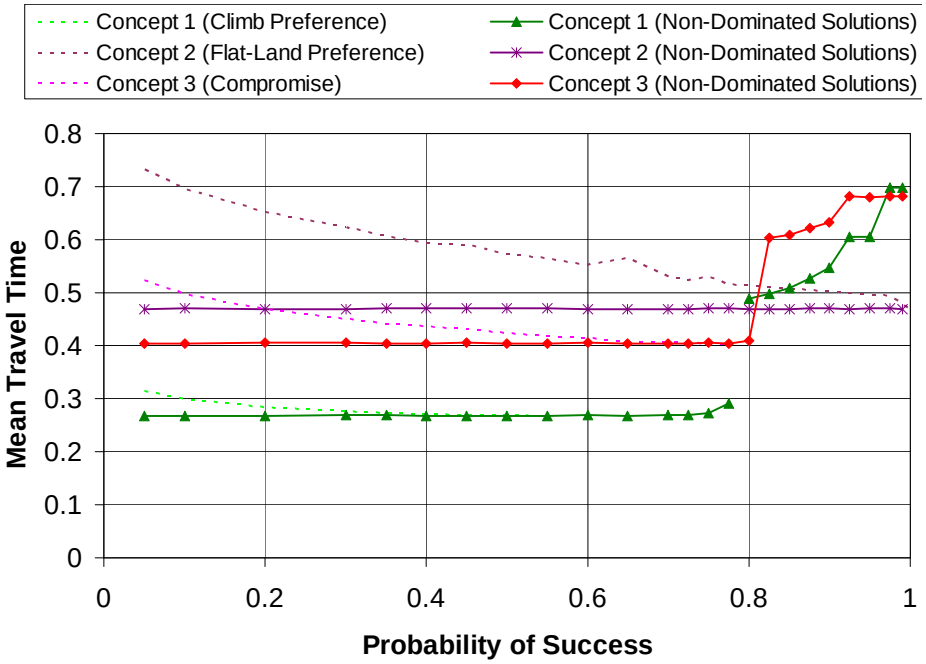

Figure 69: Optimum Objective Function versus Probability of Success for Three Alternatives with Alternate Mountain Positions

CHAPTER V

ANALYSIS TOOL DEVELOPMENT

5.1 Torpedo Optimization, Analysis, and Design Program (TOAD)

In order to conduct an analysis and optimization of torpedo systems, an unclassified analysis tool had to be created. This tool, designated TOAD, was developed specifically to conduct this research in torpedo design. The Torpedo Optimization, Analysis, and Design Program was a joint analysis program developed co-operatively between the Aerospace Systems Design Laboratory and the Naval Undersea Warfare Center. Initial development work begin in the 2001 fiscal year [159]. The TOAD program was developed as an object-oriented, parametric sizing and synthesis analysis program for torpedoes. TOAD was structured with a highly modular, object-oriented architecture, which has facilitated the development of a simplified torpedo design tool that can be easily upgraded in order to add higher degrees of sophistication and fidelity to the analysis.

The TOAD program takes advantage of the fact that torpedo sections can be sized independently [28] by employing separate sizing and analysis modules for each of the internal components and then accounting for the total performance of the vehicle based upon the calculated characteristics of the internal components. The TOAD program currently has analysis modules for several motor types, including a SCEPS engine, an electric and integrated motor propulsor (IMP), and fuel-burning piston and turbine engines. TOAD also contains a warhead module from the Naval Surface Warfare Center (NSWC), along with a custom-made propulsor performance code from the Naval Undersea Warfare Center (NUWC) and a guidance, navigation, and control (GNC) electronics sizing package from Penn State's Applied Research Lab. The TOAD program is currently used by multiple research organizations and has been used to size torpedo systems of different architectures.

A comprehensive User's Manual has been written for TOAD and provides all of the information necessary to use and understand the program [158]. Included in the manual are complete descriptions of the inputs and outputs for TOAD, the algorithms used in the program and several examples for reference. Figure 70 shows the development history for TOAD from 2001 to the present. Figure 71 shows the current analysis capabilities in TOAD and the collaborating laboratory for each.

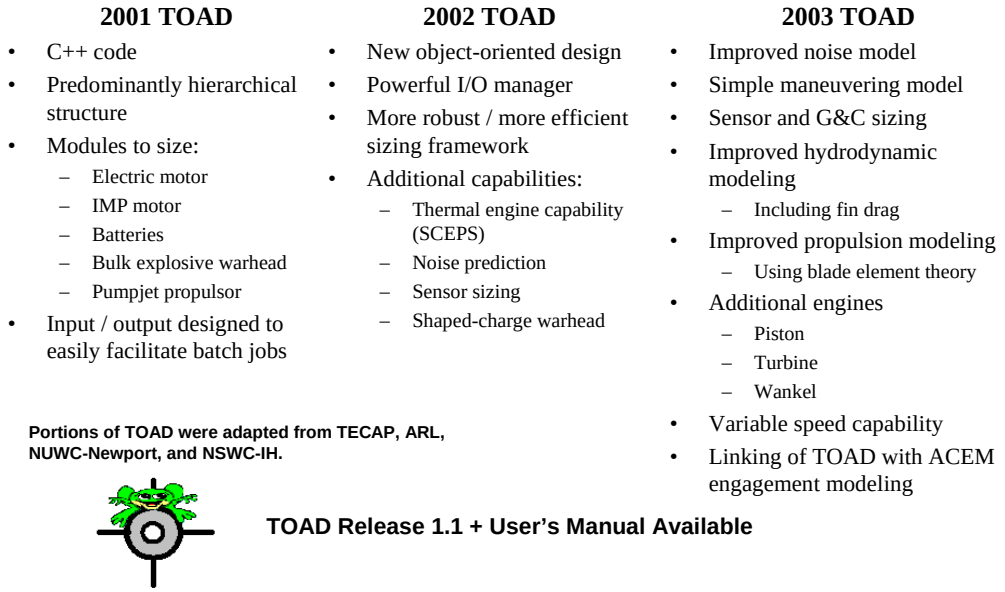

Figure 70: Evolution of the Torpedo Optimization, Analysis, and Design Program (TOAD) [237]

TOAD uses input or design variables such as the type of torpedo propulsion system, outer diameter, operating depth, energy section length, power density, and motor horsepower. It then calculates the overall torpedo length and weights, which are often constraints for launcher compatibility, and torpedo performance metrics, such as maximum velocity, range, and radiated noise. Table 5 in Section 2.1 has a very good breakdown of all the individual sub-systems modeled in TOAD, along with the inputs, outputs, and sizing rules. Key inputs and outputs for TOAD are summarized in Figure 72.

To the greatest extent possible, results from TOAD have been compared against several existing torpedoes in order to provide some preliminary validation of its results. Torpedoes

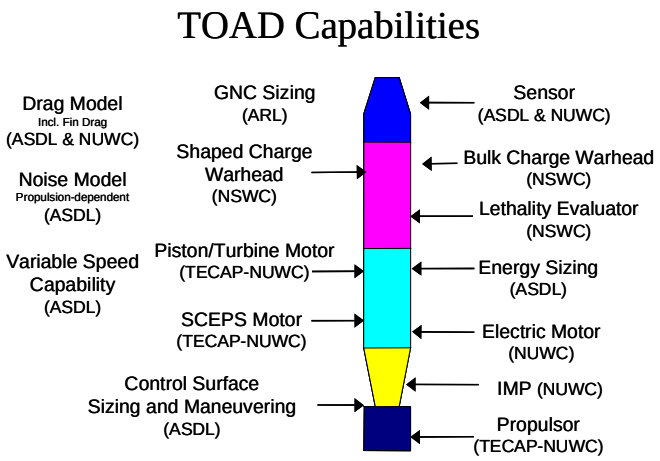

Figure 71: Components of the Torpedo Optimization, Analysis, and Design Program (TOAD)

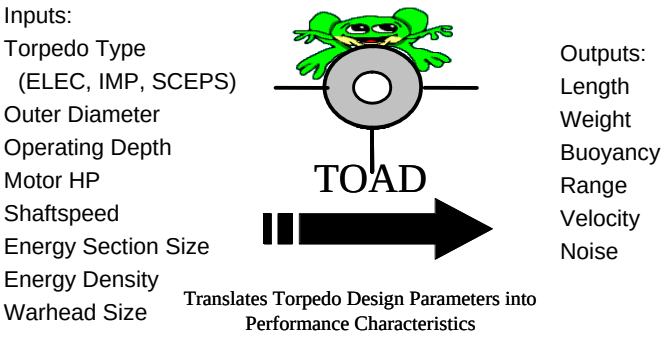

Figure 72: Inputs and Outputs of TOAD

were designed in TOAD that attempted to match the physical characteristics and performance of the Mk-46 -48 and -50. A summary of the matching cases is shown in Table 15. The results match very nicely, particularly considering that some input values were not publicly available and were estimated, such as sensor and electronics information. TOAD has been used to perform simple deterministic design space explorations for several different types of torpedo systems and now has the sophistication to produce meaningful results [71].

5.1.1 Iteration Process

The torpedo system is iteratively sized. The iterative sizing process is shown in Figure 73. To begin the iteration process, the front end of the torpedo, which includes the sonar,

Table 15: TOAD Validation Results [158] with Historical Data from [2] and [68]

	Mk-46 Piston Lightweight			Mk-48 Piston Heavyweight			Mk-50 SCEPS Lightweight		
	Historical	TOAD	Error	Historical	TOAD	Error	Historical	TOAD	Error
Diameter (in)	12.75	12.75	0.0%	21	21	0.0%	12.77	12.77	0.0%
Length (in)	102.36	100.0	2.3%	240	251.4	4.7%	114.1	121.3	6.3%
Weight (lb_m)	517.65	566.9	9.5%	4000	4085.8	2.1%	800.42	756.3	5.5%
Velocity (kts)	45	44.8	0.4%	55	53.2	3.3%	55	58.0	5.4%
Range (nmi)	6	6	0.0%	20.5	20.5	0.0%	8	8	0.0%
Power (hp)	---	90	---	---	375	---	201.2	201.2	0.0%
Warhead (lb_m)	98	98	0.0%	650	650	0.0%	100	100	0.0%

electronics, warhead, and fuel tank, is fixed at a specific size. This size is defined by the diameter of the torpedo and the individual section length inputs. The front-end of the torpedo is sized only once and remains constant for the entirety of the iteration process. Next, the motor is sized based upon the input diameter, horsepower, and RPM. The propulsor is sized last, based upon the global diameter input, along with the RPM and the horsepower delivered by the motor. For this analysis work it is assumed that there is a direct drive shaft connecting the propulsor and the motor; no gear-box is present, thus requiring both the motor and propulsor sub-systems to have identical RPM values. The propulsor uses this data to calculate the power delivered, or the power transmitted into the water to propel the vehicle. These calculations are made using traditional blade element/momentum theory for a two-element, ducted propulsor configuration [42]. Drag produced by the interactions between the propulsor and the torpedo, called the wake fraction and thrust deduction [198], are modeled with data from Mautner and Burcher and Rydill [34][148].

Once the vehicle is initially sized, the vehicle drag coefficient is estimated. This estimation is based upon drag data found in references [95], [106], and [107]. The final velocity of the vehicle is determined by conducting a force and power balance. The forces in the vertical direction: weight, buoyancy, and dynamic lift, must balance each other, as well as the forces in the horizontal direction: thrust, form drag, and induced drag. This force balance is displayed in Figure 74. Since the propulsor size is a function of the vehicle velocity, once the new vehicle velocity is determined, the propulsor must be sized again, following the iteration loop laid out in Figure 73. A detailed description of the TOAD vehicle-level

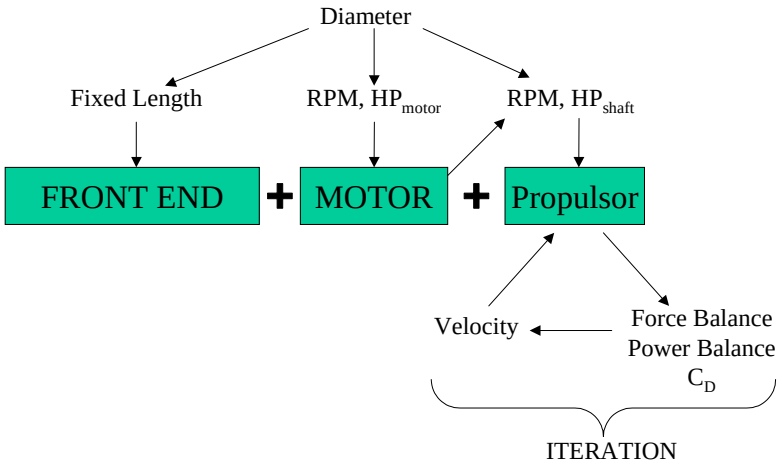

Figure 73: Iteration Procedure of TOAD

analyses for drag, velocity, range, and noise is given in Appendix B.

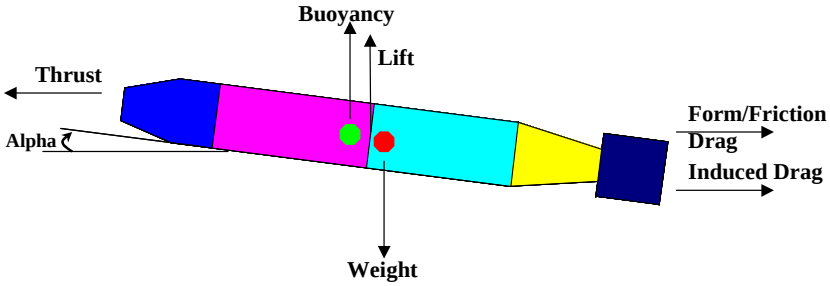

Figure 74: Force Balance in TOAD Sizing

5.1.2 TOAD Failure Modes

A key element of this research is looking at regions of the design space for which valid torpedo designs cannot be created, known as the infeasible region of the design space. There are many mechanisms that drive torpedo designs to become infeasible. In the case of the TOAD torpedo design tool, most of the reasons for failure are found in the propulsor component of the torpedo. One such failure mechanism is when the torpedo propulsor cannot meet a $C_{L_{max}}$ constraint. The propulsor is little more than an airfoil rotating in the flow. The airfoil shape being used is a NACA 66-mod(TMB) blade section, whose performance data can be found in Reference [6] and [43]. The power (or thrust) delivered

by the propulsor blade is proportional to the C_L of the airfoil and the square of its velocity relative to the flow. If a design situation occurs in which the C_L required to generate the required power is greater than the $C_{L_{max}}$ of the airfoil section, the propulsor is unable to deliver the required performance, and hits a $C_{L_{max}}$ constraint. A second failure mode occurs when the torpedo begins to cavitate. Cavitation occurs when the decrease in the fluid pressure over various blade surfaces drops below the vapor pressure of the fluid. In this situation, pockets of gaseous water vapor develop, significantly lowering propulsor efficiency, creating large amounts of noise, and potentially damaging the propulsor. A third failure occurs when the analysis program is unable to converge to a solution. This error often occurs when the force balance (Figure 74) cannot be resolved. Such a problem may occur when the torpedo does not have sufficient velocity and thus needs a larger engine, or if other propulsor modeling errors are driving the propulsor efficiency so low that the system cannot generate sufficient power. A final failure mode develops from the historically-based thrust deduction model that is being used [34][148]. If the propulsor parameters of the torpedo lie outside of the validity of the model data, an error is reported. However, this error is not a function of the physics, but simply indicates that there is insufficient data in the drag model. If necessary, the thrust deduction could be extrapolated into this region. For this work, the data was extrapolated so that this region of the design space was still considered to be 'feasible'. Table 16 provides a summary of the common modes of failure for the TOAD analysis program.

Table 16: TOAD Failure Modes

Failure Mode	Relevant Torpedo Section	Reason	Solution
C_{LMax} Constraint Violation	Propulsor	Propulsor airfoil is unable to meet the required C_L	Decrease blade loading by decreasing power requirements, or increasing diameter or RPM
Cavitation Constraint Violation	Propulsor	Propulsor airfoil has too large of a pressure difference, dropping the static pressure below the fluid's vapor pressure	Increase Diameter
Unable to Converge	Propulsor / Torpedo	Propulsor is unable to provide enough power to resolve the torpedo force-balance May also be caused by other constraint violations	Increase motor power Prevent other constaint violations
Thrust Deduction Model Outside of Bounds	Propulsor	Propulsor is operating in a regime outside of the available database	Limit propulsor designs to within previous data, or extrapolate available data

5.2 Torpedo Design Results

Several design studies have been made using the TOAD program as a stand-alone tool. In these studies, various designs of experiments were run and response surface equations constructed for metamodels. From these analysis runs and metamodels, useful results were obtained from the program. Examples of these results will be shown here. The first such result is an example Pareto chart in Figure 75, the energy section length and the outer diameter dominate the response of torpedo range, while the motor horsepower and diameter are the biggest drivers for the response of torpedo velocity. These charts show that intelligent selection of the outer diameter of a torpedo is paramount for a well-performing design.

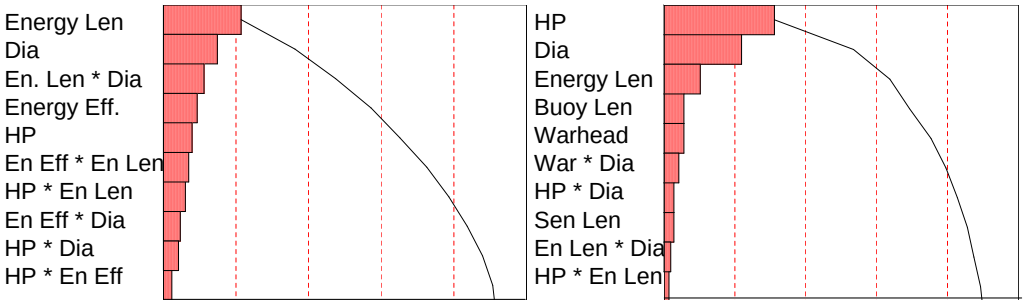

Figure 75: Pareto Plot for Range (left-hand side) and Velocity [160]

A large prediction profile was generated from the design results and is shown in Figure 76. Note that the system behaves as expected, for example, increases in outer diameter decrease the length of the torpedo, but also increase the weight. Increasing the motor horsepower increases both the velocity and radiated noise of the torpedo while decreasing the range. All are behaviors that should be expected in the torpedo system.

Another product of torpedo studies is the contour plot, Figure 78. This plot is also created in JMP using data from the metamodels created from TOAD. The contour plot in Figure 78 shows two input parameters for the electric torpedo, the length of the energy section (containing the batteries) on the x-axis, and the motor horsepower on the y-axis. Constraints were then placed on the plot, indicating a maximum noise criteria, maximum length and weight, and minimum speed and velocity constraints. These constraints very visibly define the feasible design space available to the torpedo designer. These examples

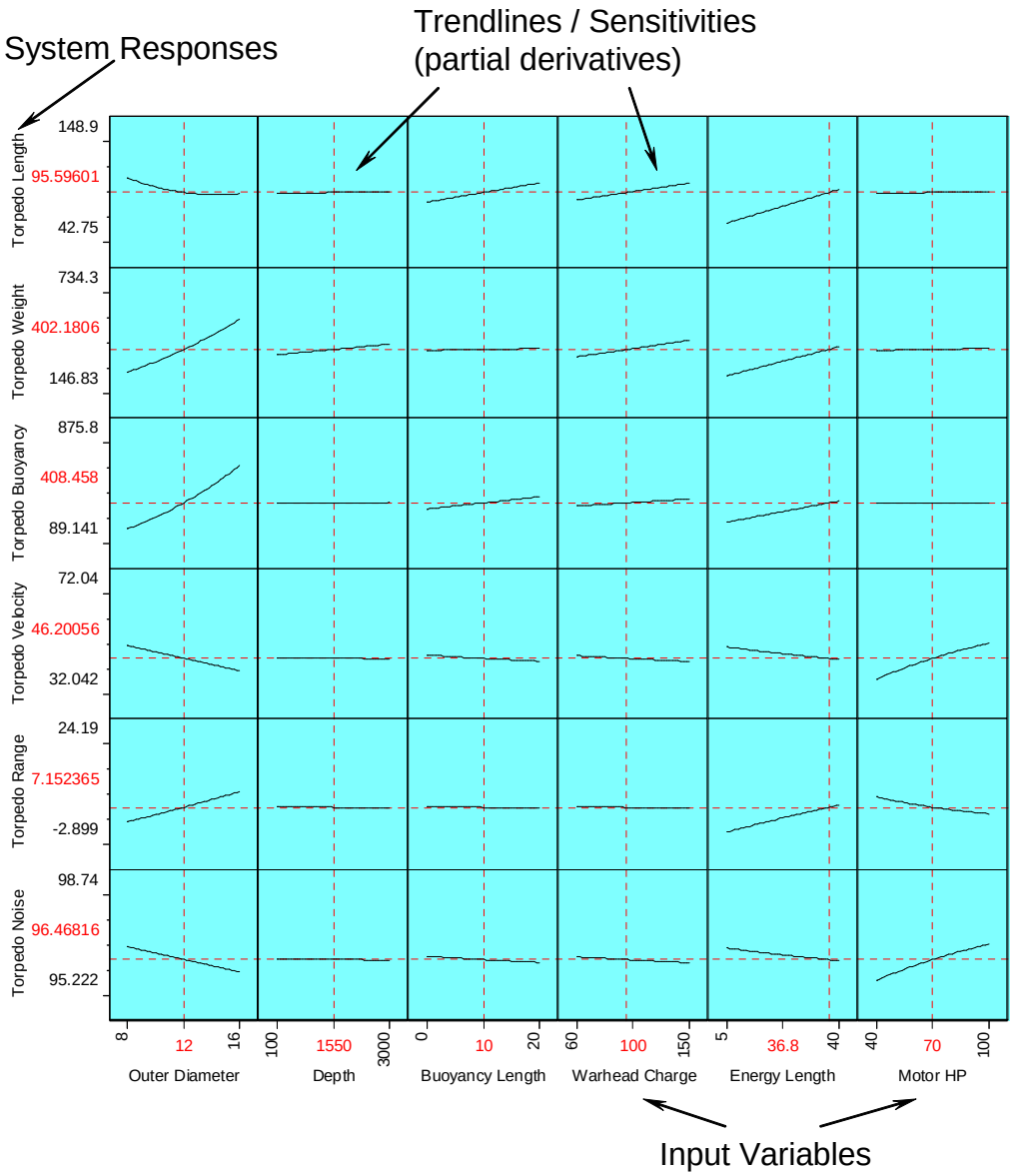

Figure 76: Prediction Profile for an Electric Torpedo [160]

serve to show how easily TOAD can be used in conjunction with the functionality of JMP and ASDL's advanced design environment [122].

5.2.1 Uncertainty Analysis using TOAD

In order to handle uncertainty, "k-factors" were added to the TOAD analysis tool. "K-factors" are often used to model the use of future technologies or uncertainty [122]. The factors work as multipliers to interim values in the code, such as estimated drag and system

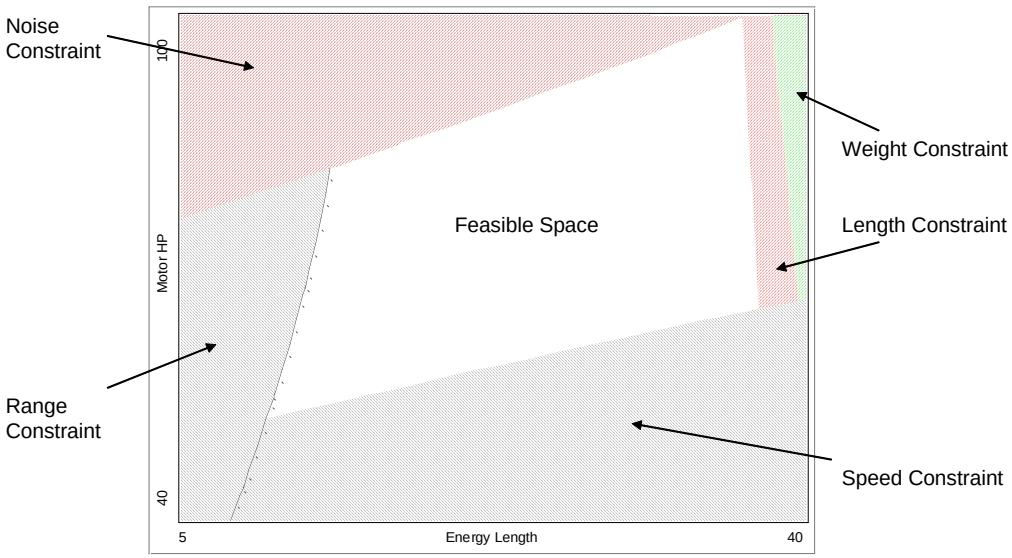

Figure 77: Contour Plot for an Electric Torpedo [160]

efficiencies. The factors thus affect the predicted performance of the system by changing internal values. In this form, the "k-factors" represent the inability of the individual analysis tools to predict the final results, i.e., the inability of the motor module to accurate predict the motor efficiency. This uncertainty would be defined as "acknowledged error" and "aleatory uncertainty" as defined by Oberkampf (Section 3.1), as it represents approximation and inaccuracies in the design program and variations in the construction of the torpedo program. These "k-factors" thus can model the uncertainty between the proposed design and the actual torpedo system. A list of the "k-factors" used in TOAD is given as Table 17.

Table 17: Uncertainty "k-factors" Built into TOAD

Uncertainty "k-factors"
Estimated Drag
Battery Efficiency
Motor Efficiency
Propulsor Efficiency
Radiated Noise

Figure 78 is a Prediction Profile that shows the relative effects of design variables and

uncertainty "k-factors" in TOAD. Note that, in many cases, such as velocity, a change in the value of the uncertainty multiplier in TOAD has a greater effect on the outcome than changes to the design variable. The prediction profile therefore shows that the effects of uncertainty is definitely of the same magnitude as the design variables. The Pareto charts in Figure 79 and Figure 80 show the Pareto charts for the torpedo range and velocity. These charts indicate the relative contribution of each input variable to the response. Note how the uncertainty "k-factors" contribute a large amount of the response for these two critical torpedo measures of merit. Therefore, any torpedo analysis that does not account for this uncertainty will potentially contain significant error.

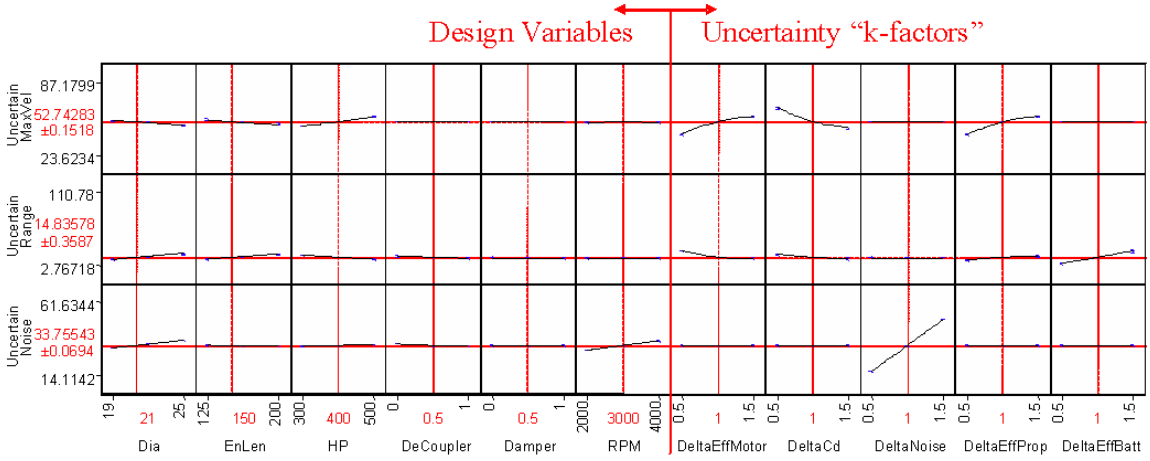

Figure 78: Contour Plot for an Electric Torpedo with "k-factors" [157]

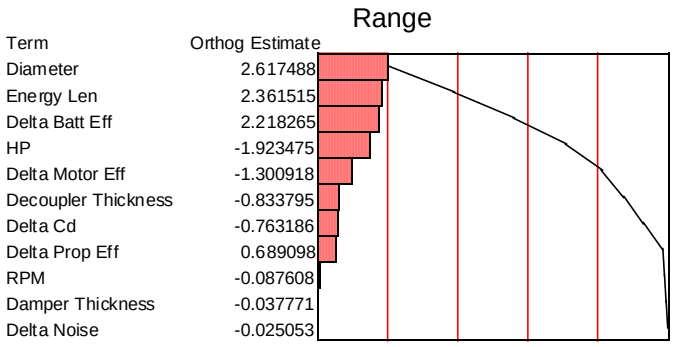

Figure 79: Pareto Chart for Torpedo Range, Including Uncertainty

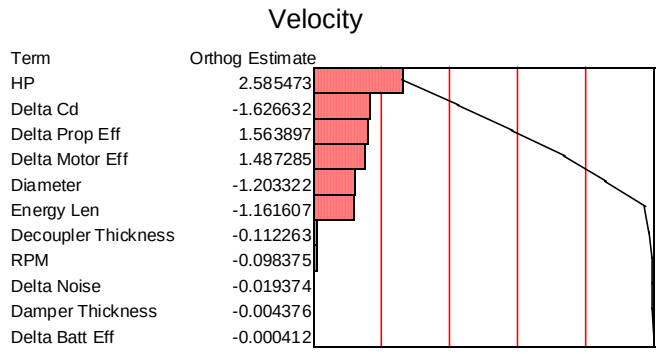

Figure 80: Pareto Chart for Torpedo Velocity, Including Uncertainty

5.3 Visualization Tool Development

Bringing a lot of probabilistic elements into the design process brings more challenges to the decision-maker. With more data available to assist the decision-maker in selecting the best design, it becomes a challenge to present the data in a concise, easy-to-understand manner. A torpedo visualization tool was developed at ASDL that can help present the probabilistic data to the designer [79] [157]. This tool was developed in Matlab and addresses many of the visualization needs required when dealing with large amounts of probabilistic data. Figure 81 is a snapshot of the visualization tool.

The visualization tool allows the designer to look at the available points in the design space and graphs these points as a function of probability of success versus any metric of merit such as weight, cost, or length. The tool automatically identifies the Pareto points for the currently selected metric and allows the user to select any design point for a more detailed investigation. Selecting a design point brings up a scaled, rotatable image of the specified torpedo design, along with the relevant design parameters and responses. The image of the torpedo is color-coded to show the multiple sections of the torpedo system. From back to front they are: sensors, warhead, fuel/energy section, motor and afterbody, and the propulsor. The visualization tool thus provides a mechanism by which the decision-maker can quickly see the relative size of makeup of torpedo systems.

In addition, as shown in Figure 82, the visualization tool can be used to simultaneously compare two torpedoes. The tool also allows the graphing of two distinct sets of data, which

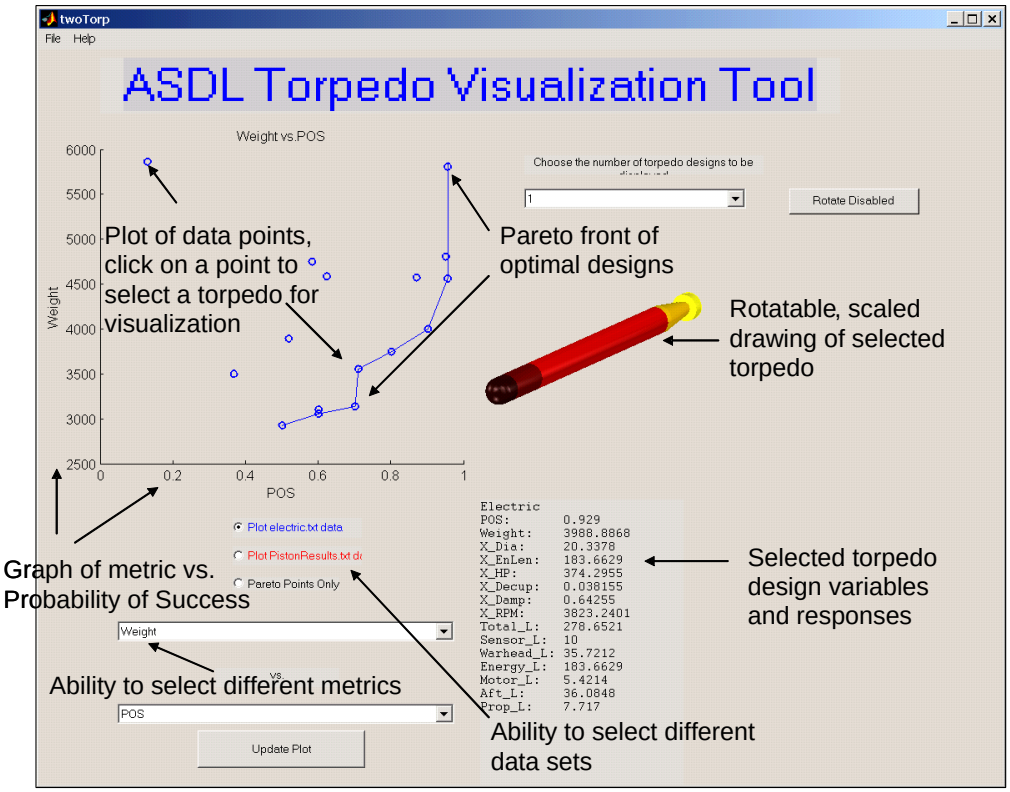

Figure 81: Snapshot of Torpedo Design Visualization Tool

allows for the comparison of two torpedo alternatives (such as electric vs. piston), or allows for the comparison of various technologies. An example of this is shown in Figure 83, with an electric torpedo shown by blue points and a piston torpedo shown by red points.

The visualization tool was developed to allow for the examination and tradeoffs between large numbers of potential torpedo designs. By quickly identifying (and reducing) the torpedo points to a Pareto set, regardless of which metric the designer chooses, the visualization tool allows for the quick examination of large numbers of runs – a particularly useful feature when genetic algorithms or random searches are used to generate large numbers of feasible designs. The tool is dynamic in nature, using pre-generated analysis sets, allowing for the decision-maker and disciplinary experts to interactively make decisions. Figure 84 shows an example where the visualization tool is used to define and examine the best designs from a large torpedo data set. The visualization tool is used extensively in the visualization of torpedo design results throughout this work, where its capabilities are further illustrated.

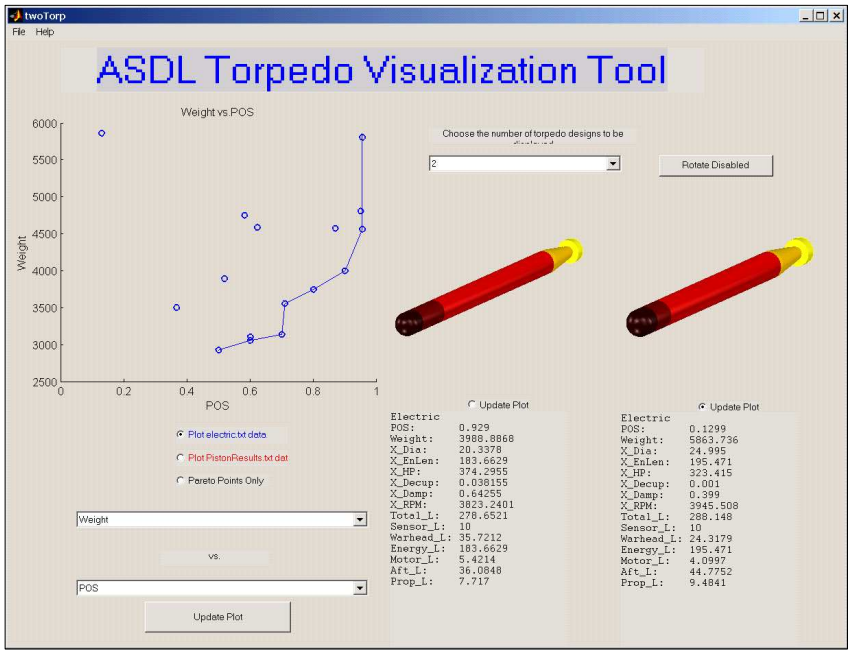

Figure 82: Visualization Tool Comparing Two Concepts

Currently, the ASDL torpedo visualization tool has the following capabilities:

- Graphically shows the relative merit of multiple design points
- Shows these design points as a function of probability of success versus any metric
- Generates an appropriately scaled rendering of any individual design point
- Color-codes the torpedo subsystems in the rendering
- Allows the user to rotate the torpedo rendering
- Displays the specific design variables and responses for the selected design point
- Displays multiple torpedoes simultaneously, allowing for direct comparisons
- Automatically identifies and highlights the Pareto points for the current metric
- Allows the interchanging of multiple data sets
- Graphs multiple data sets simultaneously so that different alternatives or technologies can be compared

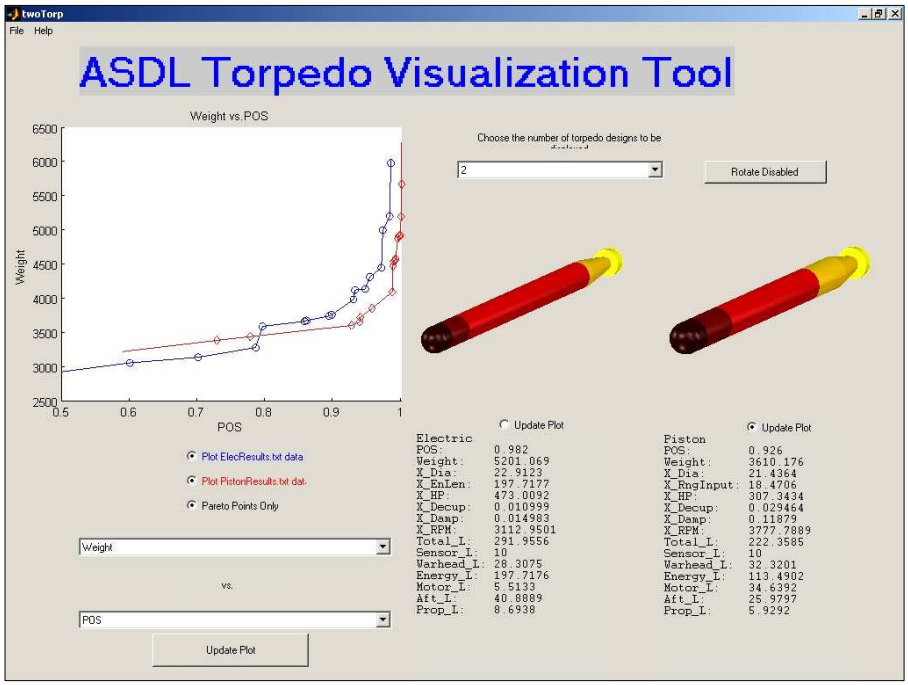

Figure 83: Visualization Tool Comparing Two Technology Sets

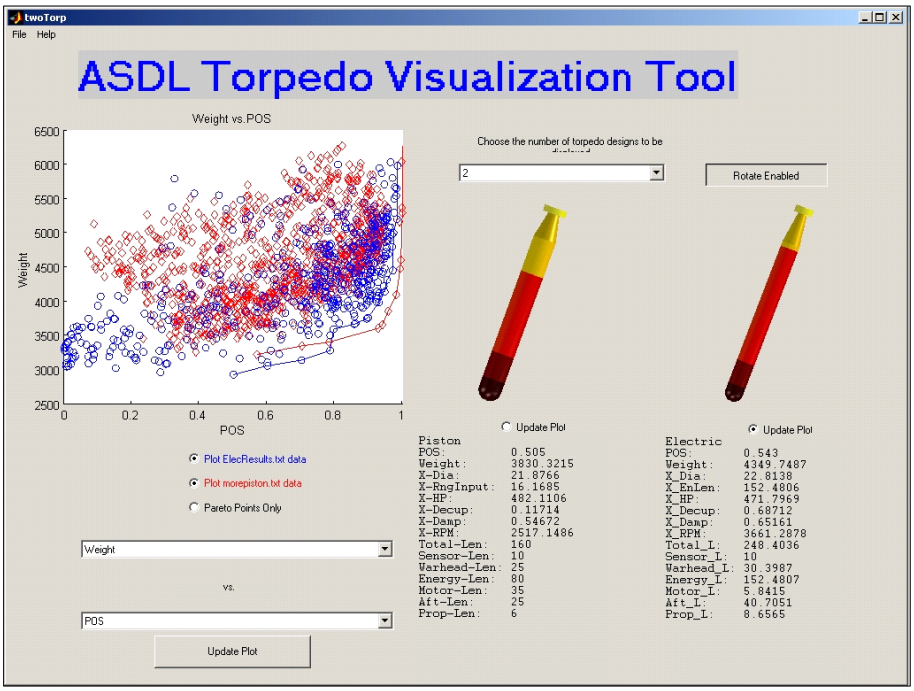

Figure 84: Visualization Tool Being Used to Identify Points from a Random Search

CHAPTER VI

IMPLEMENTATION OF ROBUST DESIGN PROCESS WITH TORPEDO SYSTEMS

The uncertainty analysis on torpedoes will use the framework for robust design discussed in Section 4.1. Uncertainty multipliers integrated into the TOAD program (Section 5.2.1) will be used for the analysis. These uncertainty multipliers are listed again in Table 18. The terms represent uncertainty that is defined as both acknowledged error and aleatory uncertainty by Oberkampf [182], which represent the designer's lack of knowledge about the final torpedo design resulting from the use of simplified analysis tools, along with variations in the manufacture of the torpedoes. Oberkampf suggests that probability distributions can be used to adequate capture this uncertainty, therefore, for this problem, probabilistic uncertainty distributions will be used in conjunction with the uncertainty parameters.

Table 18: Uncertainty Multipliers for Torpedo Design

Uncertainty Multipliers	Mean	Standard Deviation
Estimated Drag	1.0	0.1
Battery Efficiency	1.0	0.1
Motor Efficiency	1.0	0.1
Propulsor Efficiency	1.0	0.1
Radiated Noise	1.0	0.1

Due to the absence of unclassified data and real numbers available in this area, hypothetically derived normal distributions will be placed upon the uncertainty parameters defined in TOAD. In an actual analysis, historical data would be used to generate better estimates of the appropriate uncertainty distributions to use. The means and the standard deviations for the uncertainty parameters are given in Table 18.

Table 19: Design Variables for Heavyweight Torpedo Example

Design Variables	Min	Max	Units
Torpedo Diameter	19	25	in
Fuel Section Length	125	200	in
Motor Horsepower	300	500	hp
Decoupling Layer Thickness	0.0	1.0	in
Damping Layer Thickness	0.0	1.0	in
Motor/Propulsor RPM	2000	4000	rev/min

6.1 Methodology Applied to Torpedo Design Problem

The example design problem is for an all-electric, heavyweight torpedo. This problem has six design variables, or control variables, as listed in Table 19. The problem also has five noise variables, which correspond to the "k-factors" as shown in Table 18. Normal distributions were added to each of these noise variables. The goal of the design problem is to design a large diameter torpedo system, carrying a 650-lb_m warhead that meets the minimum performance characteristics listed in Table 20. The design constants for the heavyweight problem are given in Table 21. An individual torpedo design corresponds to a single deterministic setting of the design variables, with a probabilistic distribution associated for each response. A torpedo will thus have fixed, or deterministic, design variables such as diameter, horsepower, etc., but will have a probabilistic response for velocity, range and noise. Other responses, those that are not affected by the uncertainty distributions, are given as deterministic values, such as total length and weight. Table 22 lists the responses for the example problem.

Table 20: Design Requirements for Torpedo Example

Performance		Requirements
Max. Velocity	*at least*	45 kts
Max. Range	*at least*	15 nmi
Noise	*at most*	45 dB

A normal distribution, with parameters shown in Table 18, was assigned to each of the uncertainty variables, or "k-factors". The resulting response is illustrated in Figure 85. To summarize the problem: each individual torpedo design consists of a deterministic setting

Table 21: Design Constants for Heavyweight Torpedo Example

Parameter	Value	Units
Sensor Length	10	in
Sensor Weight	40	lb_f
Sensor Power	150	watts
Warhead Charge	650	lb_m
Batt Heat Value	56	watt-hr/lb_m
Batt Energy Den	2.5	watt-Hr/in^3
Motor Voltage	200	V

Table 22: Design Responses for Torpedo Example

Response	Type	Target	Units
Velocity	Probabilistic	45	kts
Range	Probabilistic	15	nmi
Noise	Probabilistic	45	dB
Length	Deterministic	*minimize*	in
Weight	Deterministic	*minimize*	lb_m

of the six design variables, along with a random value of each of the five noise variables, which corresponds to the distribution shown in Figure 85. The probability of success for each torpedo system is the probability of simultaneously meeting all of the performance characteristics listed in Table 20. The overall metric of merit for the system will be the minimization of torpedo weight. Weight was chosen because it is a first-order estimator of the manufacturing cost of a system.

In order to speed the analysis, a Design of Experiments, coupled with a response surface equation, was used around the design space. The ensuing metamodel, or response surface equation, takes as inputs both the design variables (Table 19) and noise variables (Table 18), and quickly generates a response. With this technique, the TOAD analysis program is replaced by a series of simple polynomial expressions allowing for large Monte Carlo analyses to be run quickly. Third order response surface equations were used for the metamodel, as these were shown to best capture the behavior of the system. Since Monte Carlo analysis is being used, the probability of success value is found at each design point by simply counting the number of "successful" designs versus the total number of designs. This method matches the empirical distribution function as described by Bandte [16]. These definitions complete

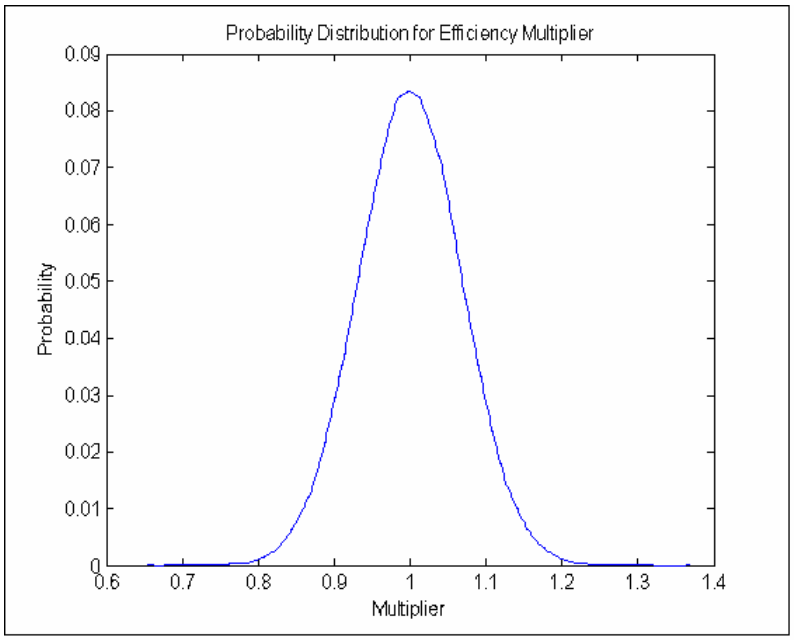

Figure 85: Uncertainty Distributions Applied to "k-factors" in TOAD

steps 1-9 of the robust design framework, as shown in Figure 86.

The next step in the design process is to identify the "optimum" design points for a range of probability of success values, thus identifying the Pareto frontier. Two separate algorithms were used to find this Pareto frontier. The first algorithm is the same gradient-based 'fmincon' optimizer in Matlab that was used for the traveller example. The gradient-based optimizer was used in conjunction with the response surface equations and Monte Carlo techniques, employing a very large number of runs per case. The large numbers of Monte Carlo runs were required in order to get accurate gradient information, which is very sensitive to noise. In addition to using a gradient-based optimizer, a random search was also employed, with a smaller number of Monte Carlo runs being used for each test case. Random search requires significantly more function calls in order to get a good solution, but, since highly precise Monte Carlo results are not required, does not need as many total runs. In terms of actual run-times, the gradient-based optimizer required a couple of days to construct the entire Pareto front. The random search could generate enough data to construct the Pareto front in only a few hours (5-6). A summary of the optimization techniques is shown in Table 23, showing the relative numbers of function calls and of Monte

Carlo trials. The complete process by which the design methodology was implemented is shown in Figure 86.

Table 23: Summary of Optimization Techniques

	Optimizer	Model	Uncertainty Analysis Technique	# of Function Calls	Total Run Time
Approach 1	Gradient-Based SQP Optimizer	Response Surface Equation	50,000 Monte Carlo Trials per Call	Dozens	1-2 Days
Approach 2	Random Search	Response Surface Equation	1,000 Monte Carlo Trials per Call	Thousands	5-6 Hours

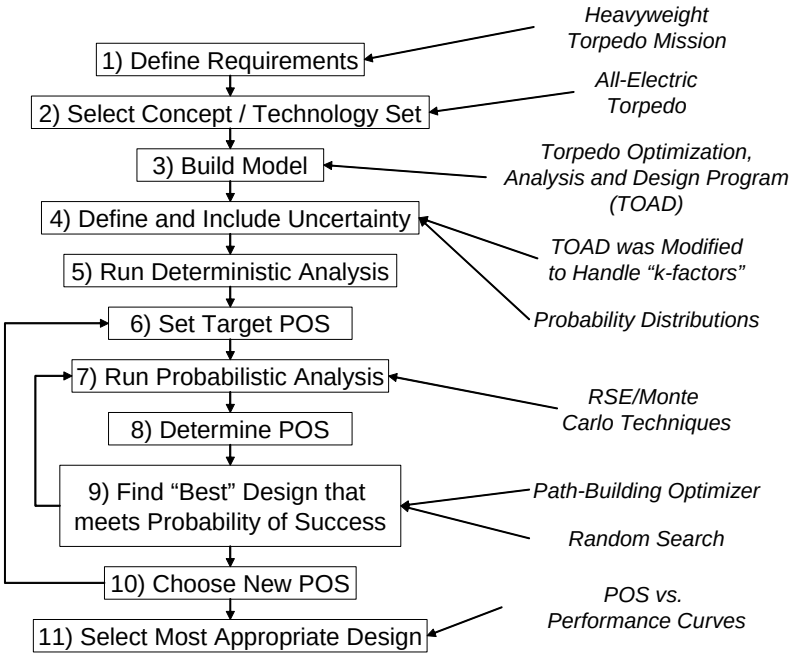

Figure 86: Design Process Implementation for Heavyweight Torpedo Analysis

6.1.1 Results

The results of the random search and the gradient-based optimization are shown in Figure 87. The figure shows that, individually, the gradient-based optimizer and the random search only partially captured the Pareto front. The gradient-based approach found the Pareto solutions that occurred at smaller probabilities of success, while the random search found

the Pareto solutions at higher probabilities of success. The complete Pareto front could only be generated by combining the results of the optimizer and the random search.

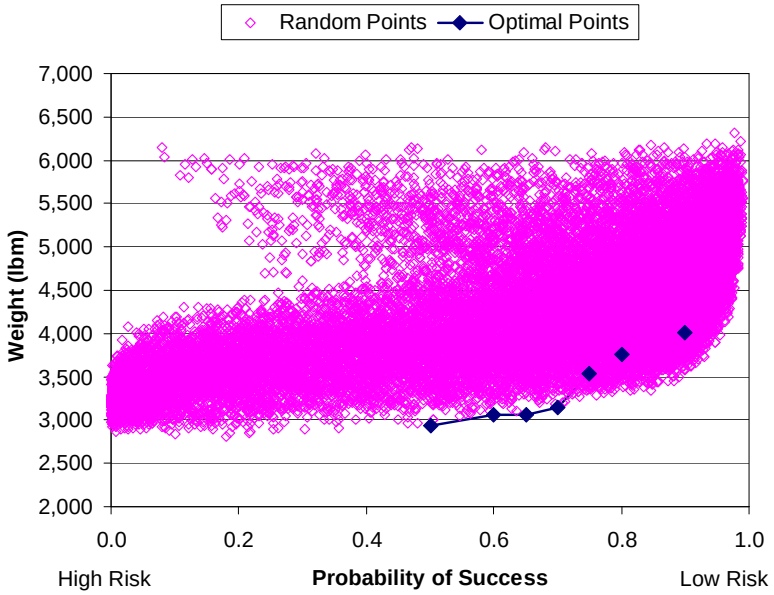

Figure 87: Comparison of Optimized Points vs. Random Points in Probability of Success Curve

The individual performances of the optimizers may be improved by a number of means. For the gradient-based optimizer, more starting points could be used to help locate the global optimum. In addition, increasing the number of Monte Carlo trials, to say, 500,000 trials or more per function call, will also decrease the noise, thereby helping the optimizer reach a good solution. For the random search, simply adding more points would better define the Pareto front. Finally, a different optimization technique altogether, such as a genetic algorithm, could be used to improve the ability of locating the Pareto Front. Genetic algorithms might be very powerful for these types of problems, as they combine the advantages of both gradient-based and random searches.

The complete Pareto front of non-dominated points, formed from the aggregate of the two approaches, is shown in Figure 88. The results in this chart behaved similarly to the results in the traveller problem, with increasing probability of success (or decreasing risk) leading to heavier, more costly solutions. The curve illustrates the basic catch-22 for

decision-makers: the higher the probability of success for the system, the higher the weight (and cost) of the system. Note that in these figures there are no discontinuities in the design space like those seen in the traveller example (Section 4.2.1). One reason for this lack of discontinuities is because of the use of response surface equations for the torpedo problem. By using second-order equations, the design space may have been smoothed so that large 'jumps' in the probability of success versus weight curve do not exist. If this work were repeated with direct function calls of the analysis program, then the more complex behavior of the previous problem might become visible.

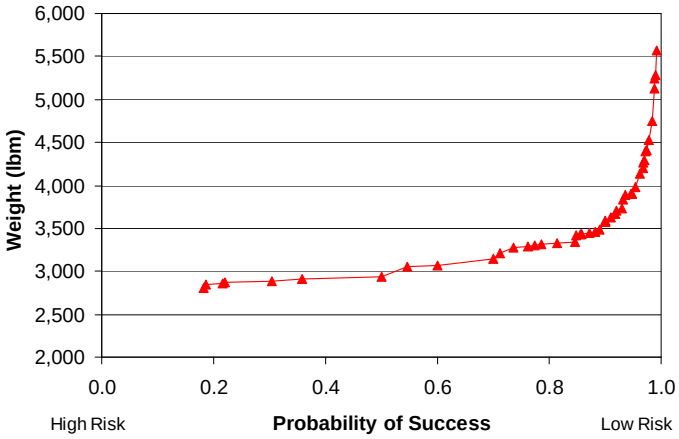

Figure 88: Probability of Success vs. Weight for an All-Electric, Heavyweight Torpedo

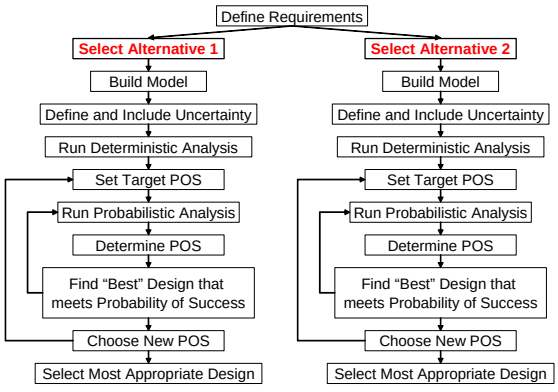

Figure 89: Design Process Implementation for Multiple Alternatives

To further illustrate the possibilities inherent in the robust design technique, two torpedo

alternatives were compared. A piston-driven system was compared to the previous results for an all-electric system. The design process in Figure 86 was repeated for the new piston concept. Since two alternatives were being examined, the design methodology was modified and is shown in Figure 89. The results of both design alternatives, the piston-engine system and the all-electric system, were compared in Figure 90. The results indicate that the two concepts are fairly similar in performance. However, if a lower probability of success (higher risk) is acceptable, then the electric system is the preferred alternative. However, if a very high probability of success is required, then the piston system is definitely the best choice. At moderate POS values, both systems had similar performance. The figure very succinctly describes when one system is preferable over another and when the two systems are comparable. Thus, these figures allow the decision-maker the opportunity to assess the relative merits of alternatives based upon his or her choice of the level of acceptable risk.

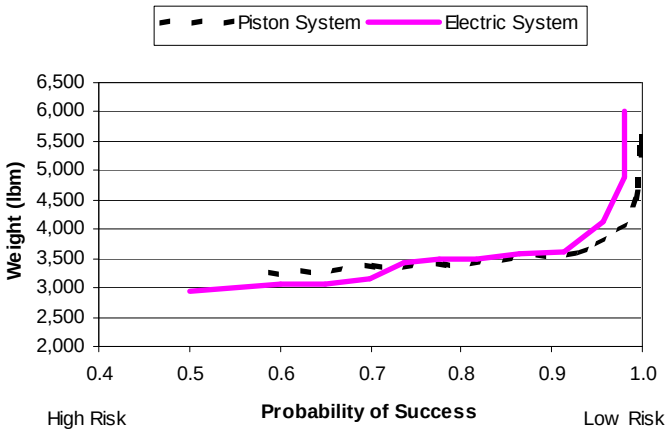

Figure 90: Probability of Success vs. Weight for Multiple Alternatives

It is important to mention that, considering the closeness of the two systems in Figure 90, the results may be inconclusive. More accurate Monte Carlo analysis should be conducted before definitively stating that the two systems have different performance. Also, had this example incorporated real uncertainty data, it is likely that more data would have been available regarding the piston-engine propulsion system, since it is a legacy system. This would imply that there would have been less uncertainty associated with the piston-engine system than the electric torpedo. However, since historical estimates of uncertainty were

not available for this research, differences in uncertainty between the piston and the electric torpedo were not modeled.

Figure 92 shows another useful application of this design technique. In Figure 92, the effect of changing requirements is shown for the electric torpedo system. The original design process from Figure 86 was repeated three times, each with a set of design requirements more stringent than the original. This new design process is illustrated in Figure 91. The various design requirements, in descending order of difficulty, are shown in Table 24. The results show that relaxing the performance requirements of the system increases the probability of success, or, stated another way: if the requirements are relaxed, there is less risk that a system of given weight will not meet the requirements. Figure 92 would be useful to a decision-maker who wanted to look at the effect of changing requirements on the risk and cost of the system.

Table 24: Changing Heavyweight Torpedo Design Requirements

Requirements	Velocity (kts)	Range (nmi)	Noise (dB)
Difficult	50	20	45
Moderate	50	15	45
Easy (Baseline)	45	15	45

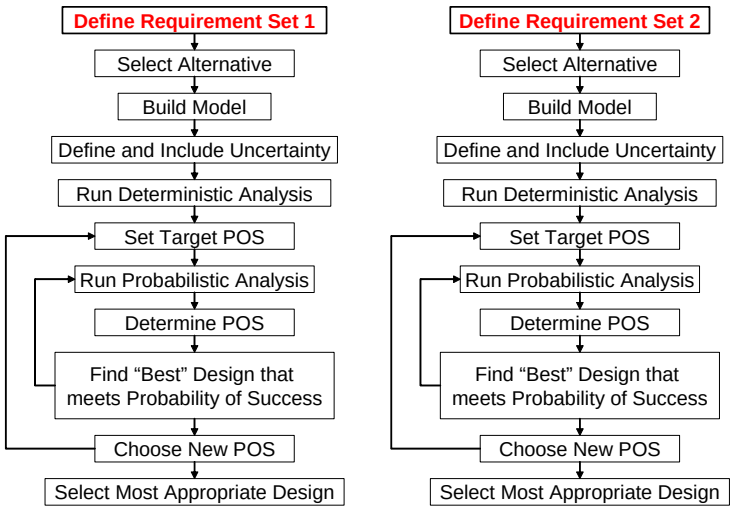

Figure 91: Design Process Implementation for Multiple Requirements

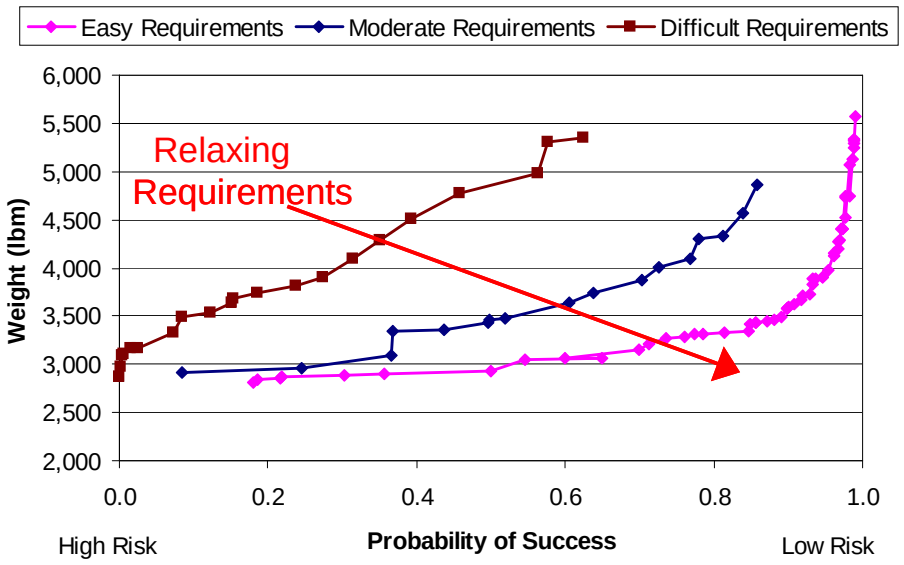

Figure 92: Probability of Success vs. Weight for Decreasing Requirements

It is important to remember that each point on the Pareto front represents not a single design, but instead a probabilistic response. Figure 93 and Figure 94 help illustrate the large amount of information behind each single Pareto point in the space. Each design point represents a single torpedo design, with corresponding fixed design variables and some deterministic responses, such as length, and weight. These deterministic responses can be used to visualize the shape of the torpedo, as shown by the torpedo renderings. However, in addition to these deterministic values, probabilistic results also exist for each point. The probabilistic results are represented by probability distributions for the responses for range and velocity. In addition, these probabilistic results can be combined together into a single joint-probability distribution. It is these probability distributions that are collapsed into the single-valued, more elegant probability of success parameter that is reflected in the Pareto frontiers. Thus, each single design on the Pareto chart reflects a summary of an entire multi-dimensional probabilistic response.

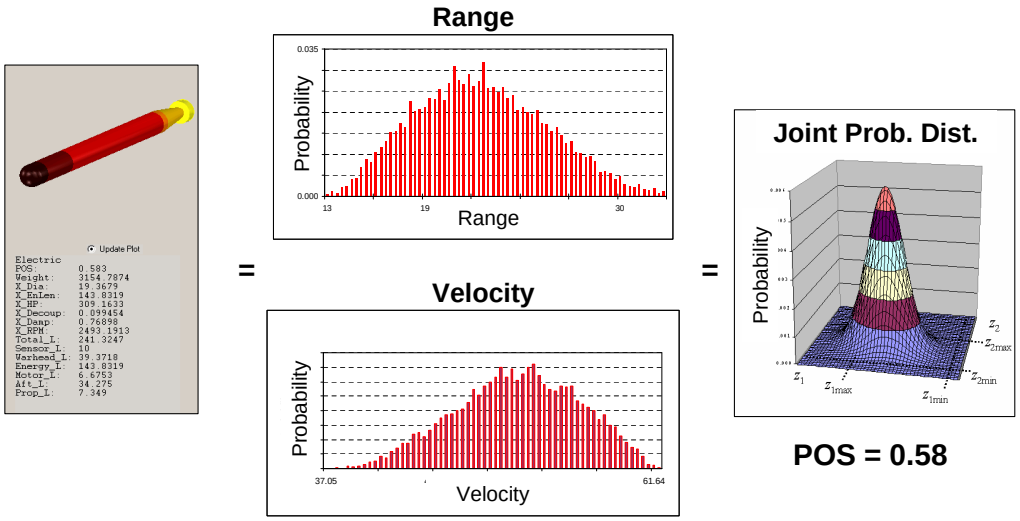

Figure 93: Expansion of Single Data Point to Show Background Data

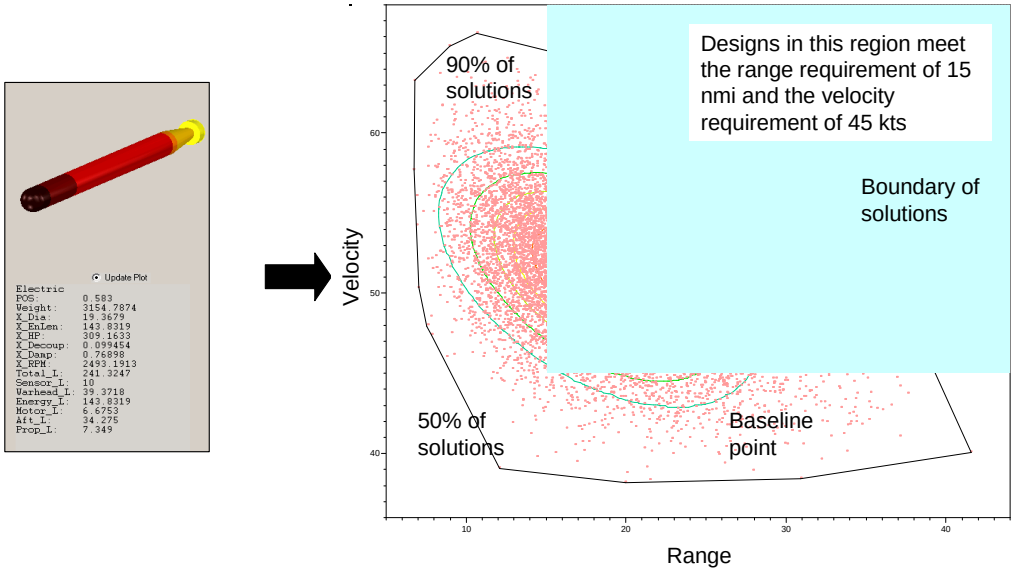

Figure 94: Expansion of Single Data Point to Show Joint Probability Information

6.2 Methodology with Direct Simulation of Torpedo Analysis

The example design problem from Section 6.1 was repeated, with the exception that direct simulation was used in the design process. Instead of sampling the torpedo design space and substituting a metamodel (in the form of a response surface equation), all of the analysis was conducted via direct calls of the TOAD analysis program. In order to enable the automated calling of TOAD, the program was linked to the optimizer through the use of Matlab, similar to the environment developed by Buonanno (Reference [33], Section 3.9). This change in the design approach has two significant benefits. The first advantage occurs because using the results as calculated by the TOAD analysis program will remove all metamodel error (which is almost always present), thereby allowing for more accurate results.

The second advantage to this technique is that any failed or infeasible cases can be counted against the probability of success. When generating response surface equations, infeasible cases are often 'discarded' from the results, as mentioned in Section 3.4. The RSE is then fit based upon the remaining data points. If the number of discarded cases is not significant, these discarded cases do not greatly affect the RSE accuracy. However, the failed cases may represent a region of the design space that is infeasible. By discarding these cases, yet still fitting an RSE over those particular design points, the RSE might be inappropriately including an 'infeasible' region in the design space. Unfortunately, there are few ways to conveniently get around this fact when using RSEs. However, direct simulation automatically accounts for this fact because it does not assume that the entire space is feasible, thereby allowing infeasible cases to be identified and immediately removed on an individual basis from the solution space.

Table 25 shows how the direct simulation differs from the previous two torpedo design examples. The last example problem was repeated, with the only difference being the direct simulation of the TOAD analysis instead of the use of a metamodel. The results of the random search with direct simulation are similar to those from the RSEs, with a large number of runs forming a well-defined Pareto front. Figure 95 shows the random points and the resulting Pareto front with direct simulation.

Table 25: Summary of Optimization Techniques

	Optimizer	Model	Uncertainty Analysis Technique	# of Function Calls	Total Run Time
Approach 1	Gradient-Based SQP Optimizer	Response Surface Equation	50,000 Monte Carlo Trials per Call	Dozens	1-2 Days
Approach 2	Random Search	Response Surface Equation	1,000 Monte Carlo Trials per Call	Thousands	5-6 Hours
Approach 3	Random Search	Direct Simulation	1,000 Monte Carlo Trials per Call	Thousands	9-12 Hours

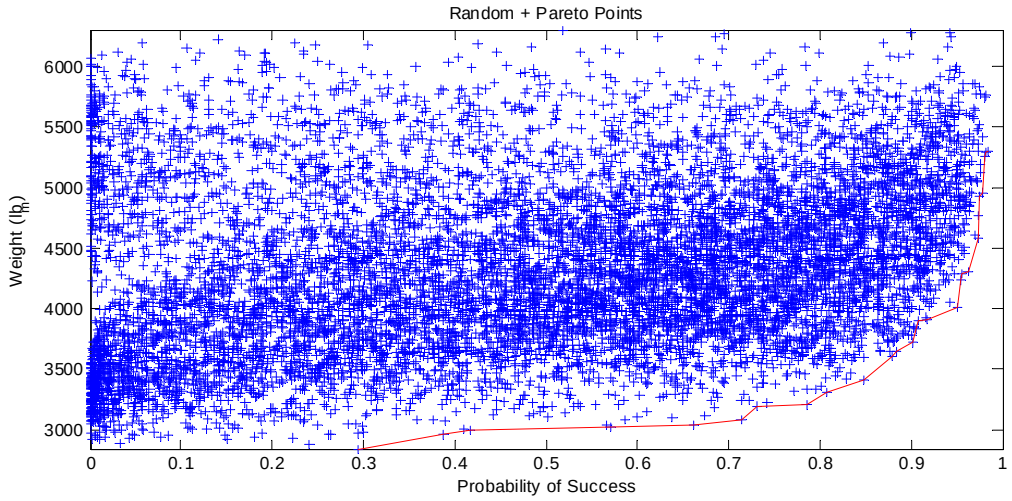

Figure 95: Pareto Points Determined from Random Runs using Direct Simulation of TOAD

Figure 96 gives a direct comparison between the results of the response surface analysis and the direct simulation. Note that the Pareto fronts are very similar for the two systems, implying that both techniques created the same results. Keep in mind that the results from the direct simulation should be considered to be more accurate than the results from the response surface equation analysis, though in this case the two systems perform similarly. There is one region, near a probability of success between 0.6 and 0.8, where the direct simulation performs slightly better than the RSE results. This improvement possibly comes from the fact that the response surface will naturally 'smooth' out regions of the design

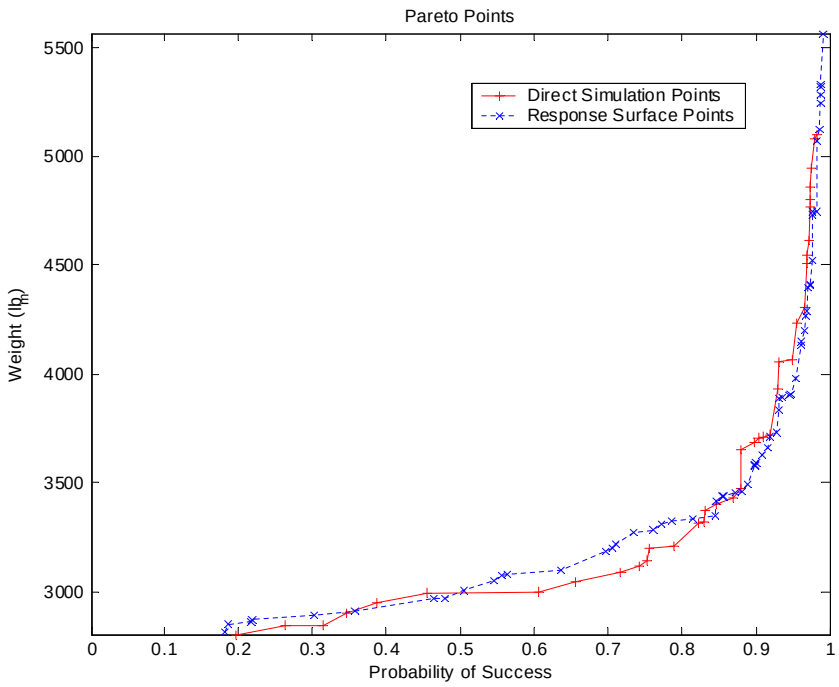

Figure 96: Comparison of Pareto Points Determined from Direct Simulation and Response Surface Equations

space, so a local minima might have been washed out by the RSE, but will still exist in direct simulation. The only disadvantage of direct simulation, other than a longer setup time, is the fact that the overall optimization took several hours longer than running response surface equations.

It is informative to use the visualization tool to better examine some of the torpedo designs. Figure 97 focuses on a torpedo that has a probability of success value of 0.455, an almost 50% chance of meeting all of the design requirements. The visualization tool displays a large amount of information about the torpedo: the key measure of merit (weight), the probability of success, the design variables, and the lengths of the overall torpedo and independent sub-sections. The figure also illustrates where the torpedo lies on the probability of success frontier and shows the relative advantages of moving to a different point on the frontier.

Even though the information shown is straightforward, it is important to recall that a large amount of probabilistic data exists for this torpedo design. This probabilistic data

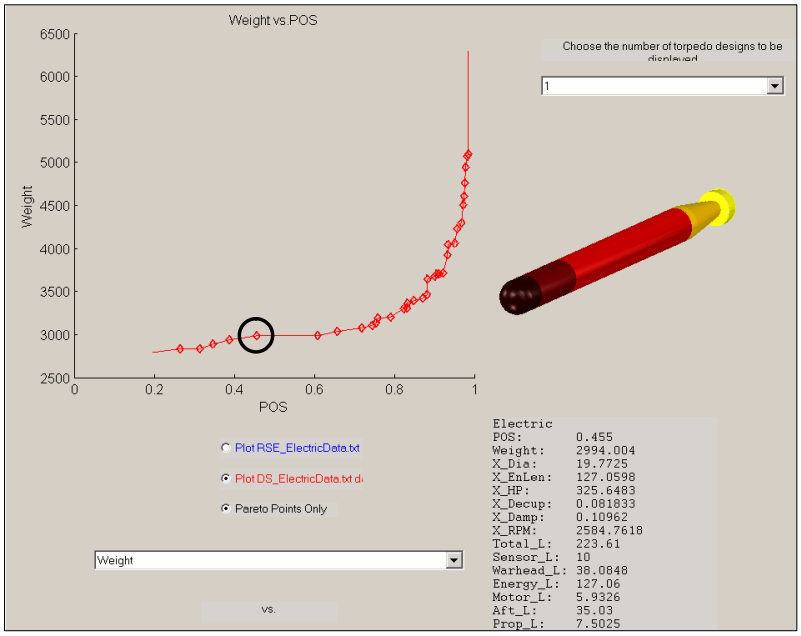

Figure 97: Examination of an Optimum Torpedo

was used to calculate the probability of success. It is informative to examine this underlying probabilistic data more closely. Figure 98 shows the probability density functions generated for this torpedo design. The PDFs for the probabilistic responses of velocity, range, and noise are given, along with the corresponding constraint values (marked by a red-dashed line). The cumulative distribution functions for the responses are shown in Figure 99. The CDFs show the probabilistic responses of the system and the cumulative likelihood of meeting each individual constraint. From this figure, it is clear that the noise and velocity constraints are easy to meet, while there is only around a 50% chance of meeting the range constraint.

Another torpedo design on the Pareto front can now be chosen to be examined. The next design chosen has a moderately high probability of success of 0.881 and is illustrated in Figure 100. Note the differences between this torpedo and the previous torpedo: it is larger, longer, and has a higher chance of meeting all of the constraints. The PDFs and CDFs for this torpedo are shown in Figure 101 and Figure 102. For this example, the mean of each of the response distributions is shifted to a higher value for the larger torpedo. This torpedo design, having more capability, can more easily meet all of the performance constraints,

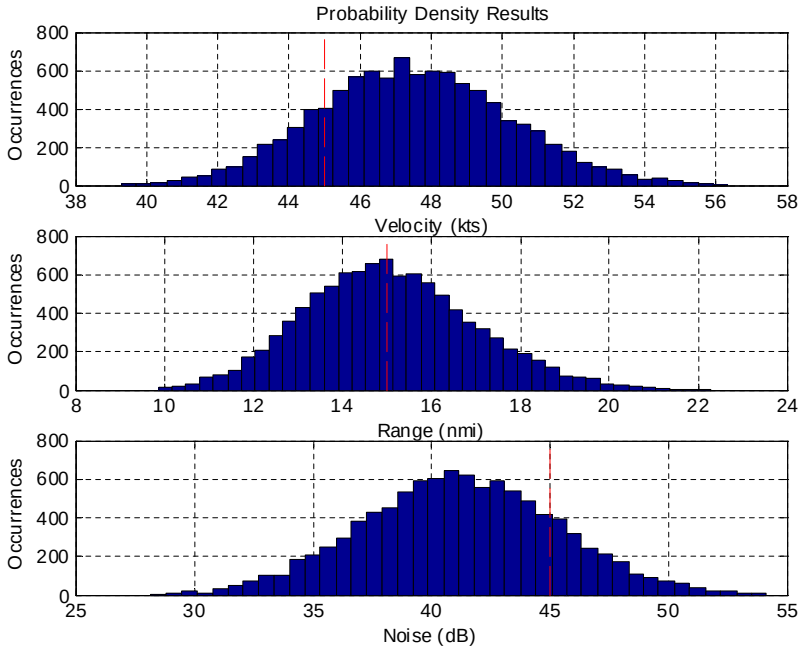

Figure 98: Probability Density Function Results for an Optimum Torpedo

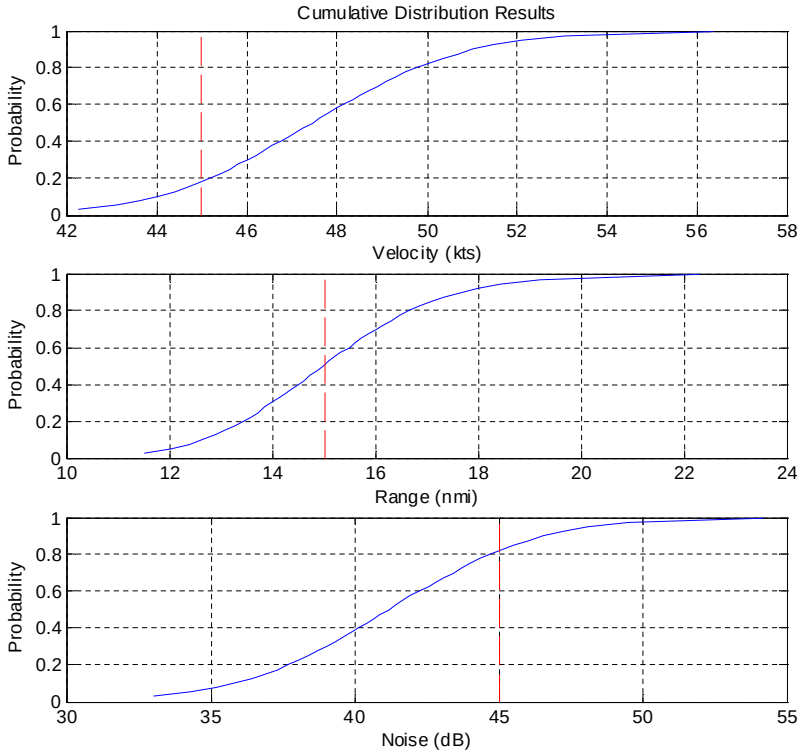

Figure 99: Cumulative Distribution Function Results for an Optimum Torpedo

thus leading to a higher probability of success, though at the cost of increasing weight.

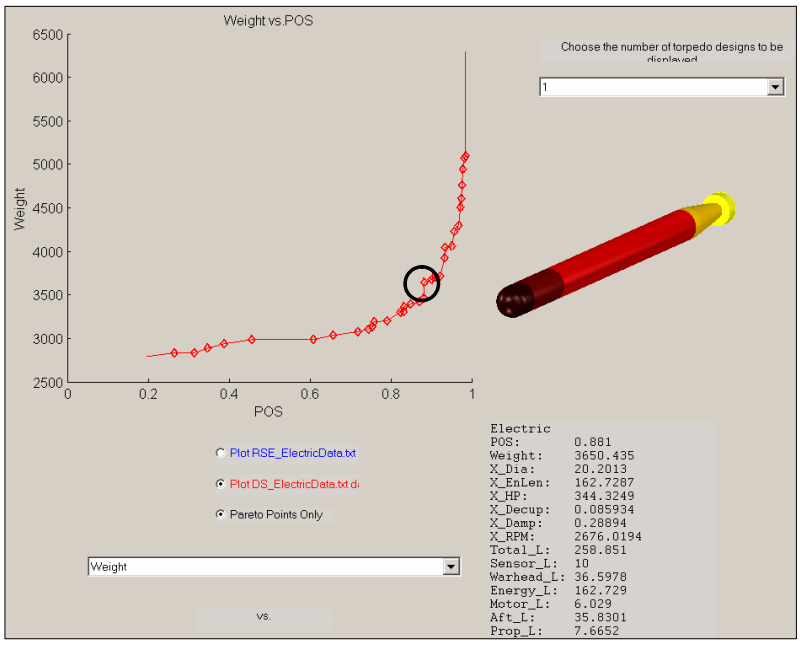

Figure 100: Examination of an Optimum Torpedo

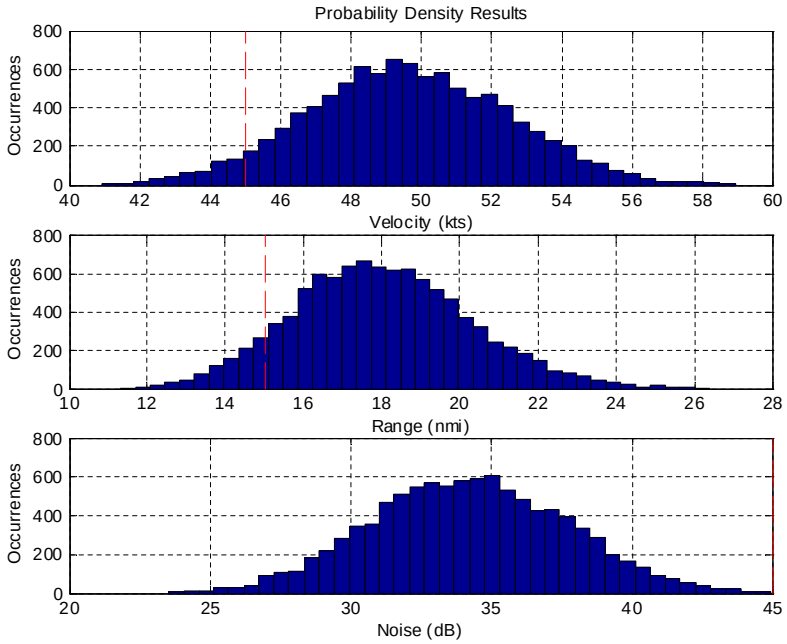

Figure 101: Probability Density Function Results for an Optimum Torpedo

Yet a third example torpedo is shown in Figure 103. This torpedo has a probability of

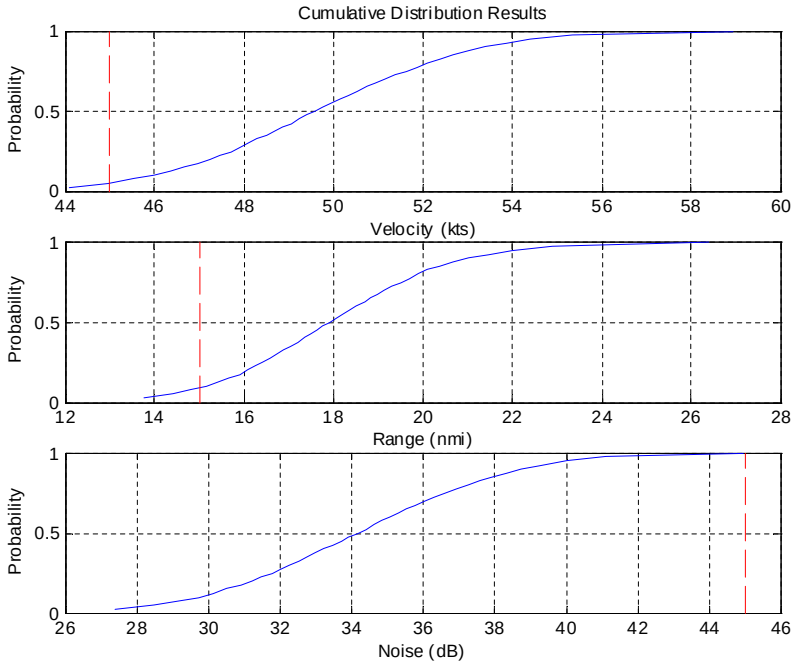

Figure 102: Cumulative Distribution Function Results for an Optimum Torpedo

success of 0.974, so it will reliably meet the requirements. However, this robustness comes at great cost, as the torpedo has a gargantuan 23 inch diameter and is over 1,000 pounds heavier than the previous systems. This torpedo illustrates the upper end of the tradeoff between cost and risk: the less risk that the decision-maker wishes to accept, the larger and more costly the system. PDFs and CDFs for this torpedo are shown in Figure 104 and Figure 105, showing the relative ease with which each constraint is met.

The last three examples illustrated how the results of this analysis, coupled with the visualization tool, can help understand the tradeoff between the probabilistic likelihood of meeting the requirements and the total system cost. The examples also showed how the torpedo designs varied along the probability of success curve. These three torpedoes are summarized side-by-side in Table 26.

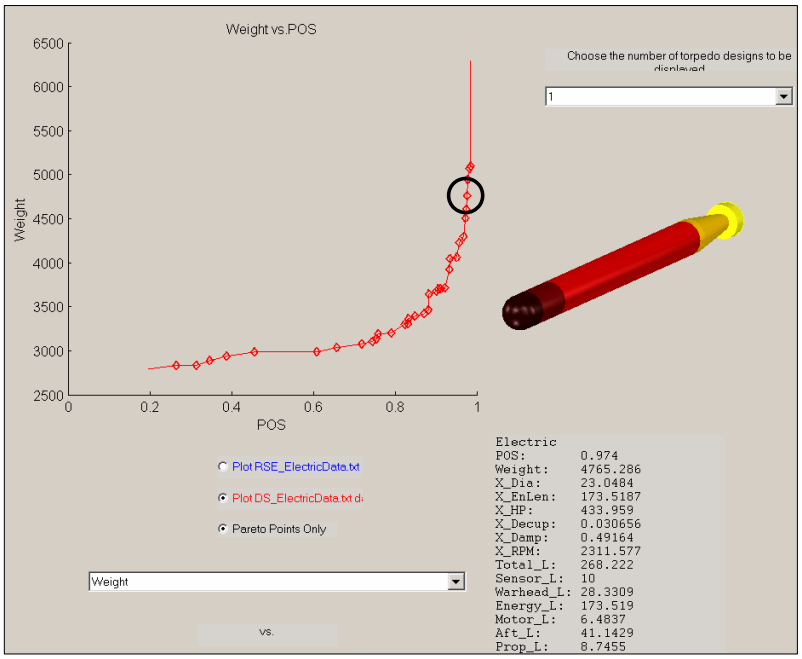

Figure 103: Examination of an Optimum Torpedo

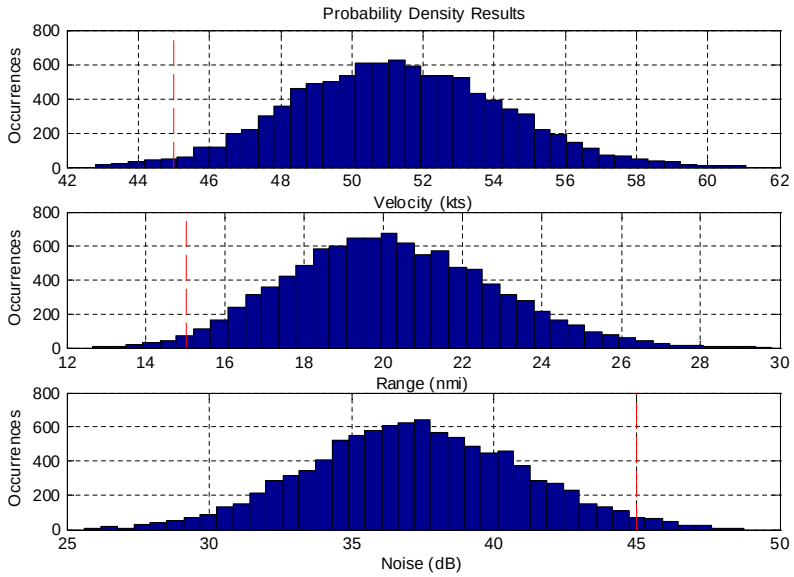

Figure 104: Probability Density Function Results for an Optimum Torpedo

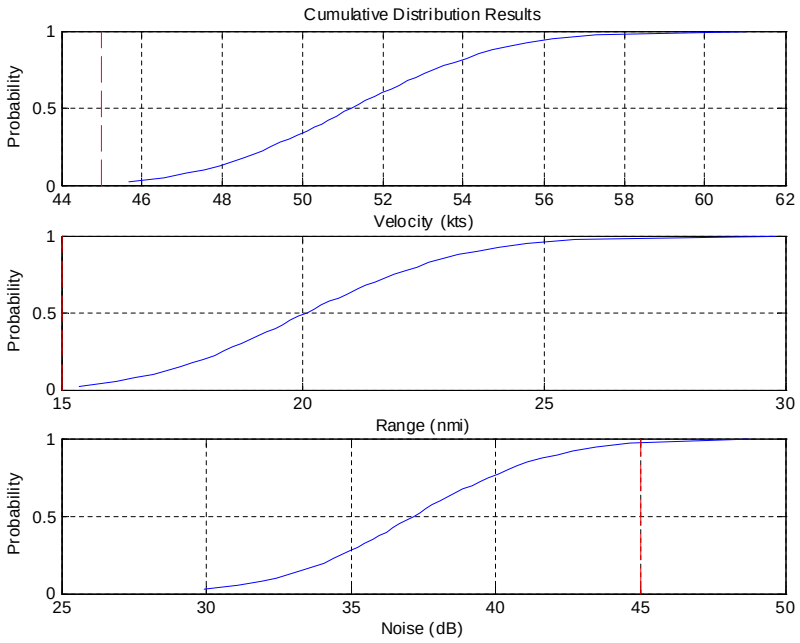

Figure 105: Cumulative Distribution Function Results for an Optimum Torpedo

Table 26: Comparison of Some Optimal Heavyweight Torpedoes

	Quantity	Units	Torpedo 1	Torpedo 2	Torpedo 3
Pareto Optimality	POS	---	**0.445**	**0.881**	**0.974**
	Weight	lb_m	2994	3650	4765
Design Variables	Diameter	in	19.8	20.2	23
	Energy Len	in	127	162	173.5
	Motor HP	hp	325	344	433
	Decoupler Thickness	in	0.08	0.08	0.03
	Damper Thickness	in	0.10	0.29	0.49
	Motor/Prop RPM	rev/min	2584	2676	2311
Deterministic Responses	Total Len	in	223.6	258.0	268.2
	Sensor Len	in	10.0	10.0	10.0
	Warhead Len	in	38.0	36.6	28.3
	Energy Len	in	127.1	163.0	173.5
	Motor Len	in	5.9	6.0	6.5
	Aftbody Len	in	35.0	35.8	41.1
	Prop Len	in	7.5	7.7	8.7
Probabilistic Responses	Velocity Mean	kts	47.5	49.7	51.3
	Velocity St. Dev.	kts	2.78	2.92	3.00
	Range Mean	nmi	15.1	18.0	20.2
	Range St. Dev.	nmi	2.41	2.33	2.64
	Noise Mean	dB	41.2	34.2	37.2
	Noise St. Dev.	dB	4.23	3.53	3.78
	Vel-R Correlation	---	-0.072	-0.004	-0.006
	Vel-N Correlation	---	0.197	0.241	0.209
	R-N Correlation	---	-0.020	-0.025	0.003

As the previous discussion showed, different styles of torpedoes are optimal at varying probability of success values. Concerns may then arise as to how the design variables vary along the Pareto front. Common questions might be whether the variables were constant, how they changed, and whether there was a large jump in their values. An examination of the design variables as they varied along the Pareto front was conducted. However, because the Pareto fronts were generated using Monte Carlo analysis, with relatively low numbers of trials $(1,000)$, there was some noise in the results, as seen in Figure 106. This noise caused a decidedly unsmooth transition in the design variables. It was decided to reduce this noise to get a clearer picture of the underlying variation in the design variables along the Pareto front. This noise was removed by instituting a running average of the results. In Figure 106, the original results for motor horsepower for both the direct simulation case and the response surface case are shown, along with the smoothed results. Note the jaggedness in the variation of horsepower that results from the noise in the system. The smoothed lines still show humps and trends, however, these trends are significantly more visible without the noise.

Figures 107 through 112 show comparisons of all the design variables for both the response surface results and the direct simulations. The results are somewhat similar between the two analysis methods, but, surprisingly, the response surface results have a lot more peaks. This difference suggests that there may be more differences between the RSE and the direct simulation than initially discussed. However, the direct simulation results should still be considered the more accurate of the two.

Looking closer at the design variables, as one might expect, as the probability of success increases, so too do the torpedo size, motor horsepower, and fuel section length, indicating again that the lower risk systems are the larger ones. However, note that there is very little variation in the damping layer thickness (Figure 111), and there is wide variation in the decoupling layer thickness (Figure 110) and the RPM (Figure 112). These results are most likely attributed to the fact that RPM, decoupling layer, and damping layer are not large drivers on the system, particularly since the noise constraints appeared to be the easiest constraints to satisfy. These design variables seem to have remained within the noise of

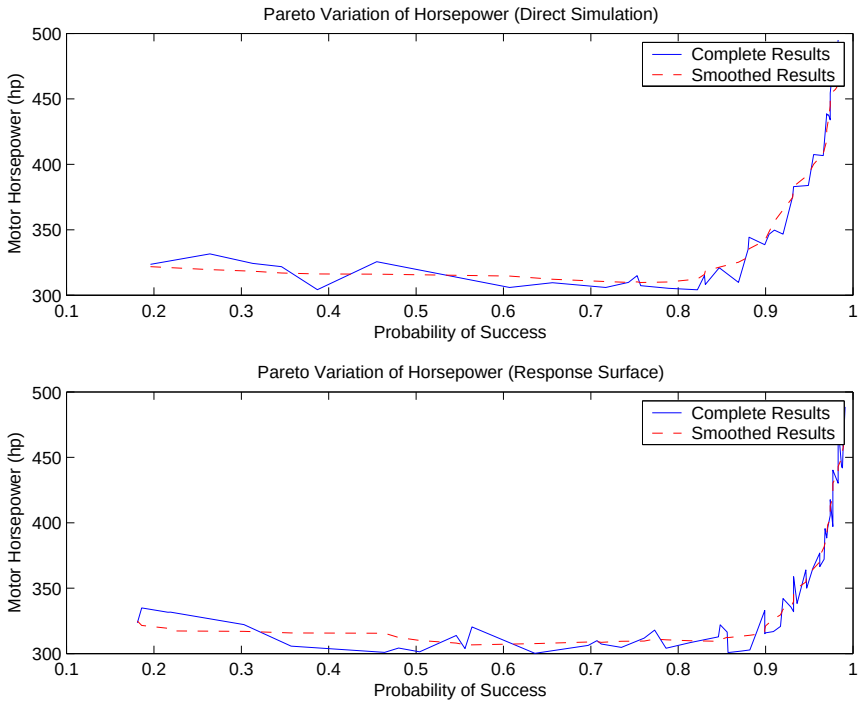

Figure 106: Variation of Motor Horsepower along the Pareto Front (smoothed and unsmoothed)

the system. To generate more interesting results, several steps could be taken: spurious design variables could be removed since they have little effect, the noise constraint could be increased so these variables become more important, or a higher fidelity analysis could be used.

In addition to looking at the variation of design variables along the Pareto frontier, it is also interesting to look at the variation in the torpedo length, a deterministic response. The variation of torpedo length is shown in Figure 113. This figure has the same behavior as the others, with the direct simulation results being much more continuous than the response surface results. Note that the length of the torpedo tends to increase as the probability of success increases. Since the weight also increases with probability, it would be expected for the length to increase as well, since the two are correlated. This fact continues to show that the higher probability of success systems tend to be the larger, over-designed, systems.

Questions may also rise about the appropriateness of using only $1,000$ Monte Carlo trials as opposed to a higher number. To answer those questions, the Pareto points from Figure

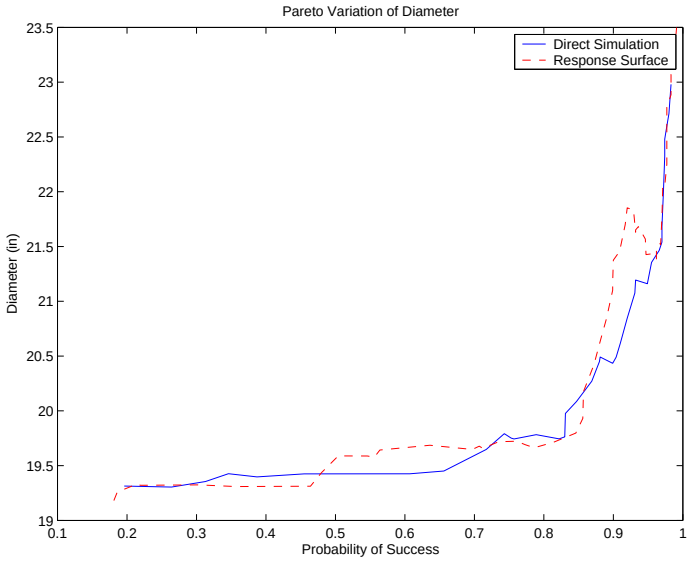

Figure 107: Variation of Torpedo Diameter along the Pareto Front

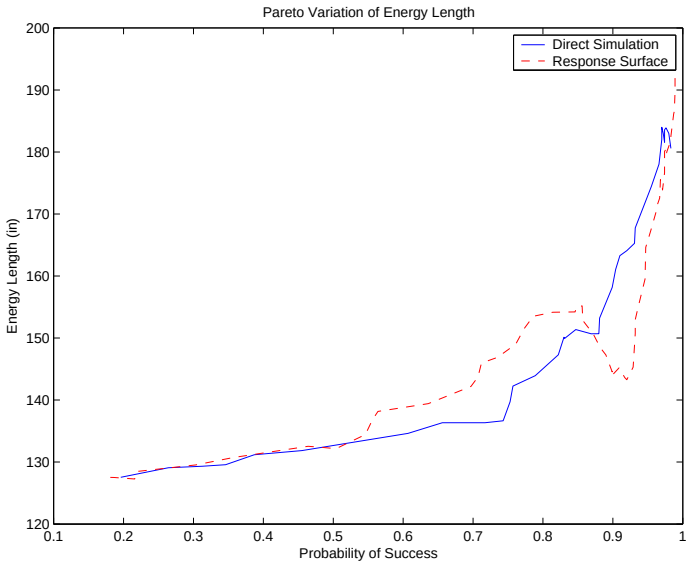

Figure 108: Variation of the Energy Section Length along the Pareto Front

95 were run again with a higher number of Monte Carlo trials (100, 000). The results of the higher fidelity Monte Carlo trials are compared against to the original results in Figure 114. The figure shows that the results are quite similar, there is not much variation between the two levels of fidelity, with many points matching exactly. However, one interesting thing to note in Figure 114 is that the higher fidelity Monte Carlo runs tend to be slightly more

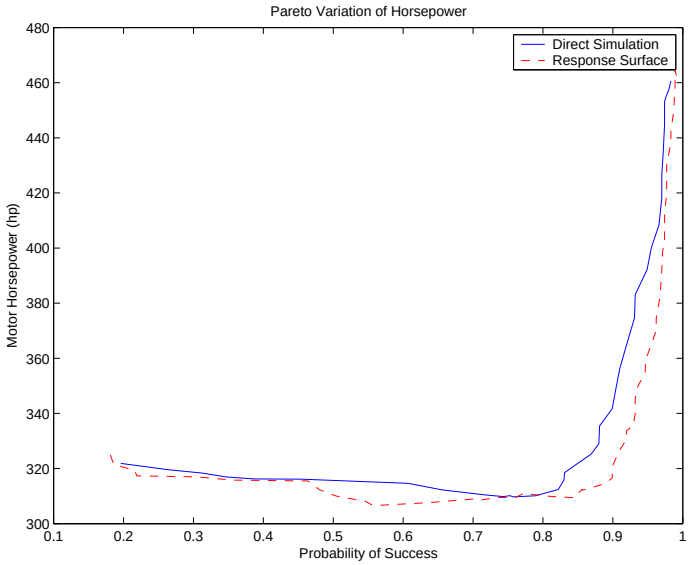

Figure 109: Variation of the Motor Horespower along the Pareto Front

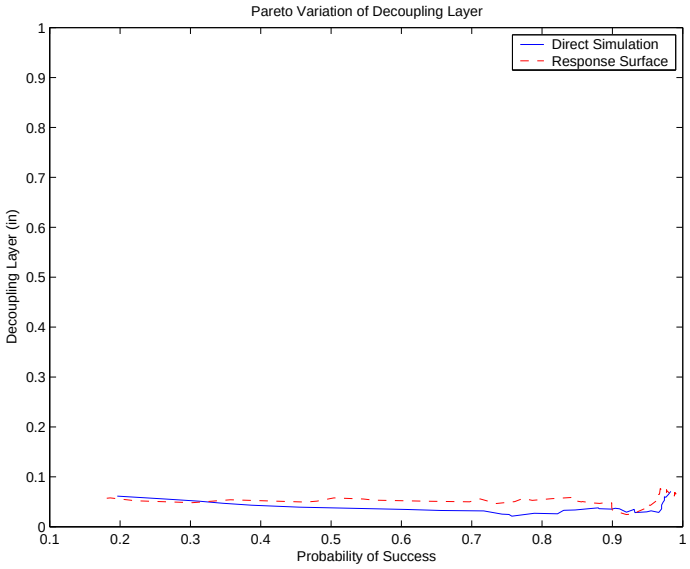

Figure 110: Variation of Decoupling Layer along the Pareto Front

conservative than the lower fidelity Monte Carlo runs. This fact should encourage the user to use as many Monte Carlo trials as possible under the time constraints available.

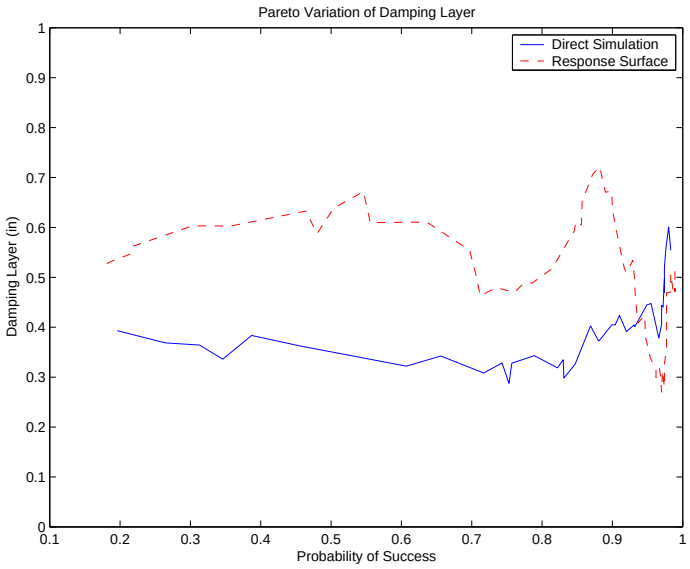

Figure 111: Variation of the Motor Damping Layer along the Pareto Front

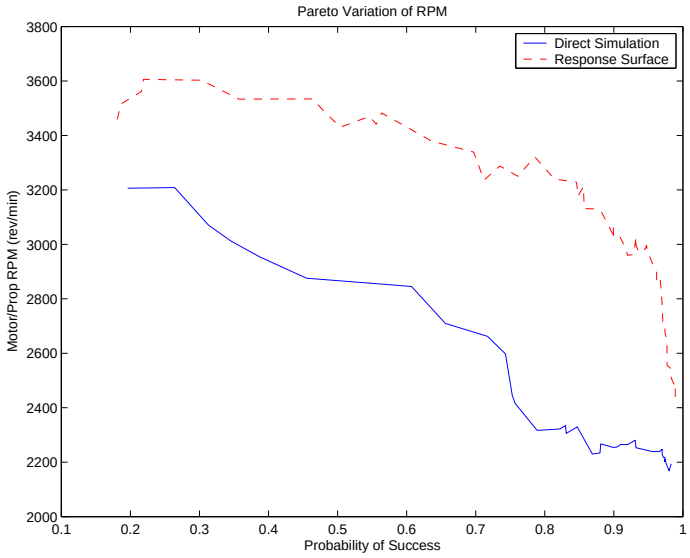

Figure 112: Variation of Motor/Propulsor RPM along the Pareto Front

6.3 Lightweight Analysis Results

The torpedo design problem was repeated for a lightweight torpedo system. Again, the torpedo system had an all-electric propulsion system, however, both the minimum range of the torpedo and the warhead size were dramatically reduced: from 15 nmi to 5 nmi and from 650 lb_m to 150 lb_m. The new design requirements are given in Table 27, with

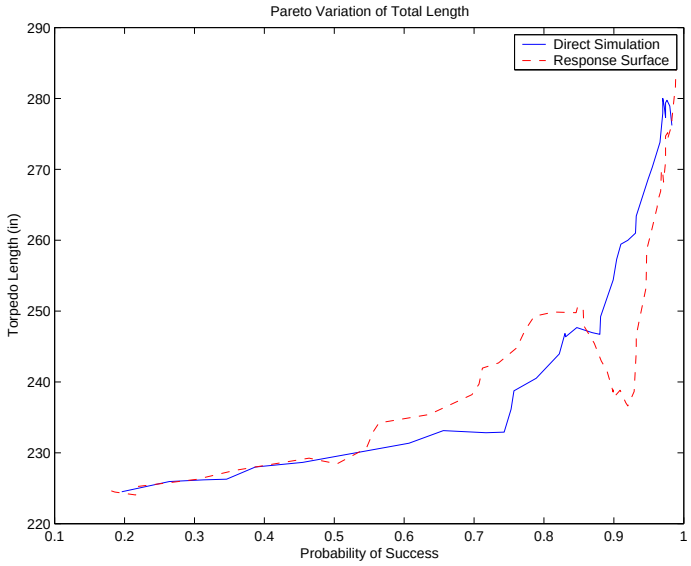

Figure 113: Variation of Torpedo Length along the Pareto Front

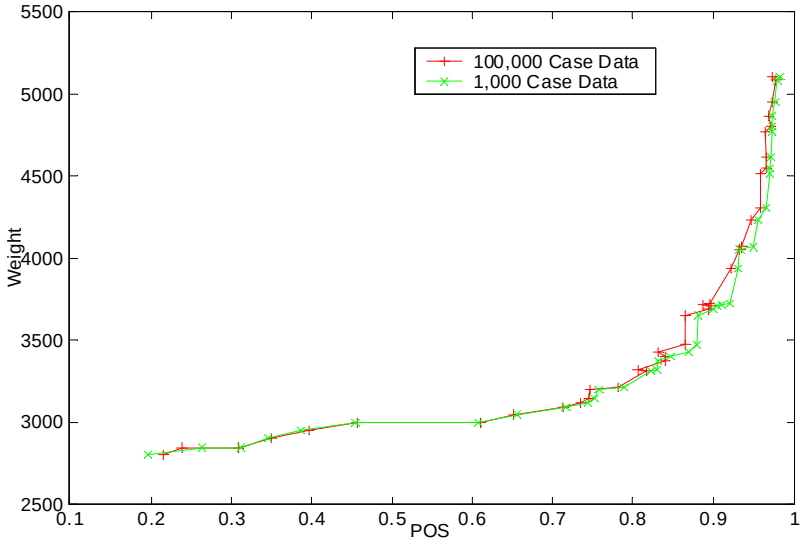

Figure 114: Comparison of Increased Monte Carlo Trials on the Pareto Front

the design constants listed in Table 28. Because the lightweight torpedoes are significantly smaller than heavyweight systems, the design variable ranges for the study were reduced to reflect a smaller system, as shown in Table 29. The previous ranges for the uncertainty multipliers, or "k-factors", were used in this study (Table 18).

The lightweight example was conducted via approach 3 from Table 25: direct simulation

Table 27: Design Requirements for Torpedo Example

Performance		Requirements
Max. Velocity	*at least*	45 kts
Max. Range	*at least*	5 nmi
Noise	*at most*	45 dB

Table 28: Design Constants for Heavyweight Torpedo Example

Parameter	Value	Units
Sensor Length	10	in
Sensor Weight	40	lb_f
Sensor Power	150	watts
Warhead Charge	150	lb_m
Batt Heat Value	56	watt-hr/lb_m
Batt Energy Den	2.5	watt-Hr/in^3
Motor Voltage	200	V

of the TOAD computer model in conjunction with Monte Carlo techniques. A random search was used for the optimization process. The implementation of the design process for the lightweight torpedo example is shown in Figure 115.

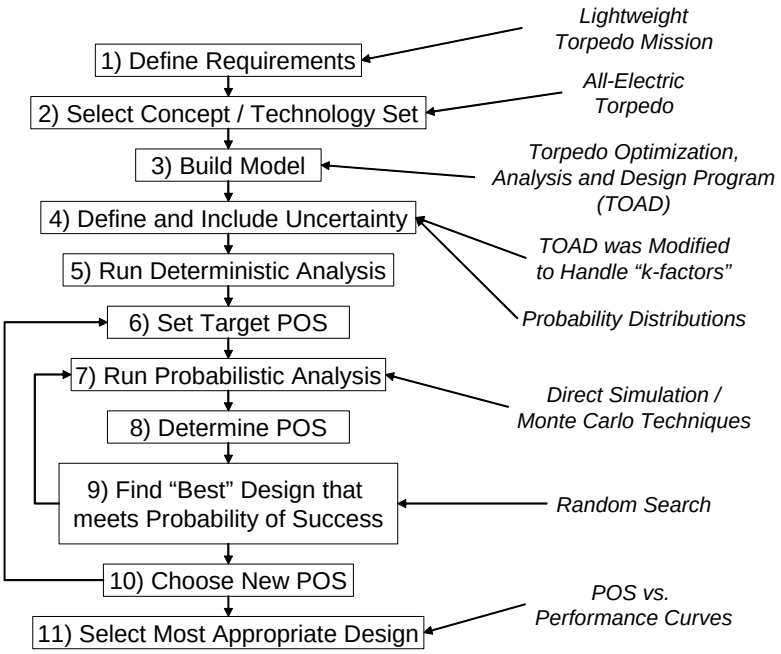

Figure 115: Design Process Implementation for Lightweight Torpedo Analysis

Table 29: Design Variables for Heavyweight Torpedo Example

Design Variables	Min	Max	Units
Torpedo Diameter	9	16	in
Fuel Section Length	25	150	in
Motor Horsepower	50	250	hp
Decoupling Layer Thickness	0.0	0.75	in
Damping Layer Thickness	0.0	0.75	in
Motor/Propulsor RPM	2000	4000	rev/min

The results of the random search are given as Figure 116. The results show two large congregations of responses, one with a probability of success near zero, and the other with a probability of success near one. The accumulation of points near the probability of success of zero indicates that there are a wide array of designs that fail to meet any design requirements. These designs may be completely infeasible. This point illustrates an advantage of direct simulation over response surface equations. Where the response surface equations tend to "smooth out" infeasible regions, direct simulation allows infeasible regions to be dealt with directly so that they can summarily be discarded, as they were in this example (as indicated by the large number of designs with zero POS). The large numbers of random points near the probability of success of one means that a great number of the designs can meet all of the design requirements. If the decision-maker desired to spread out the design points near the higher POS value, more stringent design requirements could be implemented.

A comparison between the lightweight results and the heavyweight results is given in Figure 117. Note that, for both cases, the shape of the Pareto frontier is similar, although there is less curvature for the lightweight system. This reduced curvature is due to the relative ease with which the lightweight system is meeting its design requirements. If the design requirements were increased, it is likely that more curvature would become visible. The lightweight torpedo meets its requirements at a significantly lower weight (or cost) than the heavyweight counterpart. Keep in mind, however, that this advantage for the lightweight torpedo does not come from superior performance, but from the reduced design requirements for the system (in the form of a smaller minimum range and warhead).

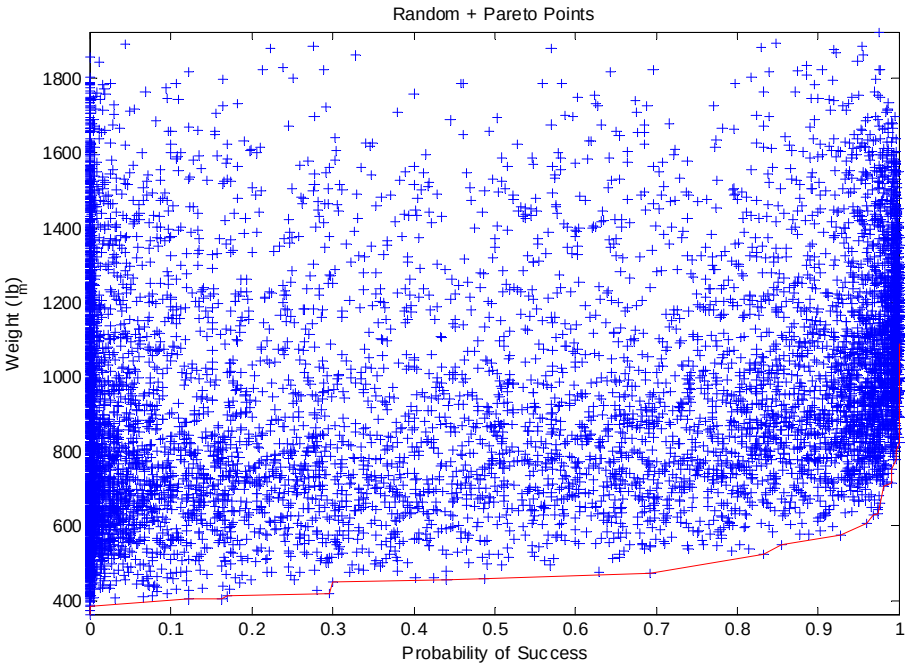

Figure 116: Random Points and the Pareto Frontier for Lightweight Torpedo

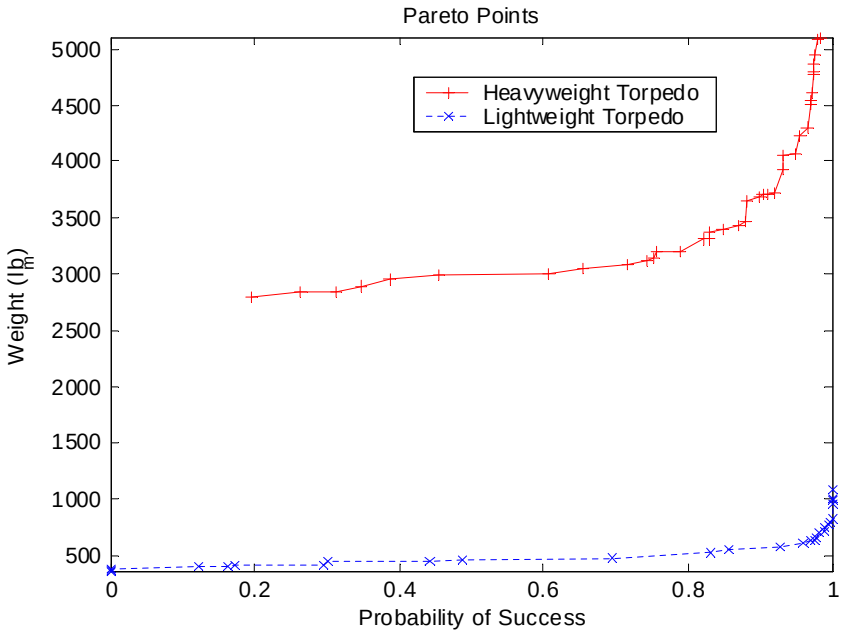

Figure 117: Comparison of Pareto Frontier for Lightweight and Heavyweight Torpedoes

The visualization tool can also be used to compare the heavyweight torpedo designs to the lightweight torpedo designs. Figure 118 shows a snapshot of the visualization tool.

In this image, a heavyweight torpedo (left-hand side) is being compared to a lightweight torpedo (right-hand side). The physical differences between the two torpedoes are striking. The heavyweight system is significantly larger than the lightweight. In addition, a majority of the heavyweight torpedo length is dedicated to the fuel tank. For the lightweight torpedo, which is thinner and has a higher fineness ratio, the warhead takes up an appreciably larger portion of the torpedo. The visualization tool allows for this quick examination of tradeoffs between distinct system concepts.

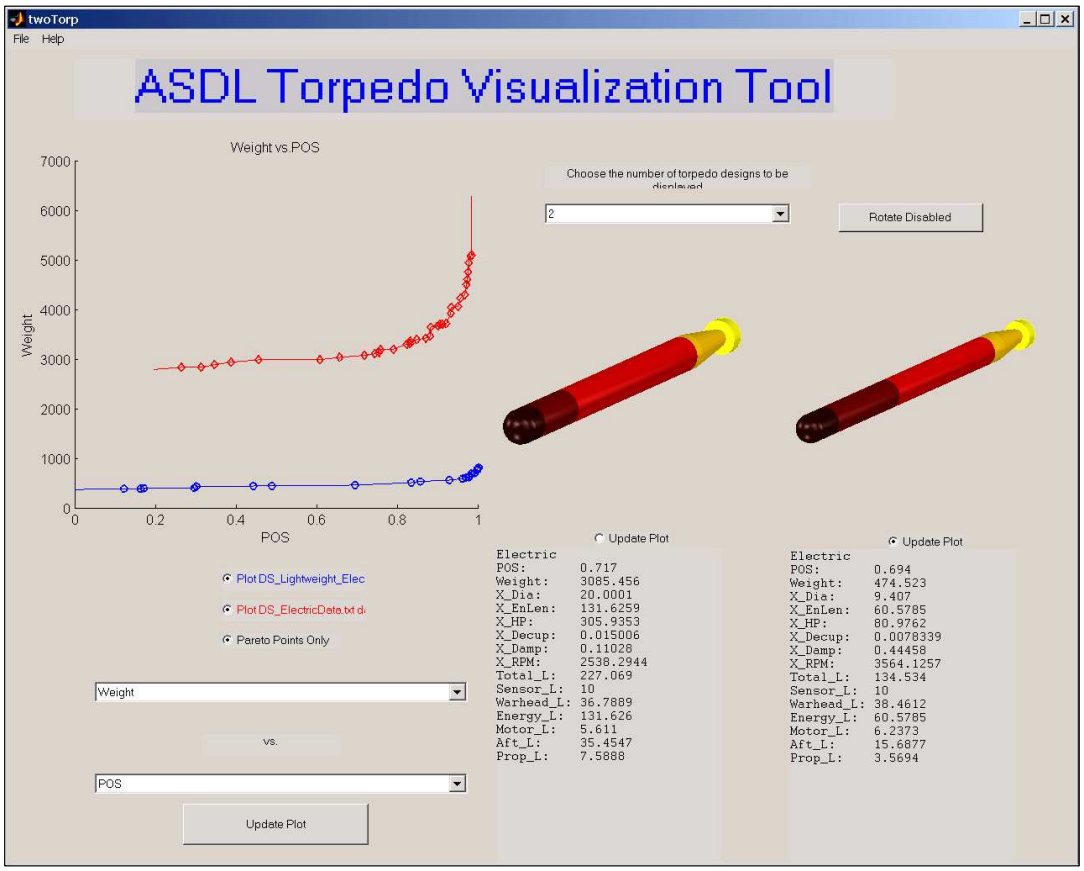

Figure 118: Visualization Tool Comparing Lightweight and Heavyweight Torpedoes

6.4 Summary

This section illustrated the use of the robust design method to analyze torpedo design problems. Two separate approaches were applied, one using a response surface metamodel and the other incorporating direct simulation of the TOAD analysis tool. Both methods

Table 30: Relative Advantages in Design Process Techniques

Concept	Technique	Advantages	Disadvantages
Optimizers	Path-Building	Works well for small dimensional problems	For large dimensions, can have difficulty finding the Pareto frontier (too multimodal and noisy)
	Random Search	Determines the Pareto front all-at-once	Requires many runs, plus creates large amounts of data to track
Modeling and Simulation Tool	Response Surface Equation	Smooths data, works well with gradient-based optimizers	Harder to capture infeasible regions, results appear to be more noisy
	Direct Simulation	More accurate, less noise	Difficult to implement, requires more CPU time

used Monte Carlo simulation as the primary mechanism for calculating the probability of success values. Due to time constraints, genetic algorithms and most-probable-point methods were not used, however, they could easily be incorporated into the analysis. The results from this section section showed that it was possible to use this approach to develop frontiers of probability of success versus weight for torpedo systems and that these frontiers could be used in decision-making. The ability to develop optimum torpedo parameters as a function of the probability of success was clearly demonstrated.

This section also illustrated a few cautionary measures concerning the robust design method. For one, great care needs to be taken when using a path-building optimizer or random search to ensure that the complete Pareto frontier has been located. In addition, the use of random searches may lead to some level of 'noise' along the Pareto front. Finally, direct simulation behaved better than the response surface equations – direct simulation should be used whenever it feasible to do so. Some of the relative merits of each technique are given in Table 30. Even though some techniques have disadvantages, the overall process is still robust, and, as illustrated in this section, is a very powerful tool to examine the complete design space of undersea weapon systems.

CHAPTER VII

INTEGRATION OF TACTICS WITH DESIGN

7.1 Examination of Tactics on Torpedo Design

A study was done to understand the implications of torpedo tactics in relation to torpedo design. This work focused on quantizing the effect that tactics have on design decisions. This analysis required the linking of a torpedo analysis tool with a mission analysis tool, commonly called an engagement model. Because no such engagement models were available in the public domain, an engagement model had to be created. For simplicity, this model focused upon the acoustically-based search abilities of the torpedo – submarine tactics were not included. To facilitate the linking between the torpedo analysis and the new engagement model, the TOAD program was not used. Instead, response surface equations were generated from the TOAD analysis program to use in conjunction with the engagement model. This framework allowed for a well-linked, fast-running, and computationally noise-free analysis environment. This type of framework also allowed for the inclusion of some aspects of torpedo design, such as system cost and a more robust sensor model, that are not available in TOAD. Equations for these parameters could be inserted into the response surface equations representing torpedo design.

Even within this relatively simple framework, the results shown here are extensible to environments in which more complex tools are employed. The final results from this analysis showed that a variation in the tactical situation had a tremendous impact on the performance of the torpedo system.

7.1.1 Analysis Tools

In terms of operational environments, undersea warfare is almost completely characterized by the lack of knowledge concerning the location of enemy vessels. Thus, a large part of undersea warfare is concerned with the means and mechanisms of acquiring information about

the target; essentially this is a combination of tactics and sonar capabilities. In addition to the tactics and sonar capabilities, accurate undersea warfare analysis also requires detailed performance data about the weapon system. In order to capture both the kinematics and the sonar capabilities of the torpedo system, a simple torpedo design program was created, using response surface equations generated from the more advanced TOAD torpedo design and analysis program (see Section 5.1). The new program was specifically designed to examine the implications of sonar performance on the overall capabilities of a fixed-length torpedo system. The analysis assumed a 240-inch long, 21-inch diameter torpedo, similar to today's heavyweight Mk-48 torpedo system. The torpedo is divided into several sections, each sized independently, as described in Table 31. The length of the nose section is a function of the directivity index (DI) and the beam-width (BW) of the sonar. In addition, the power requirement, or "hotel load", generated by the sonar is also a function of these parameters. The variation of hotel load as a function of sonar parameters is shown in Figure 119. The warhead is fixed as a 35 inch, 1,000-lb_m system. The motor provides power to the system, both for the propulsor and for the hotel load of the sonar. The length of the motor is a function of the shaft-horsepower required by the motor to provide sufficient thrust and power generation. The length is generated from a response surface equation developed from the more extensive TOAD analysis program. The back-end of the torpedo, including the afterbody, control fins, and propulsor, is fixed at a 30-inch length. Finally, the fuel section consumes the remaining length of the torpedo, sized so that the total length of the torpedo is always 240 inches.

Table 31: Torpedo Section Definitions

Section	**Purpose**	**Size**
Nose	Sonar and electronics	Function of DI and BW
Warhead	1,000 lb_m warhead	35 inches
Fuel	Fuel for motor	Remainder of 240 inch torpedo
Motor	Provide power to propulsor and sonar	Function of HP
Back-End	Rear of torpedo and propulsor	30 inches

In addition to estimating the sizes of individual torpedo sections, the torpedo analysis tool also calculates the detection range of the sonar, the total range of the torpedo, the search

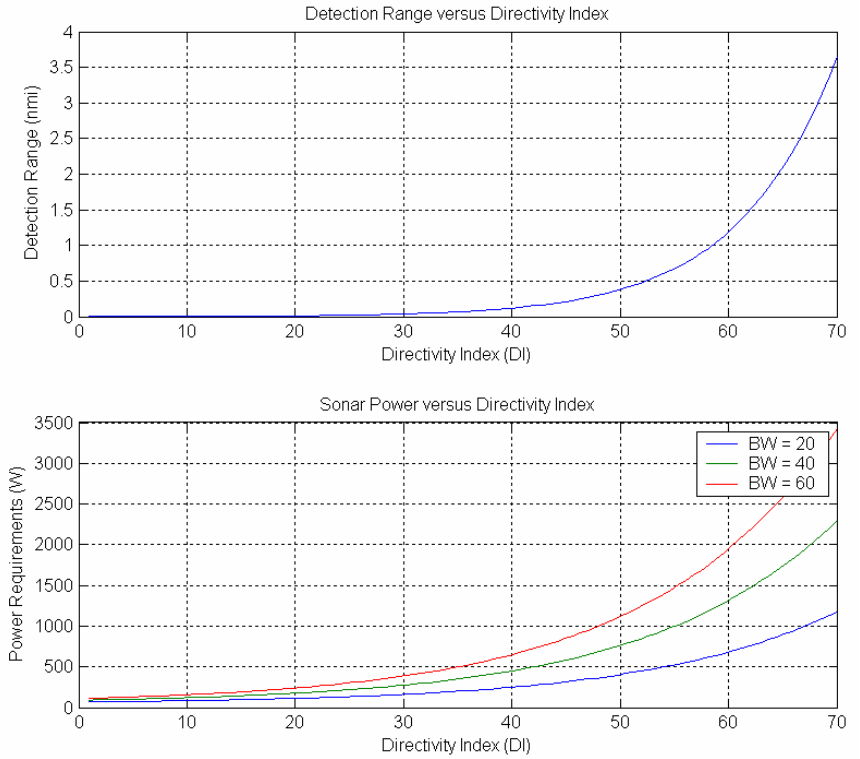

Figure 119: Variation of Directivity Index with Detection Range and Hotel Load

rate of the torpedo, and an estimate of the relative cost of the system. Two parameters are used to define the sonar system. Directivity index, in decibels, essentially tells the 'goodness' of the sonar, or its ability to distinguish a target from background noise. Directivity index directly relates to detection range, as indicated in Equation 24 [120]. The beam-width defines the width of the sonar 'beam'. This width parameter is used to define the effective search area of the sonar. The hotel power drain of the sonar system is a function of both the beam-width and the directivity index. A graph of detection range versus directivity index is given in Figure 119, along with a plot of the power drain of the sonar.

$$20 \cdot \log_{10}(range) + a \cdot range = SL - NL + DI - DT \tag{24}$$

a = Absoprtion Coefficient of Seawater (0.00006 dB/m) [120]
SL = Source Level (25 dB)
NL = Noise Level (15 dB)
DT = Detection Threshold (03 dB)
DI = Directivity Index (input dB)

The range of the torpedo is calculated by first looking at the drag of the vehicle, using the drag routines included in the TOAD analysis program. The power required to overcome the drag and the hotel load is used, along with the effective heating value (accounting for all of the auxiliary losses including unburned fuel, fuel tank structure, auxiliary system volumes, and thermal engine efficiencies) for torpedo OTTO fuel used in the TOAD program ($1.15x10^7 ft-lb_f/ft^3$) to determine the endurance, and thus range, of the torpedo. Finally, the relative cost of the system is estimated. It is assumed that from the baseline torpedo there is an exponential price increase due to improving the sonar performance, plus a milder price increase for increasing the motor horsepower. These costs are entirely notional and are based upon the assumption that higher performance components, such as the engine and sonar, will translate directly into greater costs. Figure 120 shows the relative performance and cost of the system when changing the torpedo design variables.

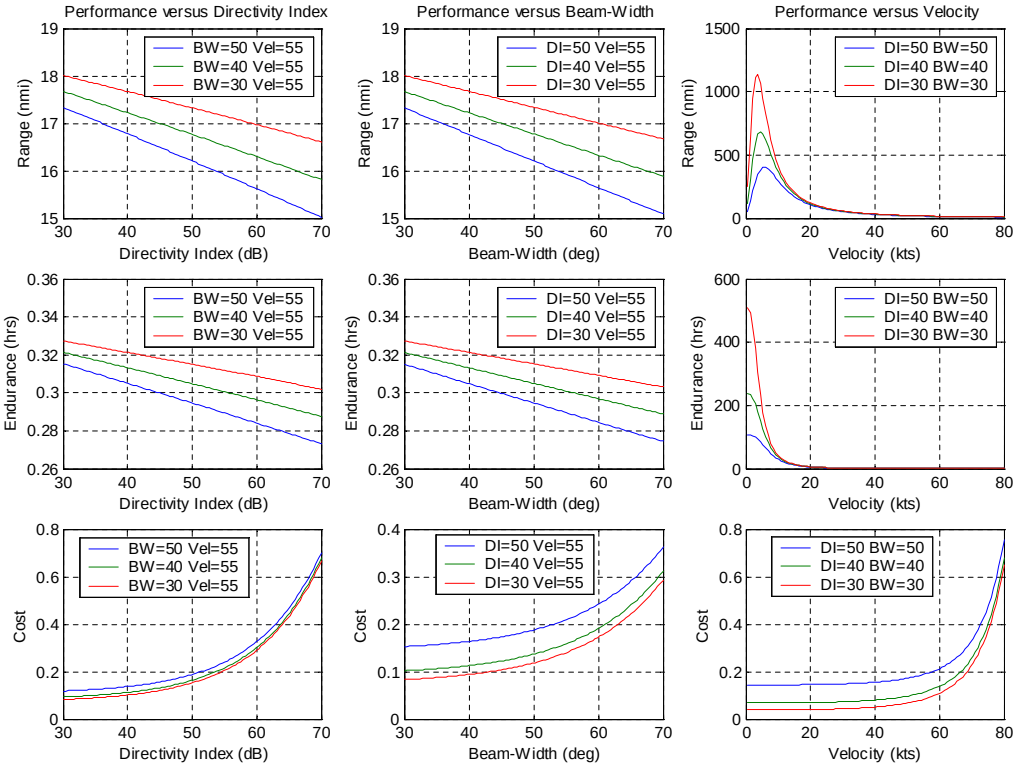

Figure 120: Hypothetical Range, Endurance, and Cost of Torpedo Systems

The search rate of the torpedo is calculated via the geometry shown in Figure 121. The search rate is calculated from the detection range (calculated from directivity index), the beam-width of the sonar, and the velocity of the torpedo, as shown in Equation 25. The search rate is essentially a calculation of how quickly the 'search front' is moved through the water. The search rate assumes that the torpedo moves at a constant velocity and can 'detect' anything that enters into the detection zone. In addition, the search rate assumes that a 'perfect' search pattern is being executed (delineated in the formula by setting η_{search}=1). This perfect search pattern assumes that no portion of the search area is examined twice and that the threat submarine never doubles-back into a previously searched area. A less efficient search, with the torpedo overlapping previously searched areas, could be modeled by setting η_{search} to a value less than one. Although a constant search rate may seem somewhat unrealistic, it is a surprisingly good reflection of the real world. Washburn showed that in a situation in which a searcher was looking for an evading target in a fixed area, the searcher's likelihood of finding the target increased at a constant rate with respect to time [236]. Washburn claimed that the magnitude of this constant search rate is extremely difficult to calculate, but that the search rate is a function of the searcher's speed advantage and sensor range, which is analogous to the formula created in Equation 25.

$$SearchRate = \eta_{search} \cdot 2\pi \cdot DetectionRange \cdot (\frac{BW_{torp}}{360}) \cdot V_{torp} \tag{25}$$

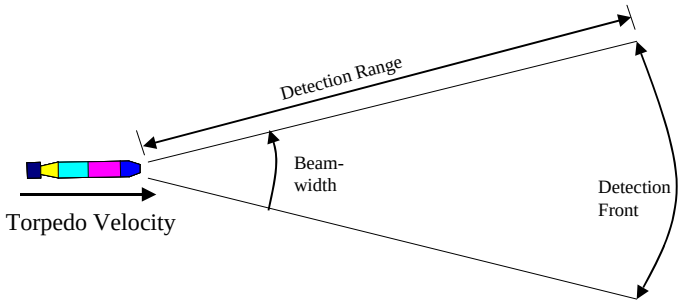

Figure 121: Calculation of Torpedo Search Rate

Two tactical parameters are defined for this problem and are illustrated in Figure 122.

The focus of these tactical parameters is not on the tactics, strategies, and maneuvers of the two submarines before firing, but instead focuses only on the tactical situation that the torpedo 'sees' immediately after launch. Thus, the relevant torpedo information includes the distance to the target, or the required transit distance, and the area of uncertainty surrounding the target, which defines the size of the region within which the target is randomly located. An additional parameter is the velocity of the threat submarine, or, the rate at which the radius of uncertainty for the threat submarine is growing. The threat submarine is assumed to maintain a slow velocity to facilitate its hiding from the searching torpedo. Figure 123 demonstrates how an encounter develops over time.

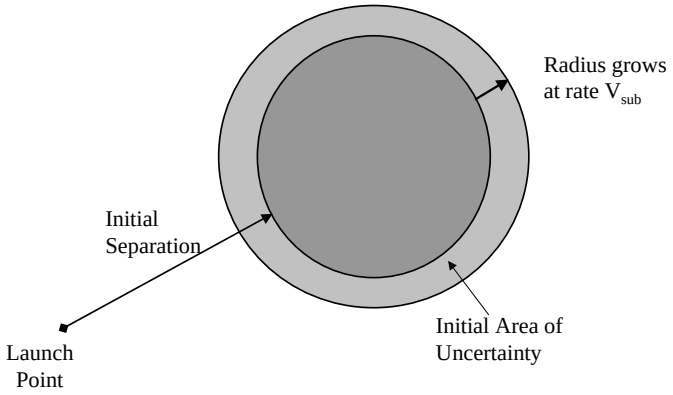

Figure 122: Torpedo Tactics Parameters Analyzed

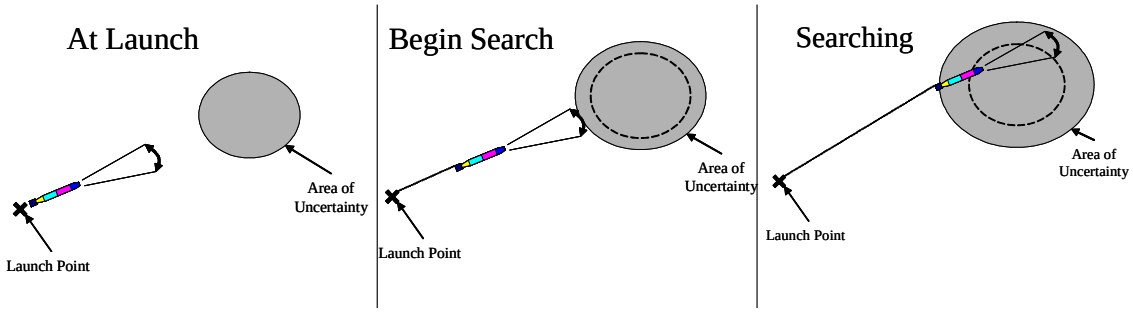

Figure 123: Timeline of Torpedo Engagement

Once launched, the torpedo transits the distance to the search area, with the required search area increasing during transit (at a rate equal to the velocity of the threat submarine). Once in the area of uncertainty, the torpedo begins its search pattern, searching at the

constant rate defined in Equation 25. While the torpedo is searching for the target, the area of uncertainty continues to increase around the threat submarine. Figure 124 shows how the two relative areas change with time: the area that has successfully been searched by the torpedo and the area of uncertainty of the submarine. The area of uncertainty increases quadratically, while the torpedo search area is flat during the torpedo transit and then increases linearly. If it is assumed that the threat submarine is randomly positioned inside the area of uncertainty, then the ratio of these two areas defines the probability of the torpedo detecting the enemy submarine. Thus, the ratio of the current aggregate search area divided by the current area of uncertainty is defined as the probability of hit. Figure 124 also shows the time-varying probability of hit, which is calculated from the ratio of the two areas. The overall, or final, probability of hit is the maximum probability of hit attained during the encounter.

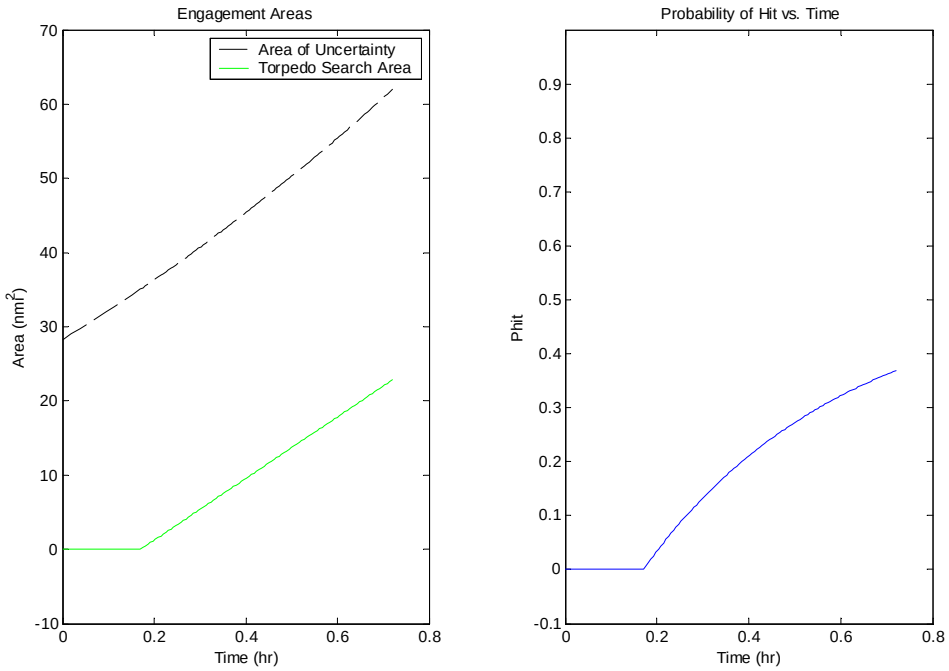

Figure 124: Time Variation of Area of Uncertainty, Search Area, and Probability of Hit

The results from the torpedo analysis tool are linked with the inputs to the engagement analysis tool. The linkages are shown in Figure 125. Using this linkage between the two analysis tools, the torpedo inputs can be translated directly into a P_{hit} value. Since the

torpedo cost is also calculated, the capabilities and cost for various torpedo systems can be compared under various operational scenarios. Table 32 summarizes the inputs and the outputs for the analysis system.

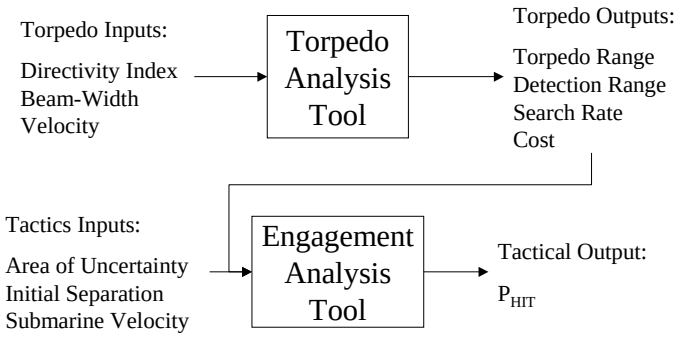

Figure 125: Layout of Tools for Torpedo Tactical Analysis Tools

Table 32: Input and Output Parameters for Tactics Problem

Parameter	Units	Description
Torpedo Input Parameters		
Directivity Index	dB	Effectiveness of sonar beam
Beam-Width	deg	Width of sonar beam
Velocity	kts	Torpedo velocity
Torpedo Output Parameters		
Torpedo Range	nmi	Range of Torpedo
Detection Range	nmi	Range when torpedo detects target
Search Rage	nmi^2/hr	Rate at which torpedo searches area
Cost	—	Estimated cost of system
Tactics Input parameters		
Area of Uncertainty	nmi^2	Initial area of uncertainty for threat
Initial Separation	nmi	Initial separation to area of uncertainty
Threat Sub Velocity	kts	Threat submarine velocity
Tactics Output Parameters		
P_{hit}	—	Probability of hitting target

Figure 126 summarizes the performance of various torpedo system designs. The figure shows the relative range, endurance, search rate, cost, and probability of hit for a torpedo system as a function of the physical attributes of the torpedo: directivity index, beam-width, and velocity. The figures provide some insight into the tradeoffs between the various torpedo attributes and overall performance. Figure 127 shows how varying the tactical

situation changes the torpedo performance. The effects of changing standoff-distance, area of uncertainty, and the threat submarine velocity are apparent on the probability of hit. The figure also demonstrates the significant improvement in probability of hit with an improvement in the sonar system. Note that the torpedo has the best P_{hit} value when used with a standoff distance of zero and an infinitesimally small area of uncertainty. This situation corresponds to an 'optimal' firing position, where the torpedo is dropped right on top of the enemy vessel and the torpedo knows the exact location of the enemy vessel.

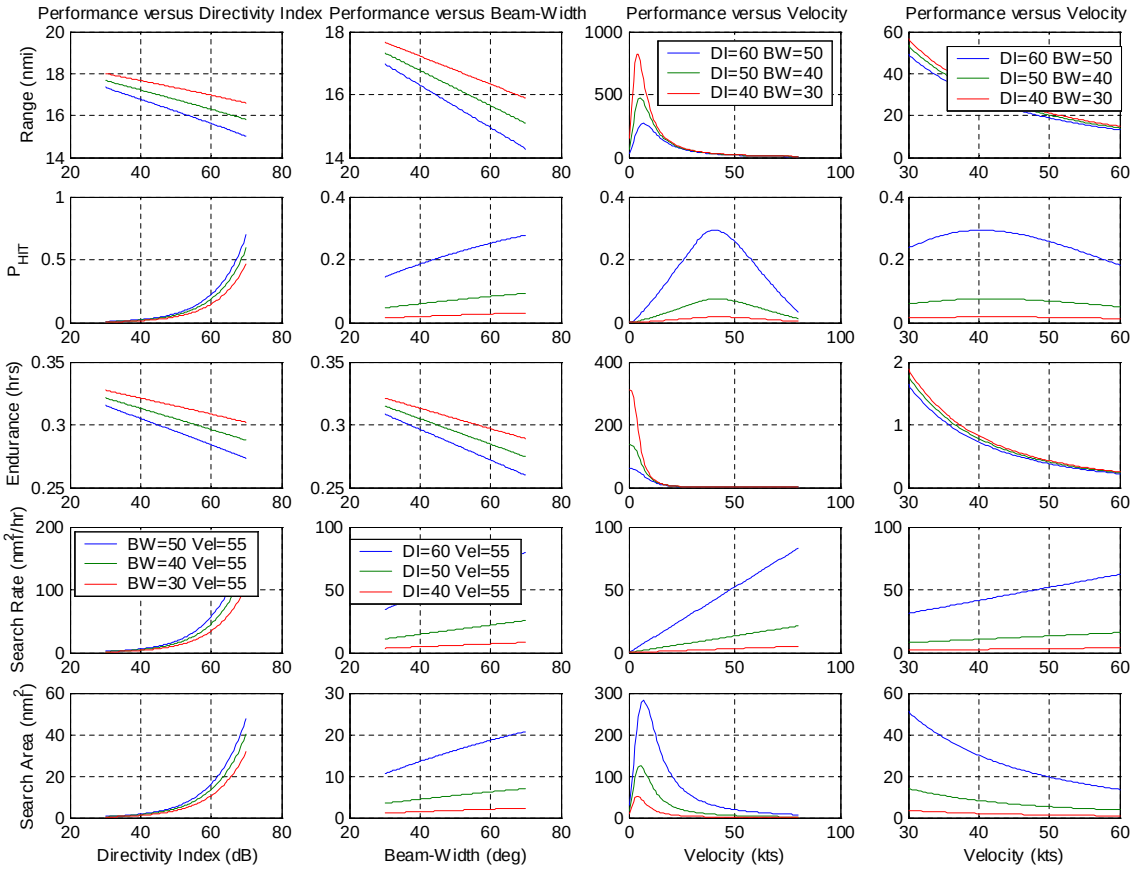

Figure 126: Overall Torpedo System Performance

7.1.2 Results

Once the analysis tools were created and linked together, they were used in conjunction with the 'fmincon' optimizer in Matlab. The analysis tools, in conjunction with the optimizer, could then be used to find the lowest cost torpedo for a fixed price, or conversely, find

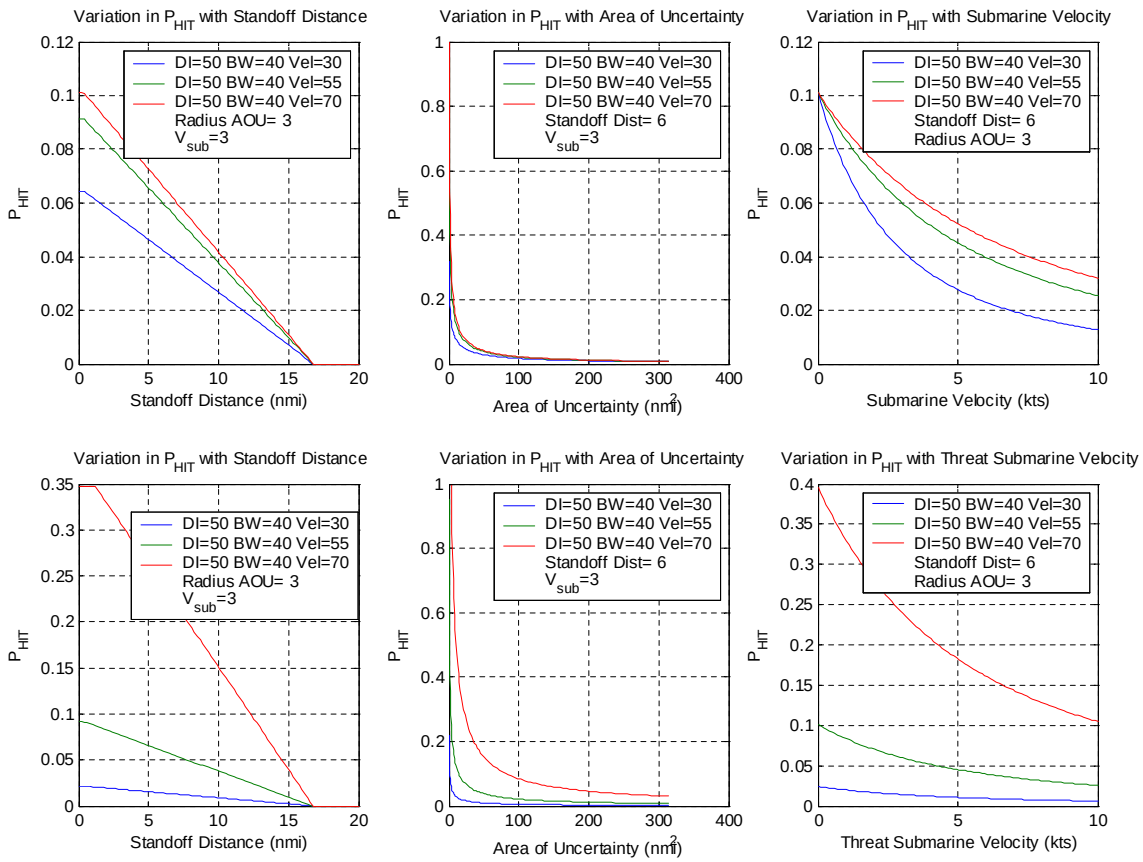

Figure 127: Variation in Torpedo Performance for Changing Tactical Environments

the best performing torpedo for a fixed price. The graph in Figure 128 shows an example iteration history for a converged solution. The figure shows the convergence of a minimum cost torpedo with a constrained P_{hit} minimum of 0.8. In this example the optimizer behaves as expected, first meeting the P_{hit} constraint by driving up the cost, then working to reduce the cost while maintaining the minimum allowed P_{hit} value of 0.8.

Because the design space is multi-modal, multiple "starting locations" were used for the optimizer to guarantee that a global minimum, not just a local minimum, was found. Figure 129 shows the convergence history of a torpedo with a cost constraint of 0.5, where the optimizer is trying to maximize the value of P_{hit}. The convergence history for three runs, each with a unique starting point, is shown in the figure.

Once the optimizer was successfully linked with the torpedo design programs, optimum torpedo designs were found for a range of constrained probability of hit values. The optimal,

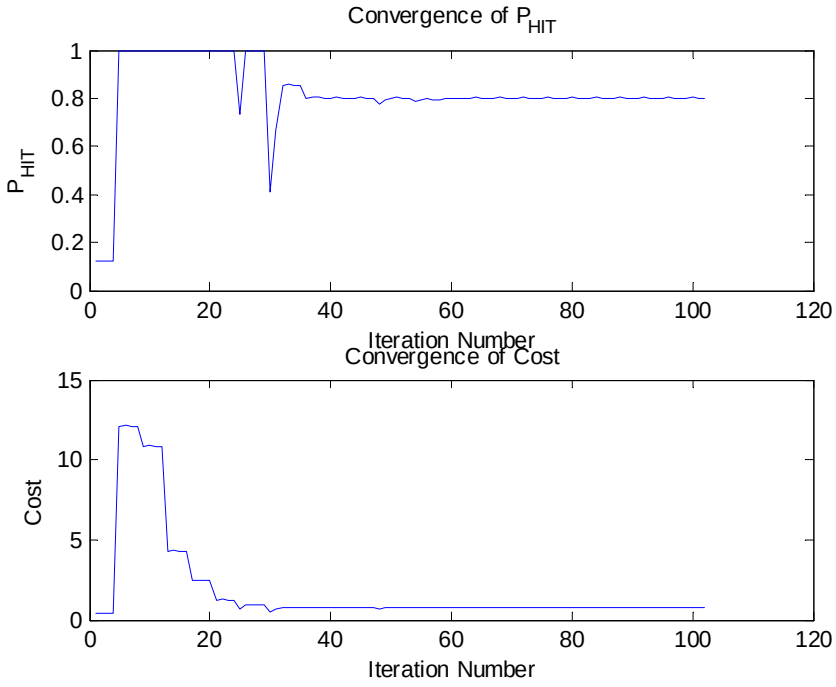

Figure 128: Convergence History for Minimum Cost Torpedo

or lowest cost torpedo, was plotted for each probability of hit, and the results are shown in Figure 130 for three sets of tactical conditions. The figure verifies that, as more performance is required of the torpedo (in the form of a higher P_{hit} value), the system will be more costly. Note also that as the tactical environment worsens, as when the torpedo is launched further from the target area and more uncertainty exists about the location of the target, a much more expensive torpedo is required to meet the same level of probability of hit. Thus, a tradeoff is demonstrated between the cost of the torpedo and the ability to launch the torpedo closer to the target. If the torpedo can be launched closer to the target, then a much lower-cost system will suffice.

Figure 131 gives more information about the optimal torpedoes for each probability of hit. The physical characteristics of each optimized torpedo: directivity index, beam-width, and velocity, are graphed, showing how the physical characteristics change for the optimal designs. Note that as the probability of hit requirement increases, both the directivity index and the beam-width increase, thus driving up the cost. Of interest is the fact that the velocity of the torpedo decreases as the required probability of success increases. This

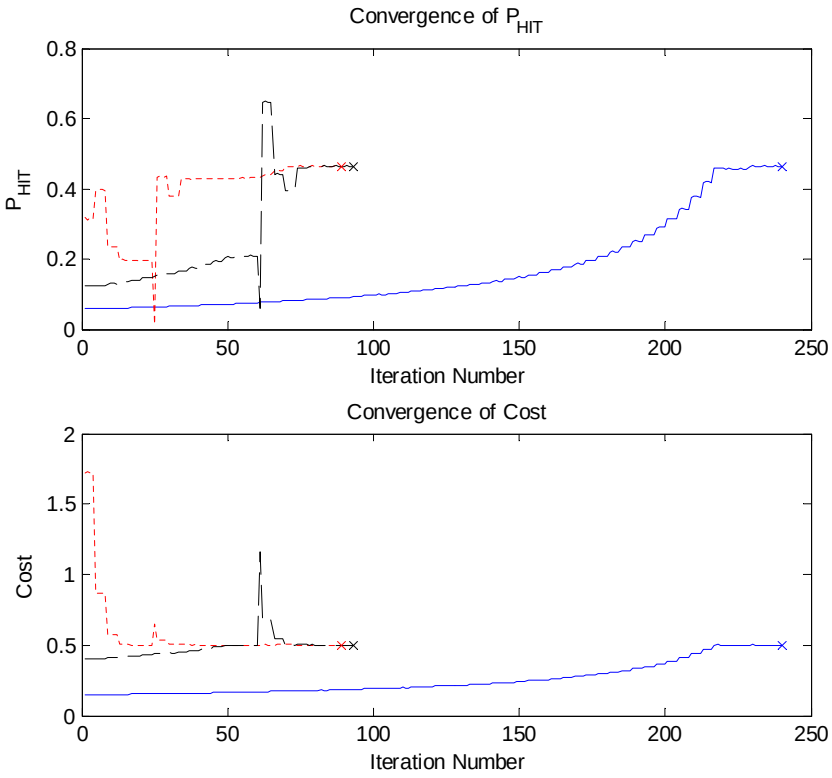

Figure 129: Convergence History of Maximum P_{hit} Torpedo with Multiple Start Points

decrease indicates that it is more important to go slower and search for the target for a longer period of time than it is to cover an area quickly, but less effectively. Lastly, of note is the fact that when the torpedo is launched close to the target (2 nmi), with a small radius of uncertainty (2 nmi), a significantly faster torpedo with a smaller sonar is preferred. If the torpedo is launched this close to the target, it is apparently best to close to the target area quickly and forego the large, expensive sonar systems required of torpedoes that must search larger areas. The charts in Figure 131 show that the best torpedo for a given mission is a direct function of the tactical situation in which the torpedo is being operated, implying that the tactics need to be developed simultaneously with the weapon so that a weapon is always designed that best fits the tactical environment.

Finally, the off-design performance of the torpedoes were tested for various tactical situations. First, a torpedo was optimized to provide the highest P_{hit} possible for a fixed cost of 0.5, in a tactical situation in which the radius of the area of uncertainty was 2.5 nmi

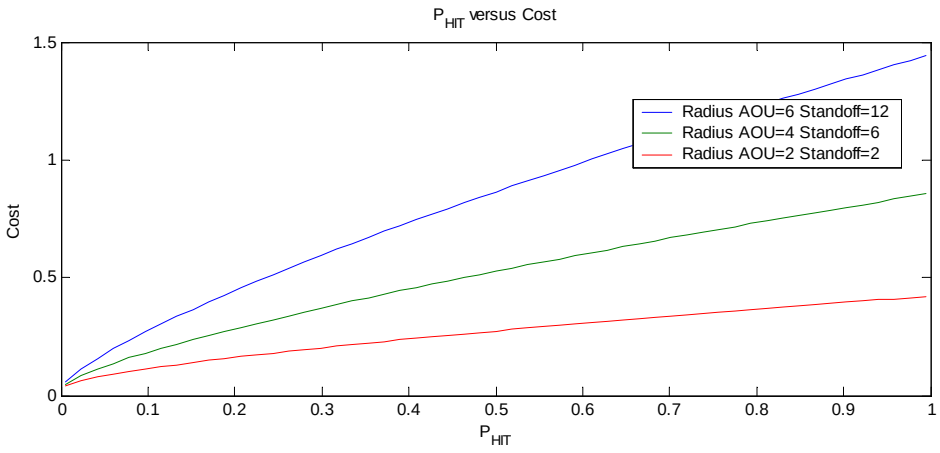

Figure 130: Lowest Cost Torpedo for a Specified P_{hit} Value

and the standoff distance was 5 nmi. Table 33 shows the optimized torpedo for this tactical situation. At a cost value of 0.5, this torpedo was able to provide a probability of hit of 0.85 for the given tactical situation. The entire range of potential tactical situations was then run for this torpedo, to see how the effectiveness of the torpedo changed in various situations; the results are shown in Figure 132. Note that the torpedo performance degrades as it moves towards a longer standoff range and a larger radius of uncertainty. Not only does this represent a significantly degraded tactical environment, but since the plot is for a fixed torpedo that is not optimized for these situations, its performance should also be expected to decrease as the torpedo is being used in sub-optimal tactical situations. The right hand side of Figure 132 shows what happens when the torpedo is locally optimized for each set of tactical parameters. At each point the torpedo is still constrained to meet the 0.5 cost requirement, however it is locally optimized for each tactical setting. Note that the same-cost torpedo performs significantly better when it is optimized for each tactical situation.

Figure 133 overlays the results of the fixed torpedo and the locally optimized torpedo. The dashed lines represent the locally optimized torpedo. Note that, near the 'optimized' point, where the radius of uncertainty is 2.5 nmi and the standoff distance is 5 nmi, the results for the fixed and locally optimized torpedoes are identical. This is expected, as

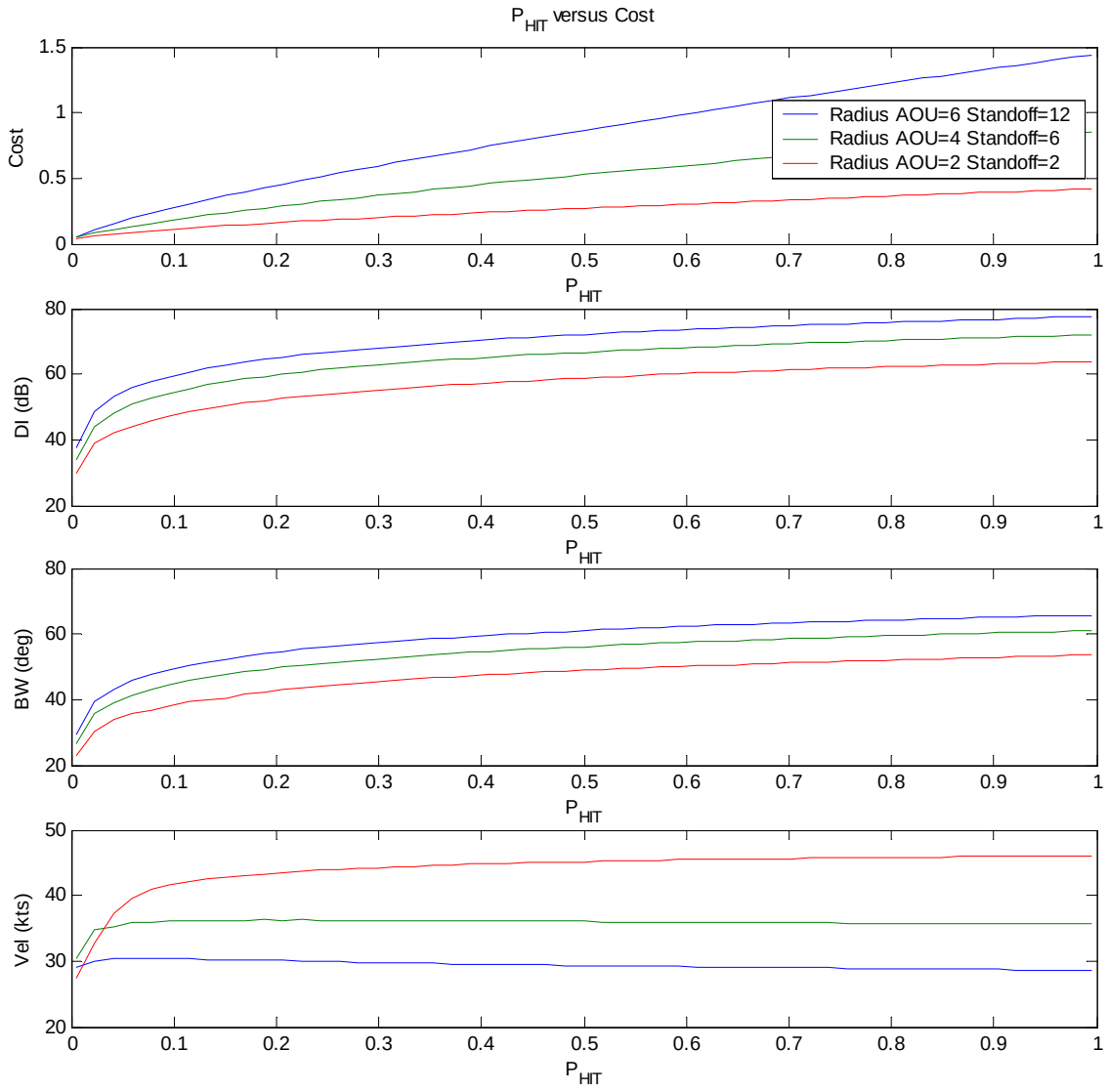

Figure 131: Optimum Torpedo Attributes to meet a Specified P_{hit} Value

both torpedoes are essentially optimized for this region. However, the further away from this optimized region, or, the greater the change that occurs in the tactics, the greater the performance difference that exists between the two torpedoes. After altering the tactics only a small amount, the locally optimized torpedo begins to perform significantly better than the fixed, or singularly optimized system. Thus, the results indicate that there are significant advantages in optimizing the tactics simultaneously with the torpedo system, because the tactics need to be fully defined at the time of designing and optimizing the

Table 33: Optimized Torpedo System

Tactical Parameters		Optimal Torpedo Parameters		System Parameters	
Radius of Uncertainty	2.5 nmi	Directivity Index	66 dB	Cost	0.5
Standoff Distance	5 nmi	BeamWidth	55.4 deg	P_{hit}	0.85
		Velocity	41.3 kts		
		Range	27.5 nmi		

torpedo. Failing to have the tactics fully defined when constructing a torpedo system will potentially lead to a sub-optimal torpedo design.

Figure 134 provides another example that is similar to the comparison of the fixed and the locally optimized torpedo from Figure 133. However, in this case, the fixed torpedo is optimized for a different tactical situation: a radius of uncertainty of 5 nmi and a standoff distance of 15 nmi. The torpedo is again constrained to have a cost no greater than 0.5. The results again show that the locally optimized torpedo behaves similarly to the fixed design near the design point (marked with a +). But, again, there is significant improvement in the effectiveness of a locally optimized torpedo in tactical situations for which the fixed torpedo was not optimized.

Figure 135 shows a third example. This example is for a compromise torpedo design, one that attempts to have good performance at both extremes of the tactical space: a close launch with good target position data and a long-range launch with bad target position data. Note that this compromise torpedo does perform moderately well throughout the tactics space, but, the locally optimized torpedo outperforms the compromise torpedo at every single point in the space. Table 34 shows a summary of the performance for the three fixed torpedoes shown in Figures 133, 134, and 135, along with a locally optimized torpedo. Note again that the locally optimized torpedo always outperforms the other torpedoes, regardless of the mission. Again, in order to achieve the best performance from a torpedo system, the tactics must be analyzed and created simultaneously with the design of the torpedo system.

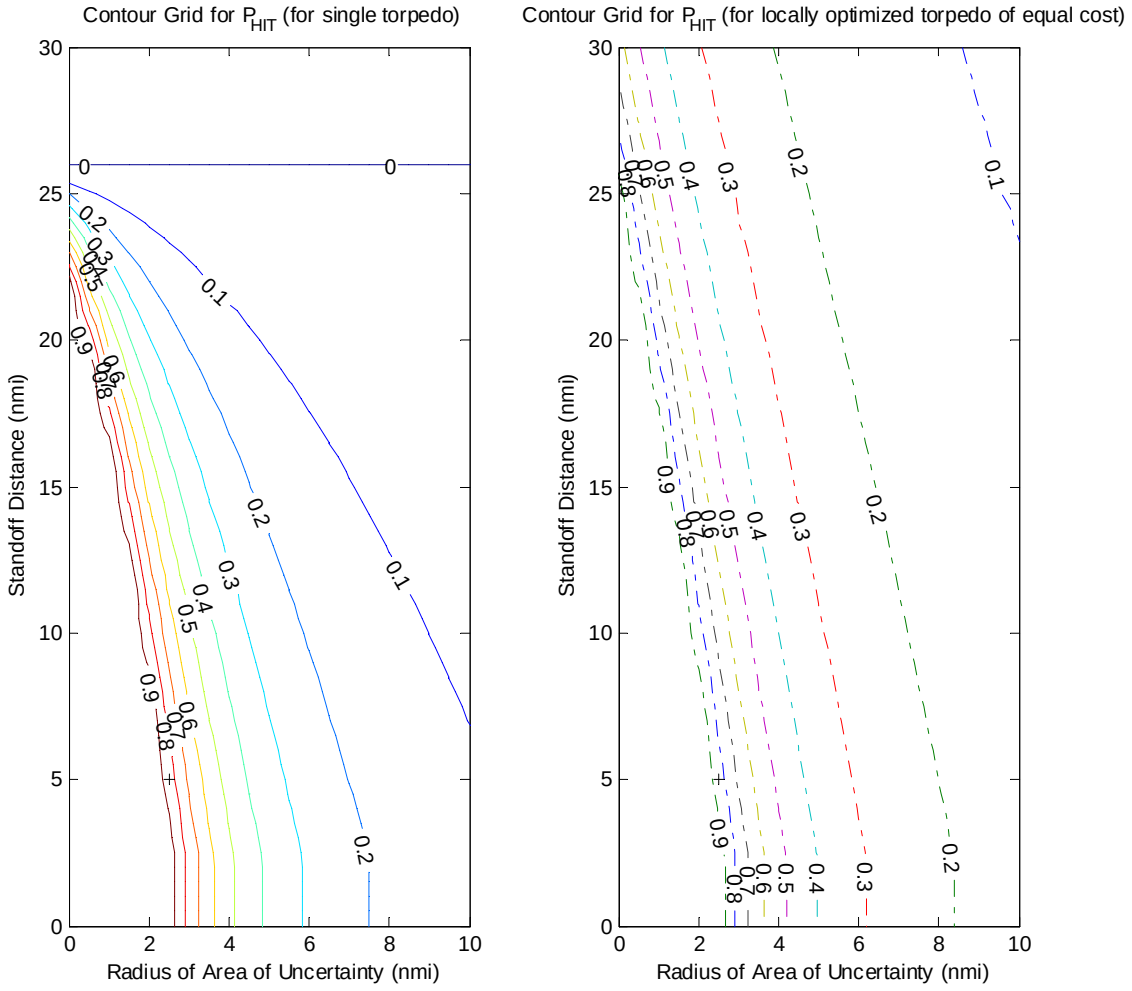

Figure 132: Contours of P_{hit} for Varying Tactics

7.1.3 Summary

The results of this analysis show that the starting tactical situation of the torpedo, or the information available to the torpedo has when it is 'launched', has a significant impact on the performance of the system. Furthermore, the torpedo can be optimized so that its performance is maximized for any tactical scenario. However, if the torpedo is optimized for any single tactical situation, its performance will then be sub-optimal for other tactical situations. Thus, in order to get the most effective torpedo system, the tactics need to be defined and refined during the design and optimization of the torpedo system. By developing the submarine tactics simultaneous with the torpedo design, the torpedo design

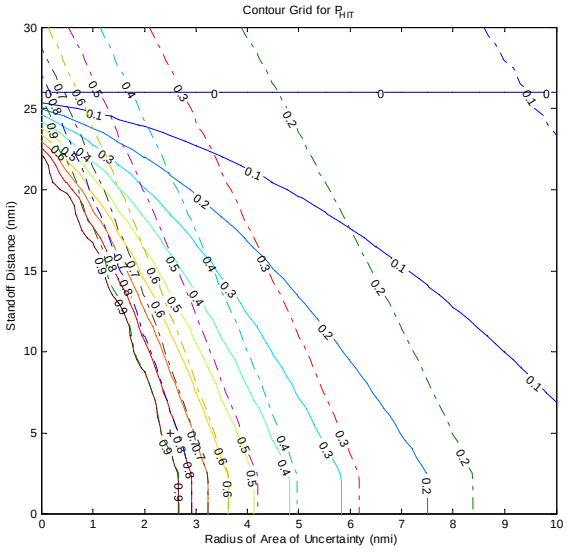

Figure 133: Overlay of Performance of Fixed Torpedo (solid line) and a Locally Optimized Torpedo (dashed line)

Table 34: Relative Performance of Various Torpedoes

			Close Range Torpedo	Long Range Torpedo	Compromise Torpedo	Locally Optimized Torpedo
		DI	66.0	66.5	66.1	varies
		BW	55.4	53.2	55.4	varies
		Velocity	41.4	30.1	37.9	varies
		Range	25.7	46.6	30.3	varies
Scenario 1 (Close In, Good Knowledge)	Radius of Uncertainty	2.5 nmi	**0.852**	0.668	0.834	**0.852**
	Standoff Distance	5 nmi				
Scenario 2 (Long Range, Bad Knowledge)	Radius of Uncertainty	5 nmi	0.174	**0.262**	0.215	**0.262**
	Standoff Distance	15 nmi				
Scenario 3 (Close In, Bad Knowledge)	Radius of Uncertainty	5 nmi	0.335	0.345	0.356	**0.364**
	Standoff Distance	5 nmi				
Scenario 4 (Long Range, Good Knowledge)	Radius of Uncertainty	2.5 nmi	0.442	0.486	0.504	**0.526**
	Standoff Distance	15 nmi				
Scenario 5 (Avg Range, Avg Knowledge)	Radius of Uncertainty	3.75 nmi	0.384	0.404	0.417	**0.430**
	Standoff Distance	10 nmi				

that best meets the tactical environments can be developed, thus ensuring the optimal, most cost-effective system. Therefore, this paper points to the need to design torpedoes in the context of the larger system (the submarine and tactical environment), thereby taking the "system of systems" approach. Only by designing the torpedo at such a level can truly optimal systems be created.

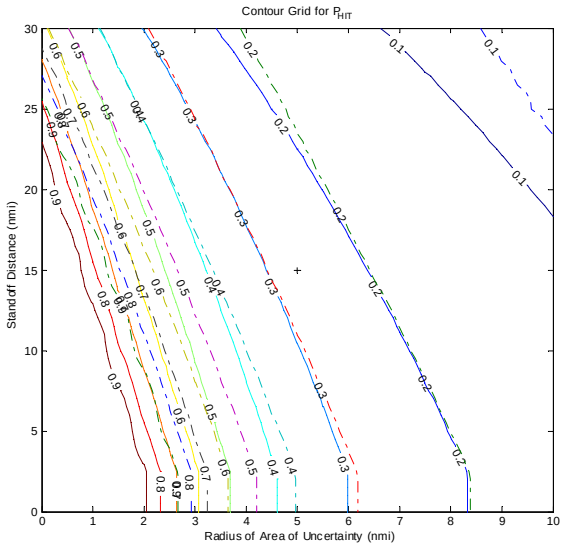

Figure 134: Overlay of Performance of Fixed Torpedo (solid line) and a Locally Optimized Torpedo (dashed line) for Different Requirements

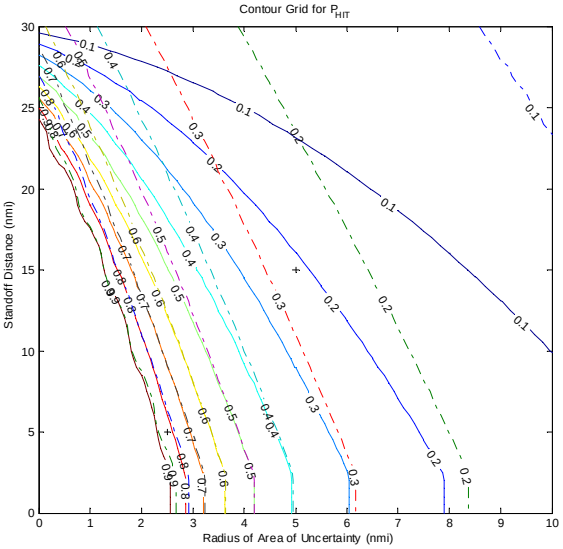

Figure 135: Overlay of Performance of Fixed Torpedo (solid line) and a Locally Optimized Torpedo (dashed line) for a Compromise Torpedo

7.2 Optimization of Mine Counter-Measure Tactics and Design

7.2.1 Analysis Tool

Several modeling tools exist to analyze mine counter-measure systems. These tools include the Surf Zone Mine Clearance Evaluator Tool, Total Mine Simulation System, and the Autonomous Littoral Warfare Systems Evaluator. At least 15 separate government simulations exist to serve these modeling needs [30]. Unfortunately, none of these models are publicly available, thus they could not be used for this research.

As such, a minehunting simulation was developed in Matlab. This program had a time-marching simulation of a minehunting vehicle as it moved through a minefield searching for, classifying, identifying, and neutralizing both mines and non-mines. The program calculates the percent of the total mines in the field that were cleared in a given time, as well as the number of non-mines that were wrongly prosecuted. The program accounts for all of the critical minehunting variables listed in Table 6, including detection probabilities, classification probabilities, classification times, etc.

The program works by time-marching a minehunter through a minefield. The minehunter is assumed to have an imperfect seeker (see Section 2.3.2). This seeker has a fixed search radius and probability of detection associated with it. If an object (either mine or non-mine) enters the radius, there is a random chance that the object is detected, based upon the probability of detection. If the object is detected, then a classification attempt is made, with the given probability of classification, which takes a time equal to the time-to-classify (t_c) value. In this manner the program follows the minehunting steps displayed in Figure 23. After the allotted search time is complete, the program terminates, with the percent clearance of the minefield returned as an output.

The minehunting analysis program has a visualization feature, whereby the user can watch the minehunter sweep through the minefield. Though the visualization can be turned off for large Monte Carlo runs, it is indispensable for debugging and validating the program. A screenshot of the initial setup for a run is given in Figure 136. The minefield to be searched is shown. Individual mines are represented by an 'x' and non-mines are represented by a

'·'. The mines and non-mines are randomly placed in the minefield at the start of the run.

The minehunter is represented by a '+' symbol. A dotted line around the '+' symbol represents the range of the 'imperfect' seeker associated with the minehunter. Any object, mine or non-mine, that enters into this radius, has a chance of being detected by the minehunter.

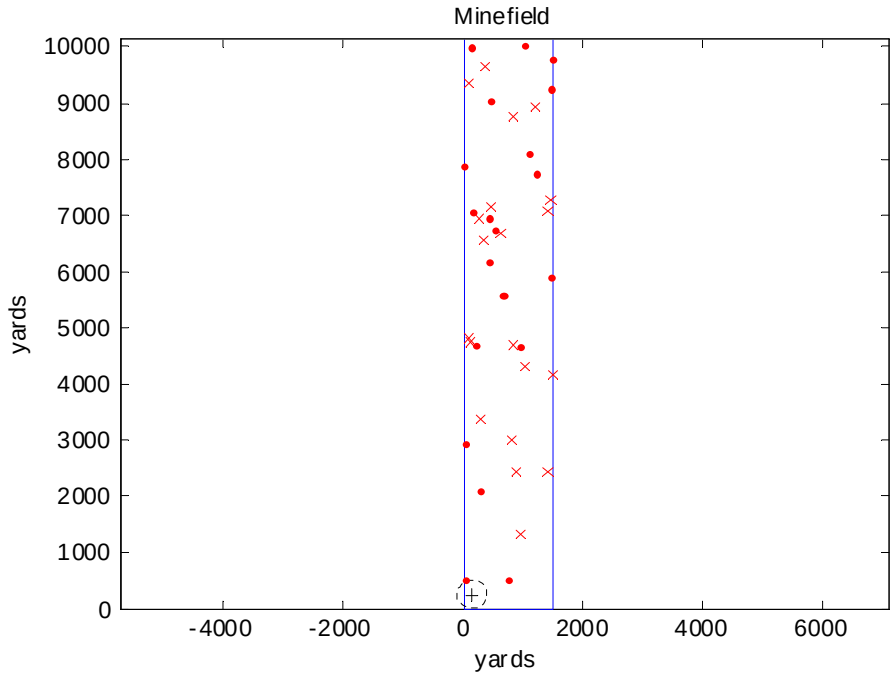

Figure 136: Initial Setup for Minehunting Analysis Tool – Mines are represented as an 'x' and non-mines by a '·'

As the minehunter moves through the minefield, it detects, classifies, identifies, and neutralizes mines. These steps are indicated in the visualization system by a sequence of colors. Red means an object has not been identified, green means it has been declared a false target (whether this is true or not), and black means that the object has been neutralized (whether a mine or not). Table 35 provides a legend for the visualization program.

Figure 137 shows an example of the situation partway through the minehunting process. Note that the minehunter, which is moving in vertical tracks, is gradually making its way towards the right-hand side of the minefield. In its wake, some mines (represented by 'x'), have not been detected (in red) or have been mistakenly marked as false target (in green),

Table 35: Legend for Minehunting Tool

Symbols	
+	Minehunter
- - -	Seeker Radius
x	Mine
·	Non-Mine
blue line	Minefield Border
Mine Colors	
red	Mine Still Active
green	Mine has been Detected Incorrectly Classified as a False Target
black	Mine has been Neutralized
Non-Mine Colors	
red	Non-Mine Has Not Been Detected
green	Non-Mine has been Detected Correctly Classified as a False Target
black	Non-Mine has been Unnecessarily Neutralized

two bad situations. However, a large number of mines have already been neutralized, as represented by the large number of black x's. Similarly, most non-mines have been safely marked as false targets, though some have not been detected or were unnecessarily neutralized (neutralization of non-mines, though not being harmful to the minehunter, represents a waste of both time and resources).

Figure 138 shows an example of a minehunter after completing its mission. The minehunter has finished several sweeps of the minefield, when most of the mines and non-mines have been detected and have either classified as false targets or have been neutralized. A perfect minehunter would have neutralized every mine and classified each non-mine as a false target. Thus, for a perfect mission, every 'x' would be black, and every '·' would be green. This situation would represent a mine clearance percentage (number of mines neutralized divided by total number of mines) of 100%. If some mines were not neutralized, the neutralization percentage would be less than 100%.

The minehunter searches by traveling back and forth across the minefield. When the minehunter reaches the end of the minefield, it moves laterally a distance equal to the track spacing, which is another input, and begins searching in the opposite direction. If the minehunter, which starts on the left-hand side of the minefield, moves the entire width of the

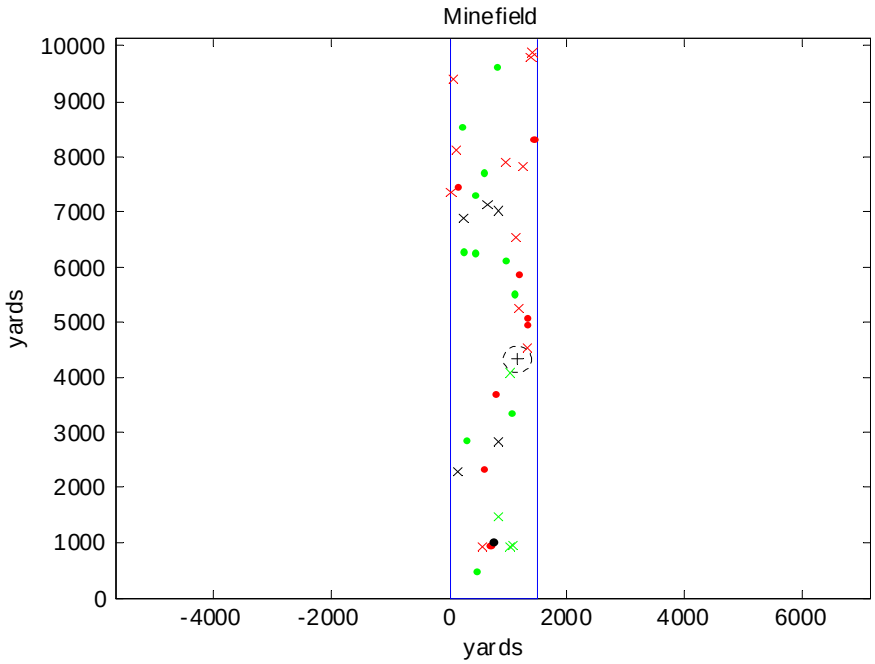

Figure 137: Example of Minehunter Progress in Minehunting Analysis Tool

minefield, it begins its next sweep by returning to the left-hand side of the minefield. Thus, the minehunter may search the entire minefield multiple times, depending on its velocity and the amount of search time it is allotted. The minehunter continues this process until it reaches the maximum allowed search time. In order to account for navigational error, the minehunter does not travel directly across the minefield. Instead, a random heading error in inserted into the minehunter's path. This heading error, or navigation error, is defined as a percentage and represents the percent error that will exist at the end of the path. For example, a 2% navigation error would indicate that after traveling 2,000 yards, the minehunter will be 40 yards from the location where it planned to be. Table 36 lists all of the input parameters used by the minehunting analysis program. It also lists that defaults that were used in the program. Some of these defaults were based upon data available in public literature. For instance, a Johns Hopkins study on the Long-Term Mine Reconnaissance System suggests a probability of detection of 0.9 and a vehicle speed of 7 knots [21] [142]. Unless stated otherwise in the analysis, the assumed values listed in Table 36 were used throughout the research.

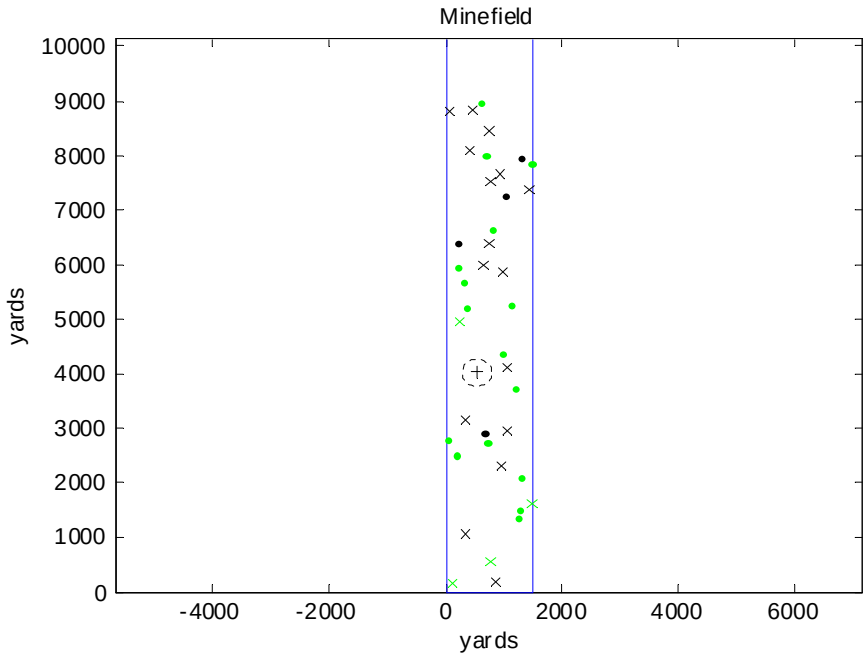

Figure 138: Example of Final Results in Minehunting Analysis Tool

7.2.2 Minehunting Results

The first step in any analysis process is to determine the relative impact of the various design variables. As mentioned in Section 3.4.3, the relative impact of design variables can be displayed in a Pareto chart. A Pareto chart for the minehunting problem is shown in Figure 139. Note that the largest drivers on the system are the endurance, or search time, seeker radius, and the velocity of the system. However, it is interesting to observe that most of the attributes tested had at least some impact on the system performance; none of the attributes could be readily be discarded as being unimportant.

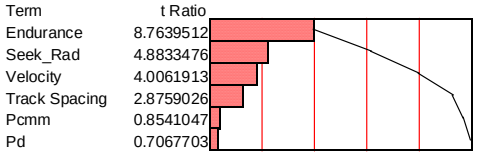

Figure 139: Pareto Plot for Minehunting Results

Table 36: Input Parameters and Assumed Values for the Minehunter Analysis Program

Parameter	Definition	Default Value
Length	Length of minefield	5 nmi
Width	Width of minefield	1000 yrd
Num_mines	Number of mines	50
Num_nonmines	Number of non-mines	50
P_d	Probability of detecting an object	0.9
P_{cmm}	Probability of classifying a mine as mine-like	0.9
P_{cnm}	Probability of classifying a non-mine as mine-like	0.3
T_c	Time to classify object	20 sec
P_{imm}	Probability of correctly identifying a mine	0.9
P_{inm}	Probability of incorrectly identifying a non-mine	0.1
T_i	Time to identify object	240 sec
P_n	Probability of neutralizing object	0.9
T_n	Time to neutralize object	60 sec
Vel	Minehunter velocity	7 kts
	Seeker radius	75 yrd
	Navigation error	2.5%
	Track spacing	150 yrd
MCT/SCT	Classification technique	MCT
	Search time	1 - 24 hrs

The second step of the analysis tool was to look at the tradeoff presented to the decision-maker. This involves examining the success of the minehunter, in terms of percent clearance of a minefield, versus the time required to sweep the minefield. Figure 140 shows how the percent clearance of the minefield increases as more time is spent in the search of the minefield.

As stated before, the minehunter problem is rife with uncertainty. This uncertainty is present because the number of mines is not fully known, the navigational error of the vehicle is random, and the sensor's likelihood of detecting and classifying a mine is dependent upon conditions. Thus, the results in Figure 140 were run with normal distributions added to the uncertain variables. Monte Carlo techniques were used to capture the probabilistic nature of the problem. The altered variables and the parameters of their normal distributions are listed in Table 37.

Since some noise will always exist in Monte-Carlo style solutions, the resulting figures were not perfectly smooth. In order to smooth out the data, a non-linear function was

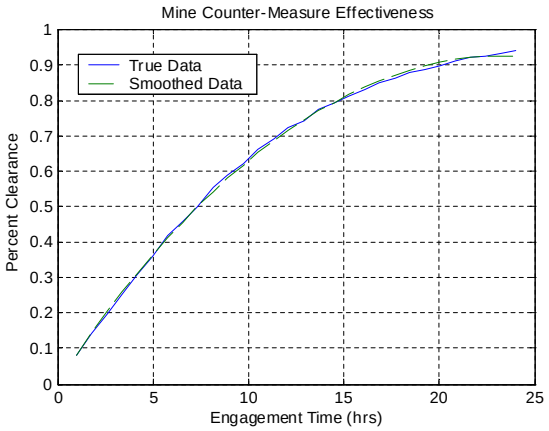

Figure 140: Minefield Clearance as a Function of Search Time

Table 37: Normal Distributions on Uncertainty Variables for Minehunting Analysis

Variable	Function	Mean	Standard Dev.
P_d	Probability of Detection	0.9	0.09
$Pcmm$	Probability of Classifying a Mine as Mine-like	0.9	0.09
Ti	Time to Identify Mine	240 sec	24 sec
Path Error	Navigation Error	2.5%	0.25%
Num_Mines	Number of Mines	50	5

regressed against the minehunting data, with the smoothed function plotted. The non-linear function is a quadratic with an exponential term added. The regression function is given in Equation 26, which is a function of five regression coefficients. The smoothed data is plotted against the original data in Figure 140.

$$Y = b_0 + b_1 \cdot x + b_2 \cdot x^2 + b_3 \cdot e^{\,b_4/x} \tag{26}$$

The results from running the analysis with the uncertainty distributions from Table 37 show that the net effect is a normal distribution on the expected percent clearance. Figure 141 shows a histogram of the results at six separate hunt-times. The resulting normal distribution can be seen for each search time. In addition, it is apparent that the mean of the distribution shifts to the right, or increases, as the search-time increases. Thus, Figure 140 can be thought of as having a histogram wrapped around each point, with only the

mean of the results being shown.

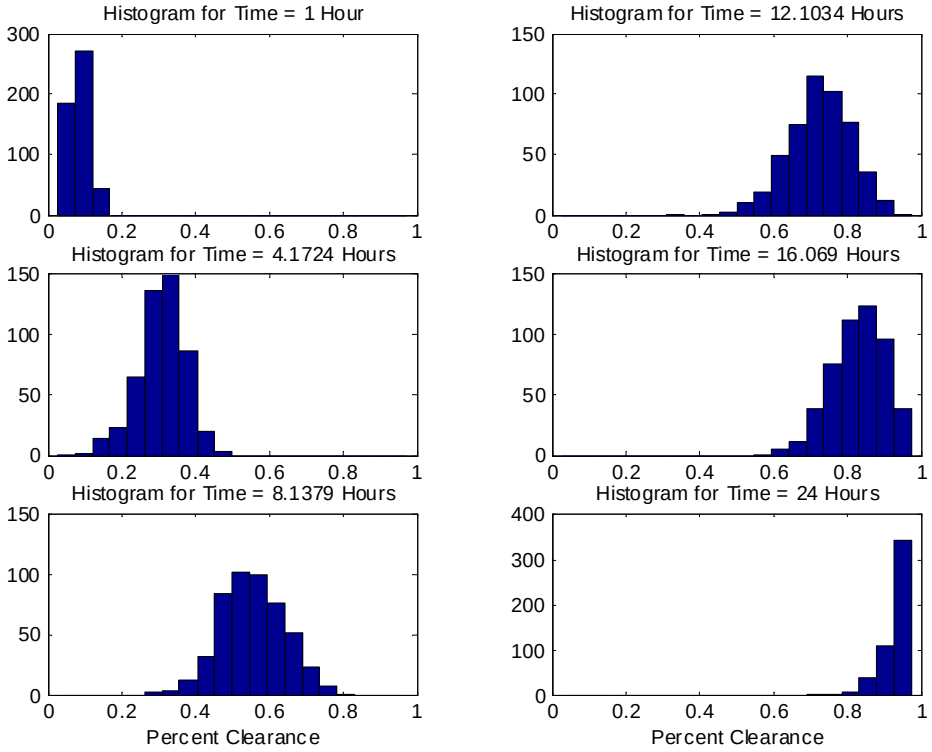

Figure 141: Uncertainty Distributions for Minefield Clearance vs. Search Time

With this new uncertainty data, the percent clearance versus search time (originally shown in Figure 140) could now be shown as a set of probabilistic lines. Figure 142 shows contours of probabilistic data. The figure shows the probabilistic confidence of meeting the percent clearance. For instance, the blue line shows the 90% confidence level. Thus, the decision-maker can, with a 90% confidence, expect the actual percent clearance of the minefield to be equal to or greater than this amount. Similarly, confidence intervals of 75%, 50%, 25%, and 10% are shown, as well as the mean value for the runs. With these charts, more information is now available for the decision-maker, as the user no longer knows what is the 'likely', or mean percent clearance, but can now address the actual confidence of meeting a clearance level for a given search time. In this manner, a probability of success value is being brought forward to the decision-maker.

Going back to the more familiar probability of success formulation, if a required clearance

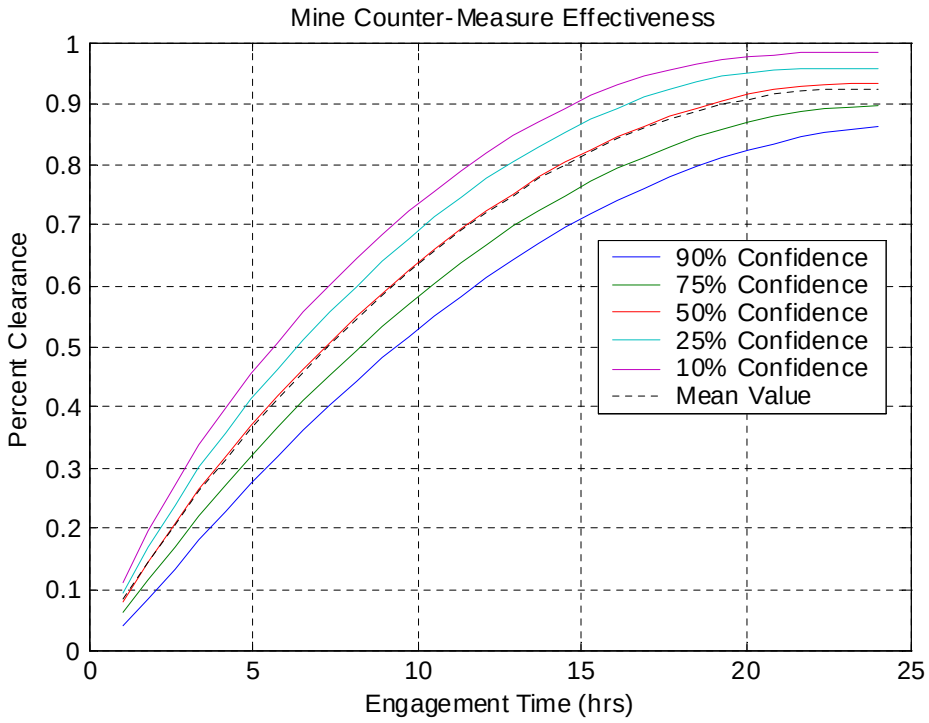

Figure 142: Probabilistic Results for Minefield Clearance vs. Search Time

level is specified, for instance, 80%, then the probability of successfully meeting that level as a function of search time can easily be calculated with the data already present. These results, comparing search time with the probability of achieving an 80% minefield clearance, are shown in Figure 143. The more familiar form of this chart is shown as Figure 144, where the smallest search time to meet a probability of success is given. These figures can be used by a decision-maker, in the same manner as described in Chapter 6, to make design decisions and design optimizations concerning the minehunter system.

7.2.3 Minehunting Tactics Results

With a means available for characterizing the effectiveness of a minehunter system, including the effects of uncertainty, the impact of design variables and tactics on the vehicle's performance could now be investigated. The first step in this investigation was to study the variation of individual parameters on the performance of the vehicle while in the presence of uncertainty. The first design parameter to vary was the probability of detection, P_d. This

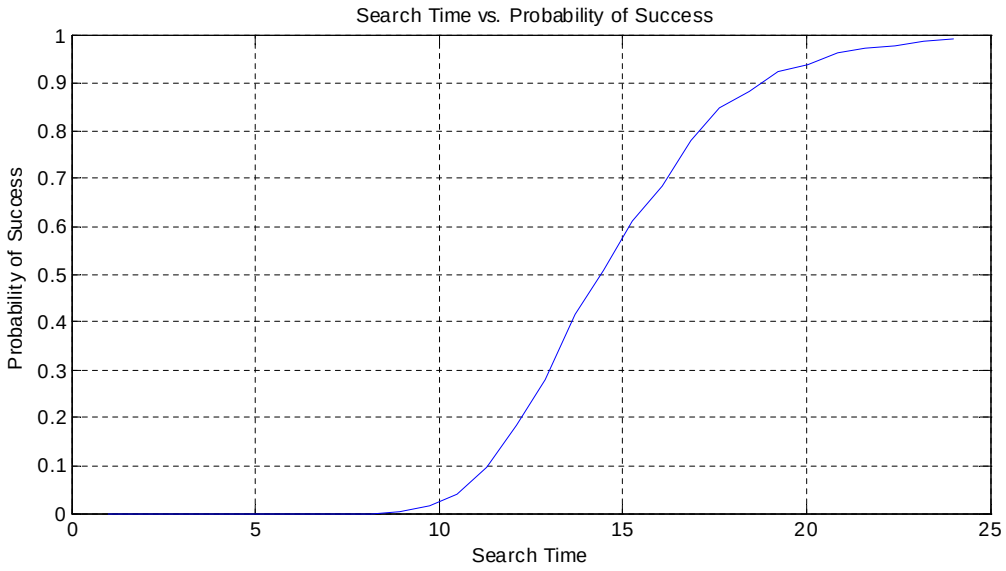

Figure 143: Probabilistic Results Comparing Search Time to Probability of Success (for a Required Mine Clearance of 80%)

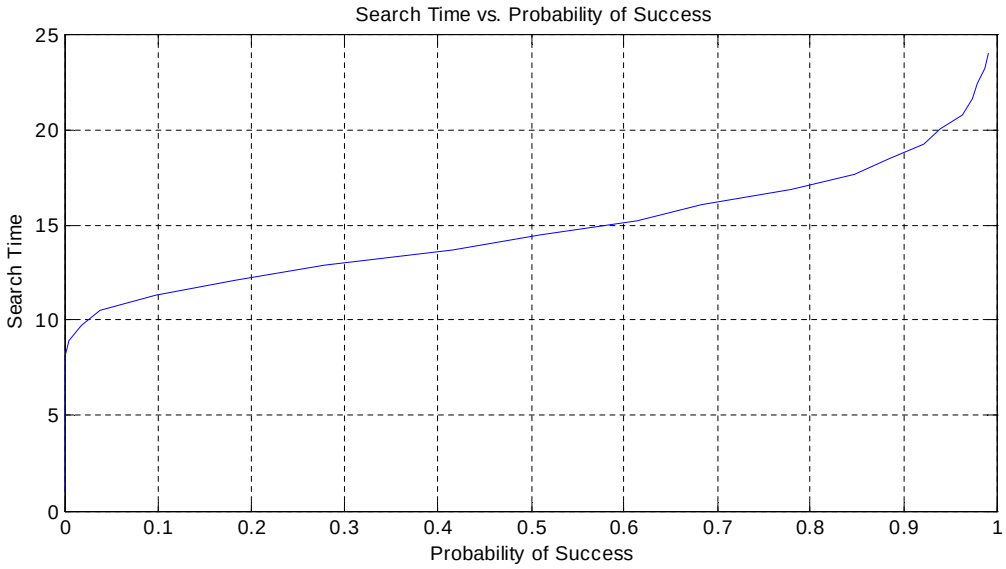

Figure 144: Probabilistic Results Probability of Success vs. Search Time (for a Required Mine Clearance of 80%)

parameter was varied from 0.6 to 0.99. The effect of varying the probability of detection on the mean performance of the vehicle is shown in Figure 145. As one would expect, an increasing probability of detection increases the minefield clearance for a given time.

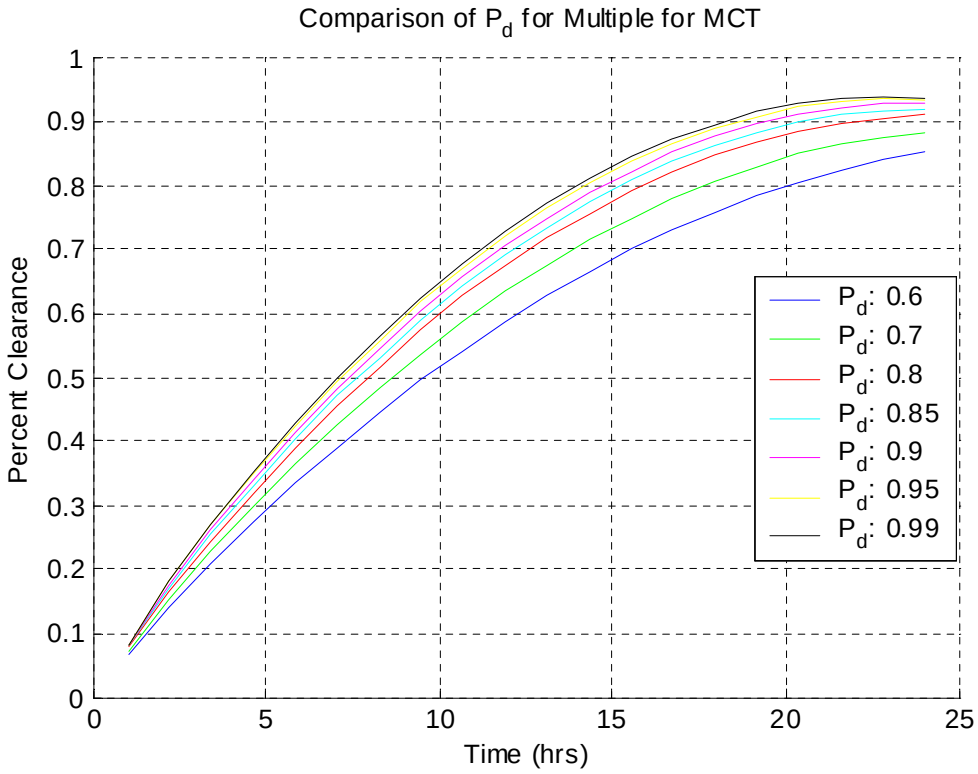

Figure 145: Effective of Varying the Probability of Detection on Minehunting Effectiveness

The track spacing, which is the distance between legs of the search pattern (see section 2.3.3), was the primary tactical variable used in this study. The effect of this parameter on the performance of the minehunter is shown in Figure 146. Note that, except at very low values of the search pattern track spacing, there was not a large effect of changing this parameter on the effectiveness of the minehunter.

Figure 146 was created using a search style known as multiple classification tactics (MCT), as discussed in Section 2.3.3. These tactics imply that additional classification attempts are made against objects every time that they are encountered, even if the object was already declared a false target on previous examination. An additional choice for tactical parameters is to use a single classification tactic (SCT), in which objects are only classified once, and, if declared to be a false target, are summarily ignored are subsequent passes. These same results, for varying track spacing, but using a single classification strategy, are shown in Figure 147. Note that the SCT strategy is more effective at smaller

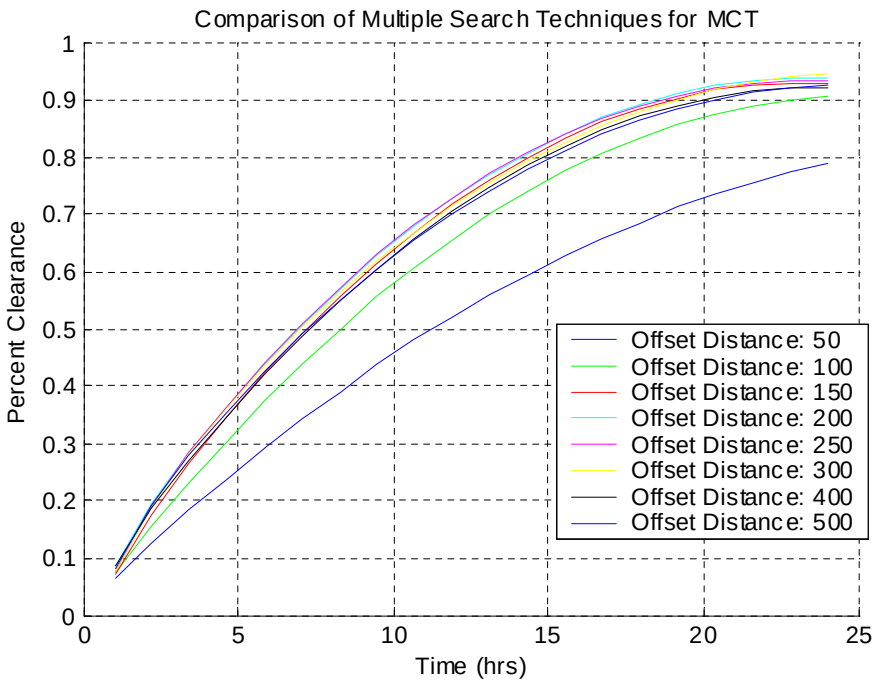

Figure 146: Effects of Varying the Track Spacing on Minehunting Effectiveness for Multiple Classification Tactics

search times, but is inferior to the multiple classification tactics at larger search times. This difference is due to the fact that SCT saves more time in the search process by not re-scanning objects, so the search proceeds at a faster rate. However, MCT techniques are more robust, as miss-diagnosed mines will be rescanned and summarily destroyed. Thus, the MCT techniques perform better at long search times. A direct comparison of the SCT and MCT results is shown in Figure 148. The same trend is evident, with SCT tactics performing better for small engagement times but MCT tactics outperforming at large engagement times. These results illustrate yet again the critical effect that tactics have on the performance of the minehunting system.

The final critical element of mine counter-measures is the minehunter search velocity. This velocity can be thought of as both a design variable and a tactics variable. The velocity is clearly a design variable, because the vehicle must be capable of sustaining the designated velocity for the entirety of the search time. However, the velocity is also a tactical parameter, because a velocity less than maximum may prove optimal for searching,

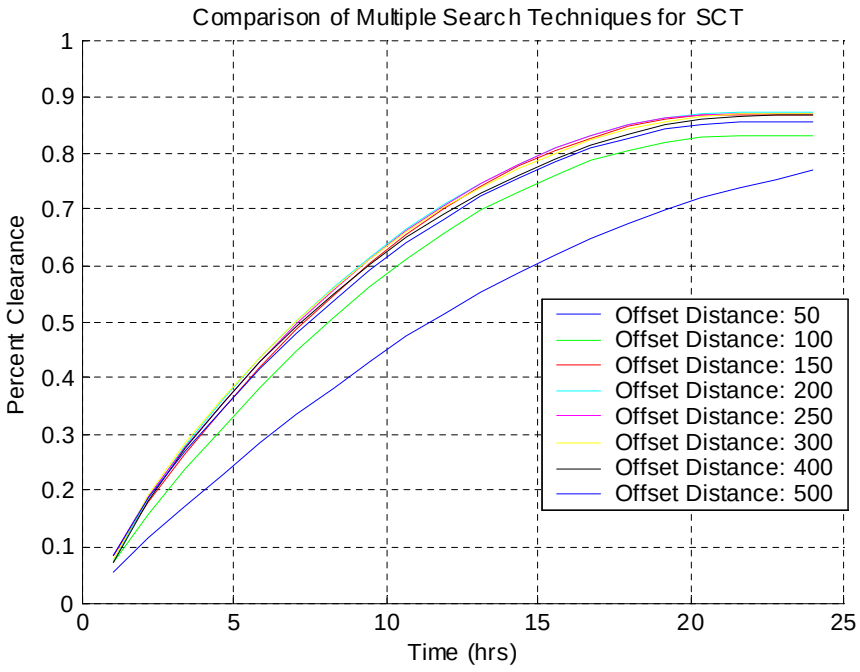

Figure 147: Effects of Varying the Track Spacing on Minehunting Effectiveness for Single Classification Tactics

especially since the probability of detection can generally be linked to the velocity of the vehicle. This linkage generally has a negative correlation: the faster the vehicle travels, the more difficult it is to detect an object. Figure 149 shows the variation of vehicle velocity on performance. Note that vehicle velocity has a very significant effect on performance, and must therefore be examined carefully in the design process.

7.2.4 Minehunter Optimization

The optimization results were undertaken for two design variables, velocity and probability of detection, and one tactics variable, the track spacing. The variables and assumptions are shown in Table 38. In order to include a tradeoff in the design space, the probability of detection was linked to the search velocity of the vehicle. It was assumed that, as the search velocity increased, the probability of detection would decrease. Three points were then conceived to fit a trend. The first point is the low value for P_d (0.6), and the high value for velocity (20 kts). The second point is the opposite, with a value of 0.95 for P_d

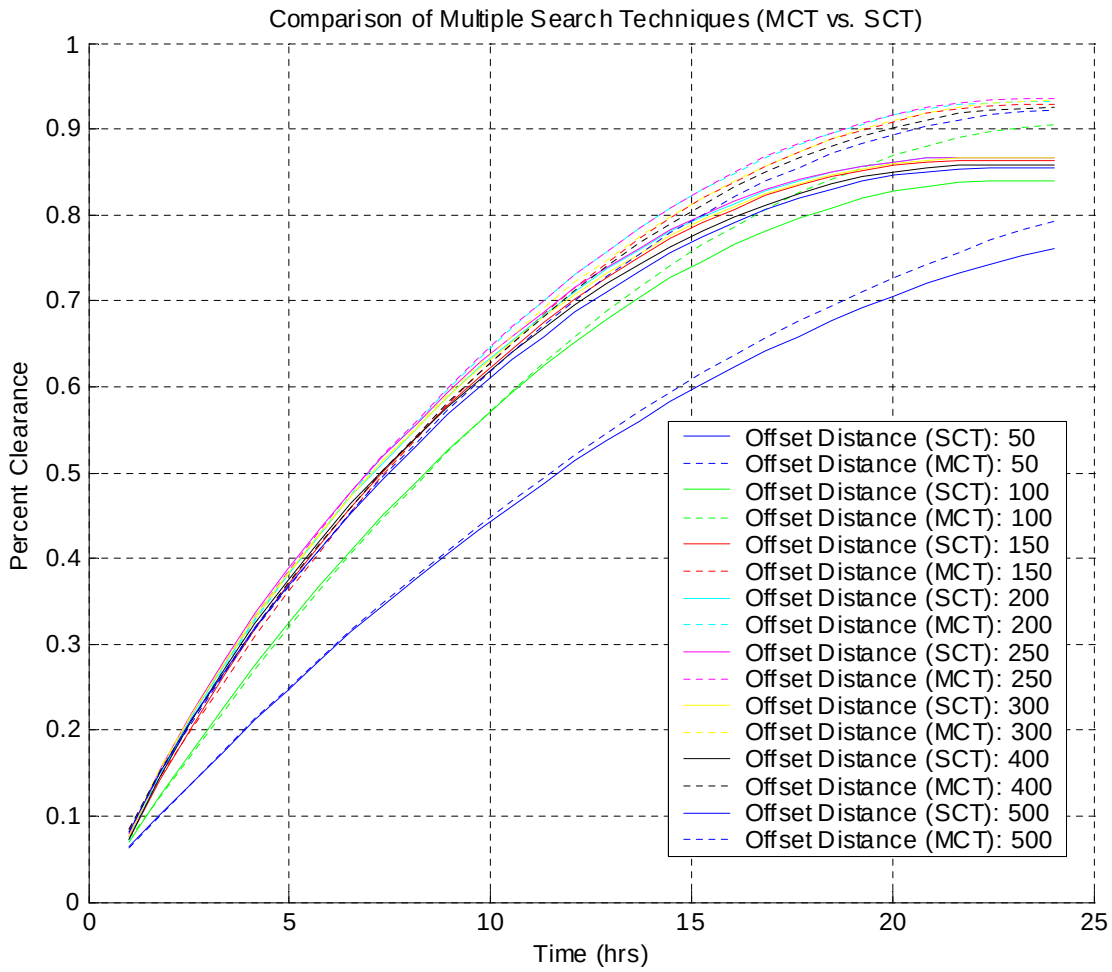

Figure 148: Effects of Varying the Track Spacing on Minehunting Effectiveness Comparing Classification Tactics

and a value of 2 kts for the velocity. Finally, an interior point was taken from Reference [21], with a P_d value of 0.9 and a velocity of 7 kts. The trend is shown in Figure 150, which represents Equation 27.

$$Vel = -4.0847 + 56.4817 \cdot P_d + 16.4429 \cdot P_d^2 - 72.749 \cdot P_d^3 \tag{27}$$

In order to find the set of optimal, or Pareto solutions, a random search was run over the design space. A 500 case random search was used for four distinct search times: 8 hours, 12 hours, 16 hours, and 24 hours. The random points that were selected are shown in Figure 151. Note in the top portion of Figure 151 that a distinct line is formed between

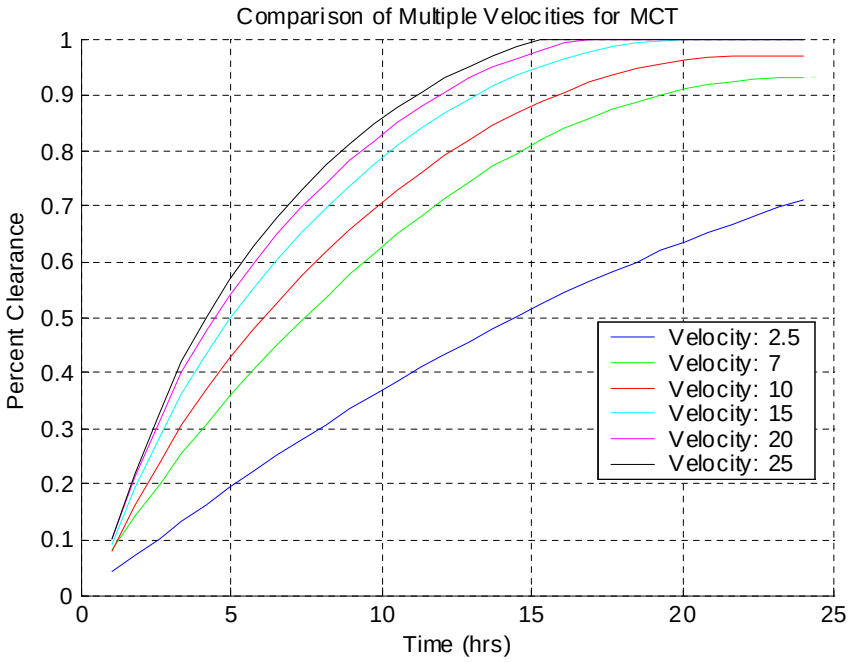

Figure 149: Effects of Varying the Vehicle Velocity on Minehunting Effectiveness

the probability of detection and the search velocity. This line occurs because the two design variables were correlated as shown in Figure 150. The lower two graphs in Figure 151 show the random nature of the selected design space.

Figure 152 shows the effectiveness, or percentage of mines neutralized, for each of the random points. The graph compares the results at each of the four sweep times. Figure 153 zooms in on these graphs. From this figure, a very important point is evident. Since all the

Table 38: Listing of Optimization Variables and Assumptions

Parameter	Definition	State	Value
Length	Length of Search Field (nmi)	Fixed	5
Width	Width of Search Field (yrd)	Fixed	1000
P_d	Probability of Detection	Var	0.6-0.95
Vel	Searcher Velocity (kts)	Var	2-20
Track Spacing	Spacing Between Parallel Search Tracks (yrd)	Var	5-500
Tactics	Raster-Scan Search Pattern	Fix	—
MCT/SCT	Classification Technique	Fix	MCT
Seeker Radius	Radius of 'Imperfect' Seeker (yrd)	Fix	75
Num_Mines	Number of Mines	Fix	50

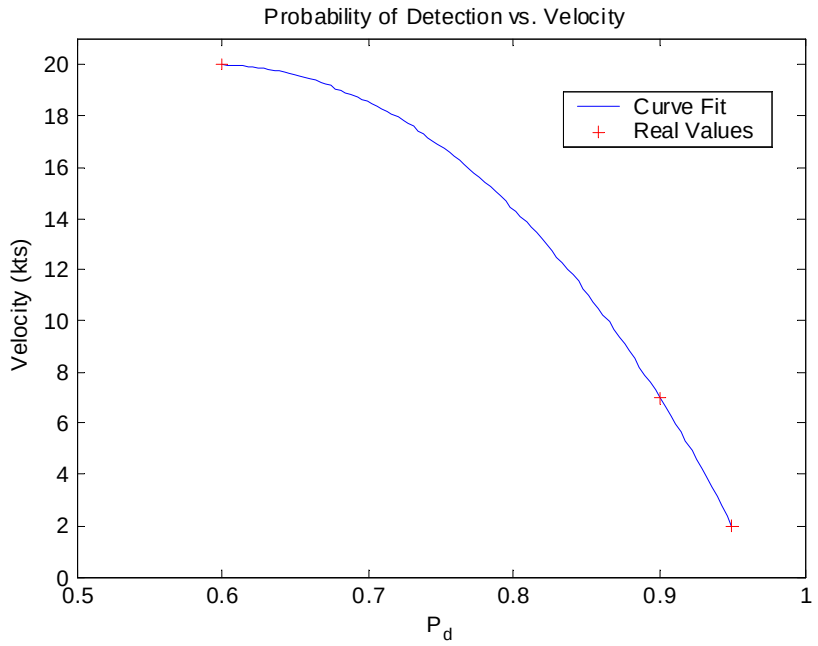

Figure 150: Estimated Correlation between Probability of Detection and Velocity

graphs show an increasing trend, this implies that an improvement in the search effectiveness at a search time of 8 hours also indicates an improvement in search effectiveness at 24 hours. Therefore, any improvement in search effectiveness at any specific time improves the search effectiveness at all times. This trend simplifies the analysis, as now a single search time can be examined and extrapolated to other search times.

Figure 154 shows the effects of the three design variables on the minefield percent clearance: probability of detection, search velocity, and track spacing. It is interesting to observe that most of the points succinctly line up with the Pareto front. Figure 155 draws the front of the best-valued points for each setting of the design variables, with the global optimum highlighted. For probability of detection, a lower detection probability leads to a higher minefield clearance. This fact is counter-intuitive, until one remembers the coupling between probability of detection and search velocity. Among other things, the results show that the performance of the system is fairly robust to variations in track spacing, except at low track spacing, which has very poor performance. In this region of the design space, it could be conjectured that the minehunter is repeating its search area too often, and thus

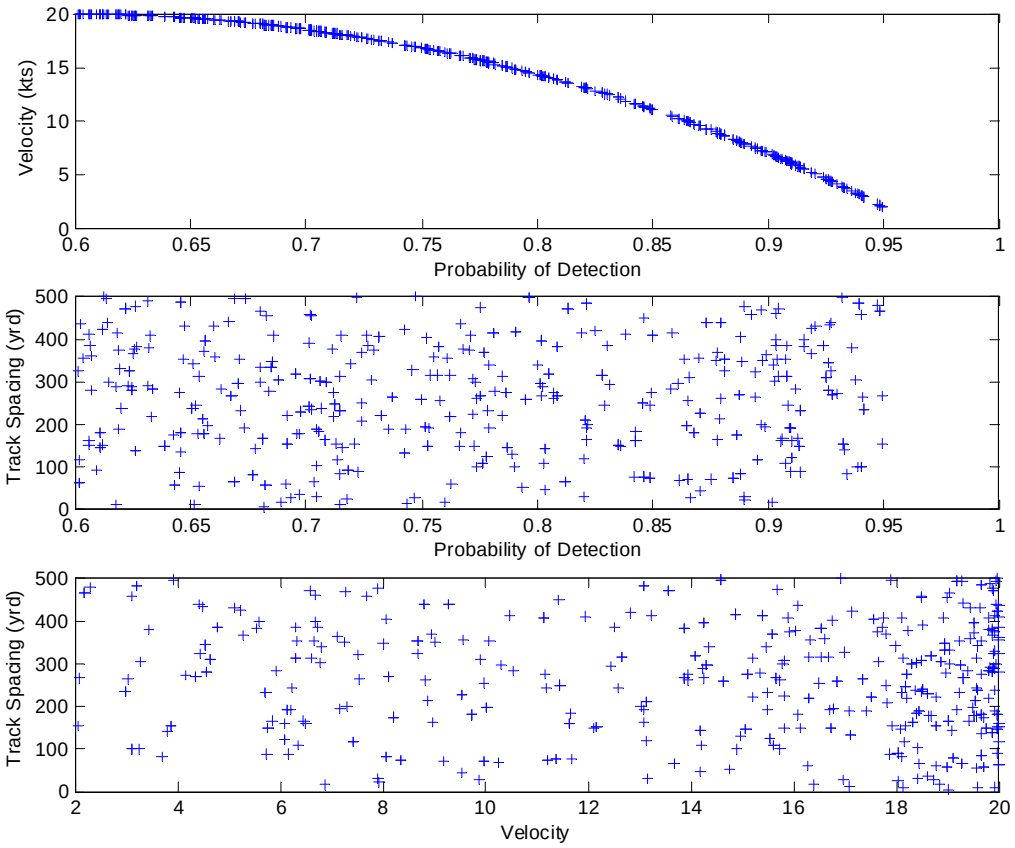

Figure 151: Randomly Selected Values of Design Variables

is performing a very inefficient search. The global optimum, shown for each variable as a cross in Figure 155, is listed in Table 39. The results show that the minehunter will likely remove 88.5% of all the mines in a minefield within a 12-hour period.

The optimum mine counter-measure system shown in Figure 155 and Table 39 was compared against a traditional design process, in which the tactics and the design variables were designed independently. Figure 156 shows the best results when an optimal minehunting system is designed *independent* from the tactics with which it is used. The design variables addressed are only probability of detection and search velocity. The results in Figure 156 compare the minehunter to the globally optimized system. Note that, at every possible setting of P_d and velocity, the minehunting system that is dually optimized with both tactics and design variables outperforms the system that is examined using only design variables. The best system has a minefield clearance of only 82.3%, versus 88.5% for the globally

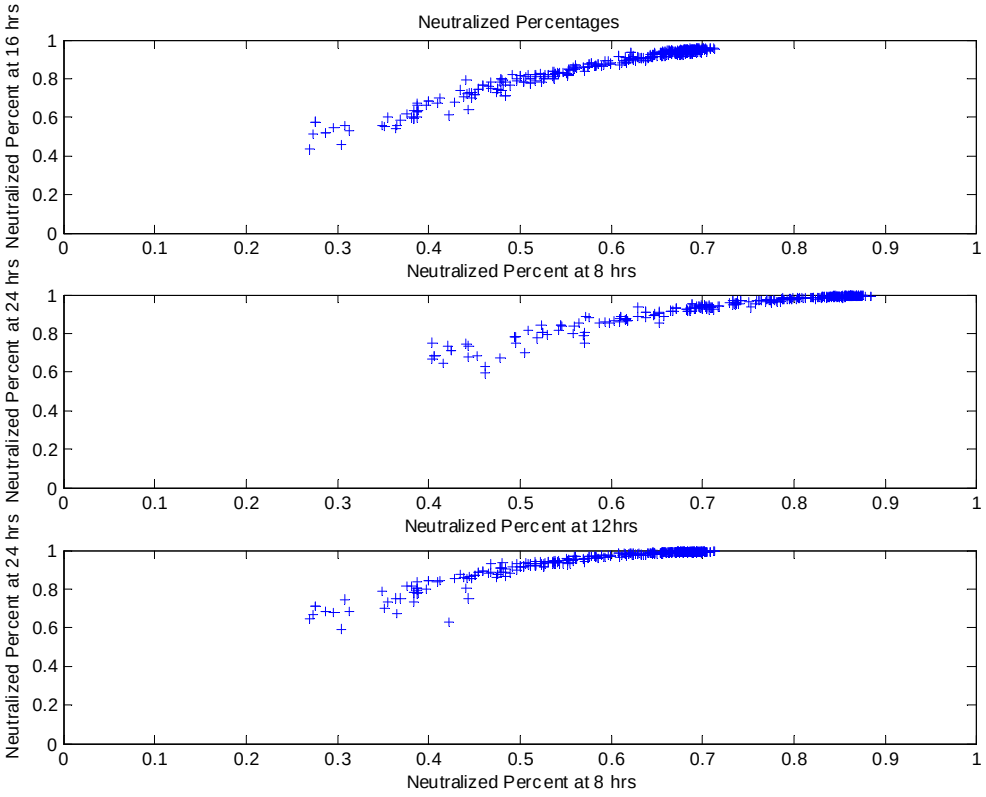

Figure 152: Resulting Mine Neutralization Percentages for Search Times of 8, 12, 16, and 24 Hours

optimized vehicle.

Figure 157 shows the opposite side of the argument. In the situation, a fixed minehunter system, i.e., a system with a fixed detection probability and velocity, is optimized to find the most appropriate tactics. The optimization is run only on the track spacing for the search process. The results indicate again that a singularly optimized system will not perform as well as a system that has been optimized with both tactics and the system design in mind. The fixed vehicle with optimized tactics will only neutralize 75.9% of the mines in the minefield, significantly less than the globally neutralized system.

A final test was conducted to explore what would happen if the independently designed vehicle was used with the independently optimized tactics. This type of situation is analagous to the discussion in Section 1.3, in which the undersea weapon (torpedo or mine counter-measure) designers are separated from the tacticians. In this case, the weapon

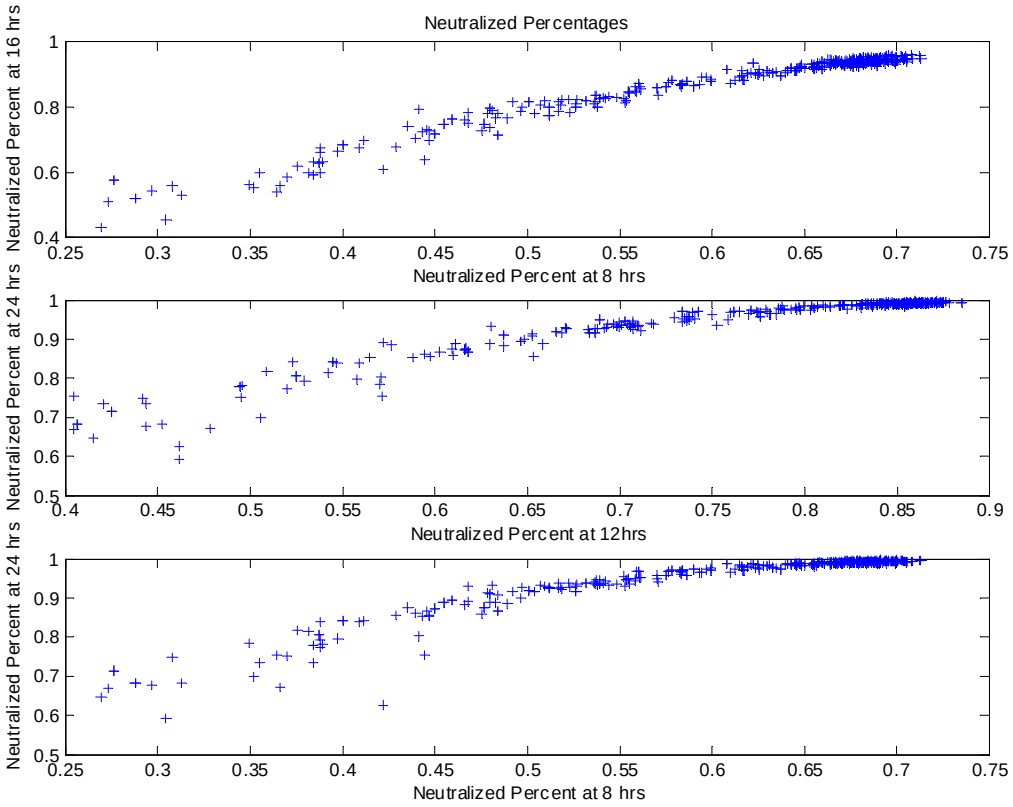

Figure 153: Zoomed Mine Neutralization Percentages for Search Times of 8, 12, 16, and 24 Hours

designers develop the best weapon that they can, and deliver it to the warfighters, who develop the best tactics possible with the weapon. For this example, the weapon designers have optimized the minehunter as shown in Figure 156, and the warfighters have developed the best tactics as shown in Figure 157. Using these 'best' tactics, coupled with the 'best' design results, in a situation in which the minehunter neutralizes 86.5% of the mines in the minefield, still less than the 88.5% neutralization achieved by the global optimization of design and tactics. Clearly, a system where the tactics and physical design are handled concurrently is superior to one in which they are developed independently. These results are summarized in Table 40.

A full probabilistic analysis was conducted for the optimum minehunter system described in Table 39 and Table 40. The probability, or confidence, of meeting each minefield clearance percentage is shown in Figure 158. This chart is analogous to the original probabilistic

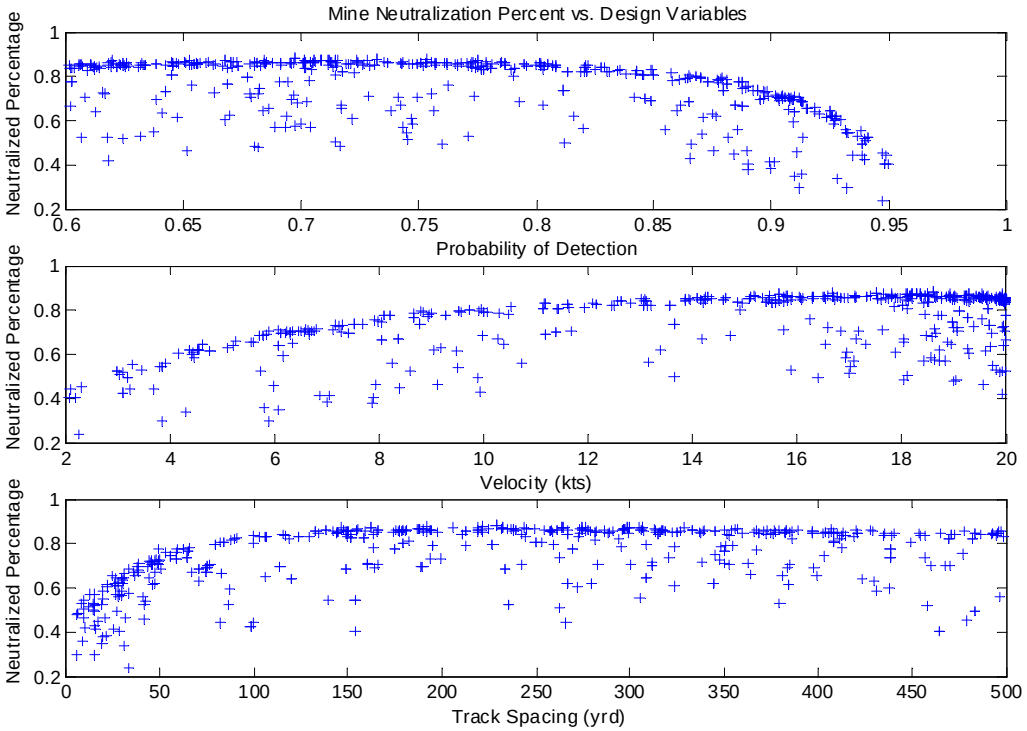

Figure 154: Mine Neutralization as a Function of Design Variables for Random Runs

Table 39: Global Optimum for Mine Counter-Measure Optimization for a 12-Hour Search Time

Variable	Value
P_d	0.698
Velocity (kts)	18.6
Track Spacing (yrd)	229
Mine Clearance Percentage	88.5%

minefield clearance in Figure 142. These figures are combined together so that the globally optimized system can be compared to the original system. This comparison is made in Figure 159. Note that in this figure, the globally optimized minehunter system always performs better than the original system, regardless of the search-time involved or the confidence level examined. In fact, the new system generally gives a 90% confidence to the same performance that the baseline system had at only a 10% confidence level. A probability of success curve for the optimized system is also compared in Figure 160, showing the advantage in decreased search times provided by the optimization. Clearly the new

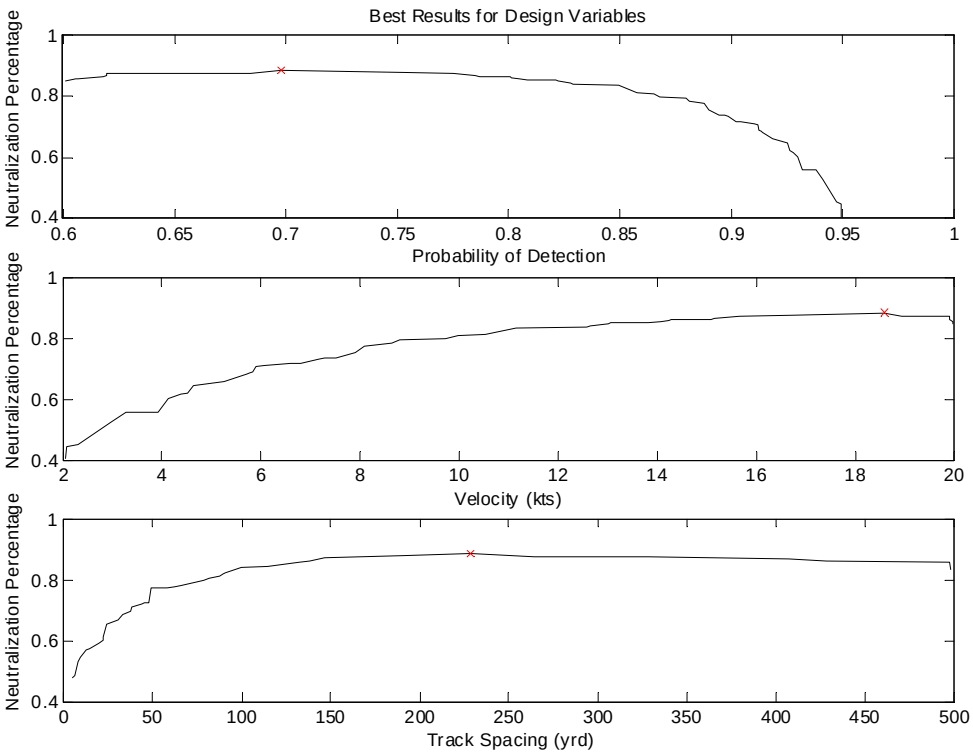

Figure 155: Best Design Variable Values for Mine Neutralization, with the Optimal Point Highlighted

minehunter system, with an optimized design and tactics, provides a dramatic performance increase over the original system.

7.2.5 Summary

A minehunting analysis program was developed for the analysis of mine counter-measure systems. This program was then used to show the type of probabilistic analysis that could be conducted for minehunting systems, accounting for the uncertainty in the system and the tactics employed. This type of analysis can be used to produce charts that illustrate the confidence of reaching a mine clearance percentage, as well as performance vs. probability of success charts.

In addition, the mine counter-measure analysis shows the advantages of optimizing a system whereby the tactics are developed concurrently with the vehicle. This approach generates an overall system that performs better and is more robust than a traditionally

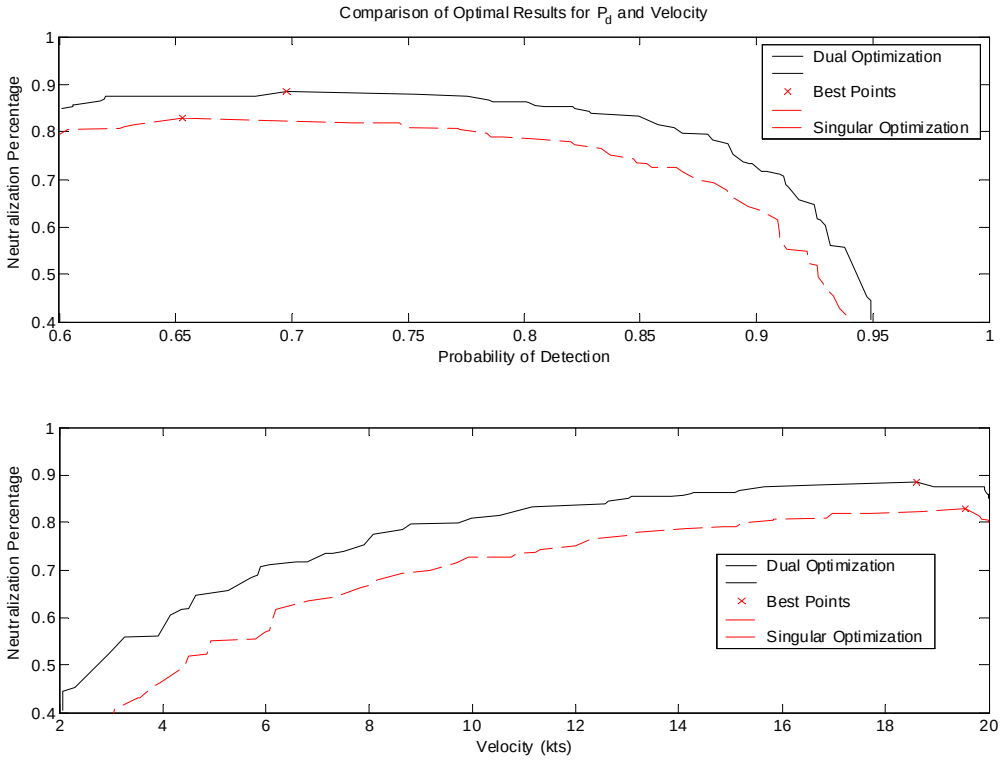

Figure 156: Comparison of Global Optimization versus Singular Optimization

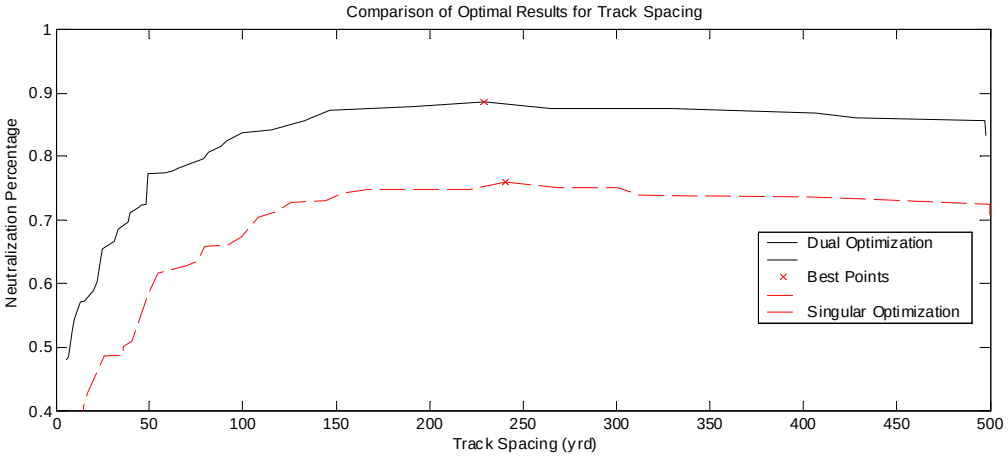

Figure 157: Comparison of Global Optimization versus Singular Optimization

developed system, where the tactics and hardware are designed independently. This type of system-of-systems approach, where the tactics are optimized in conjunction with the vehicle, is paramount in order to get as much functionality out of the vehicle as possible.

Table 40: Comparison of Multiple Optimization Techniques for Minehunter

Optimization Goal	P_d	**Vel (kts)**	**Track Spacing (yrd)**	**Mine Clearance**	**% Increase**
No Optimization	0.9	7.0	75	60.1%	0.0
Optimized Tactics	0.9	7.0	240.7	75.9%	26.3%
Optimized Vehicle	0.653	19.54	75	82.9%	37.9%
Independent Optimization	0.653	19.54	240.7	86.5%	43.9%
Simultaneous Optimization	0.698	18.60	229.0	88.5%	47.3%

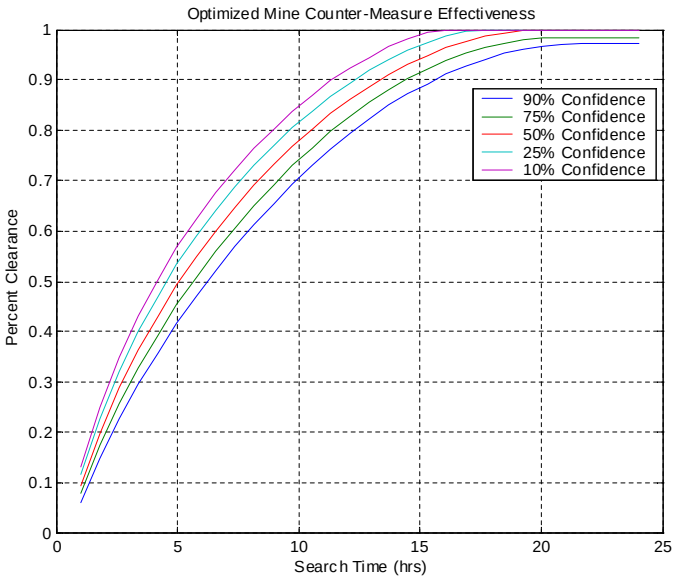

Figure 158: Probabilistically Determined Confidence Levels for an Optimized Minehunting System

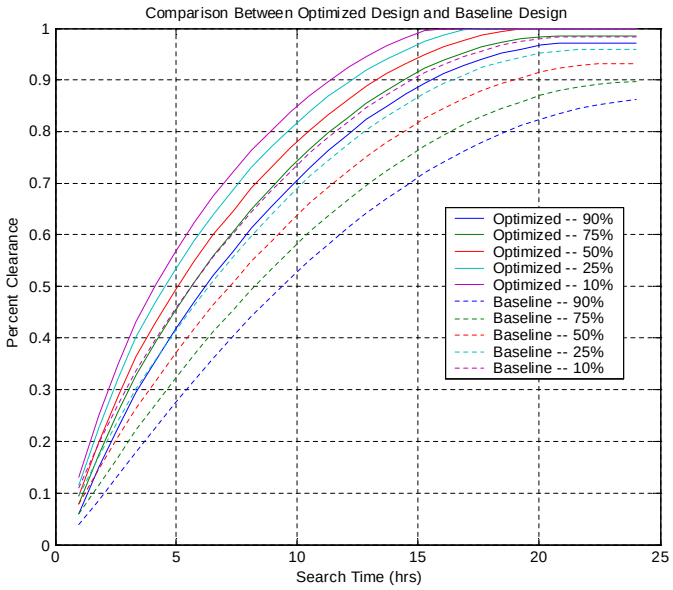

Figure 159: Comparison of Confidence Levels for Original and Optimized Minehunting Systems

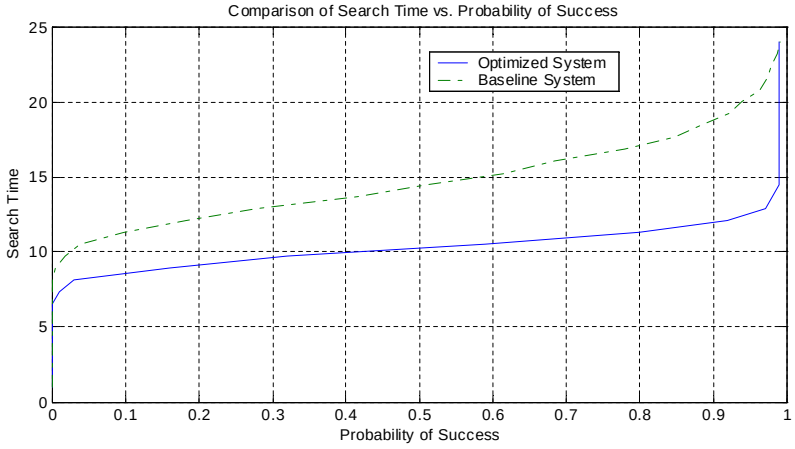

Figure 160: Comparison of Probability of Success Curves for the Minehunting System

CHAPTER VIII

NON-DIMENSIONAL PARAMETERS IN TORPEDO DESIGN

8.1 Introduction

Several techniques have been developed which illustrate a mechanism by which torpedoes can be designed in an intelligent, structured manner. This development is both robust to uncertainty and includes tactical considerations. Unfortunately, this type of analysis can be computationally intensive, particularly concerning the number of Monte Carlo runs that may need to be made. As such, it is important to choose the 'smartest' design variables faster, as these will speed the design process in general, and, in particular, will facilitate the development and execution of Designs of Experiments. This chapter studies several potential design variables for torpedoes, and provides an argument that non-dimensional parameters are most suited for torpedo design.

8.2 Exploration of Non-Dimensional Parameters

The performance of the TOAD analysis program was examined for the running of a full-factorial Design of Experiments. Particular attention was paid to regions of failure, or non-convergence, from the TOAD analysis program (these regions of TOAD failure are summarized in Table 16). Since most of the failures are related to the propulsor system, the design study focused on torpedo parameters that were closely related to the design of a propulsor system. Therefore, the following four design variables were chosen for the study because of their impact on the propulsion system: outer diameter, torpedo length, motor/propulsor RPM, and the motor horsepower. These inputs are summarized in Table 41.

Smart selection of potential Design of Experiments parameters is the first step in the implementation of this process. Traditionally used torpedo conceptual DoE parameters are

Table 41: Inputs for DoE Analysis

Input	**Units**	**Relevant Torpedo Section**
Diameter	*(in)*	Front-End Motor Propulsor
Length	*(in)*	Front-End
Motor/Prop RPM	*(revs/min)*	Motor Propulsor
Motor HP	*(hp)*	Motor Propulsor

often dimensional, non-normalized quantities, such as diameter, horsepower, propeller RPM, and internal sectional lengths (i.e., length of the fuel tank). Dimensional analysis techniques involve the creation of non-dimensional parameters from these quantities, through the comparison of units, as illustrated by the Buckingham-Pi theorem [9][139]. These techniques can be employed to develop better non-dimensional design parameters for using Design of Experiments in conjunction with torpedo design. When creating non-dimensional parameters for this analysis, it was desired to keep all of the parameter values as functions of the inputs into the TOAD analysis program, thus simplifying the execution of Designs of Experiments. Therefore, in creating these parameters, true 'non-dimensionality' was sacrificed in order to retain parameters that were a function of the TOAD analysis inputs: diameter, RPM, and horsepower.

The first parameter to be explored is the relation between two large drivers on torpedo system performance: diameter and horsepower. Dimensional analysis was used to determine the relation between these two parameters. Using the following dimensions, time (T), length (L), force (F), and mass (M), along with the fact that power is energy per unit time, the relations in Equation 28 were constructed.

$$HP = \frac{L \cdot F}{T} = \frac{L \cdot \left(\frac{M \cdot L}{T^2}\right)}{T} = \frac{M \cdot L^2}{T^3} \tag{28}$$

Thus, horsepower can be related to length squared. Diameter, with units of length,

is obviously proportional to length; therefore, horsepower should be proportional to the square of diameter, with units of mass over time cubed (Equation 29).

$$HP \propto Diam^2, \ \frac{HP}{Diam^2} = \frac{M}{T^3} \tag{29}$$

Therefore, horsepower divided by the diameter squared makes sense as a potential design parameter, because it has decreased dimensionality. The parameter is clearly not non-dimensional, because it still retains units of mass over time, however it was desired to keep each parameter a function of only two variables, so that each parameter can be used to define a unique torpedo configuration. For example, if the parameters outer diameter and HP/Diam^2 were specified, a unique combination of HP and diameter would be defined. However, if the non-dimensional parameter were a function of three variables, say HP, diameter, and shaftspeed, then the system would not be uniquely defined. Shaftspeed, or propulsor RPM, is another driving parameter that is addressed in this study. Propellers are often designed via the non-dimensional parameter called the advance coefficient [10]. The definition of advance coefficient is shown in Equation 30.

$$J = \frac{V_\infty}{\frac{RPM}{60} \cdot Diam_B} \tag{30}$$

The propulsor advance ratio would be an excellent choice of design parameter; unfortunately, the design tool, TOAD, cannot be used with this advance ratio as an input parameter. The reason TOAD cannot use advance ratio is because the freestream velocity, V_∞, is an output to the analysis program, not an input. Since the freestream velocity is not known prior to running a case, it would be impossible to use the advance ratio to set a fixed value of RPM unless an additional iteration loop was created around the analysis program - something to be avoided if possible. For analysis tools with other input/output formats, advance coefficient would likely be a strong candidate as a choice for a DoE parameter. However, even though the advance coefficient is not workable as an input parameter for this analysis tool, it does give insight into the relationship between RPM and diameter. Advance ratio suggests that the formulation of the two parameters should be inversely proportional to each other, leading to the relationship in Equation 31.

$$RPM \propto \frac{1}{Diam},\ RPM \cdot Diam = \frac{L}{T} \tag{31}$$

This equation implies that RPM times diameter is an appropriate design parameter. Again, this parameter is not non-dimensional in nature, but should better capture the design trends than using RPM and diameter independently. Yet another parameter of merit is the fineness ratio, defined as the length of the body divided by the width of the body, or the diameter. Fineness ratio is used in some aerospace fields, such as missile design [72], and is also associated with torpedo design. Two other common non-dimensional parameters used in naval engineering are based upon the thrust coefficient (K_T) and the torque coefficient (K_Q)[198]. Thrust coefficient is a parameter that non-dimensionalizes thrust. By using the relation that power is equal to thrust times velocity, the thrust coefficient can be written in terms of a power and hence renamed K_{HP}, as shown in Equation 32, where n is rotations per second, D_B is the body diameter, and T is the thrust. Unfortunately, the thrust coefficient has the same drawback as advance ratio: it is a function of a response variable from the analysis tool, V_∞.

$$K_T = \frac{T}{\rho n^2 D_B^4},\ K_{HP} = \frac{550 \cdot HP}{V_\infty} \cdot \frac{1}{\rho n^2 D_B^4} \tag{32}$$

A form of the torque coefficient can be found by multiplying the thrust coefficient by the advance ratio, as shown in Equation 33. This multiplication has the advantage that it removes velocity from the formulation, making torque coefficient useful because it is completely formulated from input parameters for the TOAD analysis program. Torque coefficient is therefore a true non-dimensional parameter that is solely a function of TOAD inputs. This fact gives the torque coefficient an advantage as a Design of Experiments parameter because it can be calculated before any TOAD runs are completed. These non-dimensional parameters have traditionally been used in naval architecture explicitly for propulsor design, but in this work their use is being expanded to include the entire undersea vehicle.

$$K_Q = K_T \cdot J = \frac{T}{\rho n^2 D_B^4} \cdot \frac{V_\infty}{n D_B} = \frac{HP}{V_\infty} \cdot \frac{1}{\rho n^2 D_B^4} \cdot \frac{V_\infty}{n D_B} = \frac{550 \cdot HP}{\rho n^3 D_B^5} \tag{33}$$

In addition to using K_{HP} or K_Q directly, it may also be beneficial to simply look at the relations that they imply between horsepower and diameter: using simply HP/D^4 or HP/D^5 as design parameters. Table 42 summarizes the potential non-dimensional parameters that were identified.

Table 42: Potential Non-Dimensional Torpedo Parameters

Non-Dimensional Parameter	Definition	Units
Advance Ratio	$J = \frac{V_\infty}{RPM/60 \cdot D_B}$	---
Thrust Coefficient	$K_{HP} = \frac{550 * HP}{V} \cdot \frac{1}{\rho n^2 D_B^4}$	---
Torque Coefficient	$K_Q = \frac{550 * HP}{\rho n^3 D_B^5}$	---
Fineness Ratio	L / D_B	---
---	HP / D_B^2	hp/in^2
---	HP / D_B^4	hp/in^4
---	HP / D_B^5	hp/in^5
---	$RPM \cdot D_B$	in/min

The example problem being explored is a lightweight torpedo system, which traditionally has a diameter of 12 3/4 inches and a power of 200 HP or less (see Table 4). The inputs and ranges that define the design space are given in Table 43. This example problem is challenging because the range of diameters available is quite large, from the short six inch torpedo to a medium-sized 14 inch torpedo. Additionally, the horsepower variation is also significant, from a lightly powered five horsepower to large 200 horsepower systems. These challenging ranges were used for a number of reasons. For one, the design space captures a wide range of possible torpedo configurations: from low-powered UUV's that could be deployed from a submarine's 6 1/2 inch counter-measure dispensers, to high-powered, large

diameter lightweight torpedoes (i.e., a 200 hp, 14 inch torpedo). Secondly, the design space is sufficiently large that regions of infeasibility will exist, thus giving the approach an opportunity to show its merit.

Table 43: Non-Dimensionalization Design Variables and Ranges

Variable	Minimum	Maximum
Diameter (in)	6	14
HP	5	200
RPM	2000	5000

Before running advanced Designs of Experiments, a grid-search was used to explore the data. The grid search was done so that the complete design space could be viewed, clearly showing regions of constraint violations. A 32x32 fine grid was used in conjunction with diameter and horsepower, while a coarse grid with four levels was run for varying RPM. The final grid search therefore comprised 4,096 total points. Figure 161 shows the 2-dimensional results with RPM held constant at 2,000. Each point on the grid represents a single run, with varying markers used to indicate the pass/fail code returned by the analysis program. Black circles are used to indicate the feasible regions, with each failure mode having its own symbol. Separate, continuous fields of failure are illuminated in the graph. The border between these fields represents a constraint line for the given failure mode. In examining this figure, the large diameter, large horsepower trials, common to today's lightweight torpedoes, execute without failure, as expected. The medium diameter, lower horsepower runs are out of the range of the thrust deduction model. However, this failure is not associated with any boundary of physics, it simply means that the program is outside the range of validity for the analysis model. If it is assumed that model extrapolations are valid (a reasonable assumption for this work), then this field of points can also be considered feasible. There are then two regions of infeasibility: the small diameter large horsepower systems are characterized by exceeding the C_{Lmax} required for the system, which eventually keeps the program from converging. On the opposite side, the very low horsepower (5 hp), large diameter systems fail to converge; this convergence failure is likely due to the analysis program's inability to complete a force balance for the torpedo.

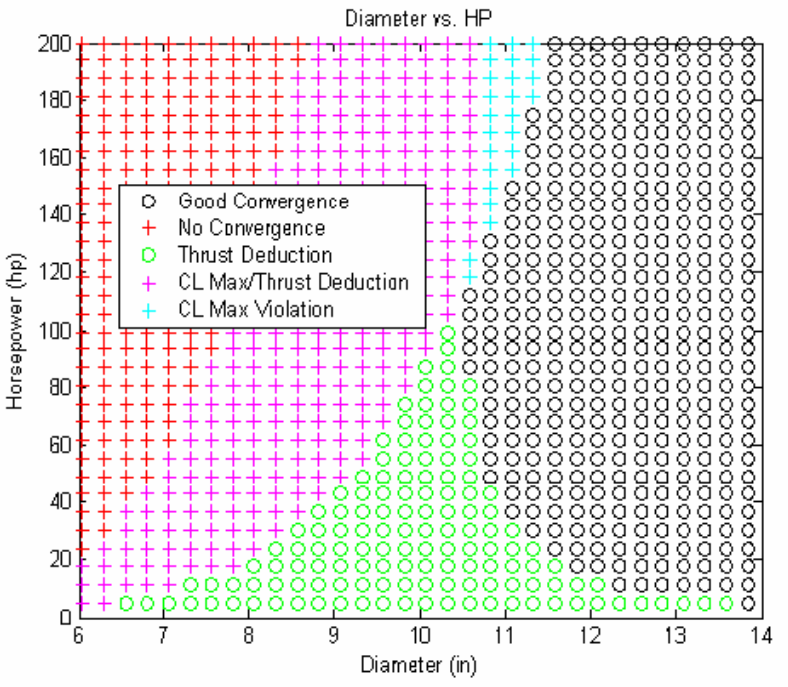

Figure 161: Grid Search Defining Constraints for Diameter and Horsepower, RPM = 2000

Figure 162 shows the three-dimensional results for all the trial runs in the grid search. Variations in the constraints as a function of RPM can now be seen. At low values of RPM, there is a large region of constraint violations for the small diameter systems. But, at these low RPMs, the large diameter, low horsepower systems perform well. As the RPMs increase, the large diameter torpedoes begin to fail, while small diameter torpedoes perform progressively better.

The next step in the non-dimensionalization process is to begin examining the design space in terms of potential non-dimensional parameters. To do so, the previous grid search was transformed so that it was charted in terms of the potential non-dimensional parameters listed in Table 42. For the transformed plots, if discrete jumps exist between feasible and infeasible cases, then the parameter being plotted is a strong candidate for use in non-dimensionalization for Designs of Experiments. In these cases, the parameter can be used to determine whether a system is valid or invalid. If there is not a discrete jump between feasible and infeasible cases for a design parameter, then that parameter is a poor candidate

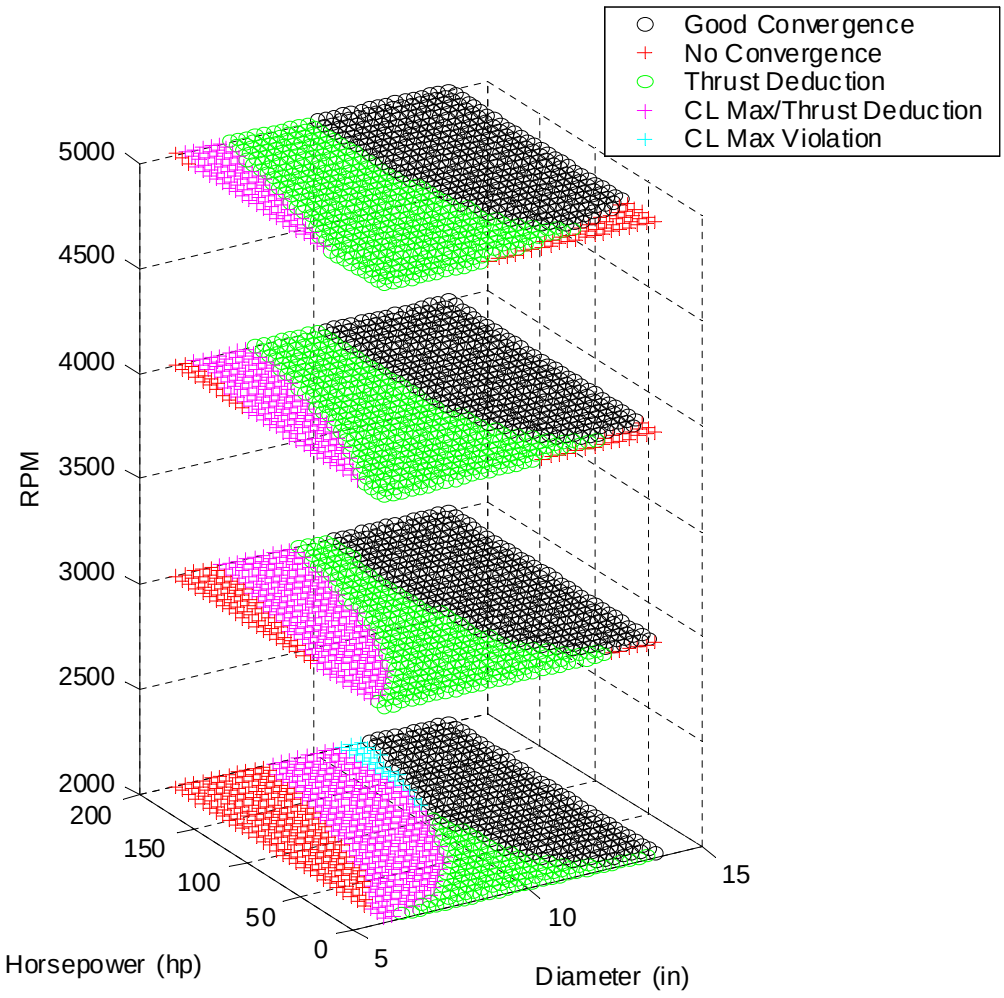

Figure 162: Grid Search Defining Constraints for Diameter, Horsepower, and RPM

for use in DoEs. Figure 163 shows some potential parameters: fineness ratio, diameter, and thrust and torque coefficients. The left-hand side of this figure shows thrust coefficient versus fineness ratio, or L/D. This figure shows a clean demarcation, or straight line, between feasible and infeasible points, indicating that K_{HP} and L/D could be used together to define a feasible model region. The right hand side of Figure 164 shows diameter and Torque Coefficient (K_Q). This figure shows that the diameter and torque coefficient can be used to clearly designate a line between feasible and infeasible design regions. Figure 164 shows how advance ratio is also useful as a DoE parameter.

System constraints in terms of these parameters are clearly visible as lines, illustrating

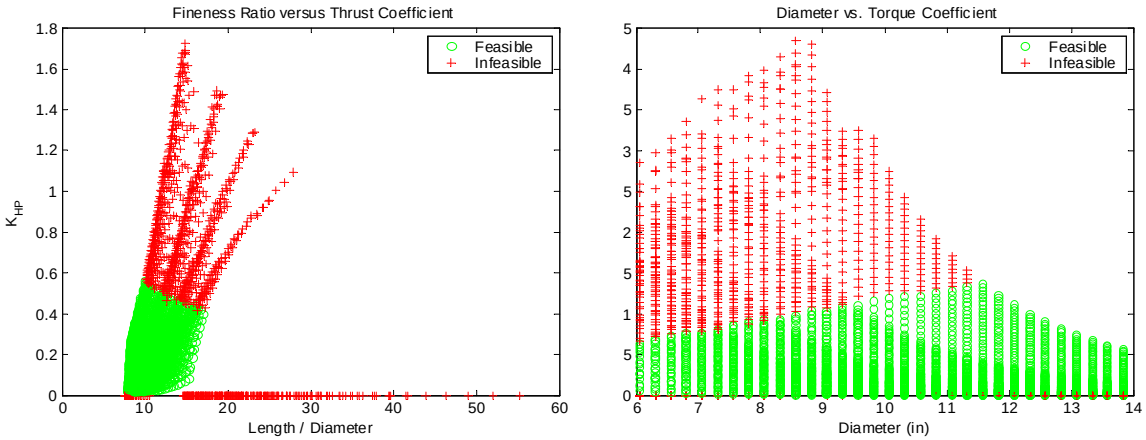

Figure 163: Illustration of Good Non-Dimensional Parameters

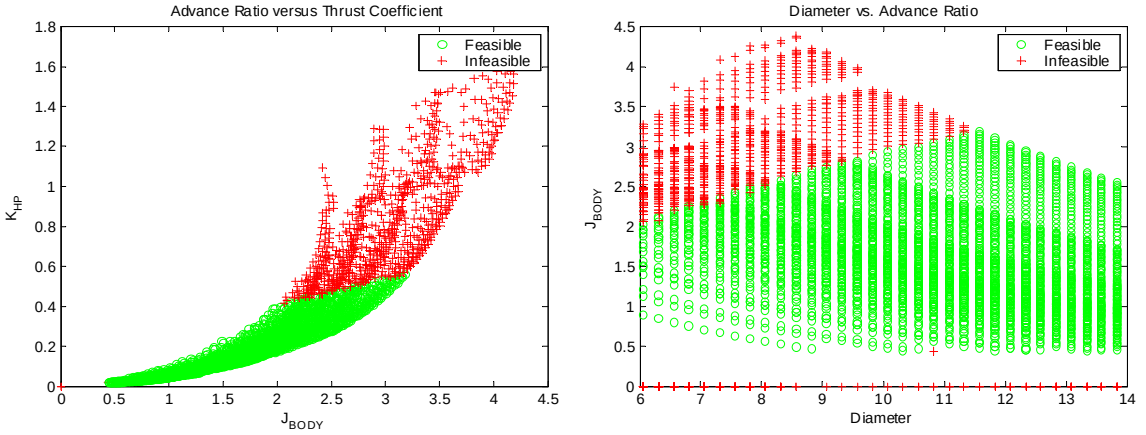

Figure 164: Illustration of Additional Good Non-Dimensional Parameters

the potential for creating engineering design rules for torpedoes from this information. For instance, from the thrust coefficient versus fineness ratio plot in Figure 163, the following design rule could be created:

$$\text{If } 5 \cdot K_{HP} + \frac{L}{D} < 19, \text{ the system is feasible} \tag{34}$$

It could also be possible to use these design rules to create a custom Design of Experiments, one specifically designed to remove infeasible or non-convergent regions from the valid design space. Reference [78] illustrates a method by which such constraint lines can be identified and custom DoEs created to exclude the non-convergent regions from the design

space.

Figure 165 shows some plots that illustrate poor potential design parameters. The left hand side shows diameter versus horsepower over diameter squared, while the right hand side of this figure shows fineness ratio versus horsepower. The fineness ratio versus horsepower chart has no clean demarcation between feasible and infeasible regions. Instead, there is a large region of overlapping between feasible and infeasible cases. The diameter versus diameter over horsepower squared has similar overlap between cases. These parameters would therefore make poor choices for use in Designs of Experiments.

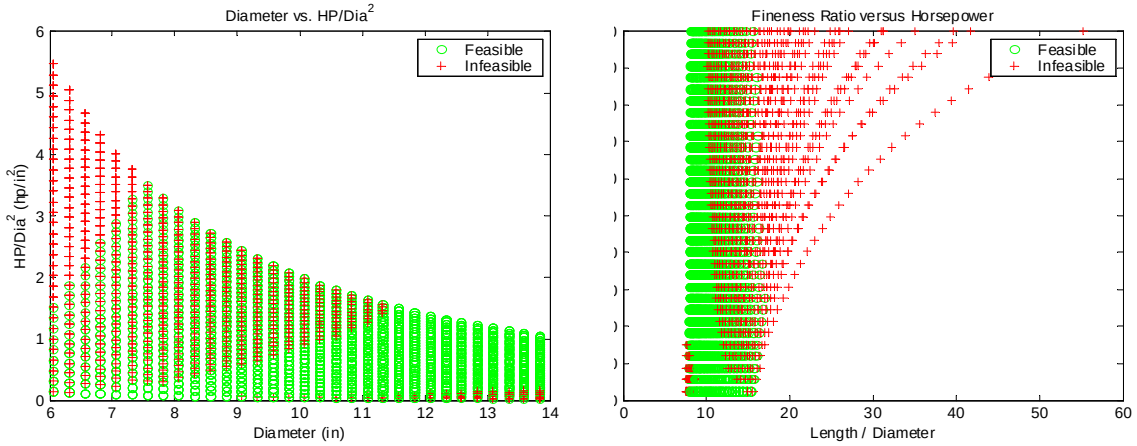

Figure 165: Illustration of Poor Non-Dimensional Parameters

All 55 combinations of the potential Design of Experiments parameters that were identified were tried against each other. Appendix A contains a complete set of 55 charts, each comparing potential DoE parameters. The results are summarized in Table 44, which shows the parameters that worked well together and which sets performed poorly. Note that the dimensional parameters tended to do poorly. Likewise the 'derived' parameters, or only partially non-dimensionalized parameters such as horsepower over diameter squared, performed equally poorly, if not worse. It was the traditionally used, fully non-dimensional parameters, such as advance ratio, fineness ratio, thrust, and torque coefficients that performed exceptionally well. These parameters would be most effective to use in a Design of Experiments for torpedo systems.

Table 44: Summary of Goodness of Non-Dimensional Torpedo Parameters

		Dimensional Parameters			Partially Non-Dimensional Parameters				Non-Dimensional Parameters			
		Diameter	Horsepower	RPM	HP/Dia^2	HP/Dia^4	HP/Dia^5	RPM*Diameter	Fineness Ratio ($^L/_D$)	Advance Ratio (J)	Thrust Coefficient (K_{HP})	Torque Coefficient (K_Q)
Dimensional Parameters	Diameter	---										
	Horsepower	B	---									
	RPM	B	B	---								
Partially Non-Dimensional Parameters	HP/Dia^2	B	B	B	---							
	HP/Dia^4	B	B	B	B	---						
	HP/Dia^5	B	B	B	B	B	---					
	RPM*Diameter	B	B	B	B	B	B	---				
Non-Dimensional Parameters	Fineness Ratio ($^L/_D$)	B	B	B	B	B	B	B	---			
	Advance Ratio (J)	**G**	B	B	B	B	B	B	**G**	---		
	Thrust Coefficient (K_{HP})	**G**	**G**	**G**	B	B	B	**G**	**G**	**G**	---	
	Torque Coefficient (K_Q)	**G**	B	B	B	B	B	B	**G**	**G**	**G**	---

B = Bad
G = Good

8.3 Results

The next step was to illustrate the use of these new design parameters in a Design of Experiments. Unfortunately, most of the parameters that performed well, such as fineness ratio, advance ratio, and thrust coefficient, are based upon responses from the TOAD analysis tool. These parameters use the overall vehicle length and the velocity of the vehicle in their calculations. Since TOAD treats these parameters as responses, they are difficult to implement as inputs into the analysis program. As such, it was decided to use the non-dimensional parameter for torque coefficient (K_Q) in the Design of Experiment, since this is the best-behaving parameter that is exclusively a function of the TOAD input variables.

Table 45: Comparison of Two Full-Factorial DoE's for Diameter and HP

	Old Parameters			New Parameters			
	Diameter	HP	Pass/Fail	Diameter	HP	KQ	Pass/Fail
Trial 1	6	5	P	6	0.28	0.02	P
Trial 2	6	102.5	**F**	6	3.67	0.26	P
Trial 3	6	200	**F**	6	7.06	0.50	P
Trial 4	10	5	P	10	3.63	0.02	P
Trial 5	10	102.5	P	10	47.23	0.26	P
Trial 6	10	200	P	10	90.83	0.50	P
Trial 7	14	5	**F**	14	19.54	0.02	P
Trial 8	14	102.5	P	14	254.03	0.26	P
Trial 9	14	200	P	14	488.52	0.50	P
		Pass Rate:	**66%**			**Pass Rate:**	**100%**

It was decided to show the effects for a simple, two-dimensional Design of Experiments. To generate a baseline case, the dimensional design variables for diameter and horsepower were used from the example problem in Table 43. These parameters were used in a three-level, full factorial experiment, for a total of 9 analysis runs. Of these 9 DoE runs, 3 of the parameter combinations failed: a 33% failure rate. Figure 166 shows a graphic of the design points and which cases failed in the analysis. A second full-factorial experiment was then run. However, instead of using diameter and horsepower as the DoE variables, diameter and torque coefficient were varied. The torque coefficient was varied from 0.02 to 0.5. This variation in K_Q resulted in a large range of horsepower, encompassing the entire range of original DoE values. The horsepower varied from less than 1.0 horsepower to nearly 500 horsepower. The original and new DoE values are compared to each other in Table 45. When running the nine cases of the new DoE, not a single failed case was reported. Thus, by running the DoE using the non-dimensional parameter for torque coefficient resulted in significantly better results than using the dimensional value of horsepower. This improvement in the Design of Experiments was obtained while still maintaining the entire original variable ranges; in fact, the variable ranges were increased for the non-dimensional case yet maintained superior performance. An overlay of the two Designs of Experiments is shown in Figure 166. The figure shows how the non-dimensional K_Q parameter steers the DoE away from the non-feasible portions of the design space while simultaneously retaining a large amount of the feasible design space. Therefore, the non-dimensional parameter K_Q can be

used with good effect in removing infeasible design space from a Design of Experiments for conceptual torpedo design.

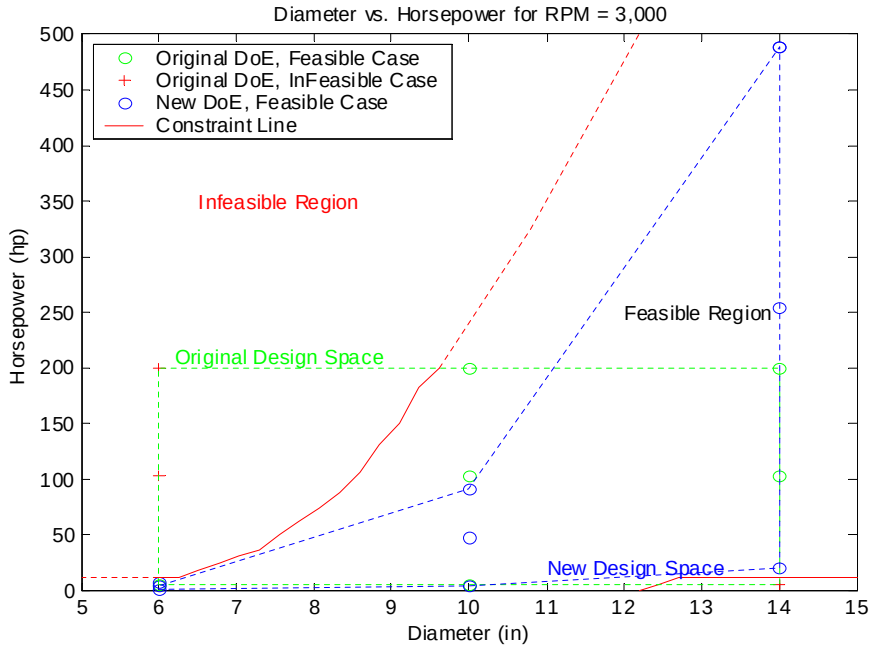

Figure 166: Comparison of Design of Experiments with Original Variables to Non-Dimensionalized Variables, with Diameter and HP

A second example is shown in Figure 167. This example, also two-dimensional, is for a design space of diameter versus RPM. The problem is solved with the motor horsepower fixed at a value of 102.5 HP. Again, a DoE for diameter and torque coefficient is compared to the original deisgn parameters of diameter and RPM. Table 46 summarizes the results. Note again that the DoE behaves significantly better for the non-dimensional parameters than the original parameters. In addition, Figure 167 shows that significantly more design space is open to the user for a similarly-sized DoE. Though not all of the cases were valid in the new DoE, the increase in design space and validity of the DoE is remarkable.

8.4 Summary

In transforming the results of the grid search to examine potential non-dimensional parameters, clear demarcations became visible that showed which sets of parameters could be used to determine whether a design would be feasible or infeasible. These plots showed that

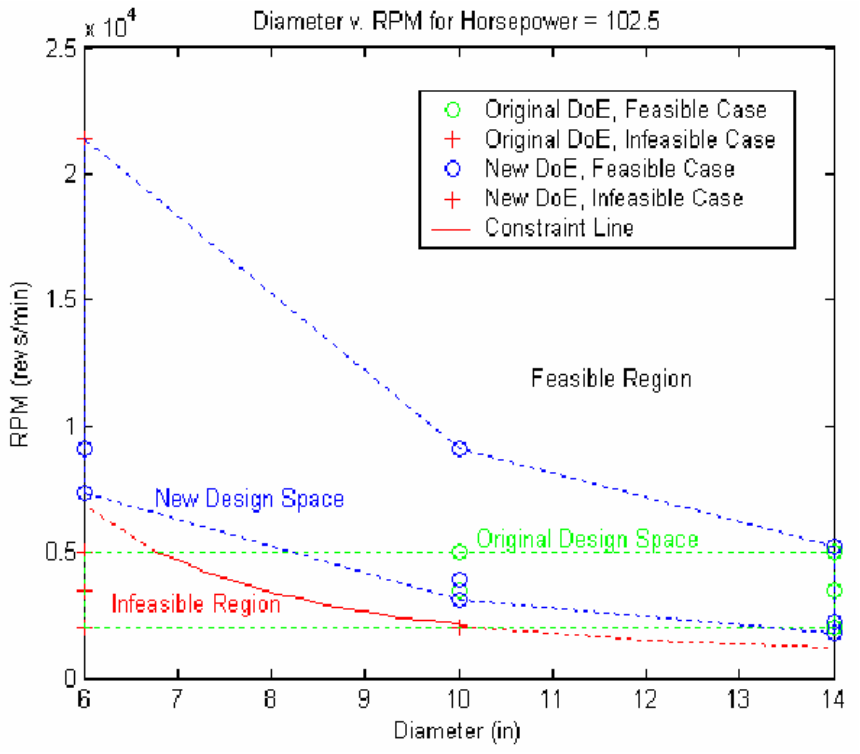

Figure 167: Comparison of Design of Experiments with Original Variables to Non-Dimensionalized Variables, with Diameter and RPM [80]

the best parameters for use in a Design of Experiments of torpedo systems are the fully non-dimensional parameters, similar to those already used in engineering disciplines, such as fineness ratio, advance ratio, thrust coefficient, and torque coefficient. When possible, sizing and synthesis programs for torpedoes should be written so that the inputs can be formulated so that they are in terms of these non-dimensional parameters.

In addition to illustrating strong non-dimensional parameters, the results show that definite constraint equations can be written in terms of these non-dimensional parameters. These equations could be used to create engineering rules of thumb for the system or could be used in the creation of custom Design of Experiments that avoids infeasible regions of the design space.

Finally, two examples employing a Design of Experiments showed that this smart selection of design parameters could significantly reduce or even eliminate the infeasible cases from the Design of Experiments, all while maintaining an aggressive range for the design

Table 46: Comparison of Two Full-Factorial DoE's for Diameter and RPM [80]

	Old Parameters			**New Parameters**			
	Diameter	RPM	Pass/Fail	Diameter	RPM	KQ	Pass/Fail
Trial 1	6	2000	**F**	6	21396.46	0.02	**F**
Trial 2	6	3500	**F**	6	9099.71	0.26	P
Trial 3	6	5000	**F**	6	7317.48	0.5	P
Trial 4	10	2000	**F**	10	9132.59	0.02	P
Trial 5	10	3500	P	10	3884.00	0.26	P
Trial 6	10	5000	P	10	3123.30	0.5	P
Trial 7	14	2000	P	14	5212.51	0.02	P
Trial 8	14	3500	P	14	2216.83	0.26	P
Trial 9	14	5000	P	14	1782.65	0.5	P
		Pass Rate:	**56%**			**Pass Rate:**	**89%**

variables. Non-dimensionalization should be considered before any large Design of Experiments study is conducted, and the parameters given in Table 44 should be used in future torpedo studies.

CHAPTER IX

CONCLUSIONS

9.1 Research Questions Answered

The following answers each of the research questions posed in Section 1.8, along with answering the research hypothesis of the dissertation. The questions and answers stand as follows:

1. *When determining total weapon effectiveness, how significant is the tactical environment with which a system is used compared to torpedo design decisions?*

   The tactical environment is very significant to the torpedo system. In many situations, the launching conditions for the torpedo have significantly more impact on torpedo performance than the actual design. However, even with the large impact of submarine tactics on torpedo effectiveness, a torpedo that is specifically optimized for its operational conditions will demonstrate a marked improvement over a torpedo that is designed for a different operational condition.

2. *If tactics account for a significant portion of total weapon effectiveness, can conceptual design decisions still be made that have more than marginal improvements on total weapon effectiveness? Can the optimization of tactics and conceptual design be synergistically combined to create an even more effective weapon system? Can this synergy be demonstrated on a mine counter-measure system?*

   Both the torpedo tactics example and the mine counter-measures problem demonstrated that although the tactics greatly influence the system performance, design decisions can still be made that improve weapon system performance. Both examples shows that the right combination of tactics and design variables produced the best-performing vehicles. The mine counter-measure system showed that tactics and

performance could be optimized simultaneously to generate the best-performing system.

3. *When dealing with uncertainty, can probability of success be treated as an independent variable in conceptual design? If so, can it be used to select the torpedo design that has the best tradeoff between cost and risk?*

   A method was developed by which probability of success could be used as an independent variable, with the decision-maker able to choose what platform, and at what cost, he or she is willing to accept based upon the probability of success, or risk, of the system. Probability of success versus weight charts were generated for torpedo design, demonstrating the trade-off between risk and cost, thereby allowing informed decisions to be made.

4. *What are the best combinations of metamodeling and uncertainty-analysis measures of merit to use when in the initial stages of robust conceptual torpedo design?*

   These combinations can be very problem-dependent. When using stochastic techniques (random searches or genetic algorithms), fast-executing metamodels like response surface equations work well. When using gradient-based optimizers to find the Pareto front, complex approximations such as most-probable-point methods (FORM and SORM) should be used, or else large numbers of Monte Carlo runs are required to find valid solutions. Joint-probability distribution functions can also be used to approximate the multi-variate design space. Whenever possible, direct simulation should be employed in lieu of a metamodel. Large numbers of Monte Carlo trials were also shown to lead to more conservative results. The applicability of each of these techniques is laid out in this dissertation.

5. *What normalization schemes for torpedo design parameters can be used to simplify the conceptual design process?*

   The results showed that the best normalization schemes to use involved fully non-dimensionalized parameters such as fineness ratio, advance ratio, thrust coefficient,

and torque coefficient. These non-dimensional parameters greatly increased the robustness of Designs of Experiments.

The answer to the research hypothesis is as follows:

A new, more effective design process can be created for conceptual torpedo design. This process, by accounting for the effects from both uncertainty and the tactical environment in which the torpedo is employed, will significantly improve on current design processes for torpedoes.

This research developed a new process for the conceptual design of undersea weapon systems. This process accounts for uncertainty in the design and decision process, as well as the effects of tactics on the system. The new design process is a significant improvement over current torpedo design processes.

9.2 Future Work

This research lays the foundation for a new design process for undersea weapon systems. The following list poses new challenges for future research that can further improve the process for undersea weapon design and optimization in particular and other complex systems-engineering problems in general.

1. A robust integrated design framework was introduced for undersea weapon systems. Theoretically, there is nothing limiting this process from being used on any complex systems-engineering design question. The process should therefore be expanded and demonstrated with additional complex systems. Good potential implementations for this process include surface and submarine design, aircraft design, missile design, and propulsion design. Examples from these fields need to be developed within this framework to prove the extensibility of the framework, as well as dealing with any minor compatibility issues that will inherently arise when the process is used with a complex system.

2. Development of engagement modeling tools is a definite need. These tools must not only be parametric in nature but also account for the myriad of tactical decisions

possible without resorting to a man-in-the-loop style of analysis. Such a capability is imperative for tactics to be fully integrated into the conceptual design and tradeoff environment.

3. A framework for including tactical decisions in design was illustrated using mine counter-measures, along with the need for such a capability in torpedo design. The torpedo design methodology should be expanded to include not only a complex torpedo analysis program, but also include a complex engagement analysis tool so that the system can be designed with tactics fully in play. In this approach, torpedoes can be designed to maximize the full probability of hit (P_{hit}) of the system while also maximizing the probability of evasion (P_{evade}) for the friendly submarine.

4. A full system-of-systems approach for undersea warfare should be implemented. This approach would not only include torpedo design and tactics analysis, but would also include submarine design. In this macroscopic, system-of-systems approach, submarine design parameters, torpedo design parameters, and appropriate tactics could all be traded-off in order to synergistically create the best performing overall system, even in the presence of uncertainty. The framework of such an over-arching undersea architecture has been laid out in this work.

5. A better accounting for the consequences of failure needs to be addressed. Does failure imply that the system performs only slightly below a subjective requirement, or does failure imply a catastrophic loss to the developer? An accounting for this type of relative consequence of failure needs to be worked into the robust design process.

9.3 Final Thoughts

This work addressed many issues, yet the cornerstone question remained the same: how can the process of conceptual design for torpedoes be improved? The solution is manyfold. For one, design uncertainty must be incorporated into any legitimate design process, particularly for undersea weapons. This work provided a mechanism to incorporate design uncertainty and introduced a new approach to exploring the results. As an additional improvement

to torpedo design, it was found that some torpedo design parameters are preferable to others. Future work should use these better-behaving design parameters. And, finally, the thesis showed that undersea weapon design cannot be done in a vacuum. Conceptual design must be done in an environment that accounts for the tactics and the capabilities of the submarines and Fleet systems that are involved. This work shows that all of these elements are crucial, and it brings them all together into an integrated robust design and tactics optimization process for undersea weapons.

APPENDIX A

NON-DIMENSIONALIZATION RESULTS

This Appendix shows the charts comparing all 55 possible combination of non-dimensional parameters that could potentially be used for torpedo design. Each combination of parameters is rated as a 'good' potential combination for design purposes or a 'bad' potential combination. This rating is based on the degree of separation of valid versus failed cases in the charts. A summary of the parameters is given in Table 47, with the complete list of figures given as Figure 168 through Figure 222.

Table 47: Summary of Goodness of Non-Dimensional Torpedo Parameters

		Dimensional Parameters			Partially Non-Dimensional Parameters				Non-Dimensional Parameters			
		Diameter	Horsepower	RPM	HP/Dia^2	HP/Dia^4	HP/Dia^5	RPM*Diameter	Fineness Ratio ($^L/_D$)	Advance Ratio (J)	Thrust Coefficient (K_{HP})	Torque Coefficient (K_Q)
Dimensional Parameters	Diameter	---										
	Horsepower	B	---									
	RPM	B	B	---								
Partially Non-Dimensional Parameters	HP/Dia^2	B	B	B	---							
	HP/Dia^4	B	B	B	B	---						
	HP/Dia^5	B	B	B	B	B	---					
	RPM*Diameter	B	B	B	B	B	B	---				
Non-Dimensional Parameters	Fineness Ratio ($^L/_D$)	B	B	B	B	B	B	B	---			
	Advance Ratio (J)	**G**	B	B	B	B	B	B	**G**	---		
	Thrust Coefficient (K_{HP})	**G**	**G**	**G**	B	B	B	**G**	**G**	**G**	---	
	Torque Coefficient (K_Q)	**G**	B	B	B	B	B	B	**G**	**G**	**G**	---

B = Bad
G = Good

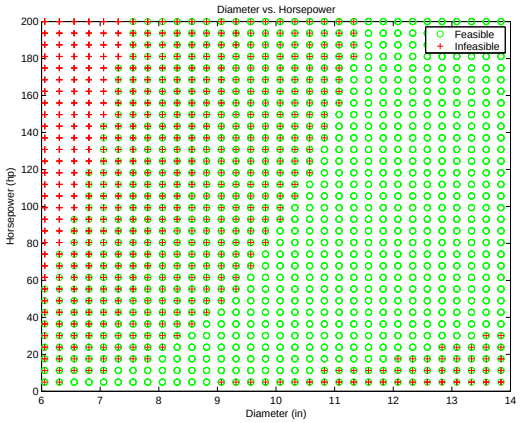

Figure 168: Diameter versus Horsepower (poor parameters)

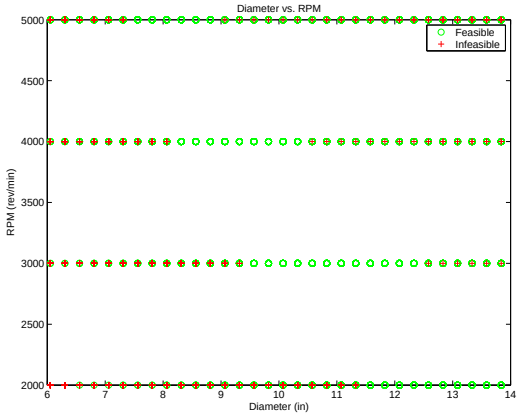

Figure 169: Diameter versus RPM (poor parameters)

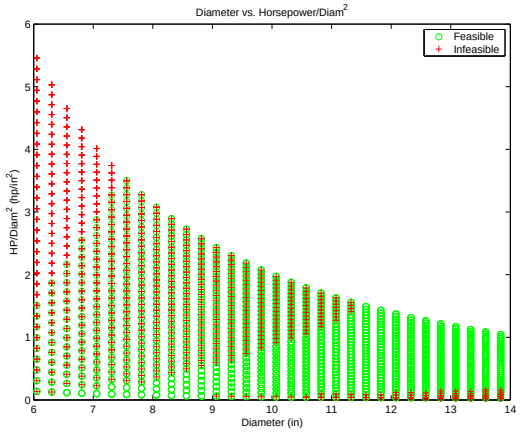

Figure 170: Diameter versus HP/Dia^2 (poor parameters)

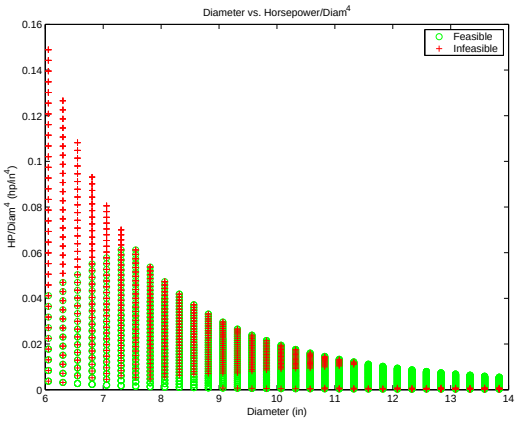

Figure 171: Diameter versus HP/Dia^4 (poor parameters)

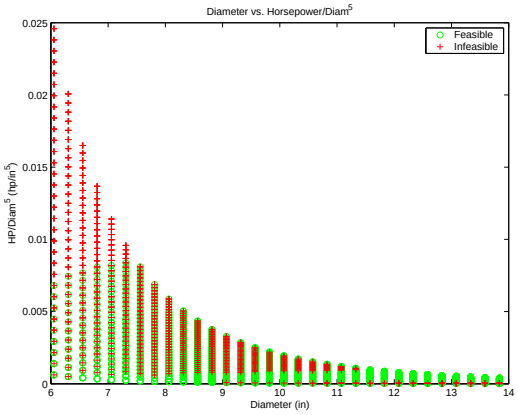

Figure 172: Diameter versus HP/Dia^5 (poor parameters)

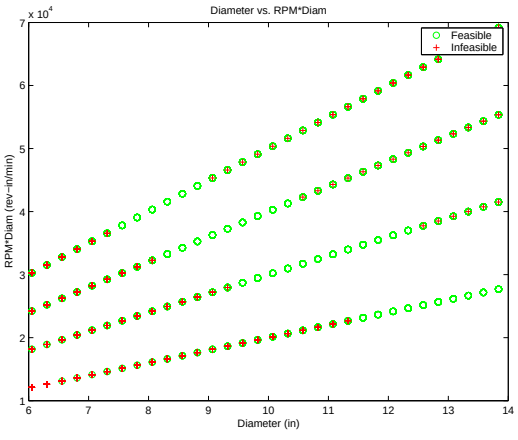

Figure 173: Diameter versus RPM·Diam (poor parameters)

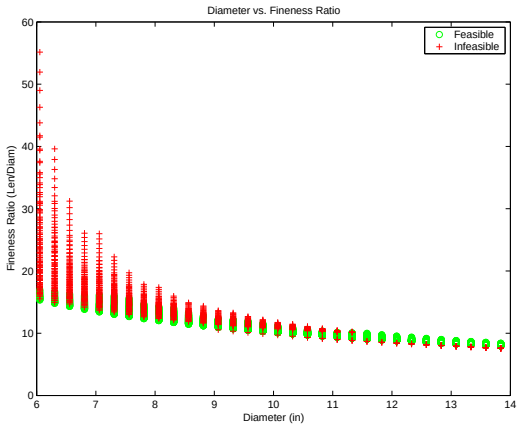

Figure 174: Diameter versus Fineness Ratio (poor parameters)

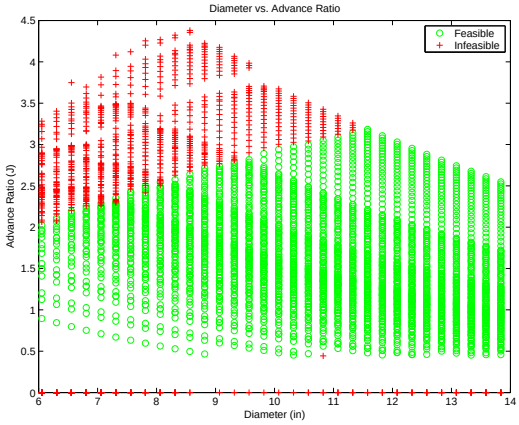

Figure 175: Diameter versus Advance Ratio (good parameters)

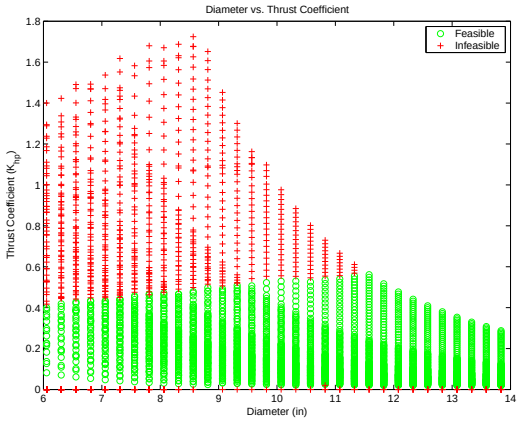

Figure 176: Diameter versus Thrust Coefficient (good parameters)

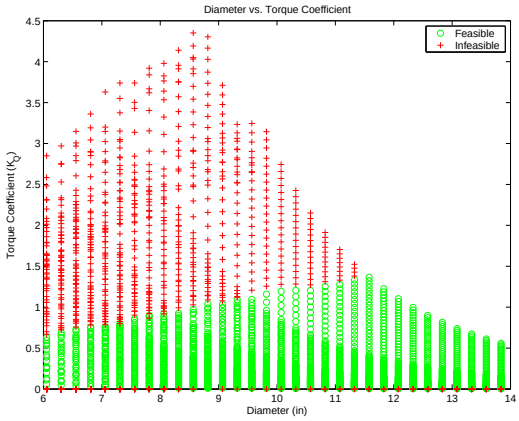

Figure 177: Diameter versus Torque Coefficient (good parameters)

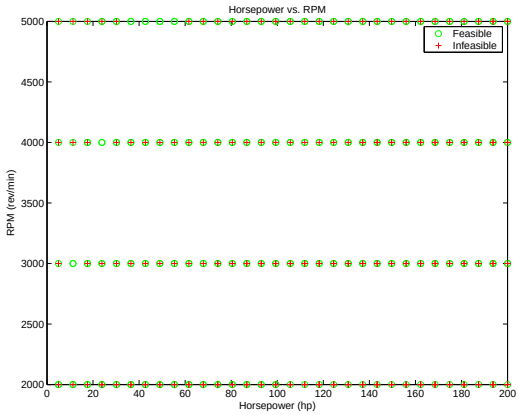

Figure 178: Horsepower versus RPM (poor parameters)

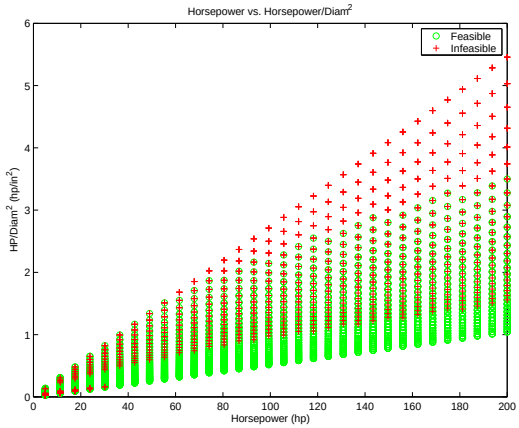

Figure 179: Horsepower versus HP/Dia^2 (poor parameters)

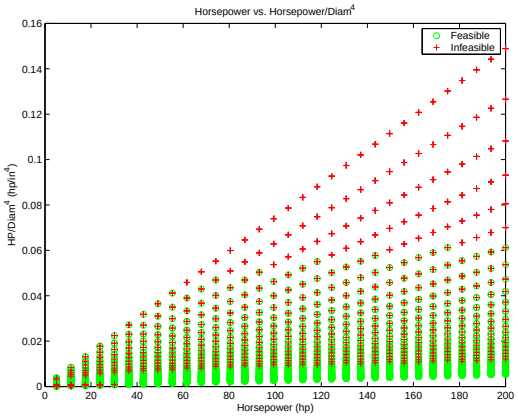

Figure 180: Horsepower versus HP/Dia^4 (poor parameters)

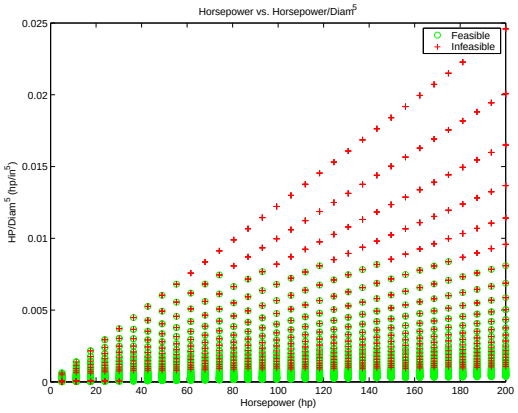

Figure 181: Horsepower versus HP/Dia^5 (poor parameters)

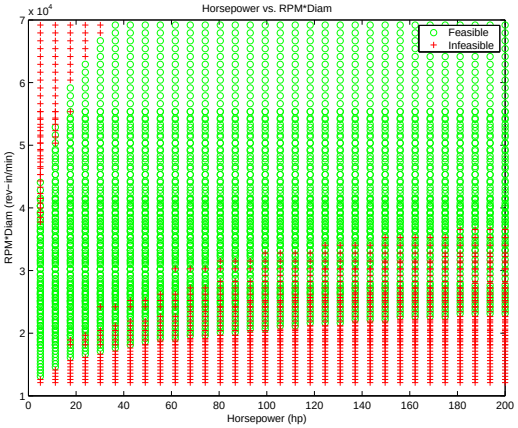

Figure 182: Horsepower versus RPM·Diam (poor parameters)

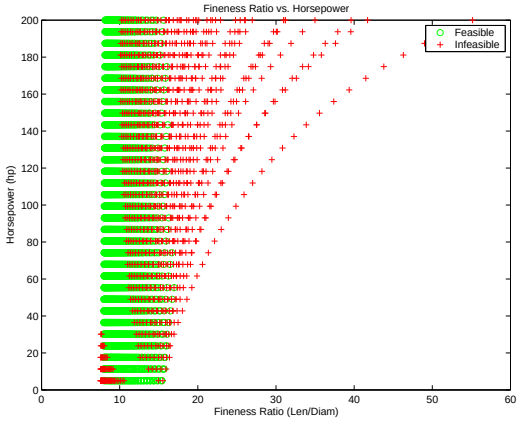

Figure 183: Fineness Ratio versus Horsepower (poor parameters)

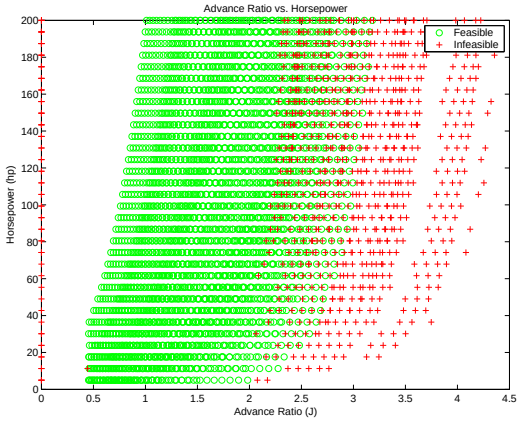

Figure 184: Advance Ratio versus Horsepower (poor parameters)

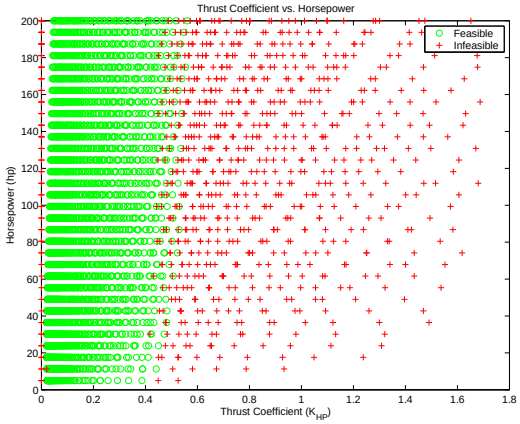

Figure 185: Thrust Coefficient versus Horsepower (good parameters)

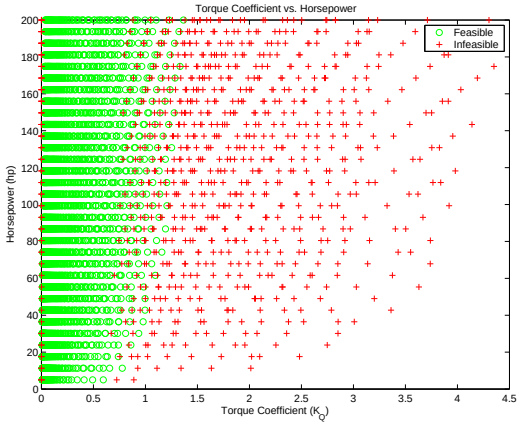

Figure 186: Torque Coefficient versus Horsepower (poor parameters)

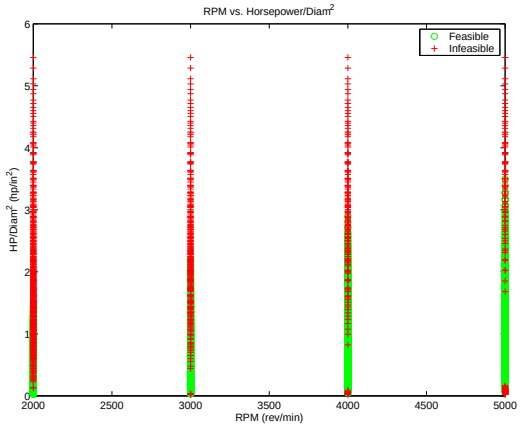

Figure 187: RPM versus HP/Dia^2 (poor parameters)

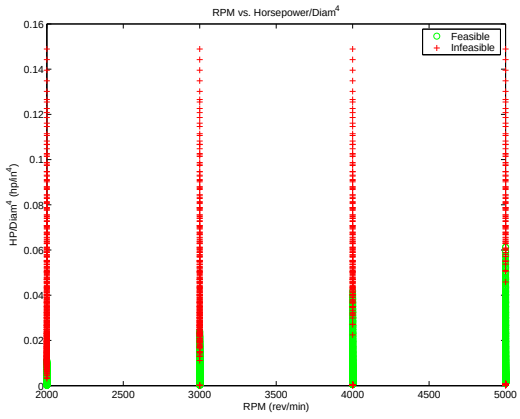

Figure 188: RPM versus HP/Dia^4 (poor parameters)

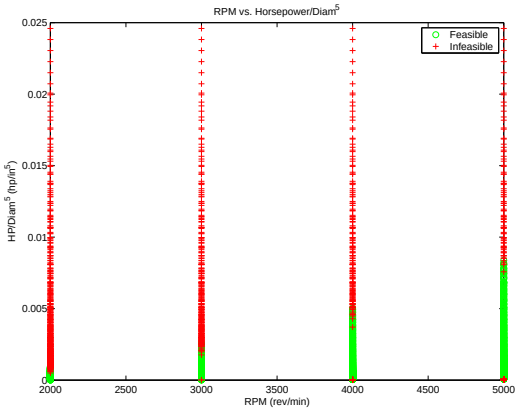

Figure 189: RPM versus HP/Dia^5 (poor parameters)

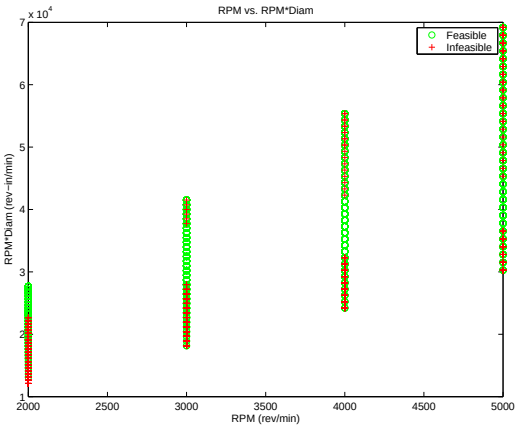

Figure 190: RPM versus RPM·Diam (poor parameters)

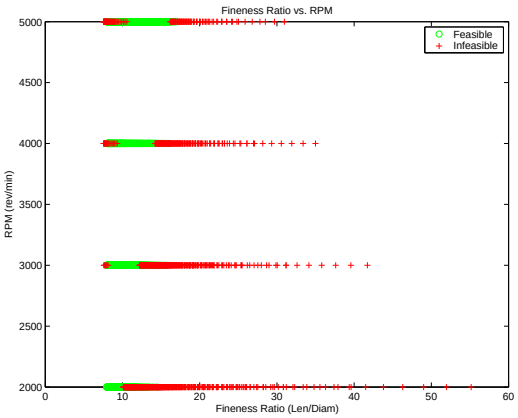

Figure 191: Fineness Ratio versus RPM (poor parameters)

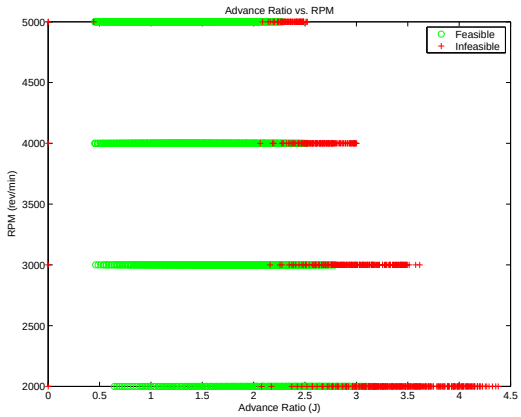

Figure 192: Advance Ratio versus RPM (poor parameters)

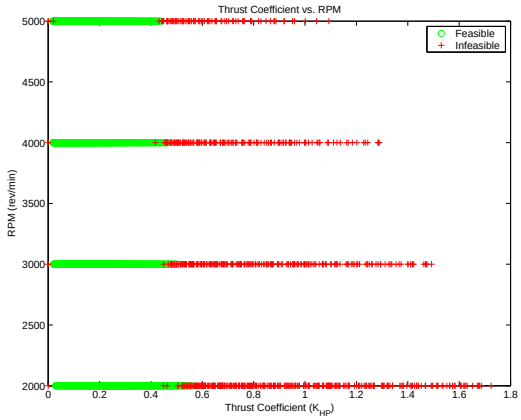

Figure 193: Thrust Coefficient versus RPM (good parameters)

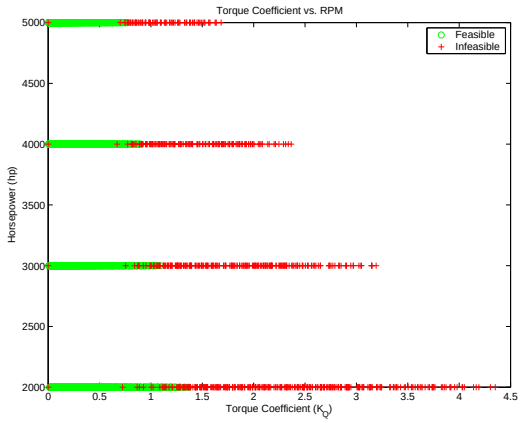

Figure 194: Torque Coefficient versus RPM (poor parameters)

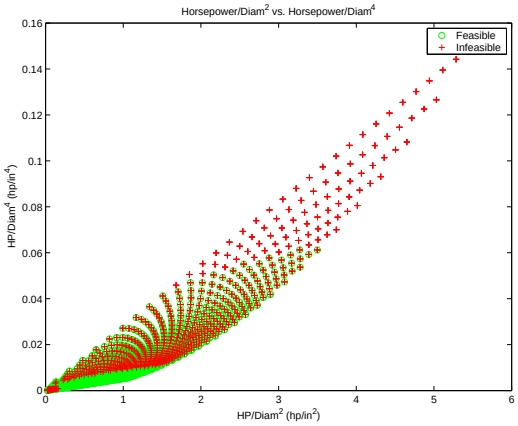

Figure 195: HP/Dia^2 versus HP/Dia^4 (poor parameters)

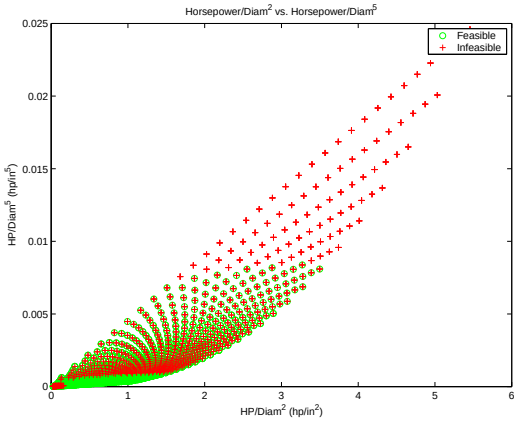

Figure 196: HP/Dia^2 versus HP/Dia^5 (poor parameters)

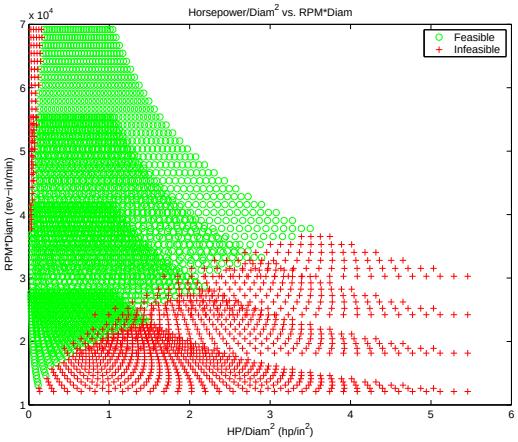

Figure 197: HP/Dia^2 versus RPM·Diam (poor parameters)

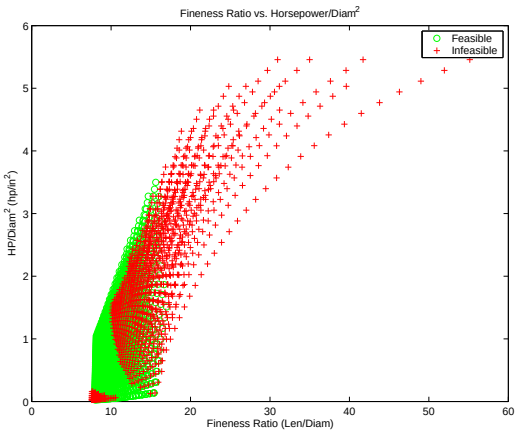

Figure 198: Fineness Ratio versus HP/Dia^2 (poor parameters)

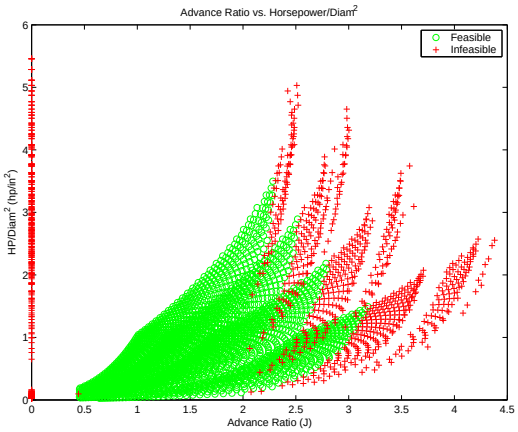

Figure 199: Advance Ratio versus HP/Dia^2 (poor parameters)

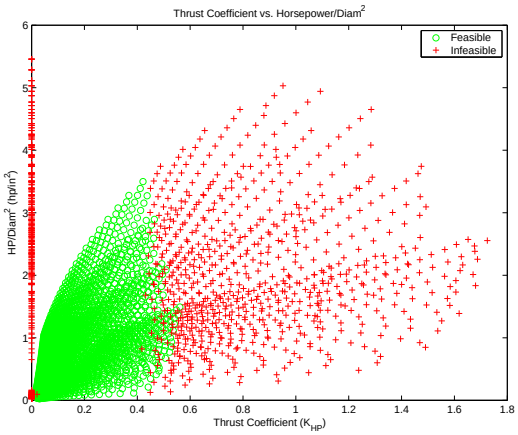

Figure 200: Thrust Coefficient versus HP/Dia^2 (poor parameters)

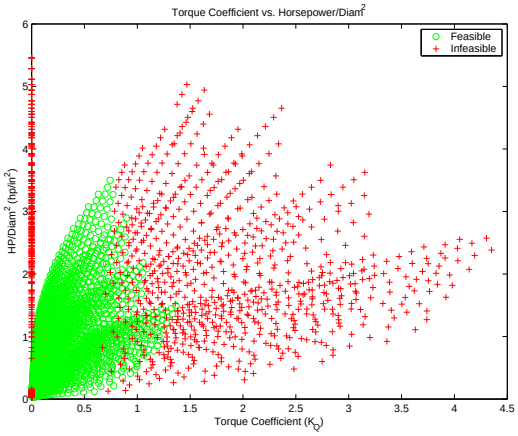

Figure 201: Torque Coefficient versus HP/Dia^2 (poor parameters)

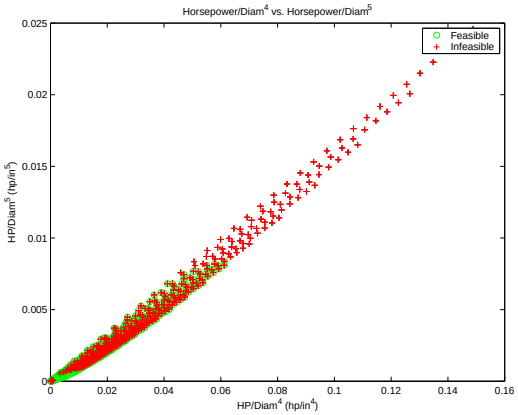

Figure 202: HP/Dia^4 versus HP/Dia^5 (poor parameters)

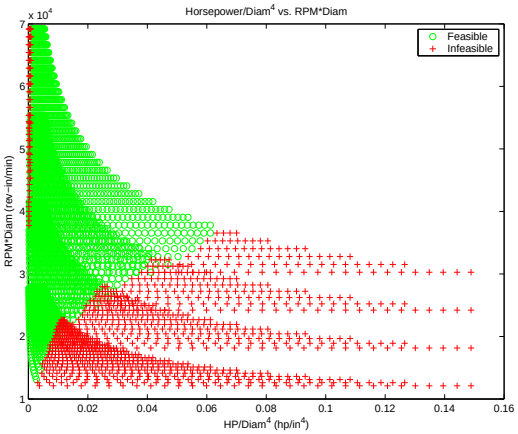

Figure 203: HP/Dia^4 versus RPM·Diam (poor parameters)

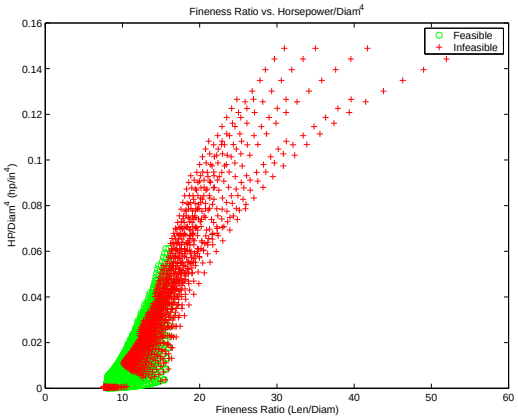

Figure 204: Fineness Ratio versus HP/Dia^4 (poor parameters)

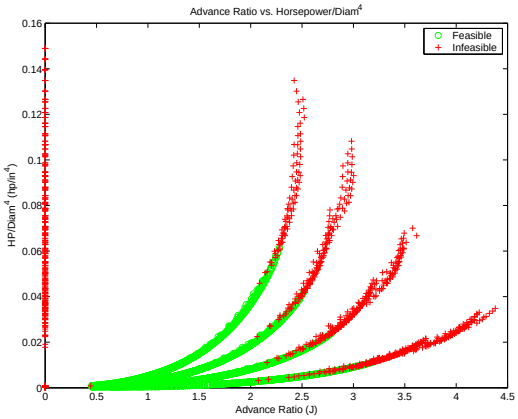

Figure 205: Advance Ratio versus HP/Dia^4 (poor parameters)

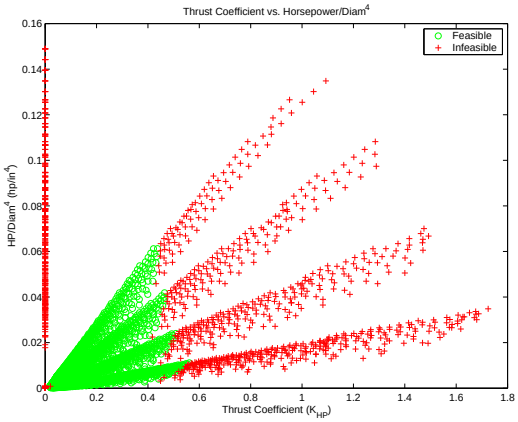

Figure 206: Thrust Coefficient versus HP/Dia^4 (poor parameters)

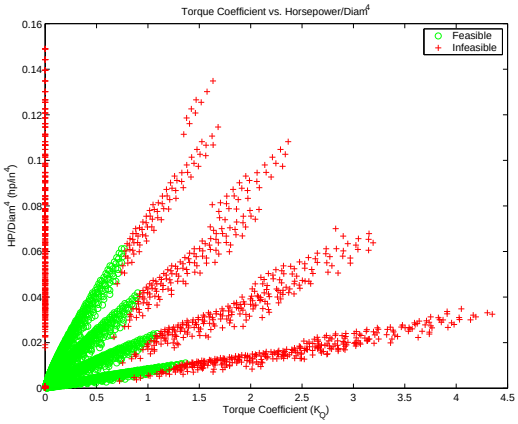

Figure 207: Torque Coefficient versus HP/Dia^4 (poor parameters)

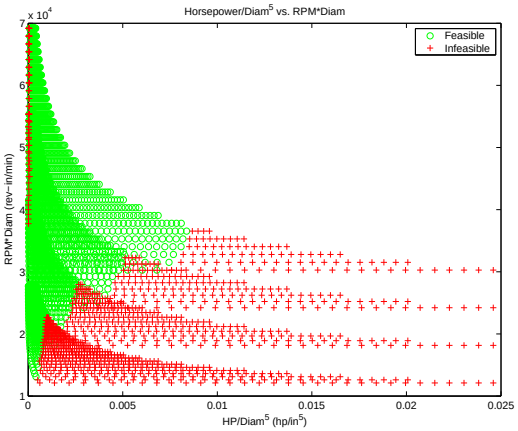

Figure 208: HP/Dia^5 versus RPM·Diam (poor parameters)

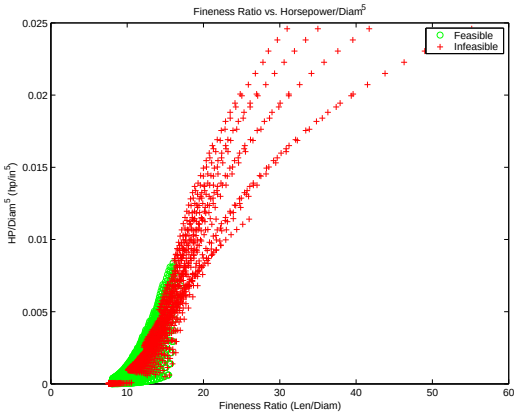

Figure 209: Fineness Ratio versus HP/Dia^5 (poor parameters)

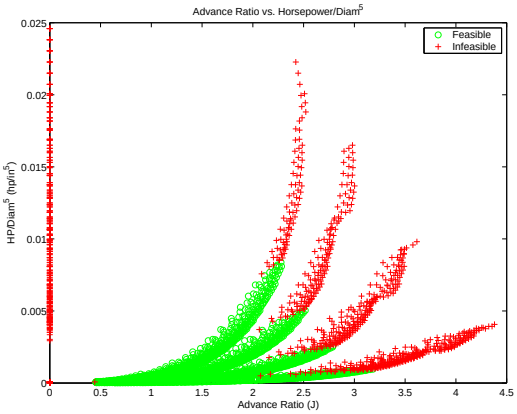

Figure 210: Advance Ratio versus HP/Dia^5 (poor parameters)

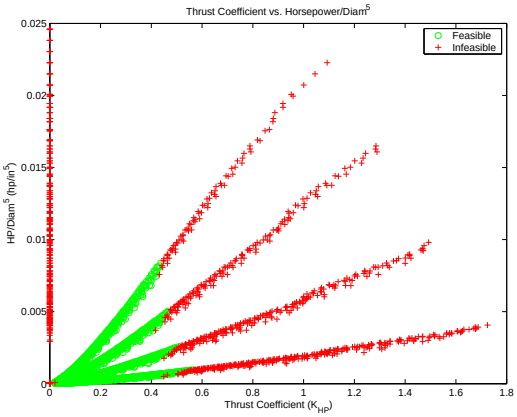

Figure 211: Thrust Coefficient versus HP/Dia^5 (poor parameters)

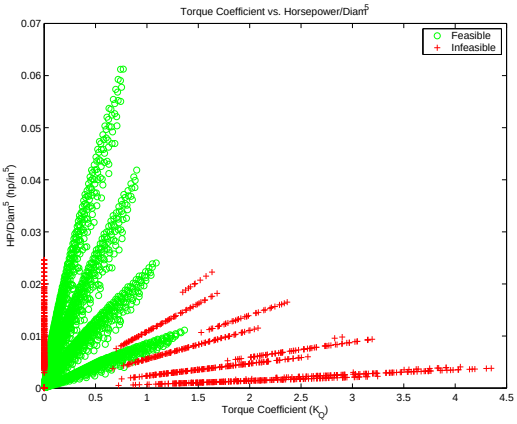

Figure 212: Torque Coefficient versus HP/Dia^5 (poor parameters)

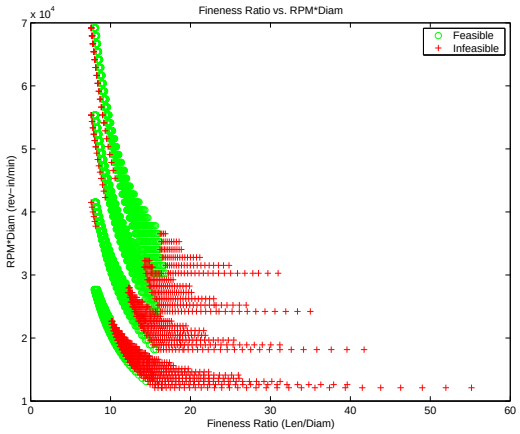

Figure 213: Fineness Ratio versus RPM·Diam (poor parameters)

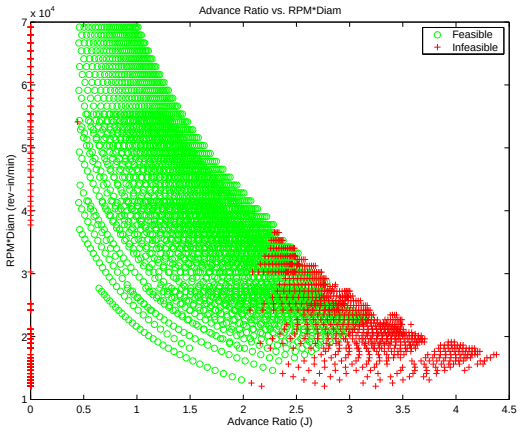

Figure 214: Advance Ratio versus RPM·Diam (poor parameters)

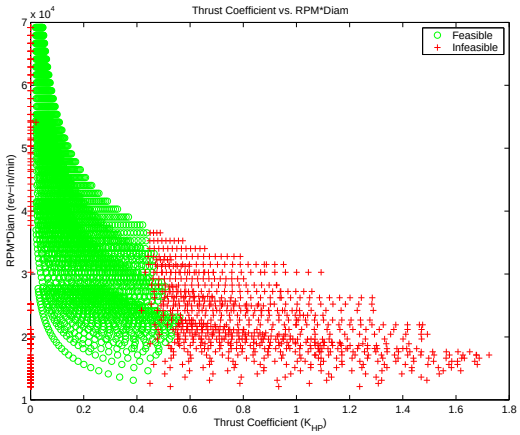

Figure 215: Thrust Coefficient versus RPM·Diam (good parameters)

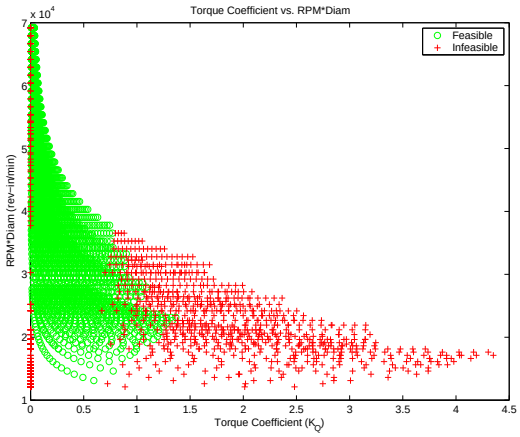

Figure 216: Torque Coefficient versus RPM·Diam (poor parameters)

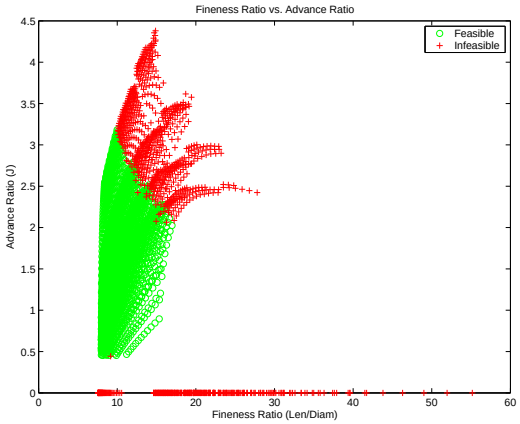

Figure 217: Fineness Ratio versus Advance Ratio (good parameters)

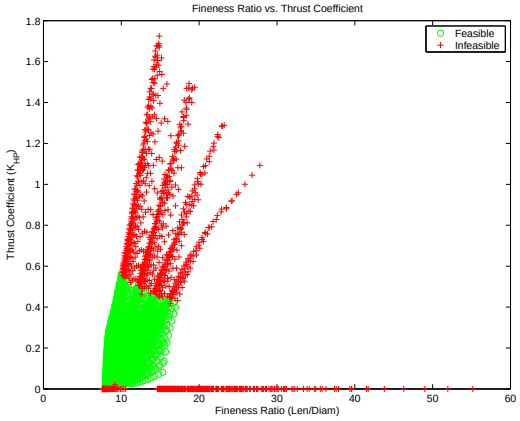

Figure 218: Fineness Ratio versus Thrust Coefficient (good parameters)

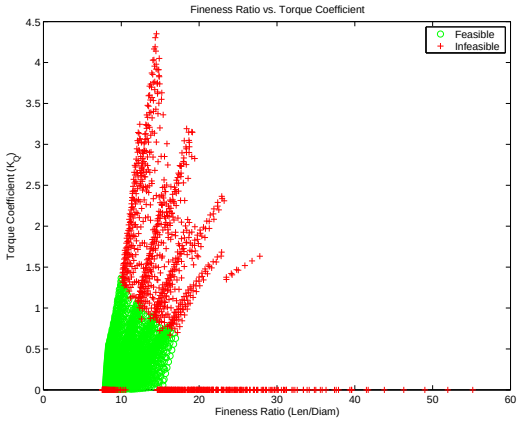

Figure 219: Fineness Ratio versus Torque Coefficient (good parameters)

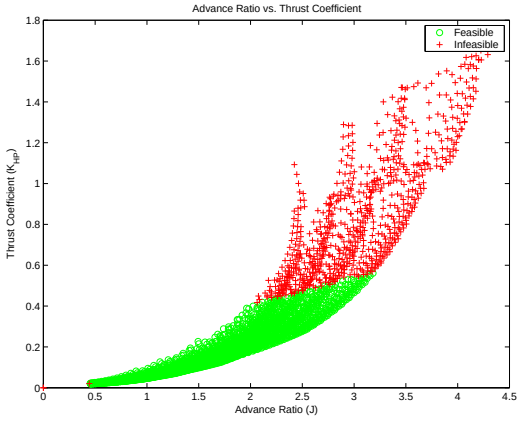

Figure 220: Advance Ratio versus Thrust Coefficient (good parameters)

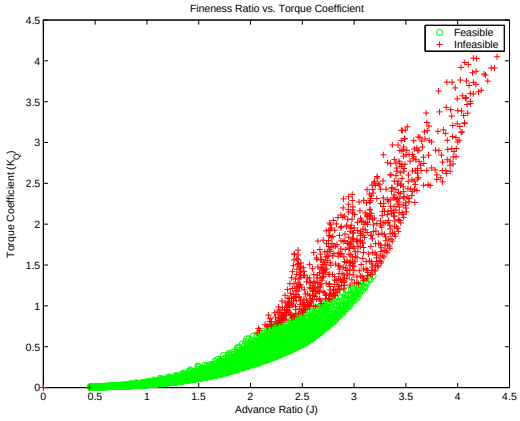

Figure 221: Advance Ratio versus Torque Coefficient (good parameters)

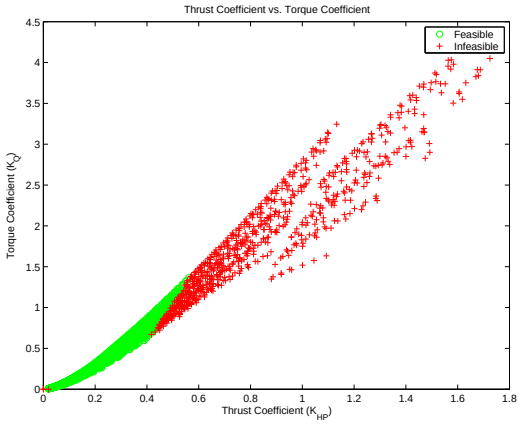

Figure 222: Thrust Coefficient versus Torque Coefficient (good parameters)

APPENDIX B

TOAD CALCULATIONS

This appendix includes some select performance algorithms from the TOAD torpedo analysis program (descriptions were taken from Reference [158]). The algorithms included here focus on the high-level "system" parameters – drag, velocity, range, and noise. Sub-system algorithms, which make up the majority of the analysis, are excluded for brevity. A complete description of analyses is available in the TOAD User's Manual, Reference [158].

B.1 Drag Calculations

The first calculation needed for drag analysis is the wetted surface area, which is a primary driver for total drag. The torpedo is modeled as a cylindrical body with a hemispherical nose and a conical afterbody. The wetted area can then be calculated by Equation 35, where f is the afterbody fraction, defined by default to be 0.10, and L and D refer to the torpedo length and diameter, respectively.

$$S_w = \frac{\pi}{4} D^2 \left(4(1-f)\frac{L}{D} + \sqrt{1 + (2f\frac{L}{D})^2} \right) \tag{35}$$

Drag coefficients for the vehicle (form drag, appendage drag, induced drag, etc.) are calculated based upon the definition of drag coefficient in Equation 36 for a drag component i.

$$C_{D_i} = \frac{D_i}{1/2 \ \rho \ V_s^2 \ S_w} \tag{36}$$

The zero-lift drag is found by summing the appendage drag (from fins, etc.) and the form drag, multiplied by a correction factor, Equation 37.

$$C_{D_0} = C_f \ F_{form} + C_{app} \tag{37}$$

The frictional drag coefficient, C_f, is based upon empirical data from Reference [95] and is shown in Equation 38, with the definition of Reynolds number in Equation 39.

$$C_f = \frac{0.0776}{\log_{10}(R_e - 1.88)^2} + \frac{60}{R_e} \tag{38}$$

$$R_e = \frac{V_s L}{\nu} \tag{39}$$

R_e = Reynolds Number

V_s = Vehicle Speed

L = Vehicle Length

ν = Fluid Kinematic Viscosity

The form correction factor, f_{form} was taken from Hoerner, Reference [107], and is shown as Equation 40.

$$f_{form} = 1 + a(1.5 + 7a) \tag{40}$$
$$a = \left(min\left(\frac{1}{2}, \frac{D}{L}\right)\right)^{3/2}$$

The drag for each fin is calculated individually, based upon the fin shape and the length of the fin that interferes with the torpedo body. The fin drag is then multiplied by the number of fins and normalized by the reference area convention of Equation 36. The calculations for appendage drag are based upon Hoerner [107] and are given in Equation 41.

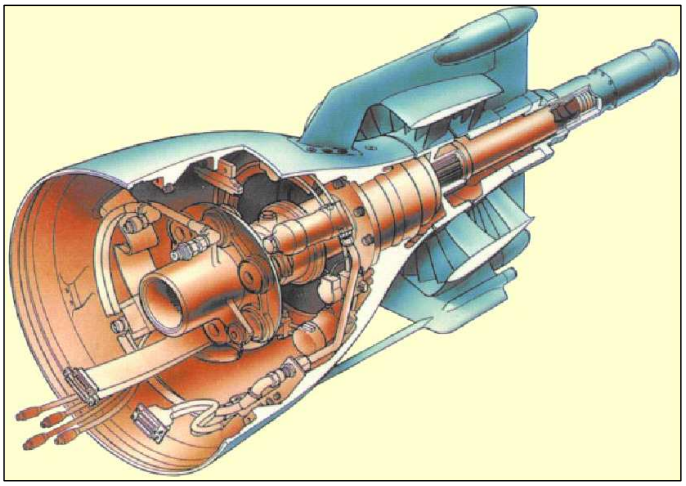

Figure 223: Close-up View of Spearfish Fin Geometry [186]

$$D_{fin} = C_f \frac{1}{2}\rho V^2 A \cdot 2\Big(1 + 1.2(t/c) + 100(t/c)^4\Big) \tag{41}$$

$$D_{int} = \frac{1}{2}\rho V^2 t^2 \Big(0.75(t/c_{int}) - 0.0003(t/c_{int})^2\Big)$$

C_f = Friction Coefficient (Equation 38)

A = Planform (one-sided) Area

t = Fin Thickness

c = Fin Chord

c_{int} = Fin Chord (with body interference)

The number and dimensions of fins are based upon the fin geometry of the British Spearfish torpedo. A schematic of the fin geometry is shown in Figure 223. Three sets of fins are listed: primary, secondary, and control surface fins. The size of each fin is given in Table B.1. The fin sizes for specific torpedoes are ratioed based upon a spearfish baseline diameter of 21 inches. For instance, if a torpedo has an 11.5 inch diameter, the fin sizes will be decreased by half to maintain the same relative size.

An induced drag component is calculated for the torpedo system. The induced lift and drag model is based upon a linear model in Reference [106]. The model is valid only at small angles of attack (less than 12 degrees). The equations for this drag are given as Equation

Table 48: Baseline Fin Sizes

Fin Type	Number of Fins	Baseline Area (in^2)	Thickness (in)	Baseline Chord (in)	Interference Length (in)	Freestream Velocity
Primary	4	40.0	0.75	16.0	chord/2	1.0
Secondary	8	20.0	0.75	4.0	chord	1.0
Control Surfaces	4	20.0	0.75	4.0	chord	1.1

42 and Equation 43.

$$
\begin{aligned}
C_{D_\alpha} &= \alpha^2(C_{L_P} + |\alpha| C_{L_P}) \qquad (42)\\
C_{L_\alpha} &= \alpha(C_{L_P} + \alpha C_{L_P})\\
C_{L_P} &= 2\frac{S_b}{S_w}\\
C_{L_V} &= \eta C_{D_C}\frac{S_p}{S_w}\\
\eta &= b_o + f_b(B_1 + f_b b_2)\\
f_b &= \sqrt{max\Big(2, min\Big(28, \frac{L}{D}\Big)\Big)}\\
S_b &= \frac{\pi}{4}D^2\\
S_p &= \frac{\pi}{4}D^2\Big(\frac{1}{2} + \Big(1 - \frac{1}{2}f\Big)\frac{4L}{\pi D}\Big)
\end{aligned}
$$

$$
\begin{aligned}
C_{D_\alpha} &= \text{Induced Drag} \\
C_{L_\alpha} &= \text{Induced Lift} \\
\alpha &= \text{Angle of Attack (radians)} \\
C_{L_P} &= \text{Potential Flow Component of Body Lift} \\
C_{L_V} &= \text{Viscous Component of Body Lift} \\
S_b &= \text{Transverse Cross-Sectional Area} \\
S_p &= \text{Planform (longitudinal cross-sectional) Area} \\
S_w &= \text{Wetted Area} \\
f &= \text{Form Correction Factor} \\
b_0 &= 0.378452 \\
b_1 &= 0.129846 \\
b_2 &= -0.00997805 \\
C_{D_C} &= 1.2
\end{aligned}
\tag{43}
$$

The total drag for the system can then be calculation via Equation 44.

$$C_D = C_{D_0} + C_{D_i} \tag{44}$$

B.2 Velocity Calculations

The velocity calculations in TOAD are developed around a power and force balance, assuming that the torpedo is travelling at a constant depth and constant velocity. The first step in the process is to calculate the power available by multiplying the shaftpower provided from the motor times the propulsor efficiency. An angle of attack (α) is then assumed, and a velocity is calculated, as shown in Equation 45.

$$V = \left(\frac{\eta_{prop} \cdot P_{shaft} \cdot \cos\alpha}{1/2\rho V^2 \cdot S_{ref}} \right)^{1/3} \tag{45}$$

Next, the forces in Figure 224 must be balanced. The estimated torpedo weight is subtracted from the buoyancy. The remaining force is equal to the 'lift' required to maintain neutral buoyancy. Note that, unlike aircraft calculations, this lift-force is not inherently upwards. In cases in which the buoyancy is greater than the weight (a positively buoyant vehicle), the lift will be in a downwards direction to maintain level travel. Positive buoyancy is a fairly common situation in torpedo design, as 'test-rounds' are always designed with positive buoyancy, so that they can easily be recovered after use.

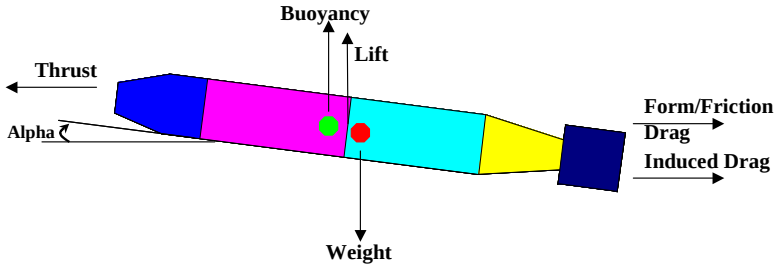

Figure 224: Force Balance in TOAD Sizing

Once the required lift has been calculated, the coefficient of lift can be calculated via Equation 46. Since the coefficient of lift is assumed to change linearly with angle of attack, a new angle of attack can be calculated based upon the required coefficient of lift.

$$C_L = \frac{\text{Buoyancy} - \text{Weight}}{1/2\rho V^2 \cdot S_{ref}} - C_D \cdot \tan(\alpha) \tag{46}$$

This new angle of attack can be used to calculate the new drag value (including induced drag, see Section B.1, Equation 44) and the power required for the system, as shown in Equation 47. The velocity analysis is then repeated, until a velocity and α value are chosen so that the two power calculations are identical.

$$P_{shaft} = \frac{C_D \cdot (1/2\rho V^2 \cdot S_{ref}) \cdot V}{\cos(\alpha)\eta_{prop}} \tag{47}$$

With a new velocity calculated for the vehicle, the TOAD program iterates and resizes the vehicle (see Figure 225), as both the propulsor sub-system and the C_{D_0} are a function of velocity. This process continues until the velocity converges and the vehicle size no longer

changes.

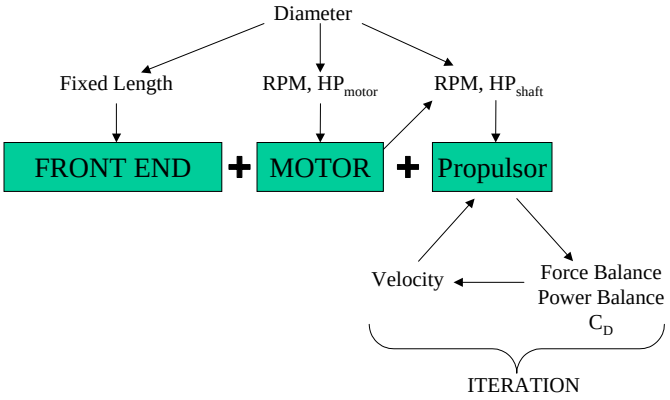

Figure 225: Iteration Procedure of TOAD

B.3 Range Calculations

The range calculations are very straightforward for the TOAD program. The total power drain of the torpedo is calculated, which accounts for the hotel power load of all the subsystems along with the power draw of the motor divided by the motor efficiency. The total energy available, in the form of either fuel or battery charge, is divided by the power drain in order to calculate the amount of time that the torpedo remains powered. This time multiplied by the torpedo velocity will generate a value for range[1]. The equations are given as Equation 48 and Equation 49.

$$\text{Power Drain} = \text{Hotel Power} + \frac{P_{Motor}}{\eta_{Motor}} \tag{48}$$

$$R = V \cdot \frac{E_{fuel}}{\text{Power Drain}} \tag{49}$$

B.4 Noise Calculations

Noise calculations are inherently complex, and, for Fleet systems, inherently classified. As such, the noise calculations for TOAD are designed to provide a simple way to show noise

[1]This formulation assumes that the torpedo will be continuously operating at its maximum-velocity condition: no accelerations or lower-speed 'cruise conditions' are present

trends (i.e., faster vehicle makes more noise, a bigger engine makes more noise) even though the magnitude of these trends may not match actual systems. In addition, the final 'noise' of the system is related through a single value of decibel level, which ignores the inherent spectral nature of system noise. The decibel levels should be considered to be 'in relation to an abstract threshold', and not an absolute amount.

The noise section calculates three distinct types of noise and then combines these three noises as an exponential sum to estimate the total noise. The three noises are flow noise, engine noise, and propulsor noise. Each noise is generated by comparing the torpedo values to a baseline criteria. Two types of noise damping materials are included in the formulation. A decoupling layer may be specified, which is an external layer attached to the hull that decreases the flow noise. Secondly, an engine damping layer may be included around the propulsion section, which decreases the engine noise. These layers do come with penalties, as the decoupling layer adds weight and decreases the inner volume available for internal components. Similarly, the engine damping layer adds both weight and length to the propulsion system. An engine damping layer may NOT be included with the IMP (integrated motor-propulsor) type propulsion system, as the motor is external to the torpedo.

The equations used to calculate the torpedo noise are shown as 50 through 53. The variables and parameter values are defined in Table 49. Note that variables with a subscript "$_0$" indicate reference values. Otherwise the variables represent torpedo values. Figure 226 shows an example of how the noise components and the total noise vary as a function of velocity. Note that engine noise dominates the system at low velocities, while flow and propulsor noise dominate the system at high velocities.

$$\text{System Noise} = 10\log_{10}\left(10^{\text{FlowNoise}/10} + 10^{\text{EngineNoise}/10} + 10^{\text{PropNoise}/10}\right) \tag{50}$$

$$\text{FlowNoise} = 60\log_{10}\left(\frac{V}{V_0}\right) - 15dB - A \cdot (\text{DecouplerThickness}) \tag{51}$$

Table 49: Torpedo Noise Variable Definitions and Reference Values

Variable	Definition	Reference Value
V	Torpedo maximum velocity	10 kts
A	Decoupler layer effectiveness	10 dB/in
HP	Motor horsepower	10 hp
B	Engine damper layer effectiveness	10 dB/in
Engine Type Noise	Extra noise due to engine type	Electric = +0dB Conventional = +10dB SCEPS = +10dB
a	Propellor radius	1.0 in
J	Propellor advance ratio	1.5
Damper Thickness	Thickness of engine-isolation layer	—
Decoupler Thickness	Thickness of body-insulation layer	—

$$\text{EngineNoise} = 10\log_{10}\left(\frac{HP}{HP_0}\right) + 10dB - B\cdot(\text{DamperThickness}) + \text{EngineTypeNoise} \quad (52)$$

$$\text{PropNoise} = 30\log_{10}\left[\frac{V}{V_0}\left(\frac{1+\left(\frac{a\pi}{J}\right)^2}{1+\left(\frac{a_0\pi}{J_0}\right)^2}\right)^{1/2}\right] - 15dB \quad (53)$$

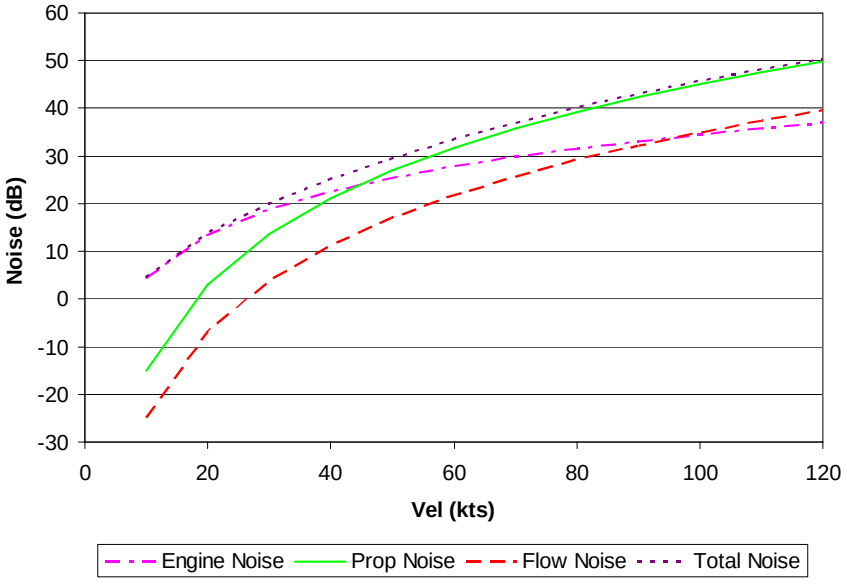

Figure 226: Torpedo Noise Contributions as a Function of Velocity

REFERENCES

[1] "Navy Strategic Planning Guidance," August 1999.

[2] *Jane's Underwater Warfare Systems*. Alexandria, VA: Jane's Information Group Limited, Sentinel House, 12th ed., 2000.

[3] "Department of Defense Directive: The Defense Acquisition System," number 5000.1, Department of Defense, *http://akss.dau.mil/dag/DoD5001/References.asp#Subject*, May 12, 2003.

[4] "Submarine Weapon Systems," *http://www.shima.demon.co.uk/subwpns.htm*, December 31, 2003.

[5] "All Hands Online," *All Hands, Magazine of the U.S. Navy, http://www.mediacen.navy.mil/pubs/allhands/Jan99/janpg30.htm*, January 1999.

[6] Abbott, I. H. and von Doenhoff, A. E., *Theory of Wing Sections*. Dover, 1959.

[7] About, inc, "U.S. Military Glossary." *http://usmilitary.about.com/library/glossary/blglossary.htm*, 2004.

[8] Alexandrov, N. and Kodiyalam, S., "Initial Results of an MDO Method Evaluation Study," (St. Louis, MO), *Presented at the 7th AIAA/USAF/NASA/ISSMO Symposium on Multidisciplinary Analysis and Optimization*, AIAA, September 1988, AIAA-98-4884.

[9] Anderson, John D., *Fundamentals of Aerodynamics*. United States of America: McGraw-Hill, 2nd ed., 1991.

[10] Anderson, John D., *Aircraft Performance and Design*. Boston: WCB McGraw-Hill, 1st ed., 1999.

[11] Ang, A. H.-S. and Tang, W. H., *Probability Concepts in Engineering Planning and Design*, vol. 1. John Wiley & Sons, 1984.

[12] Arakawa, Masao, Nakayama, Hirotaka, Sasaki, Rie, and Ishikawa, Hiroshi, "Approximate Optimization of Constraint Problem Using Radial Basis Function and Self-Organizing Maps," *8th AIAA/USAF/NASA/ISSMO Symposium on Multidisciplinary Analysis and Optimization*, AIAA, Long Beach, CA, September 6-8, 2000, AIAA-2000-4922.

[13] Ashley, Steven, "Warp Drive Underwater," *Scientific American*, May 2001.

[14] Avery, J., "The Naval Mine Threat to U.S. Surface Forces," *Surface Warfare*, pp. 4–9, May/June 1998.

[15] Baker, Andrew Paul, *The Role of Mission Requirements, Vehicle Attributes, Technologies and Uncertainty in Rotorcraft System Design*. PhD thesis, Georgia Institute of Technology, March 2002.

[16] Bandte, Oliver, *A Probabilistic Multi-Criteria Decision Making Technique for Conceptual and Preliminary Aerospace Systems Design*. PhD thesis, Georgia Institute of Technology, September 2000.

[17] Barker, Thomas B., *Engineering Quality by Design, Interpreting the Taguchi Approach*. Stastistics: Textbooks and Monographs, New York, NY: Marcel Dekker, Inc., ASQC Quality Press, 1990.

[18] Barros, P., Kirby, M., and Mavris, D., "Impact of Sampling Techniques Selection on the Creation of Response Surface Models," (Reno, NV), *Presented at the 2004 SAE World Aviation Congress*, AIAA, 2004, AIAA-2004-01-3134.

[19] Belegundu, A., "Probabilistic Optimal Design Using Second Moment Criteria," *Journal of Mechanisms, Transmissions, and Automation in Design*, vol. 110, pp. 324–329, September 1988.

[20] Belegundu, A., Halberg, E., Yukish, M., and Simpson, T., "Attribute-Based Multidisciplinary Optimization of Undersea Vehicles," (Long Beach, CA), *Presented at the 8th AIAA/USAF/NASA/ISSMO Smposium on Multidisciplinary Analysis and Optimization*, AIAA, September 6-8, 2000, AIAA-2000-4865.

[21] Benedict, J. R., "Final Report: Long-Term Mine Reconnaissance System (LMRS) Cost and Operational Effectiveness Analysis (COEA)," report NWA-96-009, Johns Hopkins University Applied Physics Laboratory, September 1996.

[22] Betancourt, Rear Adm Jose L., "Mine Warfare Physics 101." Mine Warfare Command, Corpus Christi, TX.

[23] Boeing Company, "Future Combat Systems Primer." http://www.boeing.com/defense-space/ic/fcs/bia/030707_fcs_glance.pdf, January 2004.

[24] Box, G, "Signal-to-Noise Ratios, Performance Criteria, and Transformations," *Technometrics*, vol. 30, pp. 1–17, February 1988.

[25] Boyars, A., "Warhead Integration in UWD&O," *Presented at the Undersea Weapons Design and Optimization Workshop*, Office of Naval Research, August 3, 1999.

[26] Boyars, A., Azarm, S., and Magrab, E., "Multicriteria and Multidisciplinary Optimization in Undersea Warhead Design," *Presented at the 2000 ONR Undersea Weapons Design and Optimization Workshop*, Office of Naval Research, June 7, 2000.

[27] Boyars, Art, "Warhead Design Server: Warhead Analysis Code," (Indian Head, MY), Surface Warfare Center Division, NAVSEA, Underwater Warheads and Technology Department, 2001.

[28] Boyars, Art, Kusmik, Aldo, and Yukish, Mike, "Collaborative Engineering Across Organizational Boundaries," *presented at American Society of Naval Engineer's Day*, 2002.

[29] Bracklin, William L., "Naval Orientation," training manual, Naval Education and Training Command, July 1991.

[30] Brady, John and Dorsch, Scott, "Littoral Warfare Modeling and Simulation," tech. rep., Coastal Systems Station, Panama City, FL, 2001.

[31] Brown, A. and Thomas, M., "Reengineering the Naval Ship Concept Design Process," (University of Essex, United Kingdom), p. 277, *From Research to Reality in Ship Systems Engineering Symposium*, ASNE, 1998.

[32] Brown, Cdr John, "Mine Warfare Brief." Mine Warfare Command.

[33] Buonanno, M. and Mavris, D., "Aerospace Vehicle Concept Selection Using Parallel, Variable Fidelity Genetic Algorithms," (Albany, NY), *Presented at the 2004 Multidisciplinary Analysis and Optimization Conference*, AIAA, August 30 - September 1 2004.

[34] Burcher, R. and Rydill, L., *Concepts in Submarine Design*. Cambridge University Press, 1994.

[35] Burdic, William S., *Underwater Acoustic System Analysis*. Englewood Cliffs, N.J.: Prentice Hall, 2nd ed., 1991.

[36] Burlington, Scott and Dudek, Gregory, "Spiral Search as an Efficient Mobile Robotic Search Technique," tech. rep., Center for Intelligent Machines, McGill University, January 1999.

[37] Champagne, L., Carl, R., and Hill, R., "Search Theory, Agent-Based Simulation, and U-Boats in the Bay of Biscay," *Proceedings of the 2003 Winter Simulation Conference*, December 7-10, 2003.

[38] Chen, S., Nikolaidis, E., and Cudney, H., "Comparison of Probabilistic and Fuzzy Set Methods for Designing under Uncertainty," *40th Structures Structural Dynamics and Materials Conference*, AIAA, Saint Louis, MO, 1999, AIAA-99-1579.

[39] Chen, W., Allen, J. K., Mistree, F., and Tsui, K.-L., "A Procedure for Robust Design: Minimizing Variations Caused by Noise Factors And Control Factors," *ASME Journal of Mechanical Design*, vol. 118, pp. 478–485, 1996.

[40] Chen, W., Wiecek, M., and Zhang, J, "Quality Utility – A Compromise Programming Approach to Robust Design," *ASME Journal of Mechanical Design*, vol. 121, no. 2, pp. 179–187, 1999.

[41] Clancy, T., *Submarine: A Guided Tour Inside a Nuclear Warship*. New York: Berkley Books, 2002.

[42] Comstock, J.P. (ed.), *Principles of Naval Architecture*. Society of Naval Architects and Marine Engineers, 1967 (revised edition).

[43] Coney, William B., *A method for the design of a class of optimum marine propulsors*. PhD thesis, Massachusetts Institute of Technology, 1989.

[44] Cooper, D. C., Frost, J. R., and Robe, R. Q., "Compatibility of Land SAR Procedures with Search Theory," Tech. Rep. Task Order DTCG32-02-F-000032, U.S. Department of Homeland Security, United States Coast Guard, Washington, D.C., December 30, 2003.

[45] Crespo, Luis, "Optimization of Systems with Uncertainty: Initial Developments for Performance, Robustness and Reliability Based Designs," NASA/CR-2002-211952, ICASE Report No. 2002-40, NASA, November 2002.

[46] Cressie, N., *Statistics for Spatial Data*. New York: John Wiley & Sons, 1991.

[47] Daberkow, D. and Mavris, D., "An Investigation of Metamodeling Techniques for Complex Systems Design," *Presented at the 9th AIAA/USAF/NASA/ISSMO Symposium on Multidisciplinary Analysis and Optimization*, AIAA, Atlanta, GA, September 4-6, 2002.

[48] Daberkow, Debora D., *A Formulation of Metamodel Implementation Processes for Complex Systems Design*. PhD thesis, Georgia Institute of Technology, June 2002.

[49] Das, I. and Dennis, J. E., "A Closer Look at Drawbacks of Minimizing Weighted Sums of Objectives for Pareto Set Generation in Multicriteria Optimization Problems," *Structural Optimization*, vol. 14, pp. 63–69, 1997.

[50] Das, I. and Dennis, J. E., "Normal-Boundary Intersection: A New Method for Generating the Pareto Surface in Nonlinear Multicriteria Optimization Problems," *SIAM Journal on Optimization*, vol. 8, no. 3, pp. 631–657, 1998.

[51] Dec, J. and Mitcheltree R., "Probabilistic Design of a Mars Sample Return Earth Entry Vehicle Thermal Protection System," *40th Aerospace Sciences Meeting and Exhibit*, AIAA, Reno, NV, January 14-17 2002, AIAA-2002-0910.

[52] DeLaurentis, D., Kang, T., Lim, C., Mavris, D., and Schrage, D., "System-of-systems modeling for personal air vehicles," (Atlanta, GA), *Presented at the 9th AIAA/ISSMO Symposium on Multidisciplinary Analysis and Optimization*, AIAA, September 4-6, 2002, AIAA-2002-5620.

[53] DeLaurentis, D. and Mavris, D., "Uncertainty Modeling and Management in MultiDisciplinary Analysis and Synthesis," *Presented at the 38th AIAA Aerospace Sciences Meeting and Exhibit*, AIAA, Reno, NV, January 10-13, 2000, AIAA-2000-0422.

[54] DeLaurentis, D., Pfaender, H., Mavris, D., and Schrage, D., "A Probabilistic Methodology for the Treatment of System-of-Systems Problems and Application to Future Air Transportation Architectures," *23rd International Congress of Aeronautical Sciences (ICAS)*, Toronto, Canada, September 8-13, 2002.

[55] DeLaurentis, D. A., *A Probabilistic Approach to Aircraft Design Emphasizing Stability and Control Uncertainties*. PhD thesis, Georgia Institute of Technology, November 1998.

[56] Doehring, Thoralf, "U.S. Navy," *http://navysite.de/index.htm*, December 31, 2003.

[57] Dombrowksi, P. and Ross, A., "Transforming the Navy: Punching a Feather Bed?," in *Naval War College Review*, *http://www.nwc.navy.mil/press/*, Naval War College Press, Summer 2003.

[58] Du, X. and Chen, W., "Methodology for Managing the Effect of Uncertainty in Simulation-Based Design," *AIAA Journal*, vol. 38, pp. 1471–1478, August 2000.

[59] Du, X. and Chen, W., "An Efficient Approach to Probablistic Uncertainty Analysis in Simulation-Based MultiDisciplinary Design," *the 38th AIAA Aerospace Sciences Meeting and Exhibit*, AIAA, Reno, NV 2000, AIAA 2000-0423.

[60] Du, X. and Chen, W., "Concurrent Subsystem Uncertainty Analysis in Multidisciplinary Design," *Presented at the 8th AIAA/NASA/USAF/ISSMO Symposium on Multidisciplinary Analysis and Optimization*, AIAA, Long Beach, CA, September 6-8 2000, AIAA-2000-4928.

[61] Du, X. and Chen, W., "A Hierarchical Approach to Collaborative Multidisciplinary Robust Design," *the Fourth Congress of Structural and Multidisciplinary Optimization*, Dalin, China, 2001.

[62] Eadie, J. M. and Mace, R. D., "Autonomous Littoral Warfare Systems Evalulator - Engineering Simulation," (Honolulu, HI), pp. 349–353, v. 1, *Presented at the 2001 MTS/IEEE OCEANS Conference*, IEEE, November 5-8, 2001.

[63] Eagle Picher, "Eagle Picher Product Directory – Lithium-Ion Batteries," tech. rep., Eagle Picher, http://www.the-powersource.com/E-Pspecs/li_ion.pdf, 2004.

[64] Ender, T., McClure, E., and Mavris, D., "A Probabilistic Approach to the Conceptual Design of a Ship-Launched High Speed Standoff Missile," *Presented at the AIAA 2002 Missile Sciences Conference*, AIAA, Monterey, CA, November 5-7, 2002.

[65] Engineous Software, Inc., *iSIGHT Designer's Guide*, Morrisville, NC, 1998.

[66] Erwin, Sandra I., *Navy Keeps Mine-Warfare Options Open.* National Defense Magazine, December 2002.

[67] Federation of American Scientists, "Long Term Mine Reconnaissance System [LMRS]," *http://www.fas.org/man/dod-101/sys/ship/weaps/lmrs.htm*, January 1, 1999.

[68] Federation of American Scientists, "US Navy Shipboard Combat Systems," *http://www.fas.org/man/dod-101/sys/ship/weaps/index.html*, May 15, 2003.

[69] Fieldsend, J. and Singh, S., "Pareto MultiObjective Non-Linear Regression Modelling to Aid CAPM Analogous Forecasting," *IEEE International Joint Conference on Neural Networks, part of the IEEE World Congress on Computational Intelligence*, IEEE Press, May 12-17, 2002.

[70] Filho, José C. Paes, "Javamix: A Tactical Decision Aid to Evaluate Minefield Clearance Plans," Master's thesis, Naval Postgraduate School, Monterey, CA, June 2001.

[71] Fitzgerald, C., Weston, N., Putnam, Z., and Mavris, D., "A Conceptual Design Environment for Technology Selection and Performance Optimization for Torpedoes," *Presented at the 9th Multi-Disciplinary Analysis and Optimization Symposium*, AIAA, Atlanta, GA, September 4-6, 2002, AIAA-2002-5590.

[72] Fleeman, Eugene L., *Tactical Missile Design*. AIAA Education Series, Reston, VA: American Institute of Aeronautics and Astronautics, 2001.

[73] Fletcher, Barbara, "The U.S. Navy's Master Plan: A Vision for UUV Development," *UnderWater Magazine*, July/August 2001.

[74] Fletcher, R. and Reeves, C. M., "Function Minimization by Conjugate Gradients," *British Computer Journal*, vol. 7, no. 2, pp. 149–154, 1964.

[75] Flynn, A.M., "Gnat Robots (And How They Will Change Robotics)," (Hyannis, MA), *Proceedings of the IEEE Micro Robots and Teleoperators Workshop*, November 9-11, 1987.

[76] Fowlkes, William Y. and Creveling, Clyde M., *Engineering Methods for Robust Product Design: Using Taguchi Methods in Technology and Product Development*. Engineering Process Improvement Series, Reading, MA: Addison-Wesley Publishing Company, 1st ed., 1995.

[77] Frits, A., Fleeman, E., and Mavris, D., "Use of a Conceptual Sizing Tool for Conceptual Design of Tactical Missiles (U)," *Presented at the 2002 Missile Sciences Conference*, AIAA, Monterey, CA, November 5-7, 2002.

[78] Frits, A. and Mavris, D., "A Screening Method for Customizing Designs Around Non-Convergent Regions of Design Spaces," *Presented at the 9th Multi-Disciplinary Analysis and Optimization Symposium*, AIAA, Atlanta, GA, September 4-6, 2002, AIAA-2002-5572.

[79] Frits, A. and Mavris, D., "Use of Probability of Success as an Independent Variable for Decision Making," (Chicago, IL), *Presented at the 2004 AIAA 4th Aviation Technology, Integration and Operations (ATIO) Forum*, AIAA, September 20-24, 2004, AIAA-2004-6206.

[80] Frits, A., Reynolds, K., Weston, N., and Mavris, D, "Benefits of Non-Dimensionalization in Creation of Designs of Experiments for Sizing Torpedo Systems," (Albany, NY), *Presented at the 2004 Multidisciplinary Analysis and Optimization Conference*, AIAA, August 30 - September 1, 2004, AIAA-2004-4491.

[81] Frits, A., Weston, N., Pouchet, C., Kusmik, A., Krol, W., and Mavris, D., "Examination of a Torpedo Performance Space and its Relation to the System Design Space," *Presented at the 9th Multi-Disciplinary Analysis and Optimization Symposium*, AIAA, Atlanta, GA, September 4-6, 2002, AIAA-2002-5634.

[82] Gage, D. W., "Command Control for Many-Robot Systems," *Unmanned Systems Magazine*, vol. 10, pp. 28–34, Fall 1992.

[83] Gage, D. W., "Sensor Abstractions to Support Many-Robot Systems," pp. 235–246, *Proceedings of SPIE Mobile Robots VII*, November 18-20, 1992.

[84] Gage, D. W., "Randomized Search Strategies with Imperfect Sensors," (Boston, MA), pp. 270–279, *Proceedings of the SPIE Mobile Robots VIII*, September 9-10, 1993.

[85] Gage, D. W., "Many-Robot MCM Search Systems," (Monterey, CA), pp. 9.56–9.64, *Procedures of the Autonomous Vehicles in Mine Countermeasures Symposium*, April 4-7, 1995.

[86] Garcia, E. and Mavris, D., "Framework for the Assessment of Capacity and Throughput Technologies," (San Diego, CA), *Presented at the 5th World Aviation Congress and Exposition*, SAE/AIAA, October 10-12, 2000, SAE/AIAA 2000-01-5612.

[87] Garcia, Elena, *Development of a Framework for the Assessment of Capacity and Throughput Technologies within the National Airspace System.* PhD thesis, Georgia Institute of Technology, January 2003.

[88] Gerken, Louis C., *Torpedo Technology.* American Scientific Corp., 1989.

[89] German, B., Branscome, E., Frits, A., Yiakas, N., and Mavris, D., "An Evaluation of Green Propellants for an ICBM Post Boost Propulsion System," *Presented at the 2000 Missile Sciences Conference*, AIAA, Monterey, CA, November 7-9, 2000.

[90] Girouard, W., Olson, S., and Jones, W., *Torpedo Expert Configuration Analysis Program (TECAP).* Naval Underwater Systems Center (NUSC) TM 87-2065, 1 October 1987.

[91] Global Security.org, "Type 212," *http://www.globalsecurity.org/military/world/europe/type-212.htm*, July 15, 2002.

[92] Global Security.org, "Type 214," *http://www.globalsecurity.org/military/world/europe/type-214.htm*, July 15, 2002.

[93] Goldberg, D., *Genetic Algorithms in Search, Optimization, and Machine Learning.* Reading, MA: Addison-Wesley, 1989.

[94] Golovidov, O., Kodiyalam, S., and Marineau, P., "Flexiable Implementation of Approximation Concepts in an MDO Framework," (St. Louis, MO), *Proceedings of the 7th AIAA/USAF/NASA/ISSMO Symposium on Multidisciplinary Analysis and Optimization*, AIAA, September 2-4, 1998, AIAA-98-4959.

[95] Granville, P. S., "Drag and Turbulent Boundary Layer of Flat Plates at Low Reynolds Numbers," tech. rep., DTNSRDC Report 4682, December 1975.

[96] Green, L., Lin, H., and Khalessi, M., "Probabilistic Methods for Uncertainty Propagation Applied to Aircraft Design," (St. Louis, MO), *20th AIAA Applied Aerodynamics Conference*, AIAA, June 24-26 2002, AIAA-2002-3140.

[97] Gu, X., Renaud, J., Batill, S., Brach, R., and Budhiraja, A, "Worst Case Propagated Uncetainty of Multidisciplinary Systems in Robust Design Optimization," *Structural Optimization*, vol. 20, pp. 190–213, Published by Springer-Verlag, Germany 2000.

[98] Guedes, Mauricio J. M., "A Minefield Reconnaissance Simulation," Master's thesis, Naval Postgraduate School, Monterey, CA, June 2002.

[99] Haldar, Achintya and Mahadevan, Sankaran, *Probability, Reliability and Statistical Methods in Engineering Design*. New York: John Wiley and Sons, 2000.

[100] Hayter, Anthony J., *Probability and Statistics for Engineers and Scientists*. Boston, MA: PWS Publishing Company, 1996.

[101] Hazelrigg, George A., *Systems Engineering: An Approach to Information-Based Design*. Upper Saddle River, NJ: Prentice Hall, 1996.

[102] Healey, A. J. and Kim, J., "Multiple Autonomous Vehicle Solutions to Minefield Reconnaissance and Mapping," (Sydney, Australia), *Australian-American Conference on Mine Counter-Measures*, July 15, 1999.

[103] Hezlet, Arthur, *The Submarine and Sea Power*. London: Peter Davies, 1967.

[104] Higgns, Tina, Turriff, Arthur, and Patrone, David, "Simulation-Based Undersea Warfare Assessment," *Johns Hopkins APL Technical Digest*, vol. 23, no. 4, pp. 396–402, 2002.

[105] Hines, Nathan, *A Probabilistic Methodology for Radar Cross Section Prediction in Conceptual Aircraft Design*. PhD thesis, Georgia Institute of Technology, Atlanta, GA, August 2001.

[106] Hoak, D. E. and Finck, R. D., *USAF Stability and Control DATCOM*. Wright-Patterson Air Force Base, OH: Flight Control Division, Air Force Flight Dynamics Laboratory, April 1978.

[107] Hoerner, S., *Fluid-Dynamic Drag*. (self-published), 1964.

[108] Holton, Glyn, "Contingency Analysis - The Monte Carlo Method," *www.riskglossary.com/articles/monte_carlo_method.htm*, Dec. 31, 2004.

[109] Howell, L. R., "Defining Surf Zone Crawler Search Strategies for Minefield Reconnaissance," (Honolulu, HI), *Oceans IEEE Conference and Exhibit*, IEEE, November 5-8, 2001.

[110] Hughes, Wayne P., *Military Modeling*. Military Operations Research Society, 2nd ed., 1989.

[111] Huyse, L., "Solving Problems of Optimization Under Uncertainty as Statistical Decision Problems," *42nd AIAA/ASME/ASCE/AHS/ASC 42nd Structures, Structural Dynamics, and Materials Conference and Exhibit*, AIAA, Seattle, WA, April 16-19, 2001, AIAA-2001-1519.

[112] Hwang, C.-L. and Masud, A. S. M., *Multiple Objective Decicion Making - Methods and Applications (Lecture Notes in Economics and Mathematical Systems; 164)*. Berlin: Springer-Verlag, 1979.

[113] Hwang, C.-L. and Yoon, K., *Multiple Attribute Decision Making - Methods and Applications (Lecture Notes in Economics and Mathematical Systems; 186)*. Berlin: Springer-Verlag, 1981.

[114] Jin, R., Chen, W., and Simpson, T., "Comparative Studies of Metamodeling Techniques Under Multiple Modeling Criteria," *Journal of Structural Optimization*, vol. 23, no. 1, pp. 1–13, 2001.

[115] Jin, R., Du, X., and Chen, W., "The Use of Metamodeling Techniques for Optimization Under Uncertainty," *Structural and Multidisciplinary Optimization*, vol. 25, no. 2, pp. 99–116, 2003.

[116] JMP, a Business Unit of SAS Institute, Inc., *JMP Version 5.1 User's Guide*, Cary, NC, 2003.

[117] Johnson, Adm Jay L., "Statement of radm michael g. mullen, u.s. navy director, surface warfare division before the seapower subcommittee of the senate armed services committee," March 23 2000.

[118] Johnson, Robert and Kuby, Patricia, "Just the Essentials of Elementary Statistics." Duxby Press, *http://www.duxbury.com/authors/mcclellandg/tiein/johnson/correlation.htm*, 1999.

[119] Kaminski, Paul, "Cost as an Independent Variable, Memorandum: Reducing Life Cycle Costs for New and Fielded Systems; Under Secretary of Defense for Acquitision and Technology." *http://www.ntsc.navy.mil/Resources/Library/Acqguide/caainvar.htm*, July 12, 1996.

[120] Kinsler, Lawrence E., Frey, Austin R., Coppens, Alan B., and Sanders, James V., *Fundamentals of Acoustics*. Wiley Text Books, 3rd ed., 1982.

[121] Kirby, M. and Mavris, D., "Forecasting Technology Uncertainty in Preliminary Aircraft Design," (San Francisco, CA), *Presented at the 1999 World Aviation Congress*, AIAA, October 19-21 1999, AIAA-1999-01-5631.

[122] Kirby, Michelle, *A Methodology for Technology Identification, Evaluation, and Selection in Conceptual and Preliminary Aircraft Design*. PhD thesis, Georgia Institute of Technology, March 2001.

[123] Kirby, Michelle, "TIES for Dummies: Basic How To's to Implement the TIES Method," 3rd ed., Georgia Institute of Technology, August 2, 2002.

[124] Kirsch, J., "Obtaining Group Synergy Using Swarms of Small Expendable Tactical Robots," (Washington, D.C.), *AUVS-93, the Twentieth Annual AUVS Technical Symposium*, June 29-30, 1993.

[125] Koch, P., "Probabilistic Design: Optimizing for Six Sigma Quality," *43rd AIAA/ASME/ASCE/AHS Structures, Structural Dynamics, and Materials Conference, 4th AIAA Non-Deterministic Approaches Forum*, AIAA, Denver, CO, 2002, AIAA-2002-1471.

[126] Koch, P. and Cofer, J., "Simulation-Based Design in the Face of Uncertainty," *Presented at the 51st Joint Army-Navy-NASA Air Force Propulsion Meeting*, November 18-21, 2002.

[127] Koch, P., Mavris, D., and Mistree, F., "Multi-Level, Partitioned Response Surfaces for Modeling Complex Systems," (St. Louis, MO), *Presented at the 7th AIAA/USAF/NASA/ISSMO Symposium on Multidisciplinary Analysis and Optimization*, AIAA, September 2-4, 1998, AIAA-98-4958.

[128] Koch, P., Simpson, T., Allen, J., and Mistree, F., "Statistical Approximations for Multidisciplinary Design Optimization: the Problem of Size," *Special Multidisciplinary Design Optimization Issue of Journal of Aircraft*, vol. 36, no. 1, pp. 275–286, 1999.

[129] Koch, P., Wujek, B., and Golovidov, O., "A Multi-Stage, Parallel Implementation of Probabilistic Design Optimization in an MDO Framework," (Long Beach, CA), *8th AIAA/USAF/NASA/ISSMO Symposium on Multidisciplinary Analysis and Optimization*, AIAA, September 6-8, 2000, AIAA-2000-4805.

[130] Koopman, Bernard O., *Search and Screening: General Priniciples with Historical Applications*. New York, NY: Pergamon Press, 1980.

[131] Krol, W. P. Jr., "Supercavitating Vehicle SBD Model Integration and Optimization Strategy," (University of Maryland), *Presented at the Office of Naval Research Simulation Based Design Workshop*, June 14, 2001.

[132] Kurtz, Paul, "Personal Interview." Interview from the 2004 Undersea Weapon Design and Optimization, Torpedo Stealth, and Supercavitating High-Speed Bodies Joint Workshop, June 9, 2004.

[133] Kusmik, W. Aldo, "Optimization in the Simulation Based Design Environment," *Presented at the ASME 2002 Design Engineering Technical Conference (DETC)*, September 9-12, 2001.

[134] Kusmik, W. Aldo and Glass, Richard, "Neural Network Implementation for Torpedo Design and Optimization," *Presented at the 9th Multi-Disciplinary Analysis and Optimization Symposium*, AIAA, Atlanta, GA, September 4-6, 2002.

[135] Langley, R., "Unified Approach to Probabilistic and Possibilistic Analysis of Uncertain Systems," *Journal of Engineering Mechanics*, vol. 126, No. 11, November 2000, ISSN 0733-9399.

[136] Langmaid, Kenneth, *The Approaches are Mined!* London: Jarrolds, 1965.

[137] Laplace, Marquis de, *A Philosophical Essay on Probabilities*. New York: Dover Publications, translated from the sixth French edition by F.W. Truscott and F.L. Emory, 1920, Original, 1820.

[138] Leon, R. V., Shoemaker, A. C., and Kacker, R. N., "Performance Measures Independent of Adjustment," *Technometrics*, vol. 29, pp. 253–285, 1987.

[139] Lin, C. C. and Segel, L. A., *Mathematics Applied to Deterministic Problems in the Natural Sciences*. Philadelphia, PA: Society for Industrial and Applied Mathematics, 1988.

[140] LittleJohn, W. C., "Motion Model Development for Very Shallow Water / Surf Zone Crawler," (Honolulu, HI), *Oceans IEEE Conference and Exhibit*, IEEE, November 5-8, 2001.

[141] Lopes, J. L., Folds, D. L., Paustian, I.C., and Wood-Putnam, J.L., "Acoustic Detection of Targets Buried at Steep and Subcritical Grazing Angles," (Honolulu, HI), *Oceans IEEE Conference and Exhibit*, IEEE, November 5-8, 2001.

[142] Luman, Ronald R., "Upgrading Complex Systems of Systems: A CAIV Methodology for Warfare Area Requirements Allocation," (Georgia Institute of Technology, Atlanta, GA), *Presented at the 2nd Conference on the Economics of Test and Evaluation*, November 3, 1999.

[143] Macedonia, R.M. and Sert, B., "Low Cost Mobility for Robotic Weapons," (San Diega, CA), *AUVS-88, the Fifteenth Annual AUVS Technical Symposium*, June 6-8, 1988.

[144] Martin, C. T., Kelly, C. O., Friend, H. D., Keen, C., and Wilson, S. L., "Lithium-ion Battery Development at Eagle-Picher," (Long Beach, CA), *Presented at the Fourteenth Annual Battery Conference on Applications and Advances, 1999*, IEEE, January 12-15, 1999.

[145] Matheron, G., "Principles of Geostatistics," *Economic Geology*, vol. 58, pp. 1246–1266, 1963.

[146] Matlab Manual, *The Language of Technical Computing, Version 6.0.0.88 Release 12, Online Help Guide*. The Math Works, Inc., Natick, MA, Sept 22 2000.

[147] Mattingly, J. D., Heiser, W. H., and Daley, D. H., *Aircraft Engine Design*. Washington, DC: AIAA Education Series, 1987.

[148] Mautner, Thomas S., "Comparison of the Counterrotating and Pre-Swirl Propeller Concepts for Marine Propulsion," *AIAA/ASME/SAE/ASEE 24th Joint Propulsion Conference*, 1988, AIAA-83-3088.

[149] Mavris, D., Bandte, O., and DeLaurentis, D, "Robust Design Simulation: A Probabilistic Approach to Multidisciplinary Design," *AIAA Journal of Aircraft*, vol. 36, No 1, pp. 298–307, Jan-Feb 1999.

[150] Mavris, D., Bandte, O., and Schrage, D., "Application of Probabilistic Methods for the Determination of an Economically Robust HSCT Configuration," (Bellevue, WA), *AIAA/USAF/NASA/ISSMO Multidisciplinary Analysis and Optimization Conference*, September 1996, AIAA-96-4090.

[151] Mavris, D. and DeLaurentis, D., "An Integrated Approach to Military Aircraft Selection and Concept Evaluation," (Anaheim, CA), *Presented at the 1st AIAA Aircraft Engineering, Technology, and Operations Congress*, AIAA, September 19-21, 1995, AIAA-95-3965.

[152] Mavris, D., DeLaurentis, D., Bandte, O., and Hale, M., "A Stochastic Approach to Multi-Disciplinary Aircraft Analysis and Design," (Reno, NV), *Presented at the 36th Aerospace Sciences Meeting and Exhibit*, AIAA, January 12-15, 1998, AIAA-98-0912.

[153] Mavris, D., DeLaurentis, D., and Soban, D., "Probabilistic Assessment of Handling Qualities Characteristics in Preliminary Aircraft Design," (Reno, NV), *Presented at the 36th Aerospace Sciences Meeting and Exhibit*, AIAA, January 12-15, 1998, AIAA-98-0492.

[154] Mavris, D. and Kirby, M., "Preliminary Assessment of the Economic Viability of a Family of Very Large Transport Configurations," (Los Angeles, CA), *Presented at the 1st World Aviation Congress and Exposition*, AIAA, October 21-24, 1996, AIAA-96-5516.

[155] Mavris, D. and Kirby, M., "Technology Identification, Evaluation, and Selection for Commercial Transport Aircraft," *Presented at the 58th Conference of the Society of Allied Weight Engineers*, SAWE, San Jose, CA, May 24-26 1999, SAWE Paper No. 2456.

[156] Mavris, D., Roth, B., and Macsotai, N., "A Method for Probabilistic Sensitivity Analysis of Commercial Aircraft Engines," (Florence, Italy), *Presented at the 14th ISABE*, September 1999.

[157] Mavris, D., Weston, N., and Frits, A., "Progress in the Conceptual Design of Torpedoes Incorporating Uncertainty Analysis," (State College, PA), *Presented at the Undersea Weapon Design & Optimization, Torpedo Stealth and Supercavitating High-Speed Bodies Joint Workshop*, June 8-10, 2004.

[158] Mavris, D., Weston, N., Frits, A., Pouchet, C., Fitzgerald, C., and Putnam, Z., *TOAD Torpedo Optimization, Analysis, and Design, User's Manual*. Aerospace Systems Design Laboratory, School of Aerospace Engineering, Georgia Institute of Technology, TOAD Release 1.1, May 15, 2003.

[159] Mavris, D., Weston, Neil, and Frits, Andrew, "Design Space Exploration and Technology Assessment for Torpedo Design," *Presented at the Undersea Weapon Simulation Based Design Workshop*, June 13-15, 2001, College Park, MD.

[160] Mavris, D., Weston, Neil, and Frits, Andrew, "Progress on the Development and Application of an Object-Oriented Sizing and Synthesis Tool for Torpedoes," *Presented at the Undersea Weapon Design and Optimization Workshop*, May 6-7, 2002, Newport, RI.

[161] McAllister, C., Kurtz, P., Bennett, L., and Yukish, M., "A Simulation Based Approach to Autonomous Underwater Vehicle Design," (University Park, PA), Applied Research Laboratory, Penn State University, 2002.

[162] McAllister, C., Simpson, T., Kurtz, P., and Yuksih, M., "Multidisciplinary Design Optimization Testbed Based on Autonomous Underwater Vehicle Design," (Atlanta, GA), *Presented at the 9th AIAA/ISSMO Symposium on Multidisciplinary Analysis and Optimization*, AIAA, September 4-6, 2002, AIAA-2002-5630.

[163] McDonald, Dale, Grantham, Walter J., and Tabor, Wayne L., "Response Surface Model Development for Global/Local Optimization Using Radial Basis Functions," *Presented at the 8th AIAA/USAF/NASA/ISSMO Symposium on Multidisciplinary Analysis and Optimization*, AIAA, Long Beach, CA, September 6-8, 2000, AIAA-2000-4776.

[164] McDonald, R. and Mavris, D., "Formulation, Realization, and Demonstration of a Process to Generate Aerodynamic Metamodels for Hypersonic Cruise Vehicle Design," *5th World Aviation Congress and Exposition*, AIAA, San Diego, CA, October 10-12, 2000, SAE/AIAA 2000-01-5559.

[165] Merriam-Webster, Inc., *http://www.m-w.com/*, *Merriam-Webster OnLine*, 2004.

[166] Meyers, B., Cancilliere, F., and LaPointe, K., "Torpedoes and the Next Generation of Undersea Weapons," *Undersea Warfare, The Official Magazine of the U.S. Submarine Force*, vol. 14, Winter/Spring 2002, *http://www.chinfo.navy.mil/navpalib/cno/n87/usw/issue_14/contents.html*.

[167] Mierzwicki, Timothy, "Risk Index for Multi-Objective Design Optimization of Naval Ships," Master's thesis, Ocean Engineering, Virgina Polytech Institute, Blacksburg, VA, April 24, 2003.

[168] Milford, F. J., "US Navy Torpedoes, Part One: Torpedoes Through the Thirties," *The Submarine Review, Publication of the Naval Submarine League*, April 1996.

[169] Milford, F. J., "US Navy Torpedoes, Part Two: The Great Torpedo Scandal, 1941-43," *The Submarine Review, Publication of the Naval Submarine League*, October 1996.

[170] Milford, F. J., "US Navy Torpedoes, Part Three: WW II Development of Conventional Torpedoes 1940-1946," *The Submarine Review, Publication of the Naval Submarine League*, January 1997.

[171] Montgomery, Douglas C., *Design and Analysis of Experiments*. New York: Wiley, 3rd ed., 1991.

[172] Myers, Raymond H. and Montgomery, Douglas C., *Response Surface Methodology: Process and Product Optimization Using Designed Experiments*. New York: John Wiley & Sons, 2nd ed., 2002.

[173] Naval Historical Center, "Casualties: U. S. Navy and Marine Corps Personnel Killed and Wounded in Wars, Conflicts, Terrorist Acts, and Other Hostile Incidents." *http://www.history.navy.mil/index.html*, October 20, 2004.

[174] Naval Studies Board, "Technology for the United States Navy and Marine Corps, 2000-2035: Becoming a 21st Century Force," tech. rep., National Research Council, *http://books.nap.edu/html/tec_21st/tfnf.htm*, 1997.

[175] NAVSEA, Coastal Systems Station, Panama City, "Minehunting Phases and Terminology," June 18, 2001.

[176] NAVSEA, Coastal Systems Station, Panama City, "Maritime Mine Countermeasures." *http://www.ncsc.navy.mil/Capabilities_and_Facilities/Capabilities/MaritimeMineCM/maritime_mine_countermeasures.htm*, October 3, 2004.

[177] Navy Office of Information, "Torpedoes: Mark 46, Mark 48, Mark 50," *http://www.chinfo.navy.mil/navpalib/factfile/weapons/wep-torp.html*, Washington, D.C., October 21, 2004.

[178] Neter, John, Kutner, Michael H., Nachtsheim, Christopher J., and Wasserman, William, *Applied Linear Statistical Models*. Boston, MA: McGraw-Hill, 4th ed., 1996.

[179] Ng, Kam, "2003 ONR Undersea Weapons Stealth, Propulsion, and Design Optimization Workshop," *Presented at the 2003 ONR Undersea Weapons Stealth, Propulsion and Design Optimization Workshop*, May 20-22, 2003, Newport, RI.

[180] Nixon, J. and Mavris, D., "A Multi-Level, Hierarchical Approach to Technology Selection and Optimization," *Presented at the 8th AIAA/NASA/USAF/ISSMO Symposium on Multidisciplinary Analysis and Optimization*, AIAA, Atlanta, GA, September 4-6, 2002, AIAA-2002-5423.

[181] Oberkampf, W., DeLand, S., Rutherford, B., Diegert, K., and Alvin, K., "Estimation of Total Uncertainty in Modeling and Simulation," Tech. Rep. SAND2000-0824, Sandia National Laboratories, Albuquerque, NM, April 2000.

[182] Oberkampf, W. and Helton, J., "Mathematical Representation of Uncertainty," *Non-Deterministic Approaches Forum*, AIAA, Seattle, WA, April 16-19, 2001, AIAA 2001-1645.

[183] Olds, John R., "Class Notes: Multi-Disciplinary Optimization." Georgia Institute of Technology, 2001.

[184] Olson, E. and Mavris, D., "Development of Response Surface Equations for High-Speed Civil Transport Takeoff and Landing Noise," *Presented at the 2nd World Aviation Congress and Exposition*, AIAA, Anaheim, CA, October 13-16, 1997, SAE-975570.

[185] Orr, Mark J. L., "Introduction to Radial Basis Function Networks," tech. rep., Centre for Cognitive Science, University of Edinburgh, Edinburgh, Scotland, *http://www.anc.ed.ac.uk/ mjo/intro/intro.html*, April 1996.

[186] Osborne, G. F., "The 'Spearfish' Propulsion System," *GEC Review*, vol. 13, no. 3, pp. 150–162, 1998.

[187] Padula, S. and Li, W, "Options for Robust Airfoil Optimization Under Uncertainty," *AIAA/ISSMO Symposium on Multidisciplinary Analysis and Optimization*, AIAA, Atlanta, GA, September 4-6, 2002, AIAA-2002-5602.

[188] Parks, J.M., "On Stochastic Optimization: Taguchi Methods demystified; its Limitations and Fallacy Clarified," *Probabilistic Engineering Mechanics*, vol. 16, no. 16, pp. 87–101, 2001.

[189] Phoenix Integration, *ModelCenter Basics*. Phoenix Integration, Inc., Blacksburg, VA, 2002.

[190] Powell, M. J. D., "The Theory of Radial Basis Function Approximation in 1990," in *Advances in Numerical Analysis II, Wavelets, Subdivision, and Radial Basis Functions* (Light, W., ed.), pp. 105–210, Oxford University Press, 1992.

[191] Powell, M. J. D., "An Efficient Method for Finding the Minimum of a Function of Several Variables without Calculating Derivatives," *Computer Journal*, vol. 7, no. 4, pp. 303–307, 199964.

[192] Pravda, "Does Demise of Chinese Submarine Give Hope to Russian Shipwrights?," *Pravada, News and Analysis*, August 12, 2003 *http://english.pravda.ru/main/18/89/357/9990_submarine.html*.

[193] Program Executive Office, Mine and Undersea Warfare, *PEO (MUW) INST 3370.1 – Mine and Undersea Warfare Measures of Effectiveness*. Department of the Navy, October 10, 2001.

[194] Putney, A., Savidge, L. A., Chang, S. H., and Chatham, R.E., "Bottom Crawling Synthetic Aperture Sonar for Very Shallow Water Mine Countermeasures," (Honolulu, HI), *IEEE Oceans Conference and Exhibit*, IEEE, November 5-8, 2001.

[195] Qu, X. and Haftka, R., "Probabilistic Safety Factor Based Response Surface Approach for Reliability-based Design Optimization," *Third ISSMO/AIAA Internet Conference on Approximations in Optimization*, AIAA, October 14-15, 2002.

[196] Raposa, J., Roberts, R., and Fennel, W., *User's Manual for the Electromagnetic Sizing Tool, Software for Electric Machines*. Naval Undersea Warfare Center, Electric Lightweight Torpedo Program, Newport, RI, 2002.

[197] Rasey, Stephen M., "Spotfire Communicates Portfolio Analysis of Investment Opportunities using Efficient Frontiers of Many Measures," (Hertfordshire, UK), *Presented at the Spotfire London Users Meeting*, Wiserways, LLC, May 20, 2003.

[198] Rawson, K. J. and Tupper, E. C., *Basic Ship Theory: Vol 2*. New York: Longman, Inc., 2nd ed., 1976.

[199] Raymer, Daniel P., *Aircraft Design: A Conceptual Approach*. Reston, VA: AIAA Education Series, 3rd ed., 1999.

[200] RD Designs, Webs of Interest, "Ships and Tonnage Sunk or Damaged in WW II by U.S. Submarines ," *http://www.rddesigns.com/ww2/ww2sinkings.html*, December 31, 2003.

[201] Robinson, David G., "A Survey of Probabilistic Methods Used in Reliability, Risk and Uncertainty Analysis: Analytical Techniques I," Tech. Rep. SAND98-1189, Sandia National Laboratories, Albuquerque, NM, June 1998.

[202] Roth, B., Graham, M., and Mavris, D., "Adaptive Selection of Pareto Optimal Engine Technology Solution Sets," *Presented at the 2002 ICAS Conference*, Toronto, Canada 2002, ICAS2002-5.9.4.

[203] Roth, B., Mavris, D., and Ellioitt, D., "A Probabilistic Approach to UCAV Engine Sizing," *Presented at the 34th Joint Propulsion Conference*, AIAA, Cleveland, OH, July 13-15, 1998, AIAA-98-3264.

[204] SAIC, San Diego, CA, *Integrated Theater Engagement Model (ITEM) Technical Manual*, version 8.3 ed., November 5, 1999.

[205] Saliby, E., "Descriptive Sampling: A Better Approach to Monte Carlo Simulation," *Journal of the Operational Research Society*, vol. 41, no. 12, pp. 1133–1142, 1990.

[206] Scharl, J. and Mavris, D., "Building Parameteric and Probabilistic Dynamic Vehicle Models Using Neural Networks," (Montreal, CA), *Presented at the AIAA Modeling and Simulation Conference and Exhibit*, AIAA, August 6-9, 2001, AIAA-2001-4373.

[207] Scharl, Julien, *Formulation and Implementation of a Methodology for Dynamic Modeling and Simulation in Early Aerospace Design*. PhD thesis, Georgia Institute of Technology, November 2001.

[208] Schrage, D., DeLaurentis, D., and Taggart, K., "IPPD Concept Development Process for Future Combat System," (Atlanta, GA), *Presented at the 9th AIAA/ISSMO Symposium on Multidisciplinary Analysis and Optimization*, AIAA, September 4-6, 2002, AIAA-2002-5619.

[209] Siddall, James N., *Probabilistic Engineering Design*. New York, NY: Marcel Dekker, inc., 1983.

[210] Simpson, T. W., Peplinski, J., Koch, P. N. and Allen, J. K. , "Metamodels for Computer-Based Engineering Design: Survey and Recommendations," *Engineering with Computers*, vol. 17, no. 2, pp. 129–150, 2001.

[211] Simpson, Timothy, *A Concept Exploration Method for Product Family Design*. PhD thesis, Georgia Institute of Technology, September 1998.

[212] Smith, Christina P., *MCM Analysis Portable Planning and Evaluation Resource (MAPPER) version 1.0 User's Guide*. Naval Surface Warfare Center, Panama City, FL, letter report a83-02-006 ed., June 17, 2002.

[213] Soban, Dani, *A Methodology for the Probabilistic Assessment of System Effectiveness as Applied to Aircraft Survivability and Susceptibility*. PhD thesis, Georgia Institute of Technology, December 2001.

[214] State-Ease, Inc, *Design-Expert Software, Version 6 User's Guide*, 2000.

[215] Stone, Lawrence D., *Theory of Optimal Search*, vol. 118 of *Mathematics in Science and Engineering*. New York, NY: Academic Press, 1975.

[216] Stone, Lawrence D. and Haley, Brian, *Search Theory and Applications*. NATO Conference Series, New York, NY: Plenum Press, 1980.

[217] Stroud, W., Krishnamurthy, T., and Mason, B., "Probabilistic Design of a Plate-Like Wing to Meet Flutter and Strength Requirements," *43rd AIAA/ASME/ASCE/AHS/ASC Structures, Structural Dynamics, and Materials Conference*, AIAA, Denver, CO, April 22-25, 2002, AIAA-2002-1464.

[218] Suhir, Ephraim, *Applied Probability for Engineers and Scientists*. New York: McGraw-Hill, 1997.

[219] Taguchi, Genichi, *Introduction to Quality Engineering: Designing Quality into Products and Processes*, vol. translated into English by the Asian Productivity Organization. Hong Kong: Asian Productivity Organization, 1986.

[220] Taguchi, Genichi, *Taguchi on Robust Technology Development*. Series on International Advances in Design Productivity, New York: ASME Press, 1993.

[221] Thacker, B., Riha, D., Millwater, H., and Enright, M., "Errors and Uncertainties in Probabilistic Engineering Analysis," *42nd AIAA/ASME/ASCE/AHS/ASC Structures, Structural Dynamics, and Materials Conference and Exhibit*, AIAA, Seattle, WA, April 16-19, 2001, AIAA-2001-1239.

[222] Thomas, Mark, *A Pareto Frontier for Full Stern Submarines via Genetic Algorithm*. PhD thesis, Massachussets Institute of Technology, June 1998.

[223] Tind, J. and Wiecek M., "Augmented Lagangian and Tchebycheff Approaches in Multiple Objective Programming," *Journal of Global Optimization*, vol. 14, pp. 251–266, 1999.

[224] Tong, Y. L., *The Multivariate Normal Distribution*. Springer Series in Statistics, Berlin, Germany: Springer Verlag, 1990.

[225] United States Coast Guard, "Integrated Deepwater System: Transforming America's Shield of Freedom." *http://www.uscg.mil/deepwater/faq.htm#1*, January 20, 2004.

[226] United States General Accounting Office, "Torpedo Procurement: Issues Related to the Navy's MK-50 Torpedo Propulsion System," tech. rep., GAO/NSIAD-89-8, January 1989.

[227] United States General Accounting Office, "Navy Torpedo Programs: MK-48 ADCAP Upgrades Not Adequately Justified," Tech. Rep. GAO/NSIAD-95-104, Report to the Secretary of Defense, June 1995.

[228] U.S. Navy, "Mine Warfare," NWP 3-15, NCWP 3-3.1.2 PCN 143 000008 00, Department of the Navy, Office of the Chief of Naval Operations and headquarters U.S. Marine Corps, August 1996.

[229] Vanderplaats, G. N., *Numerical Optimization Techniques for Engineering Design*. Colorado Springs, CO: Vanderplaats Research and Development, Inc, 3rd ed., 1999.

[230] Volovoi, V., Waters, M., and Mavris, D., "Comparative Assessment of Direct and Indirect Probabilistic Methods for Thermomechanical Analysis of Structural Components in Gas Turbines," *Presented at the ASME Power for Land, Sea, and Air Conference*, ASME, Atlanta, June 16-19, 2003.

[231] Volovoi, V., Zentner, J., and Mavris, D., "Assessment of the Efficiency of Partitioned Response Surface Equations in Structural Applications," *Presented at the 44th Structures, Structural Dynamics, and Materials Conference*, AIAA, Norfolk, Virginia, April 7-10, 2003.

[232] Walchak, Martin, "RAMICS - Rapid Airborne Mine Clearance System." NAVSEA, Coastal Systems Station, Panama City, October 10, 2000.

[233] Wald, Q., "Analysis of the Integral Pumpjet," *Journal of Ship Research*, pp. 307–316, December 1970.

[234] Wallace, J., *A Framework for Conducting Mechanistic Based Reliability Assessments of Components Operating in Complex Systems*. PhD thesis, Georgia Institute of Technology, Atlanta, GA, November 2003.

[235] Wallace, J., "Improved Component Reliability Assessments Using Joing Probability Modeling," (Palm Springs, CA), *6th AIAA Non-Deterministic Approaches*, AIAA, April 19-22, 2004, AIAA-2004-17901.

[236] Washburn, Alan R., *Search and Detection*. Arlington, VA: Military Applications Section, Operations Research Society of America, 1981.

[237] Weston, Neil and Frits, Andrew, "Conceptual Torpedo Design Using the Torpedo Optimization, Analysis, and Design (TOAD) Program," *Presented at the 2003 ONR Undersea Weapons Stealth, Propulsion and Design Optimization Workshop*, May 20-22, 2003, Newport, RI.

[238] Wick, C. E. and Stilwell, D. J., "A Miniature Low-Cost Autonomous Underwater Vehicle," (Honolulu, HI), *Oceans IEEE Conference and Exhibit*, IEEE, November 5-8 2001.

[239] Wilson, B., Cappelleri, D., Simpson, T., and Frecker, M, "Efficient Pareto Frontier Exploration Using Surrogate Approximations," *8th AIAA/USAF/NASA/ISSMO Symposium on Multidisciplinary Analysis and Optimization*, AIAA, Long Beach, CA, September 6-8, 2000, AIAA-2000-4895.

[240] Wood, E., Li, J., and Lin, W.-M., "An Integrated Simulation Environment for Undersea Weapon Design and Optimization," *Presented at the Undersea Weapon Design and Optimization Workshop*, May 6, 2002, Newport, RI.

[241] Wood, E., Li, J., and Lin, W.-M., "An Integrated Simulation Environment for Undersea Weapon Design and Optimization," *Presented at the 2003 ONR Undersea Weapons Stealth, Propulsion and Design Optimization Workshop*, May 21 2003, Newport, RI.

[242] Yukish, M., Bennett, L., and Kurtz, P., "Simulation-Based Design for Undersea Weapons," *Penn State-ARL Institute for Manufacturing and Sustainment Technologies Quarterly*, no. 2, pp. 3–6, 2001.

[243] Yukish, M., Bennett, L., and Simpson, T., "Requirements on MDO Imposed by the Undersea Vehicle Conceptual Design Problem," *Presented at the 8th AIAA Symposium on Multidisciplinary Analysis and Optimization*, AIAA, Long Beach, CA, September, 2000, AIAA-2000-4816.

[244] Yukish, Mike, "Personal Correspondance." July 7, 2004.

[245] Zadeh, L. A., "Fuzzy Sets," *Information and Control*, vol. 8, no. 3, pp. 338–353, 1965.

[246] Zang, T., Hemsch, M., Hilburger, M., Kenny, S., Luckring, J., Maghami, P., Padula, S., and Stroud, W., "Needs and Opportunities for Uncertainty-Based Multidisciplinary Design Methods for Aerospace Vehicles," tech. rep., NASA, July 2002, NASA/TM-2002-211462.

[247] Zhang, J., Wiecek, M., and Chen, W., "Local Approximation of the Efficient Frontier in Robust Design," *Presented at the 1999 ASME Design Engineering Technical Conferences*, ASME, Las Vegas, Nevada, September 12-15, 1999, DETC99/DAC-8566.

[248] Zhang, J., Wiecek, M, and Chen, W., "Local Approximation of the Efficient Frontier in Robust Design," *ASME Journal of Mechanical Design*, vol. 22, pp. 232–236, 2000.

VITA

Andrew P. Frits was born on November 12, 1975 in Little Rock, AR. He attended Little Rock Central High School and graduated as a National Merit Finalist. In 1994, Mr. Frits enrolled in the aerospace engineering bachelors degree program at the Georgia Institute of Technology in Atlanta, GA. He joined the cooperative education program in 1995, working with the Georgia Tech Research Institute on infrared missile guidance and countermeasures simulation. While still an undergraduate, Mr. Frits worked on warhead design in a graduate student team which won first place in an American Institute of Aeronautics and Astronautics (AIAA) missile design competition for a high speed standoff missile. In June 1999, he graduated with Highest Honors.

In August 1999, Mr. Frits enrolled in the Georgia Tech aerospace engineering graduate program with a President's Fellowship. He was awarded a graduate research assistantship at the Aerospace Systems Design Laboratory (ASDL), where he worked under the direction of Professor Dimitri Mavris. During his first year in the program, he led the trajectory and mission analysis effort on a student team for an AIAA strategic missile design competion which won first place for a design of an ICBM post-boost propulsion system. In December 2000, he graduated with his master's degree and began pursuit of the doctoral degree. As part of his graduate assistantship, Mr. Frits has assisted in sponsored research on torpedo systems for the Office of Naval Reseach (ONR), Naval Undersea Warfare Center (NUWC) and served as an intern at the NUWC facility in Newport, RI during the summers of 2003 and 2004. He has remained actively engaged with missile systems research at ASDL while taking the role of student lead on undersea weapons research.